VNIVERSITAT DE VALÈNCIA

Doctoral Program in Medicine (3139)

Department of Pediatrics, Obstetrics and Gynecology, Faculty of Medicine

PhD Thesis

Using organoids to decipher endometrial regeneration in Asherman syndrome patients

Author:

Javier González Fernández

Supervised by:

Dr. Felipe Vilella

Dr. Carlos Simón

Dr. Xavier Santamaría

Valencia, October 2024

VNIVERSITAT DE VALÈNCIA

Dr. Carlos Simón Vallés, Professor of Pediatrics, Obstetrics and Gynecology at the University of Valencia and President of Carlos Simon Foundation for Research in Women's Health; Dr. Felipe Vilella, Group Leader of materno-fetal crosstalk laboratory at the INCLIVA Health Research Institute and Senior Principal Investigator at the Carlos Simon Foundation for Research in Women's Health; Dr. Xavier Santamaría, Senior Principal Investigator at the Carlos Simon Foundation for Research in Women's Health.

CERTIFY:

That the research work entitled: "Using organoids to decipher endometrial regeneration in Asherman syndrome patients" has been carried out entirely by Mr. Javier González Fernández under their supervision. This memory is completed and meets all the requirements for its presentation and defence as a DOCTORAL THESIS before a court.

For the record, and to serve the appropriate purposes, we hereby sign this certification in:

Valencia, September 19th, 2024

SIMON VALLES CARLOS ANTONIO - 73757585N
Firmado digitalmente por SIMON VALLES CARLOS ANTONIO - 73757585N
Fecha: 2024.10.18 14:07:49 +02'00'

Signed by: Carlos Simón Vallés (Director)

VILELLA MITJANA FELIPE - 43737973T
Digitally signed by VILELLA MITJANA FELIPE - 43737973T
Date: 2024.10.18 13:23:30 +02'00'

Signed by: Felipe Vilella Mitjana (Director)

SANTAMARIA COSTA JAVIER - 43728114P
Firmado digitalmente por SANTAMARIA COSTA JAVIER - 43728114P
Fecha: 2024.10.22 06:12:42 -06'00'

Signed by: Xavier Santamaría Costa (Director)

The work presented in this doctoral thesis has been carried out at the Carlos Simon Foundation with the financial support of a “PFIS” grant from the Instituto de Salud Carlos III (Ref: FI19/00159). As a complement to the PhD program, a three-month research stay was carried out at the Stamcelinstituut in KU Leuven, under the supervision of Dr. Hugo Vankelecom. The findings from this thesis, along with those from related projects, have been successfully published and presented at various scientific conferences, as outlined below:

Research articles:

- Gonzalez-Fernandez J, Zaragozano S., Monteagudo-Sánchez A., Vilella F. Single-cell technology: the key to an improved understanding of the human endometrium in health and disease (Accepted in 2024). *American Journal of Obstetrics & Gynecology*.
- Gonzalez-Fernandez J., Moncayo-Arlandi J., Ochandio A., Simon C., Vilella F. The role of extracellular vesicles in intercellular communication in human reproduction (2023). *Clinical Science*. 137-3, pp.281-301. DOI: 10.1042/CS20220793.
- Santamaria X., Roson B., Perez-Moraga R., Venkatesan N., Pardo-Figuerez M., Gonzalez-Fernandez J., Llera-Oyola J., Fernandez E., Moreno I., Salumets A., Vankelecom H., Vilella F., Simon C. Decoding the endometrial niche of Asherman’s Syndrome at single-cell resolution (2023). *Nature Communications*. 14-5890. DOI: 10.1038/s41467-023-41656-1.
- Bolumar D., Moncayo-Arlandi J., Gonzalez-Fernandez J., Ochando A., Moreno I., Monteagudo-Sanchez A., Marin C., Diez A., Fabra P., Checa M.A., Espinos J.J., Gardner D.K., Simon C., Vilella F. Vertical transmission of maternal DNA through extracellular vesicles associates with altered embryo bioenergetics during the periconception period (2023). *Elife*. DOI: 10.7554/eLife.88008.

Oral and Poster Presentations in Scientific Meetings:

- Gonzalez-Fernandez J., Parras M., Ochando A., Perez R., Garcia J.T., Roson B., Simon C., Vilella F (2023, May 7-12). *Single-Cell analysis of endometrial cell lineages identifies endothelial and epithelial progenitors* [Oral communication].

Germinal Stem Cell Biology (Gordon Research Conference) 2023. Castelldefels, Spain.

- Zaragozano S., Gonzalez-Fernandez J., Toson B., Moncayo-Arlandi J., Grases J.P., Pardo-Figuerez M., Ochando A., Simon C., Vilella F (2024, April 8-9). *Development and Characterization of a 3D Human Endometrium-on-a-Chip Model* [Poster presentation]. 3D Organ Modelling in Health and Disease. Leuven, Belgium.

AGRADECIMIENTOS

A mis directores de tesis. Al Dr. Carlos Simón por transmitirme su devoción por la ciencia. Al Dr. Xavi Santamaría, por permitirme formar parte de esta investigación. Al Dr. Felip Vilella, por abrirme las puertas que ya creía cerradas, guiarme y creer en mí durante todo este camino.

A mis compañeros de la Fundación, los que están y estuvieron, y de los que tanto he aprendido. Gracias a todos por vuestro apoyo y ánimos constantes, pero sobre todo por los momentos y emociones que hemos compartido durante estos años. En especial a Ana y Alba, por sus recomendaciones y correcciones desinteresadas, y a María, por hacer suya esta tesis en momentos difíciles.

A mis amigos, por estar siempre pese al tiempo y la distancia, por perdonar la ausencia a pesar de las circunstancias.

A mis padres, por su amor incondicional, sus valores y el hogar eterno. Gracias por la libertad de ser y la oportunidad que me ha brindado vuestro esfuerzo, no sabéis cuanto lo valoro.

A mis hermanos y Lucía, por todos vuestros consejos y cariño. Gracias por vuestra forma de ser y por celebrar todos los logros como propios.

A Gonzalo y Alba, por robar una parte de mí, por ser una inyección de alegría y reflejar lo verdaderamente importante.

A Vero, por ser mi punto de apoyo para mover el mundo, por su generosidad y paciencia, por acompañarme en el camino, por quererme bien, por todo.

RESUMEN

Introducción

El endometrio es la capa mucosa que recubre el interior de la cavidad uterina, responsable de la implantación embrionaria y de su propia regeneración tras la menstruación (Critchley et al., 2020). Este tejido está formado por células epiteliales, estromales, inmunitarias y endoteliales, distribuidas en dos estratos diferenciados: la capa basal y la capa funcional (Makieva et al., 2018). Durante el ciclo menstrual, el endometrio sufre cambios morfológicos y fisiológicos que dependen principalmente de las secreciones cíclicas de estrógeno y progesterona (Moreno et al., 2023).

El síndrome de Asherman, en ingles *Asherman syndrome* (AS), es una patología endometrial adquirida caracterizada por la presencia de adherencias intrauterinas, en ingles *intrauterine adhesions* (IUAs). Estas adherencias suelen surgir por lesiones en la capa basal del endometrio, resultando en la sustitución del tejido endometrial normal por la transformación del estroma en tejido fibroso y la inactivación del epitelio adquiriendo una morfología cubo-columnar, afectando a la funcionalidad del útero (Smikle et al., 2023). El AS es una condición iatrogénica, comúnmente que aparece como un efecto adverso como consecuencia de intervenciones quirúrgicas como legrados o cirugías uterinas, aunque también puede desencadenarse por infecciones o endometritis aguda o crónica (Conforti et al., 2013; Sharma et al., 2008).

La prevalencia del AS varía según la población estudiada, siendo más común en países con prácticas ginecológicas menos avanzadas o donde las intervenciones para terminación del embarazo son ilegales. En la Unión Europea, la Agencia Europea de Medicamentos (EMA) ha establecido una prevalencia de 4,4 casos por cada 10.000 personas, clasificando al AS como una enfermedad rara (*Committee for Orphan Medicinal Products (COMP) | European Medicines Agency*, n.d.). La prevalencia del AS en mujeres con problemas de fertilidad varía entre el 2% y el 6%, pero puede llegar hasta el 40% en pacientes que han tenido procedimientos como la eliminación de restos placentarios o legrados repetidos (Dreisler & Kjer, 2019).

La clasificación del AS ha evolucionado desde la histerosalpingografía a clasificaciones basadas en la visualización histeroscópica de la cavidad uterina (Manchanda et al., 2021). Actualmente, su diagnóstico se basa en la clasificación de la Sociedad Americana de Fertilidad (ASRM), que divide la severidad de la patología en tres niveles: leve, moderado y severo (Buttram et al., 1988).

Su tratamiento habitual es la eliminación de las adherencias mediante adhesiolisis histeroscópica (March 2011). Sin embargo, este tratamiento tiene limitaciones debido a la tendencia a la recurrencia de las IUAs (Gharibeh et al., 2022), lo que ha llevado al uso de estrategias preventivas como geles de ácido hialurónico, tratamientos hormonales o dispositivos intrauterinos. A pesar de ello, el tratamiento suele requerir múltiples procedimientos debido a la alta tasa de recurrencia (Lekovich et al., 2017) y entre las pacientes que consiguen embarazo, la incidencia de aborto de repetición es del 17.7% (Guo et al., 2019). Las anomalías placentarias son más comunes en pacientes tratadas, presentando una mayor incidencia de placenta acreta, increta y previa debido a una decidualización endometrial inadecuada y a cicatrices residuales (Tavcar et al., 2023). Además, el parto prematuro es más frecuente en estas pacientes, con tasas que varían entre el 11.6% y el 50% (Mára et al., 2023).

En la actualidad las terapias regenerativas representan una prometedora área de estudio para el tratamiento del AS, enfocándose en el uso de células madre para regenerar el endometrio dañado. Las células madre derivadas de la médula ósea, del inglés *Bone marrow derived stem cells* (BMDSC), han mostrado un potencial significativo en estudios preclínicos, migrando al endometrio y tratando efectivamente el tejido dañado en modelos animales (Alawadhi et al., 2014). Nuestro grupo de investigación ha desarrollado un estudio experimental y un ensayo clínico de fase II utilizando BMDSCs autólogas $CD133^{+}$ para tratar pacientes con AS que no han respondido a la adhesiolisis histeroscópica y terapia de reemplazo hormonal (Santamaria et al., 2016). Este tratamiento ha mostrado mejoras en la puntuación de la enfermedad y el grosor endometrial en las pacientes, resultando en embarazos espontáneos y después de transferencias de embriones en varias de ellas. Tanto la EMA como la FDA han reconocido esta terapia como el primer tratamiento huérfano diseñado para el AS, clasificándola como un Producto Medicinal de Terapia Avanzada.

Esta tesis aborda el uso de la transcriptómica a nivel de célula única, así como un modelo *in vitro* de organoides como metodologías para ofrecer una comprensión más profunda de los mecanismos afectados en el AS, así como el efecto de la terapia celular indicada (Wang & Yu, 2018). Los recientes avances hacia la transcriptómica de célula única, del inglés *single cell RNA sequencing* (scRNA-seq), ha permitido la identificación de perfiles transcriptómicos de las células endometriales a lo largo del ciclo menstrual, mapeando los cambios celulares y moleculares en el endometrio e identificando las diferentes poblaciones celulares y sus interacciones (Wang et al., 2020).

Gran parte de los descubrimientos descritos hasta ahora se han realizado empleando biopsias endometriales (que permiten acceder a la situación específica *in vivo* del endometrio) o modelos animales (con limitaciones en la traslación del conocimiento a humanos). A pesar de que los modelos de cultivo celular presentan grandes limitaciones, su avance actual hacia modelos tridimensionales que mimetizan el desarrollo del tejido abre la puerta a investigaciones con un mayor control experimental.

Uno de estos modelos más avanzados son los organoides epiteliales de endometrio, un cultivo celular desarrollado a partir de células madre adultas residentes en el endometrio, que se diferencian en un matriz extracelular artificial (Gu et al., 2020). Este modelo se ha utilizado para estudiar la biología del endometrio, replicando características esenciales del epitelio endometrial y respondiendo a tratamientos hormonales de manera similar al tejido endometrial *in vivo* (Boretto et al., 2017; Fitzgerald et al., 2019). Asimismo, han sido caracterizados mediante scRNA-seq mostrando una composición celular heterogénea incluyendo células ciliadas y secretoras (Cochrane et al., 2020), han permitido investigar vías asociadas con la diferenciación epitelial (Garcia-Alonso et al., 2021), y han sido utilizados para estudiar diversas patologías endometriales como la endometriosis y el cáncer endometrial (Boretto et al., 2019; Cochrane et al., 2020) así como para probar nuevos tratamientos (Bi et al., 2021). En esta tesis doctoral desarrollamos organoides endometriales a partir de muestras de pacientes de AS, para verificar hasta qué punto replican las características de la enfermedad y suponen un modelo óptimo para el estudio de esta patología.

Hipótesis

El síndrome de Asherman (AS) es una patología endometrial adquirida caracterizada por la presencia de adherencias en la cavidad uterina. El desarrollo del AS implica la formación de tejido fibrótico endometrial que induce una función epitelial deteriorada.

Nuestra hipótesis es que el tejido fibrótico es la consecuencia de las intervenciones previas que lo han provocado, por lo que debe existir una patogénesis subyacente en el AS que pretendemos averiguar mediante el análisis de los perfiles transcriptómicos a nivel de célula única de las biopsias endometriales, combinando estos estudios *in vivo* con el desarrollo de un modelo *in vitro* de organoides epiteliales obtenidos de las mismas biopsias endometriales de pacientes con AS antes y después de haber recibido terapia celular dentro de un contexto de fase 1/2 autorizado por la AEMPS (Agencia Española de Medicamentos y Productos Sanitarios) y EMA (Agencia Europea de Medicamentos).

Objetivos

El objetivo principal de esta tesis doctoral es dilucidar el entorno celular dentro del endometrio afectado por el síndrome de Asherman mediante el descubrimiento de perfiles transcriptómicos celulares antes y después de haber recibido terapia celular.

Los objetivos específicos son:

1. Desarrollar un atlas de los perfiles transcriptómicos celulares del endometrio en el síndrome de Asherman que comprende las diferencias en la composición celular y la expresión génica entre los tipos celulares identificados.
2. Desarrollar un modelo de cultivo de organoides derivado del tejido patológico del síndrome de Asherman y evaluar su capacidad para reproducir con precisión las características de la enfermedad.
3. Evaluar el impacto de la terapia celular basada en BMDSC desarrollada por nuestro grupo pre y post tratamiento tanto *in vivo* como *in vitro*.

Metodología

Para la consecución de los objetivos planteados, se obtuvieron y analizaron muestras de 9 pacientes con AS, antes y después de someterse al tratamiento autólogo con células $CD133^{+}$ derivadas de la médula ósea de los propios pacientes, así como de 9 donantes

sanos como controles, realizando la toma de muestras durante la ventana de implantación. Además, los perfiles transcriptómicos de 6 muestras de donantes sanos durante la ventana de implantación, en inglés *window of implantation* (WOI), y 10 de donantes dentro de la fase secretora, se obtuvieron de nuestro set de datos previamente publicado (Wang et al., 2020).

Para el análisis transcriptómico de célula única, en inglés *single-cell RNA sequencing* (scRNA-seq) se utilizaron todas las biopsias endometriales procedentes de pacientes con AS y 6 donantes sanas (además de los datos ya secuenciados en estudios previos). Las muestras endometriales se sometieron a una disgregación enzimática y mecánica resultando en suspensiones de células individuales tras su filtrado. Tras la eliminación de las células muertas mediante la utilización de un kit comercial (MACS *dead cell removal kit*, Miltenyi), se obtuvieron las librerías de cDNA, de alrededor de 18.000 células por muestra, de cada célula aislada mediante la utilización de chips de microfluídica (10x Genomics), siguiendo las instrucciones del fabricante. Tras la cuantificación de las librerías mediante TapeStation, éstas se secuenciaron en un NovaSeq System 6000 (Illumina). Los datos obtenidos se analizaron mediante CellRanger (Lange et al., 2022), Seurat (Hao et al., 2021) y Harmony (Korsunsky et al., 2019) entre otras herramientas, tras la eliminación de las células que no cumplían los criterios de calidad en cuanto a número de genes, número de conteos y porcentaje de lecturas mitocondriales. Las poblaciones celulares identificadas se etiquetaron en base a la expresión diferencial de genes conocidos como marcadores canónicos, previamente descritos en la bibliografía. Las muestras de donantes sanos correspondientes a la fase secretora se utilizaron para la caracterización general de todas las poblaciones identificadas, mientras que las muestras correspondientes a la ventana de implantación se utilizaron para la caracterización profunda de las poblaciones de interés (epiteliales, estromales, perivasculares y musculares). Posteriormente, se llevó a cabo un análisis de expresión diferencial tanto entre las muestras de AS y los diferentes controles (de fase secretora y ventana de implantación), como entre las muestras de AS antes y después del tratamiento con células $CD133^{+}$. La abundancia celular diferencial se analizó aplicando un modelo lineal generalizado binomial negativo (NB-GLM, *Negative Binomial*

Generalizad Linear Model), y el análisis de las comunicaciones célula a célula se realizó mediante CellChat (Jin et al., 2021).

El cultivo de organoides se realizó a partir de 3 biopsias procedentes de pacientes con AS (antes y después de la terapia celular) y 3 nuevas biopsias de donantes sanos en la ventana de implantación. Las células en suspensión obtenidas tras la digestión de las biopsias se cultivaron en gotas de Matrigel® con un medio rico en factores de crecimiento y diferenciación (siguiendo el protocolo descrito previamente (Boretto et al., 2017)). Los pases del cultivo se realizaron mediante la digestión enzimática del Matrigel® y mecánica de los organoides, y, entre los pases 2 y 4, se cultivaron células de organoides durante dos días, para someterse posteriormente al tratamiento hormonal que simula el ciclo menstrual durante 6 días más. A partir de los organoides obtenidos de las diferentes biopsias se realizaron mediciones sobre su número y diámetro medio, además de utilizarse para scRNA-seq y análisis inmunohistoquímicos.

Para los análisis de inmunohistoquímica en muestras de tejido endometrial, fragmentos de las muestras de biopsia obtenidas se fijaron con paraformaldehído y embebieron en parafina. Después, se realizaron múltiples secciones del tejido empleando un microtomo y se realizaron tinciones de hematoxilina y eosina e hibridación de RNA *in situ* mediante la técnica RNAscope (siguiendo las indicaciones del fabricante), empleando sondas de reconocimiento para el mRNA del gen *SLPI.*

Los análisis de inmunohistoquímica en organoides se realizaron aislándolos de la matriz artificial mediante su digestión enzimática, para posteriormente fijarlos con paraformaldehído y permeabilizarlos con tritón. Posteriormente se realizaron tinciones de marcadores epiteliales (E-cadherina y pancitoqueratina), proliferación (Ki67), y colágeno (COL1A2). Los análisis estadísticos de los datos obtenidos se realizaron utilizando el software GraphPad Prism.

Resultados y discusión

Por medio del análisis de los perfiles transcriptómicos identificamos un total de 18 tipos celulares, que incluyen células epiteliales y epiteliales ciliadas, estromales, endoteliales, perivasculares, perivasculares contráctiles, musculares (en inglés *smooth muscle cells,* SMC), y diferentes subpoblaciones de células inmunes (como macrófagos, células

dendríticas o *natural killer* (NK) entre otros). Algunos de estos tipos celulares se subdividieron tras un análisis específico dentro de la ventana de implantación, dando lugar a la distinción entre epitelio luminar, glandular y glandular secretor (que se diferencia de la glandular por la expresión de genes relacionados con la ventana de implantación), SMC y miofibroblastos, y diferentes tipos de células perivasculares. Las muestras de pacientes de AS mostraron una reducción significativa en las poblaciones epiteliales, principalmente ciliada y glandular secretora al compararlas con las muestras control (poblaciones críticas en la receptividad endometrial (Dmowski & Greenblatt, 1969)), en concordancia con la histología del AS, en la que se observa una pérdida de la gran mayoría de las glándulas epiteliales (Smikle et al., 2023).

La anotación celular también detectó una población previamente descrita (Garcia-Alonso et al., 2021) como posible población de células madre endometriales (por su expresión del gen *SOX9*). Esta población solo apareció en las muestras control, sugiriendo que su ausencia en el endometrio de AS podría estar relacionada con la perdida de la capacidad de regeneración endometrial. Por el contrario, tanto las SMC y perivasculares contráctiles, como diferentes poblaciones inmunes presentan un incremento en el endometrio de AS, representando una mayor rigidez y un perfil pro-inflamatorio, condiciones características de la patología (Smikle et al., 2023).

Por primera vez, identificamos una nueva población asociada al AS que denominamos epitelio-AS. Esta población, que expresa genes relacionados con el estrés celular y la respuesta inflamatoria (como HSPA1A, SOCS3 o SLPI) (Carow & Rottenberg, 2014; Mongkolpathumrat et al., 2024), se encuentra casi exclusivamente en el AS, por lo que podría suponer un candidato para el diagnóstico y/o pronóstico de la enfermedad puesto que validamos su detección en tejido mediante hibridación de mRNA *in situ*.

Los análisis de expresión diferencial entre las células endometriales de pacientes con AS y los controles sanos mostraron una actividad secretora disminuida y menor expresión de genes relacionados con la ventana de implantación en las poblaciones epiteliales, indicadores de un endometrio con menor capacidad para la adhesión embrionaria. Las células estromales mostraron un incremento en la expresión de genes proliferativos y relacionados con la producción de componentes de la matriz extracelular (como el

colágeno y la fibronectina). Estos cambios en la expresión génica muestran el perfil pro-fibrótico de la enfermedad, una de las consecuencias más características del AS y principal causante de la formación de las adhesiones intrauterinas (Smikle et al., 2023)(Salama et al., 2020). Otro factor que incrementa el ambiente fibrótico de la enfermedad, y provoca la pérdida de la menstruación en las pacientes, es la disminución de la vasculatura (Santamaria, Mas, et al., 2018). En nuestro análisis identificamos su promoción mediante la expresión diferencial de señales anti-angiogénicas en pacientes de AS. De la misma forma identificamos la expansión de las poblaciones mieloides y linfoides en el AS, cuyos perfiles transcriptómicos mostraron la sobreexpresión de genes relacionados con inflamación (*NEAT1* o *S100A8/9/12*) o la producción de citoquinas (*CCL5/3* o *CC3L1*), incrementando el estado pro-inflamatorio característico de la patología.

Con el objetivo de investigar las posibles alteraciones de la comunicación célula a célula se llevó a cabo un análisis en el que se identificaron un total de 59 vías de señalización alteradas. Al comparar las muestras de SA con los controles sanos se observó una pérdida general de las interacciones entre las poblaciones epiteliales y el resto de los tipos celulares en el AS, sustituidas principalmente por la autoestimulación de las células estromales. Entre las vías de señalización más alteradas de las células epiteliales se encuentran la IL6 (relacionada con el mantenimiento del embarazo (Yoo et al., 2017)), o CDH1 y SPP1 (relacionadas con la adhesión del epitelio y la decidualización (Reardon et al., 2012; X. B. Wang et al., 2018)), contribuyendo a la disminución del revestimiento epitelial y su integridad estructural en el endometrio de las pacientes de AS. La comunicación célula a célula también mostró la activación de la producción de fibras de la matriz extracelular (colágeno, laminina y fibronectina) y vías pro-fibróticas (FGF y PERIOSTIN) principalmente mediante la auto-estimulación del estroma, sugiriendo que el estroma es un actor principal en la acumulación de matriz extracelular y la fibrotización del tejido (Smith et al., 2018)(Dmowski & Greenblatt, 1969). En cuanto a las células inmunes y endoteliales, las vías de señalización relacionadas con la migración celular (ICAM o PECAM1 (P. J. Murray & Wynn, 2011)) y sus interacciones con las células epiteliales, indican la continua atracción de células inmunes hacia el endometrio, especialmente hacia el epitelio endometrial, incrementando su ambiente pro-

inflamatorio, que podría estar regulado mediante receptores de estrógeno y progesterona, cuya expresión se encuentra incrementada en las células del AS.

Un hallazgo importante relacionado con la comunicación celular radica en la importancia de las vías de señalización WNT y NOTCH. Estas vías han sido relacionadas con la regeneración endometrial mediante la expansión y el mantenimiento de la quiescencia en células madre (Boland et al., 2004; Ling et al., 2009). Las interacciones celulares mediante esta vía analizadas en pacientes de AS mostraron su desaparición en la comunicación entre epitelio y estroma, principalmente en el epitelio $SOX9^{+}$. Mientras que la pérdida de la comunicación mediante WNT7a podría limitar la renovación del epitelio $SOX9^{+}$, la ausencia de WNT5a afectaría a su expansión, disminuyendo la capacidad regenerativa del endometrio. Estas alteraciones, sumadas a la disminución observada en la señalización vía NOTCH, afectarían además al epitelio luminal y glandular, ya que el equilibrio WNT/NOTCH juega un papel fundamental en la diferenciación del epitelio (Garcia-Alonso et al., 2021).

Para abordar el impacto de la terapia celular desarrollada por nuestro grupo (basada en la administración de BMDSCs $CD133^{+}$) en la transcriptómica del tejido endometrial, analizamos mediante scRNA-seq 9 biopsias endometriales tomadas después de la terapia celular a los mismos pacientes analizados previamente. Este análisis mostró la reversión de algunas de las alteraciones observadas en la patología, mostrando una tendencia en el aumento de las poblaciones epiteliales, endoteliales y perivasculares, y una disminución significativa del epitelio-AS y algunas células inmunes (como los macrófagos). Estos cambios sugieren una recuperación hacia el estado definido en el endometrio sano, concordando con los resultados obtenidos en estudios previos, en los que se observó una recuperación en el grosor y el número de glándulas en modelos animales de AS sometidos a terapias con BMDSCs (Cervelló et al., 2015; Yuan et al., 2022). Basándonos en estudios previos, hipotetizamos que el mecanismo de acción de nuestra terapia puede estar basado en la secreción de factores paracrinos (como la trombospondina I o IGF1 (Cervelló et al., 2015)) y exosomas (X. Zhang et al., 2023) que induzcan una acción regeneradora de las células presentes en el endometrio, y/o mediante la diferenciación de las propias células $CD133^{+}$ en células endoteliales y perivasculares (Urbich & Dimmeler, 2004).

A pesar de la recuperación de ciertas poblaciones, no detectamos la presencia de células $SOX9^{+}$ tras la administración de la terapia con BMDSCS $CD133^{+}$, lo que sugiere que el efecto regenerativo de la terapia celular no consigue el restablecimiento de esta población. Esto puede significar que la terapia no restablece la capacidad regenerativa natural del endometrio, dando lugar a un efecto temporal que coincide con los resultados previos obtenidos en nuestro grupo (Santamaria et al., 2016), donde se recupera el estado patológico meses después de la aplicación de la terapia. Cabe destacar que si se alcanzó un estado similar al sano con respecto a la población epitelio-AS, puesto que ésta disminuyó significativamente tras la terapia. Este efecto podría desarrollarse por la secreción de citoquinas anti-inflamatorias tal y como se ha demostrado que hacen las células mesenquimales de la médula ósea (Salama et al., 2020), y apoya la utilización del marcador *SLPI* para el diagnóstico y el análisis del efecto de la terapia en las pacientes de AS.

La expresión diferencial tras la administración de nuestra terapia celular mostró diferencias notables. El epitelio incrementó la expresión de genes con función secretora y proliferativa, mientras que las células estromales mostraron la sobreexpresión de genes relacionados con estabilización de la matriz extracelular (*TPM1*) y la autofagia (*DIO2*). Estos resultados refuerzan la hipótesis de que las células BMDSCs pueden inducir la proliferación de un tejido dañado y mejorar la función endometrial (Fu et al., 2019; Mohsen et al., 2019), mediante la recuperación del epitelio y la reducción de la fibrosis, a la vez que lo que coincide con los resultados obtenidos en nuestro estudio previo (Santamaria et al., 2016), en el que las pacientes experimentaron un incremento del grosor endometrial tras la terapia, alcanzando en algunos casos el embarazo. Las células estromales también modificaron su perfil anti-angiogénico, modificando la expresión de *IGFBP3* por genes pro-angiogénicos como *PTN* e *IGFBP2*. Estos resultados muestran como la terapia celular promueve el desarrollo de capilares sanguíneos, aunque probablemente se trate de un efecto temporal, tal y como pudimos comprobar con la pérdida de la menstruación en pacientes de AS seis meses después de ser tratadas con nuestra terapia (Santamaria et al., 2016).

Adicionalmente, la terapia redujo la expresión de genes musculares (como *MYL9*) en SMC y células perivasculares, ocasionando la reducción del perfil muscular de estas

células y con ello la rigidez del tejido (X. Qin et al., 2024)). Con respecto a las células inmunes, la administración de las BMDSC CD133^{+} redujo la expresión de genes pro-inflamatorios (*S100A* o *MTRNR2L1)* o de atracción de células inmunes. A pesar de desconocer el mecanismo por el cual se produce esta reducción de la respuesta inflamatoria, probablemente se produzca mediante la secreción de citocinas anti-inflamatorias tal y como se ha descrito para las BMDSCs en tejidos como el pulmón (Su et al., 2019).

El análisis de la comunicación intercelular comparando el endometrio AS antes y después de la terapia celular mostró la recuperación de diferentes vías de señalización afectadas en la patología. La vía WNT se recuperó entre las células estromales y epiteliales, aunque con ligandos diferentes (WNT2 y WNT4) a los observados en donantes sanos. Esto puede implicar la expansión y renovación de células madre, pero posiblemente no la recuperación de las descritas células SOX9^{+}, posible causa de la recuperación temporal obtenida tras la terapia. La comunicación entre el estroma y el endotelio mediante el factor anti-angiogénico *ANGPTL1* se sustituyó por *ANGPTL2* (un promotor de la angiogénesis) habiéndose demostrado que este balance induce la regeneración vascular (Carbone et al., 2018), y se redujeron las interacciones que implicaban ligandos relacionados con la fibrosis (*ITGB2* and *FGF2*) (Tan et al., 2020). Estos cambios provocan la reducción de la fibrosis endometrial, transformando la matriz extracelular en un entorno más dinámico y con menor rigidez que posibilita la restructuración del epitelio, pero que continúa sintetizando fibras de la matriz extracelular mayores a las de un endometrio sano, una posible causa de la nueva formación de adhesiones intrauterinas tras la aplicación del tratamiento que observamos en nuestro estudio previo (Santamaria et al., 2016).

A pesar del progreso en la comprensión de la patología en el AS, la utilización de modelos animales y biopsias endometriales han limitado la investigación sobre esta enfermedad debido a sus limitaciones intrínsecas. Para solventar algunas de las limitaciones, desarrollamos por primera vez un modelo de cultivo de organoides en 3D a partir de biopsias de pacientes con AS (antes y después de la administración de la terapia celular) y controles sanos en la ventana de implantación. Este modelo, denominado organoides epiteliales endometriales (en inglés *Endometrial Epithelial Organoids,* EEOs), replica la

funcionalidad y estructura del epitelio (Clevers, 2016) y se ha utilizado ampliamente en el estudio del endometrio sano (Boretto et al., 2017; Garcia-Alonso et al., 2021) y en la modelización de enfermedades como la endometriosis (Boretto et al., 2019) o el cáncer endometrial (Katcher et al., 2023).

En nuestro estudio demostramos el desarrollo de EEOs de AS utilizando un protocolo descrito para muestras de donantes sanos (Boretto et al., 2017), para después establecer un estado similar a la ventana de implantación mediante tratamiento hormonal. Las evaluaciones inmunohistoquímicas revelaron que los EEO de AS consistían en células epiteliales diferenciadas y polarizadas, al igual que en los EEO de controles sanos, y que mostraban una capacidad de generación de organoides menor que los EEO control. Además, los EEO de AS mostraron diámetro y niveles de proliferación menores que los EEO control, sugiriendo un menor número de células madre adultas (o un deterioro en su funcionalidad) en el endometrio afectado por AS y una menor capacidad de crecimiento y división celular en las células de los EEOs de AS, lo que en conjunto demuestra la replicación de algunas de las características en el epitelio de esta patología.

Con el fin de caracterizar los EEOs de AS a nivel transcriptómico y comparar sus perfiles con el tejido *in vivo*, los organoides desarrollados antes y después del tratamiento (n=6) y donantes sanos (n=3) se analizaron mediante scRNA-seq. En este análisis identificamos poblaciones con perfiles asociados con células ciliadas, glandulares y glandulares secretoras (que expresan genes relacionados con la ventana de implantación). Además, detectamos varias poblaciones proliferativas, cada una distinguida por un perfil de expresión específico que incluye genes asociados con proliferación y matriz extracelular. Al comparar EEOs de AS antes de la terapia celular con EEOs control, encontramos un número menor de células ciliadas y una proporción de células glandulares secretoras inferior a las glandulares. Esta distribución de poblaciones coincide con los resultados observados en biopsias de pacientes, que muestran una disminución del epitelio ciliado y glandular secretor, con la mayoría de las células epiteliales en la población glandular. Entre las poblaciones de organoides no identificamos epitelio-AS, previamente descrito en muestras de tejido endometrial de pacientes, lo que podría atribuirse a un ambiente menos inflamatorio presente en las condiciones de cultivo celular en comparación con el endometrio afectado por AS.

Al realizar una comparativa entre las poblaciones detectadas en biopsias endometriales y las identificadas en EEOs, observamos que células glandulares de biopsia se asemejaban a los EEOs de AS, mientras que las glandulares secretoras se asemejan a los EEO control. Esto se puede deber a su perfil transcriptómico, ya que los organoides de pacientes presentan mayor expresión de genes inflamatorios y menor de genes relacionados con la receptividad endometrial, recapitulando las características de la enfermedad.

A pesar de que el modelo de cultivo solo representa la fracción epitelial del tejido, éste sirve como punto de partida para incrementar su complejidad, por ejemplo, incluyendo otros tipos celulares (Rawlings et al., 2021), lo que puede ser útil para estudiar las alteraciones en las interacciones entre las células que componen el endometrio.

Al comparar los EEOs obtenidos a partir de muestras de pacientes antes y después del tratamiento con células $CD133^+$, descubrimos que el efecto pro-regenerativo/reparador del tratamiento observado in vivo se reflejaba en las características de los organoides. Los EEOs de AS post-tratamiento presentaron una mayor tasa de crecimiento, mayor diámetro y mayor proliferación en comparación con los EEOs de AS pre-tratamiento, sugiriendo que los EEOs de AS reflejan el impacto de la administración de $CD133^+$ BMDSC *in vivo*, aumentando el valor de este modelo. Sin embargo, los valores recuperados tras la terapia no alcanzan los observados en los EEOs de muestras control, mostrando una recuperación parcial al igual que se describió en nuestro primer estudio (Santamaria et al., 2016). Además, el tratamiento modificó la composición celular de los EEOs de AS, incrementando el número de células ciliadas y proliferativas que expresaban genes asociados con EMT, mientras que el grupo glandular pasó a ser proporcionalmente menor que el grupo glandular secretor, lo que indica una mayor proliferación y diferenciación celular. La expresión de genes EMT puede representar un efecto secundario del uso de un inhibidor de la vía WNT durante el tratamiento hormonal de los EEOs (Kagawa et al., 2022; Yuan et al., 2022). Finalmente, el análisis de expresión génica reveló que los EEOs de AS post-tratamiento redujeron la expresión de genes de colágeno y respuesta inmune, junto con un aumento en los relacionados con la diferenciación celular, como efecto de la terapia celular.

Estos hallazgos muestran cómo nuestro modelo de organoides de AS respondió a la mejora de la enfermedad, recapitulando cambios observados en el tejido y postulándose como una herramienta valiosa para estudiar el AS y los mecanismos que regulan la regeneración epitelial endometrial en pacientes con esta patología tras la terapia celular. Este modelo también puede usarse para estudiar los efectos de diferentes terapias aplicadas directamente a los EEOs disminuyendo la necesidad de muestras de pacientes.

En resumen, nuestros resultados proporcionan una descripción detallada del estado celular del endometrio afectado por AS, creando un atlas que servirá como referencia para numerosos estudios futuros. Hemos demostrado el impacto de la terapia celular con BMDSCS CD133^{+} en los mecanismos patológicos del AS, lo que ha llevado a mejoras significativas, y nuestra caracterización de un nuevo modelo de cultivo de EEO para la enfermedad amplía las vías para investigar nuevas terapias o tratamientos combinados.

Conclusiones

1. Nuestro estudio a nivel de célula única del endometrio en pacientes con AS demuestra la existencia de 5 poblaciones celulares mayores, que incluyen 18 subpoblaciones definidas transcriptómicamente.
2. El endometrio en pacientes con AS presenta una disminución del epitelio glandular secretor y epitelio ciliado con respecto al endometrio sano. Además, la menor actividad secretora y la pérdida de la comunicación epitelio-estroma mediadas por las vías de señalización CDH1 y SPP1, puede afectar a la receptividad endometrial.
3. En el endometrio de pacientes con AS identificamos una nueva población celular epitelial (epitelio-AS), que expresa genes relacionados con estrés celular y respuesta inflamatoria. Esta población está asociada al AS y disminuye significativamente tras la terapia con células BMDSCs CD133^{+}, posibilitando la utilización del epitelio-AS como marcador diagnóstico y pronóstico mediante el marcador SLPI.
4. El endometrio en pacientes con AS carece de células epiteliales *SOX9*$^{+}$, que se caracterizan por ser una población de células progenitoras en el endometrio normal, probablemente por la pérdida de comunicación mediante WNT7a y

WNT5a. Esta podría ser una de las causas de la pérdida de regeneración endometrial en AS.

5. Esta patología endometrial induce un perfil pro-inflamatorio, caracterizado por el aumento de diferentes poblaciones inmunes que sobre expresan diversos genes inflamatorios como *NEAT1* y *S100A8/9/12*, citoquinas *CCL5/3* y *CC3L1*, y por la atracción de células inmunes mediante las vías de señalización ICAM, PECAM1 y VCAM.
6. Así mismo, la fibrosis endometrial en AS es debida a estímulos paracrinos de las de las vías pro-fibróticas FGF y PERIOSTIN en las células estromales, originando un incremento en la producción de colágeno y el incremento de las poblaciones contráctiles (células de músculo liso y perivasculares contráctiles), que provocan la expansión de la matriz extracelular e incrementan su rigidez.
7. El endometrio del AS muestra una alteración anti-angiogénica, caracterizada por la pérdida de vasculatura endometrial debido a la sobreexpresión de factores anti-angiogénicos como *IGFBP3 e IGFBP5* por parte de las células estromales, endoteliales y perivasculares.
8. La terapia celular, basada en la administración de BMDSCs $CD133^{+}$ autólogas, induce una recuperación parcial del perfil pro-inflamatorio, profibrótico y anti-angiogénico del endometrio de las pacientes con AS.
9. La terapia celular induce un aumento de la capacidad secretora endometrial y una disminución de la expresión de genes pro-inflamatorios. También provoca una disminución del perfil pro-fibrótico en el endometrio mediante la reducción de la expresión de genes como *MYL9*, *ITGB2*, o *TPM1* en el estroma y/o células contráctiles. Finalmente, induce la angiogénesis mediante la expresión de *PTN, IGFBP2*, *KLF2*, y la comunicación a través de la vía ANGPTL.
10. El desarrollo de organoides epiteliales endometriales a partir de biopsias endometriales de pacientes con AS replica parcialmente las características del epitelio, así como su recuperación parcial tras tratamiento mediante esta terapia celular, permitiendo su uso como *modelo in vitro* para el estudio del AS.

ABSTRACT

Asherman syndrome (AS) is an acquired endometrial pathology characterized by the presence of intrauterine adhesions. Endometrial injury within the *stratum basalis* frequently triggers the formation of fibrotic tissues, resulting in functional impairment as normal endometrial tissue becomes substituted by non-functional fibrotic tissue and adhesions within the uterine wall. The European Medicines Agency classifies AS, which has a prevalence of 4.4 cases per 10,000 people, as a rare iatrogenic condition that can cause pelvic/abdominal pain, alterations in menstruation, and, ultimately, infertility. Hysteroscopy represents the gold standard for AS diagnosis *and* treatment (through adhesion removal), which can restore fertility in certain patients but often encounters restricted long-term clinical outcomes. Poor outcomes are primarily due to the tendency for intrauterine adhesion recurrence, which may result in recurrent pregnancy loss, placental abnormalities, preterm birth, and lower birth weight. Alternative endometrial regeneration-promoting therapies based on stem cells have emerged in response to the limited number of treatment options. Some therapies have reached the clinical trial phase in AS patients, including an approach from our group that employs autologous $CD133^+$ bone marrow-derived stem cells (BMDSCs) to enhance endometrial thickness and improve reproductive function.

This doctoral thesis aims to investigate the cellular environment of the AS-affected endometrium in human patients by obtaining endometrial cell transcriptomic profiles and analyzing the potential therapeutic effect of our autologous cell therapy *in vitro* and *in vivo*, combining single-cell sequencing techniques and a three-dimensional organoid culture model.

We performed single-cell RNA sequencing (scRNA-seq) analyses on nine AS patients and six healthy donors (to which we added ten previously processed samples), covering the secretory phase and the window of implantation. Single-cell transcriptomics helped us to classify eighteen cell identities, which included epithelial, endothelial, stromal, immune, perivascular, and smooth muscle cells. These cell populations displayed significant differences when comparing AS and healthy controls, such as significant reductions in ciliated and glandular secretory epithelial subpopulations or the

disappearance of a potentially stem-cell-containing SOX9$^+$ cell population in the AS endometrium. Furthermore, the scRNA-seq analysis identified a disease-associated population – the AS-epithelium - exclusively present in AS samples. Consequently, we targeted the detection of this cell population using RNAscope via characteristic *SLPI* gene expression as a marker for AS pathology. We also encountered apparent differences in the transcriptomic profiles of cell populations between AS and healthy controls, including the downregulation of genes associated with secretory and receptive functions and the upregulation of genes related to proliferation and extracellular matrix (ECM) synthesis in the AS-affected endometrium. Likewise, we discovered impaired cell-to-cell communication (CCC) analysis associated with AS, featuring enriched pathways (e.g., COLLAGEN, FGF, or ICAM) that supported AS's pro-fibrotic and pro-inflammatory nature. Overall, this approach enabled the establishment of an endometrial "atlas" with cell population and gene expression changes associated with AS, which will serve as a reference for future studies.

To address the therapeutic impact of autologous CD133$^+$ BMDSC therapy, we analyzed endometrial biopsies from AS patients after administration via scRNA-seq. This approach demonstrated the reversal of particular disease-associated alterations observed in AS patients, such as an increase in epithelial populations and a significant decrease in the AS-epithelium (supporting the analysis of the AS-epithelium as a diagnostic marker) but without recovering SOX9$^+$ cells, suggesting that endometrial regeneration would not occur through the activity of this cell population. Differential expression analysis after CD133$^+$ BMDSC administration revealed the upregulated expression of angiogenic genes (*IGFBP2 and KLF2)* and genes related to secretory function and ECM stabilization (*TPM1)*, indicating a reversal of the pathological profiles and the development of new blood vessels. CCC analysis also highlighted restored CCC between the epithelium and stroma and reduced signaling pathway activity related to fibrosis (ITGB2 and FGF2) and inflammation (ICAM and LIGHT).

In the hope of addressing the inherent limitations of endometrial biopsies, we developed a three-dimensional epithelial organoid culture model derived from biopsies of AS patients. Beyond demonstrating the successful development of AS organoids, we assessed their ability to mimic specific disease patterns, such as restricted growth or

reduced proliferation. Overall, cells of the AS epithelial organoids resembled the cell population patterns seen previously in endometrial biopsies. While we did not detect the AS-epithelium, AS epithelial organoids derived from $CD133^+$ BMDSC-treated patient biopsies exhibited a healthy-like profile, highlighting the potential of this model for future research.

Altogether, our findings provide a comprehensive overview of the cellular state of the AS-affected endometrium, establish a reference atlas, and describe the therapeutic effect of autologous $CD133^+$ BMDSC therapy, which results in marked improvements in disease pathology. Developing a novel epithelial organoid culture model for the AS endometrium also opens new possibilities for exploring novel treatments or developing combination therapies.

INDEX

LIST OF FIGURES

LIST OF TABLES

LIST OF ANNEXES

ABBREVIATIONS

Ab	**A**nti**b**ody
AEMPS	***A**gencia **E**spañola de **M**edicamentos y **P**roductos **S**anitarios*
AF	**A**lexa **F**luor
AFS	**A**merican **F**ertility **S**ociety
ANOVA	**An**alysis **O**f **Va**riance
AS	**A**sherman **S**yndrome
ASC	**A**dult **S**tem **C**ell
BMDSC	**B**one **M**arrow-**D**erived **S**tem **C**ell
BMI	**B**ody **M**ass **I**ndex
BSA	**B**ovine **S**erun **A**lbumin
cAMP	**C**yclic **A**denosine **M**onophosphate
CCC	**C**ell-to-**C**ell **C**ommunication
cDNA	**C**omplementary **DNA**
CEPC	**C**irculating **E**ndothelial **P**rogenitor **C**ell
CO2	**C**arbon **D**ioxide
COMP	**C**ommittee for **O**rphan **M**edicinal **P**roducts
DA	**D**ifferential **A**bundance
DAPI	4',6'-**dia**midino-2-**p**henylindole
DC	**D**endritic **C**ell
DMEM	**D**ulbeco's **M**odified **E**agle **M**edium
DN	**D**ouble **N**egative
DNA	**D**eoxyribo**n**ucleic **A**cid
EC	**E**ndothelial **C**ell
ECM	**E**xtra**c**ellular **M**atrix
EEO	**E**ndometrial **E**pithelial **O**rganoid
EGF	**E**pidermal **G**rowth **F**actor
EMA	**E**uropean **M**edicines **A**gency
EMT	**E**pithelial-**M**esenchymal **T**ransition
Epi	**Epi**thelium
ERA	**E**ndometrial **R**eceptivity **A**nalysis
ESH	**E**uropean **S**ociety of **H**ysteroscopy
EU-CTR	**E**uropean **U**nion **C**linical **T**rials **R**egister
EV	Extracellular Vesicle
EVT	**E**xtra**v**illous **T**rophoblast
FACS	**F**luorescence-**A**ctivated **C**ell **S**orting
FBS	**F**etal **B**ovine **S**erum
FDA	**F**ood and **D**rug **A**dministration
FDR	**F**alse **D**iscovery **R**ate
FFPW	**F**ormalin-**f**ixed **P**araffin-**e**mbedded
FGF	**F**ibroblast **G**rowth **F**actor
G-CSF	**G**ranulocyte-**C**olony **S**timulating **F**actor
GEM	**G**el Beads-In-**Em**ulsion
H&E	**H**ematoxylin and **E**osin
H_2O	Di**h**ydrogen M**o**noxide
HRT	**H**ormone **R**eplacement **T**herapy
IMP	**I**nvestigational **M**edical **P**roduct

ITS	**I**nsulin-**T**ransferrin-**S**elenium
IUA	**I**ntra**u**terine **A**dhesion
MAD	**M**edian **A**bsolute **D**eviation
MAIT	**M**ucosal-**a**ssociated **I**nvariant **T**
MenSC	**Men**strual blood **S**tem **C**ell
MET	**M**esenchymal-**E**pithelial **T**ransition
MMP	**M**atrix **M**etallo**p**roteinase
MPA	**M**edroxi**p**rogesterone **A**cetate
mRNA	**M**esenger **RNA**
MSC	**M**esenchymal **S**tem **C**ell
NB-GLM	**N**egative **B**inomial **G**eneralized **L**inear **M**odel
NGS	**N**ext **G**eneration **S**equencing
NK	**N**atural **K**iller
OD	**O**rphan **D**rug
PANCK	**Pan**-**c**yto**k**eratin
PBS	**P**hosphate-**B**uffered **S**aline
PCA	**P**rincipal **C**omponent **A**nalysis
PFA	**P**ara**f**orm**a**ldehyde
PSC	**P**luripotent **S**tem **C**ell
PV	**P**eri**v**ascular
REec	***R**egistro **E**spañol de **E**studios **C**línicos*
RIF	**R**ecurrent **I**mplantation **F**ailure
RNA	**R**ibo**n**ucleic **A**cid
RNA-seq	**RNA seq**uencing
RT	**R**oom **T**emperature
scRNA-seq	**S**ingle **C**ell **RNA Seq**uencing
SD	**S**tandard **D**eviation
SMC	**S**mooth **M**uscle **C**ell
spRNA-seq	**Sp**atial **RNA seq**uencing
UC-MSC	**U**mbilical **C**ord-derived **M**esenchymal **S**tem **C**ell
UMAP	**U**niform **M**anifold **A**pproximation and **P**rojection
UMI	**U**nique **M**olecular **I**dentifier
uNK	**U**terine **N**atural **K**iller
WOI	**W**indow **O**f **I**mplantation
2D	Two-**D**imensional
3D	Three-**D**imensional

GENE/PROTEIN LIST

Feature	Full name	Feature	Full name
ACKR1	Atypical Chemokine Receptor 1	**Ki67**	Kiel 67
ACTA2	Actin Alpha 2	**KLF2**	Kruppel-Like Factor 2
ACTB	Actin-Beta	**KLRB1**	Killer Cell Lectin Like Receptor B1
ALCAM	Activated Leukocyte Cell Adhesion Molecule	**KLRG1**	Killer Cell Lectin Like Receptor G1
ANGPTL	Angiopoietin Like	**KRT17**	Keratin 17
ANXA1	Annexin A1	**KRT19**	Keratin 19
ANXA4	Annexin A4	**KRT5**	Keratin 5
ATF3	Activating Transcription Factor 3	**LAMA2**	Laminin Subunit Alpha 2
BMP2	Bone Morphogenetic Protein 2	**LAMB1**	Laminin Subunit Beta 1
BMP7	Bone Morphogenetic Protein 7	**LAMB3**	Laminin Subunit Beta 3
BSG	Basigin	**LCK**	Lymphocyte Cell-Specific Protein-Tyrosine Kinase
BTG2	BTG Anti-Proliferation Factor 2	**LEFTY2**	Left-right determination factor 2
CADM	Cell Adhesion Molecule	**LGALS1**	Galectin 1
cAMP	Cyclic Adenosine Monophosphate	**LGR5**	Leucine Rich Repeat Containing G Protein-Coupled Receptor 5
CAP1	Cyclase Associated Actin Cytoskeleton Regulatory Protein 1	**LH**	Luteinizing Hormone
CAPS	Calcyphosine	**LIF**	Leukemia Inhibitory Factor
CCL	C-C Motif Chemokine Ligand	**LIGHT**	Tumor Necrosis Factor Superfamily, Member 14
CCL11	C-C Motif Chemokine Ligand 11	**LMO4**	LIM Domain Only Protein 4
CCL2	C-C Motif Chemokine Ligand 2	**LRP6**	Low-Density Lipoprotein Receptor-Related Protein 6
CCL3	C-C Motif Chemokine Ligand 3	**LT**	Lymphotoxin Alpha
CCL3L1	C-C Motif Chemokine Ligand 3 Like 1	**LTB**	Lymphotoxin Beta
CCL5	C-C Motif Chemokine Ligand 5	**LUM**	Lumican Proteoglycan
CCR1	C-C Motif Chemokine Receptor 1	**LYZ**	Lysozyme
CD133	Prominin 1	**MALAT1**	Metastasis Associated Lung Adenocarcinoma Transcript 1
CD22	T-Cell Surface Antigen Leu-14	**MATN2**	Matrilin 2
CD226	CD226 Molecule	**MCAM**	Melanoma Cell Adhesion Molecule

CD3D	CD3 Delta Subunit Of T-Cell Receptor Complex	**MGP**	Matrix Gla Protein
CD44	Chondroitin Sulfate Proteoglycan 8	**MHC-I**	Major Histocompatibility Complex, Class I
CD52	Epididymal Secretory Protein E5	**MHC-II**	Major Histocompatibility Complex, Class II
CD6	T-Cell Differentiation Antigen CD6	**MIF**	Macrophage Migration Inhibitory Factor
CD74	Invariant Polypeptide of Major Histocompatibility Complex CD74	**MMP1**	Matrix Metallopeptidase 1
CD86	T-Lymphocyte Activation Antigen CD86	**MMP3**	Matrix Metallopeptidase 3
CDH1	Cadherin 1	**MMP7**	Matrix Metallopeptidase 7
CDHR3	Cadherin Related Family Member 3	**MMP9**	Matrix Metallopeptidase 9
CILP	Cartilage Intermediate Layer Protein	**MPIF-1**	Myeloid progenitor inhibitory factor
CKB	Creatine Kinase B	**MRAP2**	Melanocortin 2 Receptor Accessory Protein 2
CLDN4	Claudin 4	**MSLN**	Mesothelin
CNR1	Cannabinoid Receptor 1	**MSX2**	Msh Homeobox 2
COL1A1	Collagen Type I Alpha 1 Chain	**MT1E**	Metallothionein 1E
COL1A2	Collagen Type I Alpha 2 Chain	**MT1F**	Metallothionein 1F
COL3A1	Collagen Type III Alpha 1 Chain	**MT1G**	Metallothionein 1G
COL4A1	Collagen Type IV Alpha 1 Chain	**MT1H**	Metallothionein 1H
COL4A2	Collagen Type IV Alpha 2 Chain	**MT1M**	Metallothionein 1M
COL6A1	Collagen Type VI Alpha 1 Chain	**MT1X**	Metallothionein 1X
COL6A2	Collagen Type VI Alpha 2 Chain	**MT2A**	Metallothionein 2A
COL6A3	Collagen Type VI Alpha 3 Chain	**MT-ATP6**	Mitochondrially Encoded ATP Synthase Membrane Subunit 6
CRYAB	Crystallin Alpha B	**MT-ND2**	Mitochondrially Encoded NADH-Ubiquinone Oxidoreductase Core Subunit 2
CSF2	Colony Stimulating Factor 2	**MTRNR2L12**	Long non-coding RNA HN12
CSF2RA	Colony Stimulating Factor 2 Receptor Subunit Alpha	**MUC1**	Mucin 1
CSF2RB	Colony Stimulating Factor 2 Receptor Subunit Beta	**MUC5B**	Mucin 5B
CXC3	C-X-C Motif 3	**MYH11**	Myosin Heavy Chain 11
CXCL	C-X-C Motif Chemokine Ligand	**MYL9**	Myosin Light Chain 9

CXCL10	C-X-C Motif Chemokine Ligand 10	**MYL12A**	Myosin Light Chain 12A
CXCL12	C-X-C Motif Chemokine Ligand 12	**MYLK**	Myosin Light Chain Kinase
CXCL14	C-X-C Motif Chemokine Ligand 14	**NCAM**	Neural Cell Adhesion Molecule
CXCL8	C-X-C Motif Chemokine Ligand 8	**NEAT1**	Nuclear Paraspeckle Assembly Transcript 1
CXCR4	C-X-C Motif Chemokine Receptor 4	**NECTIN**	Nectin Cell Adhesion Molecule 1
CYP1B1	Cytochrome P450 Family 1 Subfamily B Member 1	**NF-κB**	Nuclear Factor Kappa-Light-Chain-Enhancer of Activated B Cells
DCN	Decorin	**NKG7**	Natural Killer Cell Granule Protein 7
DEFB1	Defensin Beta 1	**NOTCH**	Neurogenic Locus NTOCH Protein
DIO2	Iodothyronine Deiodinase 2	**NOTCH2**	Neurogenic Locus NTOCH Protein 2
DKK1	Dickkopf WNT Signaling Pathway Inhibitor 1	**NRG**	Neuregulin
DMKN	Dermokine	**NRG2**	Neuregulin 2
DPP4	Dipeptidyl Peptidase 4	**OLFM4**	Olfactomedin 4
E_2	Estradiol	**OVGP1**	Oviductal Glycoprotein 1
EGR	Early Growth Response	**P_4**	Progesterone
EMILIN1	Elastin Microfibril Interfacer 1	**PAGE4**	Prostate-Associated Gene Protein 4
EPCAM	Epithelial Cell Adhesion Molecule	**PAX8**	Paired Box 8
ERBB2	Erb-B2 Receptor Tyrosine Kinase 2	**PDGFRA**	Platelet Derived Growth Factor Receptor Alpha
ERBB3	Erb-B2 Receptor Tyrosine Kinase 3	**PDGFRB**	Platelet Derived Growth Factor Receptor Beta
ERα	Estrogen receptor α	**PECAM1**	Platelet And Endothelial Cell Adhesion Molecule 1
ERβ	Estrogen receptor β	**PECAM-1**	Platelet endothelial cell adhesion molecule
ESR1	Estrogen Receptor 1	**PEP**	Progesterone-associated protein
FAM183A	Cilia and Flagella Associated Protein 144	**PGR**	Progesterone receptor
FAU	Ubiquitin Like FUBI-Ribosomal Protein S30 Fusion	**PIFO**	Ciliary Microtubule Associated Protein 3
FGF	Fibroblast growth factor	**PLCG2**	Phospholipase C Gamma 2
FGF2	Fibroblast Growth Factor 2	**PP14**	Placental protein 14
FGF7	Fibroblast Growth Factor 7	**PRA**	Progesterone receptor A
FGF10	Fibroblast Growth Factor 10	**PRB**	Progesterone receptor B
FGFBP1	Fibroblast Growth Factor Binding Protein 1	**PRF1**	Perforin 1
FGFR1	Fibroblast Growth Factor Receptor 1	**PRL**	Prolactin
FN1	Fibronectin 1	**PTGS1**	Prostaglandin-Endoperoxide Synthase 1

FOS	Proto-Oncogene C-Fos	**PTN**	Pleiotrophin
FOSB	Proto-Oncogene FosB	**PTPRM**	Protein Tyrosine Phosphatase Receptor Type M
FOXA2	Forkhead Box A2	**RETN**	Resistin
FOXJ1	Forkhead Box J1	**RGS5**	G protein signaling 5
FOXO1	Forkhead Box O1	**RhoA**	Ras Homolog Family Member A
FSH	Follicle Stimulation Hormone	**ROCK1**	Rho Associated Coiled-Coil Containing Protein Kinase 1
FZD4	Frizzled Class Receptor 4	**RPL31**	Ribosomal Protein L31
FZD5	Frizzled Class Receptor 5	**RPL37A**	Ribosomal Protein L37a
GADD45B	Growth Arrest and DNA Damage Inducible Beta	**S100A10**	S100 Calcium Binding Protein A10
GDF	Growth Differentiation Factor	**S100A11**	S100 Calcium Binding Protein A11
GDF15	Growth Differentiation Factor 15	**S100A12**	S100 Calcium Binding Protein A12
GM-CSF	Granulocyte-Macrophage Colony-Stimulating Factor	**S100A4**	S100 Calcium Binding Protein A4
GNLY	Granulysin	**S100A6**	S100 Calcium Binding Protein A6
GnRH	Gonadotropin-Releasing Hormone	**S100A8**	S100 Calcium Binding Protein A8
GOS2	G0/G1 Switch 2	**S100A9**	S100 Calcium Binding Protein A9
GPX3	Glutathione Peroxidase 3	**SCGB1D2**	Secretoglobin Family 1D Member 2
GZMH	Granzyme H	**SCGB2A1**	Secretoglobin Family 2A Member 1
HAP1	Huntingtin Associated Protein 1	**SCGB2A2**	Secretoglobin Family 2A Member 2
hCG	Human Chorionic Gonadotropin	**SELPLG**	Selectin P Ligand
HLA-DPA2	Major Histocompatibility Complex, Class II, DP Alpha 2	**SEMA6**	Semaphorin 6
HLA-DPB1	Major Histocompatibility Complex, Class II, DP Beta 1	**SERPINF1**	Serpin Family F Member 1
HLA-DRA	Major Histocompatibility Complex, Class II, DR Alpha	**SERPING1**	Serpin Family G Member 1
HLA-DRB1	Major Histocompatibility Complex, Class II, DR Beta 1	**SFRP1**	Secreted Frizzled Related Protein 1
HLA-DRB5	Major Histocompatibility Complex, Class II, DR Beta 5	**SLC18A2**	Solute Carrier Family 18 Member A2
HMGB2	High Mobility Group Box 2	**SLF2**	SMC5-SMC6 Complex Localization Factor 2
HSPA1A	Heat Shock Protein Family A (Hsp70) Member 1A	**SLPI**	Secretory Leukocyte Peptidase Inhibitor
HSPA1B	Heat Shock Protein Family A Member 1B	**SMAD9**	Mother Against Decapentaplegic Homolog 9
HSPH1	Heat Shock Protein Family H (Hsp110) Member 1	**SNHG9**	Small Nucleolar RNA Host Gene 9
ICAM	Intercellular Adhesion Molecule	**SOCS3**	Suppressor Of Cytokine Signaling 3

ICOS	Inducible T Cell Costimulator	**SOD2**	Superoxide Dismutase 2
IER3	Immediate Early Response 3	**SOX4**	SRY-Box Transcription Factor 4
IFNG	Interferon Gamma	**SOX9**	SRY-Box Transcription Factor 9
IGF	Insulin Like growth factor	**SPARCL1**	SPARC Like 1
IGF1	Insulin Like Growth Factor 1	**SPP1**	Secreted Phosphoprotein 1
IGF2	Insulin Like Growth Factor 2	**STAT3**	Signal Transducer and Activator of Transcription 3
IGFBP1	Insulin Like Growth Factor Binding Protein 1	**STEAP4**	Six-Transmembrane Epithelial Antigen of Prostate 4
IGFBP2	Insulin Like Growth Factor Binding Protein 2	**SUSD2**	Sushi Domain Containing 2
IGFBP3	Insulin Like Growth Factor Binding Protein 3	**SYNE2**	Spectrin Repeat Containing Nuclear Envelope Protein 2
IGFBP5	Insulin Like Growth Factor Binding Protein 5	**TAGLN**	Transgelin
IGFBP7	Insulin Like Growth Factor Binding Protein 7	**TCR**	Invariant αβ T Cell Receptor
IHH	Indian Hedgehog	**TFF1**	Trefoil Factor 1
IL10	Interleukin 10	**TFPI2**	Tissue Factor Pathway Inhibitor 2
IL11	Interleukin 11	**TGFBR2**	Transforming Growth Factor Beta Receptor 2
IL15	Interleukin 15	**TGF-β**	Transforming growth factor-beta
IL1β	Interleukin 1-beta	**THR**	Thyrotropin-releasing hormone
IL23R	Interleukin 23 Receptor	**THY1**	Thy-1 Cell Surface Antigen
IL32	Interleukin 32	**TIGIT**	T Cell Immunoreceptor with Ig And ITIM Domains
IL4	Interleukin 4	**TLR4**	Toll Like Receptor 4
IL4I1	Interleukin 4 Induced 1	**TMC5**	Transmembrane Channel Like 5
IL6	Interleukin 6	**TMEM101**	Transmembrane Protein 101
IL6R	Interleukin 6 Receptor	**TMSB10**	Thymosin Beta 10
IL6ST	Interleukin 6 Cytokine Family Signal Transducer	**TMSB4X**	Thymosin Beta 4 X-Linked
IL7R	Interleukin 7 Receptor	**TNF**	Tumor necrosis factor
ISG15	Ubiquitin Like Protein ISG15	**TOP2A**	DNA Topoisomerase II Alpha
ITGA1	Integrin Subunit Alpha 1	**TPM1**	Tropomyosin 1
ITGA2	Integrin Subunit Alpha 2	**TPP3**	Tubulin Polymerization Promoting Protein
ITGA5	Integrin Subunit Alpha 5	**TRBC2**	T Cell Receptor Beta Constant 2
ITGAV	Integrin Subunit Alpha V	**TWEAK**	Tumor Necrosis Factor Member 12
ITGB1	Integrin Subunit Beta 1	**VCAM**	Vascular Cell Adhesion Molecule
ITGB2	Integrin Subunit Beta 2	**VEGF**	Vascular endothelial growth factor
ITGB8	Integrin Subunit Beta 8	**WFDC2**	WAP Four-Disulfide Core Domain 2
IκB	NF-κB primary inhibitor	**WNT**	Wingless-Related Integration Site
JAK	Janus Kinase	**WNT2**	Wnt Family Member 2

JAM	Junctional Adhesion Molecule	**WNT4**	Wnt Family Member 4
JUN	Transcription Factor AP-1 Subunit Jun	**WNT5A**	Wnt Family Member 5A
JUNB	Transcription Factor AP-1 Subunit JunB	**WNT7A**	Wnt Family Member 7A
JUND	Transcription Factor AP-1 Subunit JunD	**ZCCHC12**	Zinc Finger CCHC-Type Containing 12
KCNQ1OT1	KCNQ1 Opposite Strand/Antisense Transcript 1	**ZFYVE21**	Zinc finger FYVE-type containing 21

I. Introduction

I. Introduction

1. The uterus

1.1. Definition, morphogenesis, and structure

The uterus is a hollow and muscular organ that harbors the embryo, initiating and maintaining its development during pregnancy. From an anatomical perspective, the uterus presents an inverted pear shape, transversely expanded and ventrodorsally flattened. The uterus is located within the female pelvic cavity, positioned anterior to the bladder and posterior to the rectum, with which it shares two convex surfaces. Following a caudal to cranial direction, we encounter three primary anatomical regions: the cervix (connected with the vagina), the body (separated from the cervix by a short isthmus, which presents as an enlargement of the uterine cavity), and the fundus (above the entrances of the fallopian tubes in the uterine horns that, together with the body, represent two-thirds of the uterus) (Vaamonde et al., 2016) (**Figure 1**).

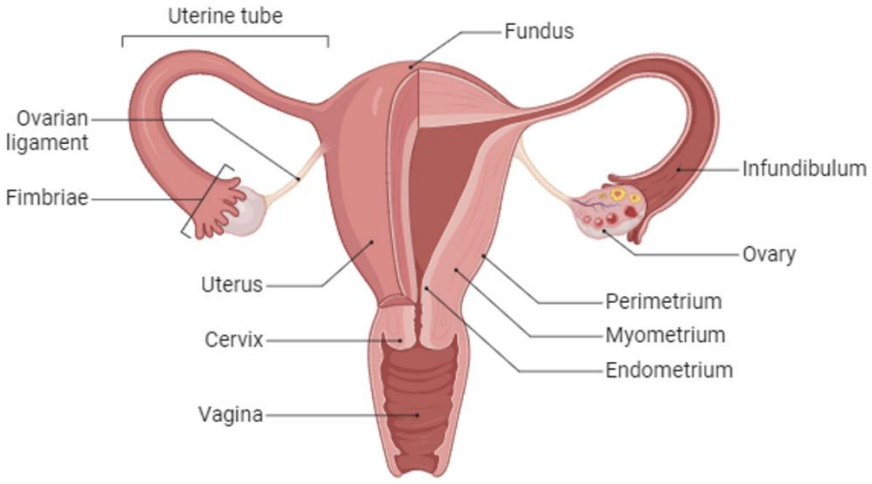

Figure 1. Illustrative diagram depicting the anatomy of the human uterus.

The uterus plays a crucial role in providing security and nourishment for the human embryo as it matures and, eventually, in expelling the fetus from the female body when fully developed at parturition. Uterine morphogenesis occurs from the mesoderm layer

around the tenth week of fetal development when it grows from the fusion of the two Müllerian (paramesonephric) ducts (Habiba et al., 2021). At 14-15 weeks of gestation, uterine glands appear, and the body divides into two primordial layers: the endometrium (that will be lined by columnar epithelium and present elongated and branched glands between 20-26 weeks of gestation) (de Jolinière et al., 2012; Robboy et al., 2017) and the myometrium (appears to originate from the mesenchymal cells that surround the primitive endometrium and will present immature smooth muscle like-cells around the eighteenth week) (Habiba et al., 2021). Significant changes occur after birth, with the uterus experiencing the gradual maturation process around menarche and into adolescence needed to acquire the capability to accommodate the tissue remodeling processes that take place during deep placentation (I. Brosens et al., 2019). Therefore, uterine volume increases considerably from the onset of puberty until the second decade (Habiba et al., 2021), which is determined by biological and sociodemographic factors (I. Brosens et al., 2017).

The developed uterine wall becomes structured into three layers: the endometrium, the myometrium, and the perimetrium (**Figure 1**). The endometrium forms the internal mucosal layer of the uterine cavity. The innermost part of the endometrium is formed by the *stratum basale* layer (contiguous to the myometrium), which is not shed during menstruation and functions to renew the outermost *stratum functionalis* layer, which contains most of the glandular tissue and becomes discarded during menstruation. The *stratum functionalis* supports the implantation and maintenance of the fertilized oocyte in the case of pregnancy; otherwise, this layer undergoes regeneration during menstruation (Critchley et al., 2020). The myometrium comprises a layer of smooth muscle with a thickness of 12-15 mm in a non-pregnant state; however, this layer undergoes substantial thickening during pregnancy (Vaamonde et al., 2016). The myometrium houses the main blood vessels and nerves that nourish the uterus and functions to deliver the fetus through contractions, thanks to the longitudinal orientation of its fibrillar bundles (Wray & Prendergast, 2019). The perimetrium represents a serosal layer that envelops the uterine body and fundus and sits atop a slender layer of

connective tissue. This outer covering seamlessly connects with the mesothelium in the region associated with the bladder and rectum (Vaamonde et al., 2016).

1.2. Menstrual cycle

The period of reproductive functionality in the human female is marked by the menstrual cycle in the uterine endometrium, which is governed by the ovarian cycle. Both cycles exhibit a high level of coordination through mutual interaction and are controlled by endocrine, autocrine, and paracrine factors. The average duration of the reproductive lifespan in women is 36 years, starting from menarche (between 8.5 to 13 years) and ending with menopause (around 51 years). The standard reproductive years are defined by monthly, cyclical fluctuations in the secretion of sex hormones, along with corresponding changes in the ovaries and endometrium (Mihm et al., 2011).

The ovarian cycle generally ranges from 21-35 days and is driven by the secretion of the Gonadotropin-releasing hormone (GnRH) in the hypothalamus, which induces pituitary gland cells to produce luteinizing hormone (LH) and follicle stimulation hormone (FSH). In turn, LH and FSH stimulate granulosa cells, which produce estradiol (E_2), and theca cells, which produce progesterone (P_4) and androgens (Vaamonde et al., 2016). The whole cycle comprises two phases separated by ovulation: the follicular and luteal phases (**Figure 2**). The follicular phase covers menses to ovulation, during which time the developing group of follicles (under the influence of increasing levels of FSH) undergo rapid mitosis and initiate E_2 production. Although increased E_2 initially has a negative effect on the initiating pulse, higher levels of E_2 overcome this effect and induce a positive effect on GnRH, LH, and FSH production. At this point, high levels of LH induce P_4 synthesis, initiating a hormone pulse that will predominate in the next phase. These episodes result in the formation of a mature ovum, primed for fertilization, and the enlargement and bursting of the Graafian follicle, enabling the release of the ovum. After ovulation, the remaining granulosa and theca cells form the corpus luteum, which produces both E_2 and P_4. In this second phase (the luteal phase), the corpus luteum becomes sustained by LH levels, with the synthesis of LH and FSH restrained by E_2 and P_4 concentrations. If an embryo is not formed and implanted, reduced LH concentrations

initiate degeneration of the corpus luteum, leading to a decline in P_4 and E_2 levels. This mechanism, in turn, prompts a fresh surge in FSH and LH, restarting the cycle by stimulating the development of a new cohort of follicles (Messinis et al., 2014; Richards, 2018).

The endometrial cycle encompasses the entirety of the changes the endometrium undergoes during the menstrual cycle and is affected by the same sex hormone pulses (E_2 and P_4) as observed in the ovarian cycle (**Figure 2**). Overall, these hormones are pivotal in coordinating the two cycles, ensuring reproductive functionality. The endometrial cycle is divided into two phases separated by ovulation: the proliferative phase and the secretory phase. In the proliferative phase, covering the end of menses to ovulation (around day 14), the endometrium reacts to elevated E_2 levels by promoting the thickening of the *stratum functionalis* through increasing cell proliferation. This layer experiences significant growth mainly by the gradual extension of the glands, which become convoluted within the mesenchyme, and vascular network development for blood supply to both *strata* to renew the endometrium (Henriet et al., 2012). In the secretory phase, which starts after ovulation, the *stratum functionalis* undergoes differentiation under the influence of P_4 (which also inhibits endometrial growth) produced by the corpus luteum. The morphological changes that affect the endometrium during this phase involve several cell types (discussed in more depth in upcoming sections) and result in the preparation of the tissue for embryo implantation. The corpus luteum ceases E_2 and P_4 production if implantation does not occur. This withdrawal of this hormone, added to the absence of human chorionic gonadotropin (hCG) secretion, leads to artery constriction, causing the shedding of the *stratum functionalis* and initiating menstrual bleeding (Henriet et al., 2012; Mihm et al., 2011).

Although the uterus requires all components for optimal functionality, this physiological complexity makes a comprehensive approach difficult; therefore, we will focus on the endometrium, providing a background to fully understand the work carried out in this thesis.

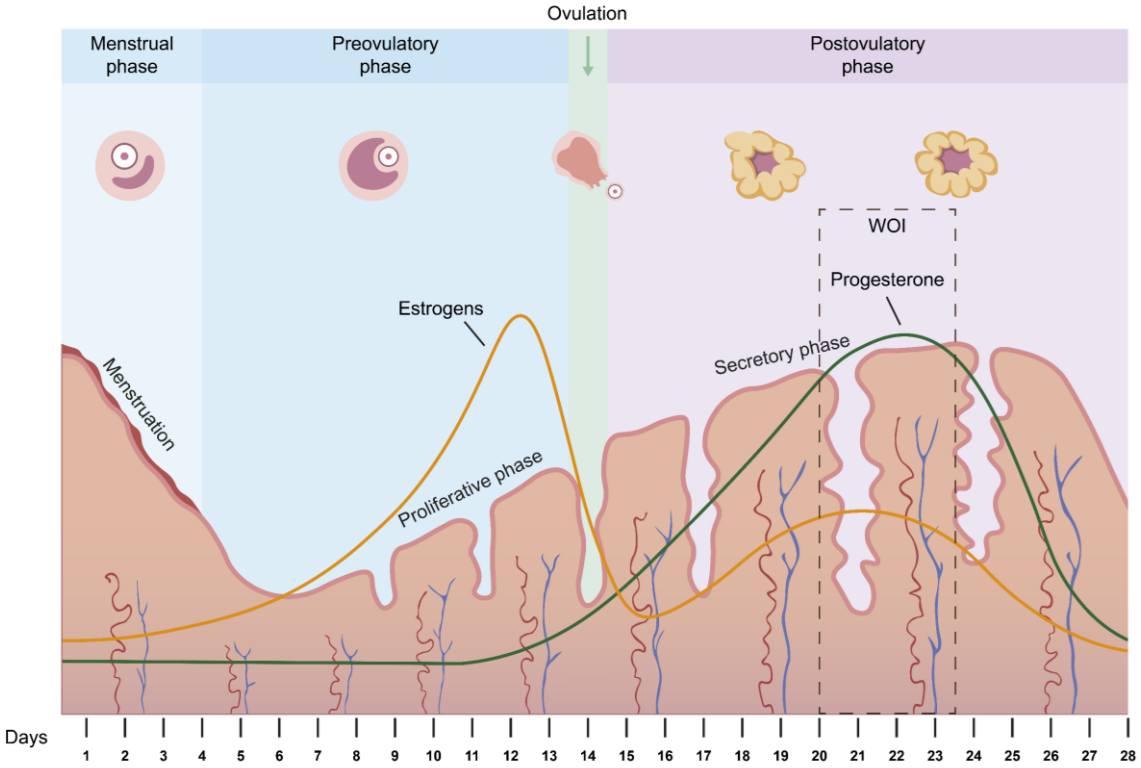

Figure 2. The human menstrual cycle. Estradiol exerts primary hormonal influence on the endometrium and the ovary throughout the proliferative and follicular phases. The secretory and luteal phases occur after ovulation, when progesterone has the most significant impact. The yellow line represents estrogen and the green line progesterone levels across the menstrual cycle. Abbreviations - WOI (window of implantation).

2. Architecture and physiology of the endometrium

2.1. Endometrial structure

The intricate interaction between circulating ovarian steroid hormones and their corresponding receptors involves multiple endometrial cell types that undergo significant alterations during the menstrual cycle. Considering this heterogeneous composition, we must acknowledge and identify each cellular element. The classic histological classification of endometrial cell types has described epithelial, stromal, immune, and endothelial cells (Makieva et al., 2018) (**Figure 3**).

The endometrial epithelium comprises a single layer of polarized cube-shaped cells that line the interior of the uterine cavity, comprising both a luminal and a glandular

component. Like other mucous membranes, this monolayer protects against pathogens entering the endometrial cavity and regulates embryo implantation (Moreno et al., 2023). The primary crucial role of the endometrial epithelium involves regulating the attachment of the embryo to the stroma and blood vessels within the endometrium, serving as the initial mediator in the interaction between the embryo and the maternal endometrium (Dominguez et al., 2005). The luminal epithelium represents the initial point of contact for an implanting embryo and acts as the temporary stay for embryo implantation and successful embryo development within the uterus. The glandular epithelium contains the endometrial glands responsible for producing and releasing essential molecules that nourish the blastocyst and facilitate implantation (Ye, 2020).

The endometrial stroma, lined by the epithelium and connected with the myometrium, comprises connective tissue consisting of cells and an extracellular matrix (ECM). This layer mainly hosts the fibroblast-like stromal cells essential to modifying the ECM during the menstrual cycle. In addition, the endometrial stroma includes a variety of tubular glands continuous with the luminal surface and spiral arteries and a changing influx of recruited innate immune cells (Noyes et al., 1975). The epithelium and most of the stroma form part of the *stratum functionalis*, which regenerates every menstrual cycle. The remaining stromal components form part of the *stratum basale* and retain a plexus network of endometrial glands, with a horizontally expanding structure of the basal glands (Yamaguchi et al., 2021).

The uterus's intricate vascular structure, mainly composed of endothelial cells, originates in the myometrium. The uterine arteries form arcuate arteries, which, in turn, give rise to radial arteries. The radial arteries traverse through the thickness of the endometrium, eventually reaching the juncture between the endometrium and myometrium, where they transform into basal arteries, which create an anastomotic network from which spiral arteries emerge. These terminal spiral arteries function to maintain the basal layer. The division and branching of the spiral arteries primarily occur in the *stratum functionalis* (Simón, 2009).

Immune cells present in the endometrium play a crucial role in its physiology. Their primary function involves regulating the local immune response to safeguard the genital tract from infections and prevent immune rejection during embryo implantation. In the normal endometrium, the leukocyte population typically accounts for around 10-15% of the stromal cell composition, although this percentage can vary depending on the menstrual cycle phase (Simón, 2009). The immune cell population primarily comprises uterine natural killer cells (uNK) concentrated near the endometrial glands, which regulate trophoblast invasion and spiral artery remodeling. Additionally, T lymphocytes play roles in immunosuppression and promote the growth of placental cells, B lymphocytes, macrophages, and monocytes, which present antigens to T lymphocytes and activate immune responses. T lymphocytes originate from the in-situ proliferation of resident immune cells, recruitment of hematopoietic precursors that differentiate within the endometrium, or circulation through the bloodstream (Lee et al., 2015).

As previously reviewed by Gargett and Masuda, substantial evidence supports the existence of an adult stem cell population within the endometrium (Gargett & Masuda, 2010). This population - commonly named endometrial progenitor cells - would primarily be found in the *stratum basale* (Santamaria, Mas, et al., 2018) and has the potential to differentiate into epithelial and stromal cells. Therefore, putative endometrial progenitor cells may play a crucial role in efficiently replenishing and maintaining the endometrium, which is necessary for restoring endometrial integrity during menstruation.

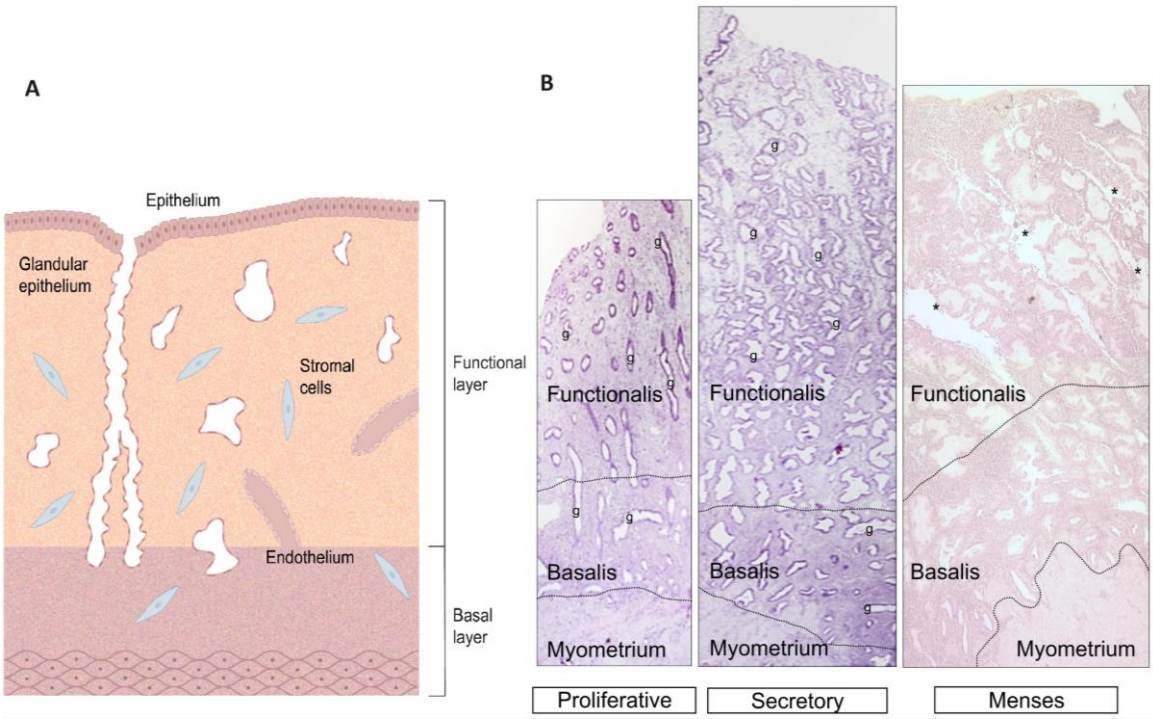

*Figure 3. Structure of human endometrium during menstrual cycle. A) Scheme of the functional layers of the endometrium and its main cell types. B) Hematoxylin and eosin-stained histological sections of pre-menopausal human endometrium during the proliferative, secretory, and menses stages, showing functional, basal, and myometrial layers. *Endometrial tissue breaks down early in the menstrual stage. g indicates glands. Dotted lines limit the different endometrial layers. Figure 1b from Oxford University Press* (Nguyen et al., 2012).

2.2. The endometrium during menstrual cycle

Connecting the above-described information regarding the endometrial structure and the menstrual cycle defines the endometrium as a sophisticated, multicellular, and steroid-sensitive tissue that undergoes monthly shedding in the absence of pregnancy. Communication with the endocrine and immune systems remains crucial for adequate tissue dynamism, ensuring efficient endometrial shedding and injured tissue repair (Critchley et al., 2020). Hence, the morphological and physiological changes in the endometrium mainly depend on the cyclic secretion of estrogens and P_4 by the ovaries.

2.2.1. Steroids and receptors

Steroid hormones act on the epithelium, stroma, and endothelium of the endometrium via specific receptors, which immunohistochemical techniques can detect. The primary receptors include the estrogen receptors alpha (ERα) and beta (ERβ), which are transcription factors found in the nuclei of glandular, stromal, and endothelial cells during the estrogen-dominant proliferative phase (**Figure 4**). The ERs promote the proliferation of these three types of cells, but their activity then decreases through the P_4-dominant secretory phase (Critchley et al., 2002; Ruiz-Alonso et al., 2012). Additionally, two progesterone receptor variants (PRA and PRB) also locate to the nuclei of stromal and epithelial cells during the proliferative phase. In this case, PRs influence the differentiation of endometrial cells, with PRA as the predominant isoform during the secretory phase, which supports the responsiveness of stromal cells to P_4 through the secretory phase (Moreno et al., 2023).

Conversely, PRs persist throughout the menstrual cycle in the *stratum basale* (Lessey et al., 1988; Snijders et al., 1992). P_4 and estrogens influence the abundance of their receptors by regulating receptor presence during both cycle phases (Bergeron, 2006). In addition, substantial evidence indicates that locally produced steroids (e.g., estrogens, androgens, and glucocorticoids) have significant roles in regulating endometrial function. Receptors to these steroids occur at differing levels in endometrial cells throughout the menstrual cycle and relate to cell proliferation and the control of inflammation or angiogenesis (Critchley et al., 2020).

2.2.2. Proliferative phase

The proliferative phase (which lasts until the 14th day) involves a notable increase in the proliferation of stromal tissue, glands, and blood vessels, resulting in the expansion of the volume of the endometrial mucosal. An elevated number of cell divisions and the elevated synthesis of DNA and RNA also occur during this phase, with these changes more pronounced in the *stratum functionalis*. The initially straight and perpendicular glands observed at the start of the proliferative phase undergo significant transformation, becoming more substantial and winding in their structure, surrounded

by a pseudostratified epithelium comprised of cylindrical cells with oval nuclei (Dabbs et al., 1986; Wynn, 1989). The glandular plexus architecture within the *stratum basale* remains intact throughout the menstrual cycle, with the occluded glands exhibiting a more significant volume during the secretory phase than the proliferative phase. As these occluded glands cannot release their secretions into the uterine cavity, they accumulate and thicken within the glands, ultimately causing cystic expansion of the glands (Yamaguchi et al., 2021). Simultaneously, the endometrial epithelium exhibits positive staining for both cytokeratin and vimentin (**Figure 4**), which are two varieties of intermediate filaments present in endometrial mesenchymal and/or epithelial cells commonly used as markers in determining cell types and the classification/prognosis of endometrial cancer (Lien et al., 2023; Vasilevska et al., 2022). The stromal tissue primarily comprises vimentin-positive/cytokeratin-negative undifferentiated cells, with the additional presence of lymphoid aggregates (Bergeron, 2006; Dabbs et al., 1986).

2.2.3. Secretory phase

During the secretory phase (which runs until the 28th day), P_4 levels inhibit endometrial growth and instead promote stromal and glandular cell differentiation by inhibiting the production of ERs (Mihm et al., 2011). P_4 promotes the conversion of E_2 into estrone via the activity of 17β-hydroxysteroid dehydrogenase, a form with low affinity for ERs (Bergeron, 2006). Structural alterations that occur during this phase include the appearance of pinopodia, small cytoplasmic projections situated on the apical surface of epithelial cells, which indicates the ability of the superficial endometrial epithelium to accept a blastocyst (Nikas & Psychoyos, 1997). Additional protein components secreted during this phase in the epithelium include endometrial progesterone-associated protein (PEP) (Joshi, 1987), leukemia inhibitory factor (LIF, related to cytotrophoblast to syncytiotrophoblast differentiation) (Stewart et al., 1992), insulin-like growth factor type 2 (IGF-2), glycodelin, placental protein 14 (PP14, which has immunosuppressive properties) (Waites et al., 1988), integrins, and mucin 1 (MUC1) (Aplin et al., 1996) (**Figure 4**). Furthermore, the cell polarity of epithelial cells becomes disrupted due to reduced levels of adhesion molecule E-cadherin on the cell surface, the inhibition of

MUC1, and the emergence of apical pinopodes. Overall, this transition - involving alterations to tissue function and structure in the receptive epithelium - facilitates blastocyst adhesion (Moreno et al., 2023).

During the secretory phase, stromal cells undergo significant alterations in a process known as decidualization, which comprises the progression that stromal cells suffer to its secretory variant, decidual cells, which comprise substantial morphological and secretory changes.

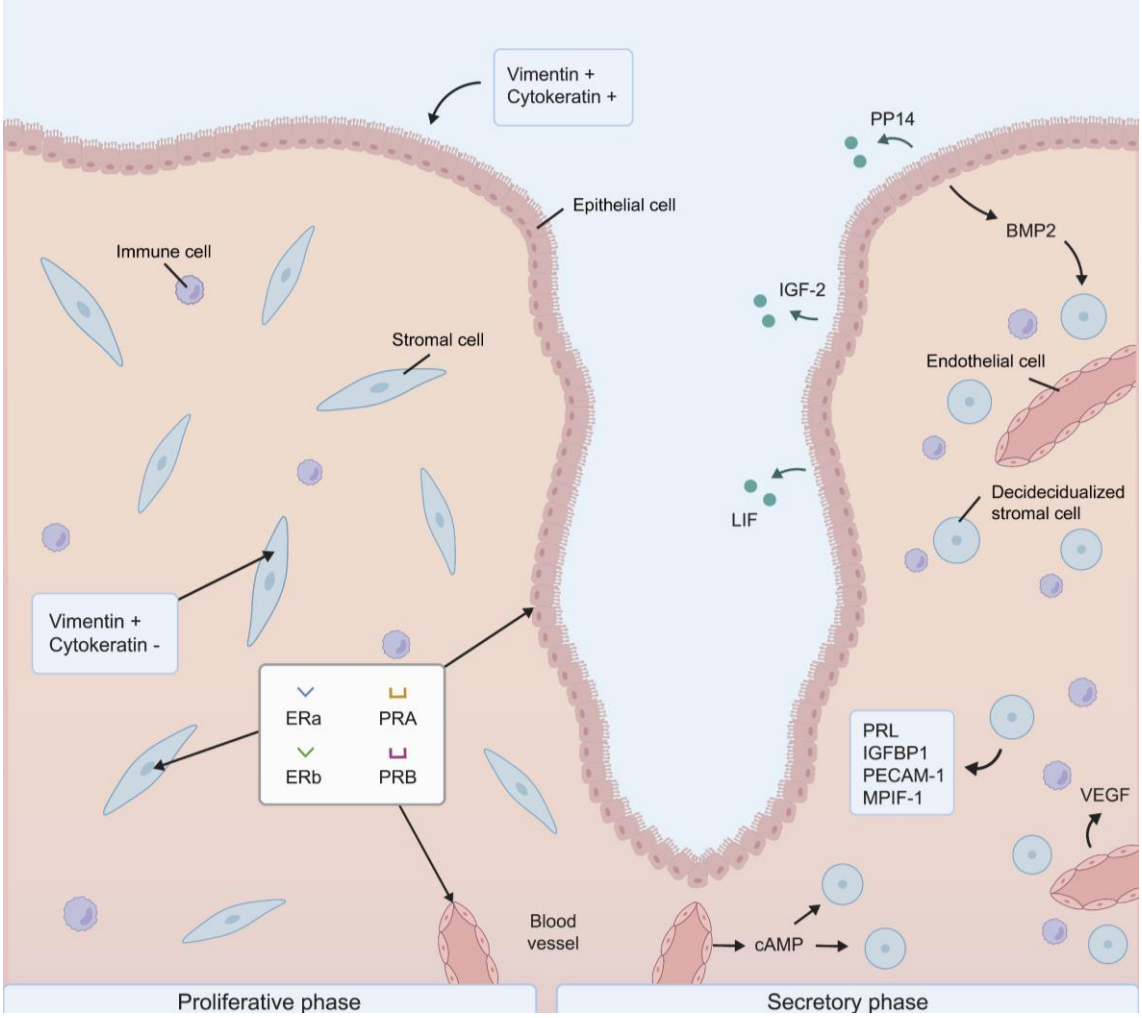

Figure 4. Schematic representation of the changes occurring and factors involved during the passage of the endometrium through the proliferative and secretory phases. Blue cells represent the stroma, red cells represent the epithelium, purple cells represent immune cells, and pink cells surrounding the blood vessels are the endothelial cells. Abbreviations - BMP2 (bone morphogenetic protein 2), cAMP (cyclic adenosine monophosphate), ERa (estrogen receptor a), ERb (estrogen receptor b), IGFBP1 (insulin growth factor 1), IGF-2 (insulin-like growth factor 2), LIF (leukemia inhibitory factor), MPIF-1 (myeloid progenitor inhibitory factor 1), PECAM-1 (platelet endothelial cell adhesion molecule), PP14 (placental protein 14), PRA (progesterone receptor A), PRB (progesterone receptor B), PRL (prolactin). Adapted from Moreno et al. 2023.

2.2.3.1. Decidualization

During decidualization, stromal cells create a nurturing and receptive cellular microenvironment crucial for embryo implantation and subsequent placental development. A successful pregnancy requires proper decidualization, as this process remains pivotal in controlling the effective implantation of the conceptus (Gellersen & Brosens, 2014). Hormonal, biochemical, and immunological factors collaborate to fine-tune endometrial changes for this purpose (**Table 1**). In addition to P_4, acting as the primary regulator thanks to the high expression of PRA in endometrial cells, additional biochemical factors influence the regulation of decidualization. Said factors include hCG, which induces the secretion of the corticotropin-releasing hormone and relaxin, and cyclic adenosine monophosphate (cAMP), which induces decidualization and maintains implantation (Moreno et al., 2023).

Table 1: Main factors in the regulation of decidualization

Decidualization regulators	**Type**	**Reference**
Progesterone (P_4)	Hormonal	Kastner et al., 1990
Estradiol (E_2)	Hormonal	Pawar et al., 2015
hCG	Hormonal	Einspanier et al., 2009; Palejwala et al., 2002
cAMP	Biochemical factor	
BMP2	Biochemical factor	Li et al., 2007
TGF-β	Biochemical factor	Kim et al., 2005
IL-1β	Immunological factor	Christian et al., 2001; Cullinan et al., 1996; Salamonsen et al., 2000; Tamura et al., 2002
LIF	Immunological factor	
IL-11	Immunological factor	
IL-10	Immunological factor	Robertson et al., 1994
LEFTY2	Immunological factor	Tang et al., 2010
Lysophosphatidic acid	Lipid mediator	Aikawa et al., 2017

Morphological shifts in decidualization begin with cAMP generation by perivascular endometrial stromal cells; later, the influence of cAMP spreads to impact the entire stroma (J. J. Brosens et al., 1999). The most critical alterations involve the transformation of elongated, fibroblast-like cells into an extended population of polygonal/round cells accompanied by ultrastructural modifications facilitated by complex cytoskeletal reorganization (McKay et al., 1992). Decidualized cells release signaling molecules such as prolactin (PRL) and insulin-like growth factor binding protein 1 (IGFBP1), serving as indicators of extravillous trophoblast (EVT) invasion and representing established markers of decidualization (Irwin et al., 1989). Additionally, other proteins have been identified as differentially secreted by decidual cells, such as PECAM-1 or MPIF-1, and expressed, such as actin beta (ACTB) or transglutaminase 2 (Loke et al., 1989) (**Figure 4**). Effective communication between epithelial and stromal elements remains crucial for coordinating decidualization, ensuring the maintenance of an ideal uterine microenvironment throughout pregnancy (X. Wang et al., 2017). Paracrine agents such as bone morphogenetic protein 2 (BMP2; secreted by epithelial cells) operate downstream of the Indian Hedgehog (IHH) pathway, establishing a gradient signal for decidualization to stromal cells. Stromal PR signaling pathways function via paracrine mechanisms targeting decidualization-associated genes such as MMP9, MSX2, or CNR1 (Bhurke et al., 2016).

The ECM - a three-dimensional macromolecular dynamic network composed of fibrillar (such as collagens or fibronectin) and non-fibrillar elements (such as proteoglycans or glycoproteins) – serves to support the cell within a tissue context (Theocharis et al., 2019). The ECM also plays a significant role during decidualization and undergoes significant changes in composition and function. Laminin's presence near decidualized cells and absence in the myometrium govern embryo invasion (Irwin et al., 1989; Loke et al., 1989). Fibronectin levels remain concentrated around decidual cells with an arginine-glycine-aspartic acid motif linked with IGFBP1, potentially serving as an anchoring factor (Aplin et al., 1988). An additional decrease in the levels of enzymes related to ECM synthesis (MMP1 and MMP3) (Schatz et al., 1995) and the increase of EVT migration inductors (EMILIN1) (Spessotto et al., 2006) creates a supportive

environment for trophoblast expansion and cell anchorage, orchestrating trophoblast invasion by actively enveloping the implanting blastocyst (McKay et al., 1992).

During decidualization, the functional layer also undergoes a growing compaction due to the infiltration of leukocytes, particularly natural killer (NK) cells, associated with the maternal tolerance of trophoblasts. NK cells acquire a more active profile with increased expression of cytotoxic granule genes and cell communication with stromal cells via interleukins. NK cell levels rise near spiral arterioles and proximity to EVTs, and a complex gradient of chemokines determines their position, which remains critical as the distribution of NK cells relates to reproductive success and imbalances associated with reproductive failure. Concurrently, macrophage levels become elevated within the decidua, particularly near infiltrating EVTs, likely contributing to tolerance for invading trophoblast cells. When considered collectively, decidualization emerges as a critical player in the immune regulation of pregnancy (Co et al., 2013; Quenby et al., 2009; Van Den Heuvel et al., 2005; Wang et al., 2020).

Endothelial cells also experience alterations during decidualization, as remodeling the endometrial vasculature is crucial during the secretory phase. Remodeling is mainly facilitated by the angiogenic vascular endothelial growth factor (VEGF), which triggers the formation of new blood vessels and vascular permeability crucial for entering leukocytes and vasoconstriction (Mihm et al., 2011).

All cellular and molecular changes in the endometrium aim to transform the tissue into a state receptive to embryo implantation. Despite this seemingly long journey, the actual period of implantation occurs in a limited interval of time known as the window of implantation (WOI) (**Figure 2**), established at the mid-secretory phase (which occurs 6-10 days after ovulation) (Maenhoudt et al., 2022). The WOI enables the adherence of the blastocyst and initiates the finalization of decidualization in the stromal compartments, regulating trophoblast invasion and subsequent placentation (Moreno et al., 2023). In most healthy pregnancies, implantation typically takes place 8 to 10 days after ovulation, and early loss arises when the implantation window becomes delayed

(Llen et al., 1999). Identifying characteristic gene expression profiles (explained in Section 3) has supported substantial progress in understanding the WOI.

2.2.4. Menstruation

Corpus luteum regression occurs in the absence of pregnancy initiation, and the consequent decline in P_4 levels triggers the expression of inflammatory cytokines, chemokines, and MMPs. This process contributes to the onset of endometrial inflammation and the beginning of menstruation (Hiby et al., 1997). The sequential endometrial events caused by P_4 withdrawal in women are traditionally divided into two phases (Kelly et al., 2001). After P_4 withdrawal, the initial phase involves heightened exposure of the endometrium to cytokines and prostaglandins (J. Evans & Salamonsen, 2014). Chemokines, specialized cytokines with chemoattractant properties, play a crucial role in orchestrating the movement and activation of leukocytes within the endometrium. The expression of inflammatory mediators after P_4 withdrawal includes IL-6, chemokines (such as CCL11, CCL2, CXCL8, or CXCL10), and granulocyte-macrophage colony-stimulating factor (GM-CSF). Nuclear factor kappa-light-chain-enhancer of activated B cells (NF-κB) activity facilitates the orchestration of this cellular response, promoting the expression of inflammatory response genes (J. Evans & Salamonsen, 2014). P_4 inhibits the NF-κB pathway by increasing the levels of an NF-κB primary inhibitor (IκB) or competing for NF-κB recognition sites (King et al., 2001). The second phase (considered unrelated to the actions of P_4/PR) begins with heightened cytokine production, followed by the influx of innate immune cells into the nearby endometrial environment. The activation and release of MMPs accompanies the second phase, which prompts ECM destruction (Q. Wang et al., 2013).

The resolution of inflammation in the menstrual endometrium is intricately regulated in a means comparable to the controlled inflammatory reactions observed in other body areas. Like other tissues, the restricted production of pro-inflammatory mediators and breakdown of pre-existing inflammatory mediators constrain the recruitment of leukocytes and promote the restoration of vascular integrity. The localized inflammatory resolution also encompasses the phagocytosis of apoptotic neutrophils, promoting the

elevated transcription and release of anti-inflammatory cytokines such as IL-10 or TGF-β (Huynh et al., 2002). Multiple studies have reported the increased transcription of the above-noted cytokines and other cytokines/chemokines (e.g., CCL2, CXCL8, IL-6, and TNF) in response to a drop in P_4 levels in the human endometrium (Armstrong et al., 2017; Jones et al., 1997; Milne et al., 1999). This increase, in turn, is accompanied by an increased number of neutrophils and mononuclear phagocytes in areas of tissue repair, as observed in models of menstruation (Armstrong et al., 2017; Cousins et al., 2016). The likely rationale for adopting an inflammatory and tissue regenerative model might derive from the metabolic burden on the mother during the luteal phase, as regenerating and shedding the endometrium would be more economical than continuously maintaining a fully secretory state, preventing loss of function. Menstrual bleeding is perceived as a low-cost phenomenon, possibly arising as a side-effect of blood volume not being re-absorbed during endometrial regression (Strassmann, 1996).

Menstruation, as a pivotal physiological event, represents a compelling example where the mesenchymal-epithelial transition (MET) and epithelial-mesenchymal transition (EMT) remain essential for successful endometrial function, as the menstruating endometrium serves as a physiological illustration of an injured surface that needs to undergo rapid monthly repair (Owusu-Akyaw et al., 2019). In murine models, MET forms part of the decidualization process during morphological changes in stromal cells, which become transformed into epithelioid-like secretory cells (Gellersen et al., 2007; Owusu-Akyaw et al., 2019), a claim supported by changes consistent with MET, such as glycogen accumulation, endoplasmic reticulum expansion, and reorganization of the actin microfilament cytoskeleton. In addition, human and rodent stromal cells demonstrate a reversible MET process, in which they present an epithelial-like morphology after culturing with a decidualization medium and fibroblast characteristics upon P_4, E_2, and cAMP decay (Abrahamsohn & Zorn, 1993; Gellersen & Brosens, 2014; L. Yu et al., 2016; X. H. Zhang et al., 2013). Several studies also suggest that stromal cells contribute to stromal and epithelial regeneration. They support this hypothesis in the presence of stromal and epithelial markers in stromal populations following artificial menstrual cycle and followed by a decrease in stromal markers and an increase in epithelial markers after

P_4 withdrawal, suggesting a role for MET in the endometrial regenerative process (Cousins et al., 2014; Patterson et al., 2013).

2.3. Endometrial regeneration

Tissue remodeling processes, such as in the skin or intestine, typically associate with the existence and functioning of tissue-resident stem cells (Clevers et al., 2014). As the endometrium undergoes a process of remodeling and renewal during the menstrual cycle (as described in section 2.2), the accommodation of stem cells participating in dynamic regeneration processes remains a reasonable hypothesis. Definitions of stem cells include self-renewing undifferentiated cells capable of transforming into other specialized cell types. Stem cells are categorized into various types based on their developmental potential, ranging from totipotent cells (like the zygote, capable of differentiating into any germ layer and extra-embryonic structure) to unipotent cells (such as dermatocytes, which can only differentiate into a specific cell type) (Zakrzewski et al., 2019). Adult (or somatic) stem cells are tissue-specific stem cells with limited differentiation possibilities residing in most postnatal tissues and organs that play a crucial role in preserving cellular homeostasis within the tissue or organ (Gargett, 2007). Nevertheless, the existence and characterization of putative endometrial stem cells and their potential role in endometrial physiology remain unresolved. Despite ongoing investigations, no evidence has established whether stem cells play a definitive role in regeneration and proliferation following menstruation and/or during the proliferative phase (Maenhoudt et al., 2022).

Stem cells commonly exist within a specialized microenvironment called the stem cell niche, which comprises supportive and regulatory cells that safeguard stem cells. They oversee their progression, maintenance, expansion into amplifying intermediate progenitor cells, and differentiation towards mature cells through the activity of specific ECM components and secreted molecules (Blanpain & Fuchs, 2014; Morrison & Spradling, 2008). As for the stem cells themselves, a definition of an endometrial stem cell niche remains elusive (Maenhoudt et al., 2022).

The cyclical renewal capacity of the human endometrium throughout each menstrual cycle supports the idea that a specific region within the endometrial tissue may serve as a niche for a small population of endometrial stem cells, which may become activated in response to steroid hormones during each menstrual cycle without undergoing shedding (Prianishnikov, 1978; Teixeira et al., 2008). Numerous studies have attempted to identify uterine tissue-resident stem cells using distinct approaches. The prevailing opinion suggests that while there are observable stem cells in the functional layer that shed during menstruation, known as "menstrual blood stem cells" (MenSCs)(Bozorgmehr et al., 2020; Gurung et al., 2020) a stem cell population would reside in the basal layer, persisting after the menstrual cycle, and enabling the regeneration of the endometrium (Hong, 2023).

Meanwhile, related studies have proposed that a limited number of bone marrow-derived stem cells (BMDSCs) may colonize diverse tissues (Blau et al., 2001). This framework supports a subset of endometrial stem cells originating from circulating BMDSCs, even given the prevailing belief that most endometrial stem cells originate from the endometrial tissue (Santamaria, Mas et al., 2018). Several studies support this theory. Endometrial tissue biopsy samples from recipients of BMDSCs have revealed the presence of donor-derived endometrial cells in humans (including stromal and epithelial cells) (Taylor, 2004), while further evidence comes from studies of allogeneic bone marrow stem cell transplant recipients (Cervelló et al., 2012; Ikoma et al., 2009) concerning endometrial endothelial cells within the endometrial vasculature (Mints et al., 2008).

Nevertheless, whether endometrial tissue consistently attracts BMDSCs in normal conditions or exclusively under diseased circumstances remains uncertain. Increased estrogen secretion may promote the migration of circulating endothelial progenitor cells (CEPCs) into the blood vessels of the endometrium during the early stages of the menstrual cycle (Masuda et al., 2007) or in response to pathological stimuli (Alawadhi et al., 2014; Du et al., 2012). *In vitro* studies have demonstrated that the estrogen-triggered release of CXCL12 and its receptor CXCR4 from endometrial stromal cells can enhance

the migration of BMDSCs (X. Wang et al., 2015), and these cells then undergo differentiation into decidual stromal cells (Tal et al., 2019). These studies support the development of a subset of endometrial cells from BMDSCs, but identifying distinct markers or traits that distinguish endometrial stem cells of exogenous origin from those of endogenous origin remains elusive (Hong, 2023). The ultimate goal of the uterus is to nurture a pregnancy, requiring the endometrium and optimized and synchronized cyclic processes; nevertheless, various endometrial pathologies can prompt disruption, resulting in abnormalities that may lead to infertility. Transcriptomics-based analyses have been extensively applied to study the endometrium, identifying gene expression patterns and states in individual cells, offering a more profound comprehension of these processes.

3. Transcriptomics of the endometrium

Randomized studies have questioned the clinical utility of traditional histological dating methods (Noyes et al., 1950, 1975) used for endometrium characterization and disease diagnosis (Coutifaris et al., 2004; M. J. Murray et al., 2004). This motivated the integration of improved techniques such as transcriptomics, which has provided vital information for the objective assessment of endometrial characterization and diagnosis. In recent years, groundbreaking research has shown the pivotal nature of high throughput "omics" (including genomics, transcriptomics, epigenomics, proteomics, and metabolomics) in the realm of endometrial research (Altmäe et al., 2014).

Microarray-based gene expression technology, which simultaneously monitors the expression of thousands of genes (Altmäe et al., 2014), represented the first transcriptomic technique widely used in endometrial research. This approach was first applied in the endometrium to profile gene expression during the secretory phase, targeting the identification of the WOI (Carson et al., 2002; Kao et al., 2002; Mirkin et al., 2005; Riesewijk et al., 2003). Since then, this technology has aided i) the study of healthy endometrium and embryo implantation (Aghajanova et al., 2008; Giudice, 2006; Horcajadas et al., 2007; Koot et al., 2012; Ruiz-Alonso et al., 2012; Toth et al., 2011); ii) the development of receptivity diagnostic tools (Díaz-Gimeno et al., 2011), iii) in

exploring diseases such as endometriosis or endometrial cancer (Doll et al., 2008; Matsuzaki, 2011), and iv) in the characterization of cellular compartments by physical separation (G. E. Evans et al., 2012; Spitzer et al., 2012; Yanaihara et al., 2005).

Even given this early success, disadvantages associated with microarrays and the contemporaneous progress in transcriptomic technology led to a shift towards applying another more advanced technique - bulk RNA sequencing (RNA-seq).

3.1. Endometrial characterization with bulk RNA sequencing

Bulk RNA-seq employs next-generation sequencing (NGS) to uncover the presence and abundance of RNA within a pooled cell population, tissue section, or biopsy and assays the whole transcriptome. This method represents a straightforward and economical approach to studying mRNA and provides gene expression profiles from the studied sample or pool of samples (X. Li & Wang, 2021).

The first comparative studies between RNA-seq and microarrays in the endometrium of animal models unveiled a persistent overlap in results, with a substantially greater number of genes exhibiting differential expression in RNA-seq approaches (Malone & Oliver, 2011; Ulbrich et al., 2013). The transcriptomic study of human endometrial biopsies indicated a link between altered gene expression profiles and the transition of the human endometrium from a pre-receptive (early secretory phase) to a receptive (mid-secretory phase) state in a natural menstrual cycle (Wang & Yu, 2018). The combined results of RNA-seq and DNA microarray studies revealed a common subset of differentially expressed genes that characterized the transition of the endometrium to a receptive state (e.g., *SPP1, IL15,* and *SERPING1*) (Garrido-Gómez et al., 2013; Macdonald et al., 2011; Ruiz-Alonso et al., 2013). Due to the ability to detect a higher number of exons, alternative splicing events, and transcripts with low abundance, RNA-seq has produced an extensive catalog of additional genes that could contribute to endometrial receptivity (e.g., *OVGP1, ZCCHC12, HAP1,* and *MRAP2*) (Hu et al., 2014; Wang & Yu, 2018), embryo implantation process (e.g., *ITGB1, SPP1, BSG,* and *LGALS1*) (Koel et al.,

2022), recurrent implantation failure (RIF) (Zhou et al., 2019), or adenomyosis (Prašnikar et al., 2022).

While transcriptomic studies vary in their findings, they unanimously acknowledged the presence of specific transcriptomic profiles throughout the menstrual cycle, mainly in the WOI (Wang & Yu, 2018). As the masking of expression profiles of rare cell populations by the average profile of all analyzed cells represents a significant drawback of RNA-seq, a separate analysis of endometrial compartments - offering a deeper understanding of endometrial physiology and elucidating interactions between cell types and their regulatory mechanisms – had remained a pending task. The emergence of single-cell RNA-seq (scRNA-seq) has recently helped to overcome this significant biological challenge (Li & Wang, 2021).

3.2. Endometrial characterization with scRNA sequencing

scRNA-seq technology allows gene expression profiling in a heterogeneous sample at the single-cell level. Gene expression profiles correspond to individual cells and not to an average of the expression of all cells within a sample; therefore, the individual characteristics of each cell are represented. Since 2017, scRNA-seq has emerged as a widely embraced genomic tool for analyzing transcriptome diversity, such as in the identification of rare cell types and states within healthy donor samples or diverse tumor samples (Li & Wang, 2021). scRNA-seq can support the characterization of the transcriptome of every human cell type, encompassing those located in the reproductive organs (Vilella et al., 2021) and involving the emergence of intriguing insights into endometrial function during menstruation and implantation (Vento-Tormo et al., 2018).

Endometrial tissue characterization at a single-cell level began before the popularization of scRNA-seq; the first single-cell technique employed fluorescence-activated cell sorting (FACS), a procedure that isolates cells based on antibodies against typical cell markers (Krjutškov et al., 2016). This FACS-based research focused on endometrial stromal cells and revealed transcriptomic differences between freshly isolated cells and cultured cells, observing upregulated genes (e.g., *FOS* and *SERPINF1*) and downregulated genes (e.g., *TMSB10* and *MYL12A*). Although this approach provided valuable information, the

difficulty of using independent reactions in wells limited its applicability; in addition, FACS results only covered known, previously isolated populations requiring specific cell markers. Of note, microfluidic techniques later coupled to these protocols allowed for the more advanced characterization of cell populations in a heterogeneous sample.

A recent study from our group utilized modern single-cell microfluidics, C1 Fluidigm, and a 10x genomics system to map cellular and molecular changes in the endometrium throughout the menstrual cycle, characterizing diverse cell populations (Wang et al., 2020). We employed endometrial biopsies covering the entire menstrual cycle, analyzed the transcriptomic information of more than 73,000 cells, and clustered them into seven distinct groups based on the expression profiles. We identified four cell types based on gene expression differences and canonical markers (endothelial cells, stromal fibroblasts, lymphocytes, and macrophages) and a small population of smooth muscle expressing *PDGFRB, MCAM,* and *SUSD2*, which suggested that the population might include cells previously classified as mesenchymal progenitor cells (Masuda et al., 2012; Schwab & Gargett, 2007). Finally, two remaining cell types expressed markers associated with epithelial cells, with gene expression profiles allowing the distinction between ciliated and unciliated epithelial cells. Employing RNA and protein co-staining, we observed the spatial arrangement of cells in situ and validated four genes (*C20orf85, FAM183A, C11orf88,* and *CDHR3*) as highly indicative markers of ciliated epithelial cells, which displayed the consistent co-expression of *FOXJ1* (a canonical regulator of cilia function) (Wang et al., 2020). The investigation of transcriptomic changes across the menstrual cycle established four main phases based on the transcriptome analysis of unciliated epithelial cells and stromal cells as leading players in endometrial transformation. A discontinuity in unciliated epithelia trajectory dynamics led to the identification of an abrupt activation of several genes at the early beginning of phase 4 (e.g., *PAEP, GPX3,* and *CXCL14*) that consistently displayed overexpression in whole-tissue transcriptomic datasets during the WOI (**Figure 5**) (Horcajadas et al., 2007). Thus, we linked the beginning of the WOI to the entrance into phase 4, starting with an abrupt transcriptional activation in the unciliated epithelium but with gradual and discrete dynamic changes in stromal cells. The changes in gene expression profiles in stromal cells

included the upregulation of *DKK1, CRYAB, FOXO1,* and *IL15*, with the latter demonstrating the onset of decidualization prior to the opening of the WOI.

In contrast, the closure of the WOI associated with gradual transitional transcriptional dynamics in both epithelium and stroma. We integrated the four phases with traditional histologically determined phases by studying cellular mitosis as a differential characteristic between the proliferative and secretory phases. We determined the transition between the proliferative and secretory phase between transcriptomic phases 2 and 3 so that phase 3 corresponds to an early secretory phase and phases 1 and 2 correspond to early and late proliferative phases (**Figure 5**). This new classification at the transcriptomic level allowed the establishment of new histologically unrecognizable subphases, representing a paradigm shift in the transition of the endometrium during the menstrual cycle.

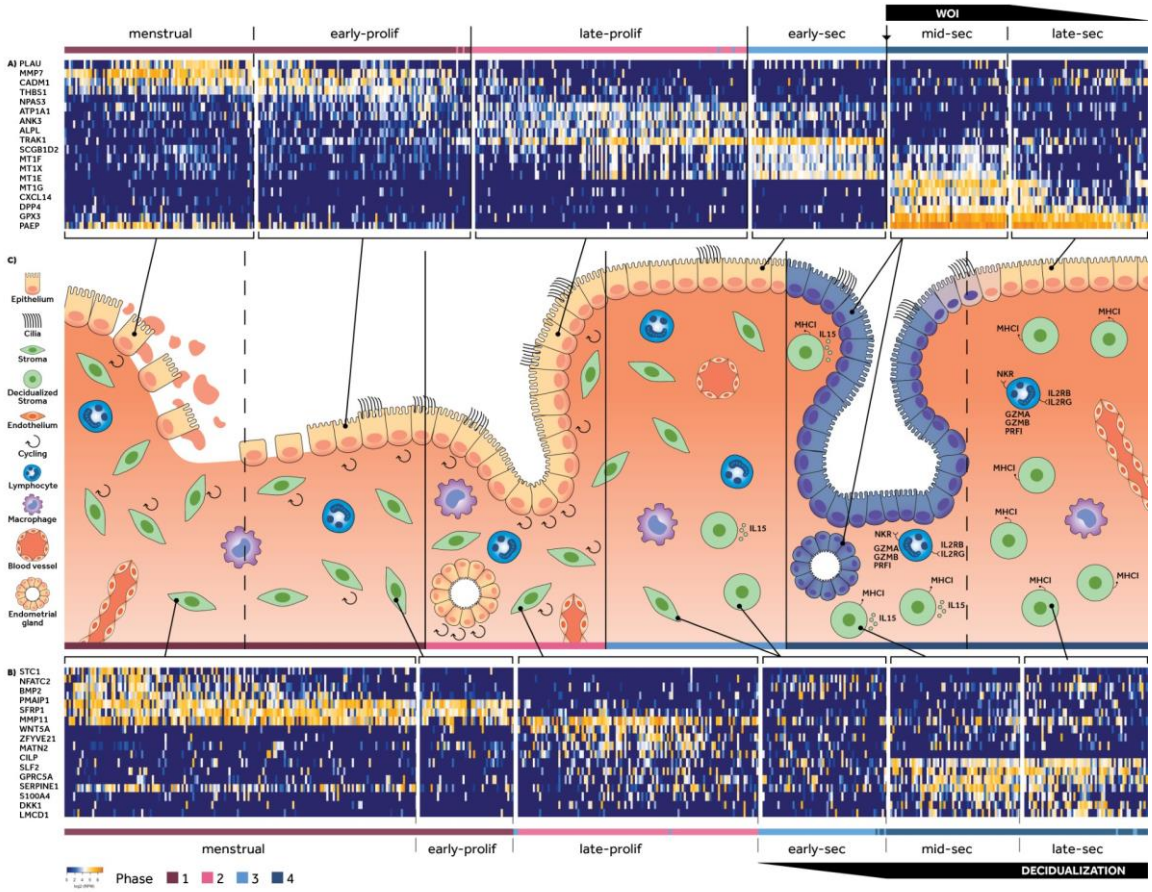

Figure 5. Fluctuating gene expression in the endometrium throughout the human menstrual cycle. A-C, Phase, and sub-phase defining genes, and the relationship between transcriptomically defined and histologically defined (canonical) endometrial phases for (a) unciliated epithelia (epi) and (b) stromal fibroblasts (str) across (c) a human menstrual cycle. Genes shown are differentially expressed (-log10(p.adj of a Wilcoxon's rank sum test)>10, log2(FC)>1) in a phase or sub-phase and are not differentially expressed between luminal and glandular cells in the phase where the gene peaked. Genes were further filtered for their potential to be deconvoluted between unciliated epithelia and stromal fibroblasts in bulk data to obtain those that are temporally in synchrony between the two cell types or those with negligible expression in one cell type across the cycle but significant phase-specific dynamics in another. (Cells (column) were ordered by pseudotime. Dashed lines: within-phase transition; Solid lines: boundaries between the four phases. Abbreviations - WOI (window of implantation), pro (proliferative), sec (secretory). Figure reproduced with permission from Wang et al. (2020).

Other studies used a novel technique known as spatial RNA sequencing (spRNA-seq) that combines the information from global transcriptional analysis of bulk RNA-seq and in situ hybridization to link transcriptomics with spatial information (Li & Wang, 2021). Garcia-Alonso et a. (2021) used an integrated approach for merging information from the initial menstrual cycle atlas (Wang et al., 2020) with newly produced single-cell and

spatial transcriptomics data from endometrial biopsies and whole endometrium samples within proliferative and secretory phases. Through this integration, the authors analyzed the transcriptome of nearly 100,000 cells, identifying 14 clusters and grouping them into five main cellular types (immune, epithelial, endothelial, supporting, and stromal cells) based on known marker expression. They carried out a detailed examination of the epithelial cell population, initially categorizing them into four groups based on cell marker expression: $SOX9^+$ cells (with high expression of *MMP7* and *ESR1*), ciliated cells (*TPP3* and *PIFO*), glandular cells (*SCGB2A2, PAEP* and *CXCL8*) and luminal cells (*PTGS1, KRT5* and *LGR5*) (**Table 2**). scRNA-seq data integration and spRNA-seq data subdivided the $SOX9^+$ epithelial cell cluster into three groups with a defined specific spatial location. $SOX9^+$ and $LGR5^+$ cells (expressing *KRT17* and *WNT7A*) located to the surface epithelium, $SOX9^+$ and $LGR5^-$ cells (expressing *IHH*) displayed enrichment in the basal glands, and $SOX9^+$ cells in G2M/S phase (either $LGR5^+$ or $LGR5^-$) located to glands within the regenerative superficial layer (**Figure 6**). Across the menstrual cycle, ciliated cells were present in proliferative and secretory phases, while $PAEP^+$ and $SOX9^+$ secretory cells appeared after the P_4 effect during ovulation. Focusing on the transcription factors controlling epithelial differentiation through the menstrual cycle, the authors revealed the upregulation of *NOTCH2* expression in glands as they move away from the lumen, whereas *WNT7A* expression remains higher in the luminal epithelium than in the glands. In addition, deducing ligand-receptor interaction among cell types inferred distinct yet complementary roles for NOTCH and WNT signaling in the development and differentiation of secretory and ciliated epithelial cells. Specifically, more robust WNT signaling than NOTCH resulted in differentiation into the ciliated cell lineage, while prevailing NOTCH signaling over WNT generated the secretory cell lineage. They functionally assessed this level of regulation using three-dimensional (3D) culture models (organoids) by activating and inhibiting the WNT or NOTCH pathways (as discussed in section 4).

Table 2: Subdivision of epithelial populations by single-cell RNA sequencing. Data from Garcia-Alonso et al. (2021)

Cell populations	Expressed marker genes
SOX9$^+$	*MMP7* and *ESR1*
Ciliated	*TPP3* and *PIFO*
Glandular	*SCGB2A2*, *PAEP* and *CXCL8*
Luminal	*PTGS1*, *KRT5* and *LGR5*

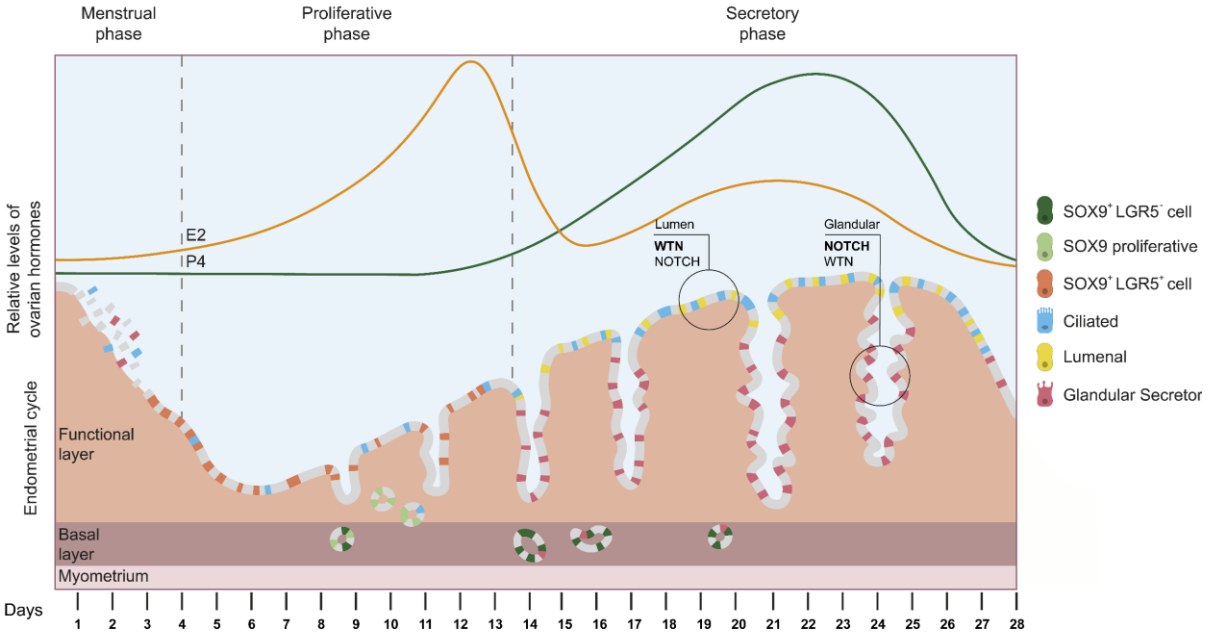

Figure 6. Schematic illustration of the proposed model for the temporal and spatial distribution of epithelial subsets obtained by single-cell RNA sequencing. Reproduced with permission from Garcia-Alonso et al. (2021).

Collectively, single-cell transcriptomic "atlases" (Garcia-Alonso et al., 2021; Wang et al., 2020) provide a comprehensive depiction of the normal human endometrium; however, other research groups have also contributed to the characterization of the endometrium. Queckbörner et al. reported ten different stromal cell types and two subsets of pericytes depending on cell markers expression (e.g., *ISG15, THY1, ACTA2,* and *BMP7*), indicating the presence of distinct stromal niches capable of regulating inflammation and ECM composition (Queckbörner et al., 2021). Diniz-da-Costa et al. characterized a novel discrete population of highly proliferative mesenchymal cells

during the WOI-expressing genes related to vascular transmigration and chemotaxis (Diniz-da-Costa et al., 2021). Finally, Kirkwood et al. employed in silico trajectories to indicate that stromal cell populations ($PDGFRB^{+}$) expressing genes typically associated with epithelial cells were stromal fibroblasts undergoing MET (Kirkwood et al., 2022).

Single-cell profiling studies also unveiled a significant fraction of endometrial immune cells, whose composition undergoes notable changes during the menstrual cycle. The leukocyte population comprises NK, T, and B cells, macrophages, neutrophils, dendritic cells, and mast cells (Maenhoudt et al., 2022). Tissue-resident immune cells distribute themselves across the epithelial and stromal functional layers, suggesting a dynamic interaction between these three cell types (Queckbörner et al., 2021). scRNA-seq revealed an increase in the number of uterine NK (uNK) cells during the secretory phase, representing the primary type of immune cell. uNK cells target senescent decidual cells and increase blood flow by secreting angiogenic factors (e.g., VEGF) at the maternal-fetal interface (Brighton et al., 2017; Rawlings et al., 2021). Recently, Cheng et al. reported the first endometrial gene signature associated with pregnancy, which contains various genes regulating immune and metabolic activity (Cheng et al., 2023).

These findings serve as valuable sources for studying endometrial alterations; therefore, scRNA-seq-based research has shifted its focus to endometrial pathologies. Garcia-Alonso et al. compared previous data on endometrial cancer and endometriotic lesions to their endometrial cell atlas, finding a dominant $SOX9^{+}$ population in tumors with subclusters (e.g., $SOX9^{+}/LGR5^{+}$ or $SOX9^{+}/LGR5^{-}$) related to different cancer stages and subtypes and endometriotic peritoneal lesions (Garcia-Alonso et al., 2021). Lucas et al. revealed a link between uNK cell deficiency and recurrent pregnancy loss co-occurring with a transition from the predominant presence of decidual cells to an increased prevalence of senescent decidual cells (Lucas et al., 2020). Liu et al. discovered a subpopulation of cells with high copy number variation levels in ectopic lesions of adenomyosis (Liu et al., 2021). Lv et al. reported that the decreased expression of proliferation-associated genes and an increase in those linked to cellular senescence in both stromal and epithelial cells in thin endometrium samples may relate to patient infertility (Lv et al., 2022). Finally, the transcriptomic profiles of endometrial cells

associated with conditions such as preeclampsia (Luo et al., 2023), RIF (Lai et al., 2022), or endometriosis (Fonseca et al., 2023; Huang et al. 2023; Ma et al., 2021; Tan et al., 2022) have facilitated their study and associated subpopulation changes or the emergence of new populations with each condition. This research exemplifies the potential of scRNA-seq in exploring both the physiological and pathological aspects of the endometrium (Li & Wang, 2021).

Transcriptomic studies can be supported using cell culture models that recapitulate pathological or physiological tissues. The existing conceptual framework for this approach in the human endometrium involves 2D culture research, which suffers from inherent limitations (Cousins et al., 2021). Progress in 3D culture models, coupled with cell characterization through scRNA-seq, provides an opportunity to overcome the constraints associated with 2D culture. 3D models for endometrial cell culture include scaffold matrices, organ-on-a-chip systems, and organoids (Li et al., 2022);however, due to the opportunities they provide, this doctoral thesis focuses explicitly on developing and using endometrial organoids generated from biopsy cells.

4. Endometrial *in vitro* models: organoids

Traditional 2D cell cultures have been widely employed for investigating *in vitro* endometrial biology and have made significant contributions. Despite benefits such as long-term expandability and user-friendly attributes, the associated drawbacks pose a significant challenge. Culturing primary endometrial cells results in the loss of their phenotype and hormone responsiveness over time. The inability to expand epithelial cells and the abnormal karyotypic and physiological characteristics of immortalized lines further compound the lack of the intricate 3D physiology found in the original tissue (Maenhoudt et al., 2022). As a result, recent research has redirected its focus toward creating 3D culture models that more accurately recapitulate endometrial structure and physiology.

Organoid culture, as a promising 3D culture platform, involves generating intricate structures from stem cells. Their development requires cell culture within an ECM in

specific culture media, which includes different growth and signaling factors (Schutgens & Clevers, 2020). Organoids can be developed from two distinct stem cell categories: i) pluripotent stem cells (PSCs), which can replicate the embryonic development of the organ, and ii) adult stem cells (ASCs), which faithfully replicate both the phenotypic and functional traits of epithelial cells of the tissue (through proliferation, self-organization, and self-renewal processes), exhibiting long-term expandability while maintaining biological properties and genomic stability (Clevers, 2016). While PSC-derived organoids develop several cell types simultaneously, ASC-derived organoids only represent the epithelial component of the organ, resulting in a more limited model. Although more intricate, PSC-derived organoids frequently harbor abnormal cell types, persist in a specific state of immaturity, and lack the capacity for expansion (Fatehullah et al., 2016). The pioneering achievement in creating a viable organoid model from ASCs came from utilizing $LGR5^+$ intestinal tissue stem cells (Sato et al., 2009); since then, organoid models have been generated from diverse tissues of both mouse and human origin (J. Kim et al., 2020).

4.1. Endometrial epithelial organoids

Endometrial epithelial organoids (EEOs) obtained from adult stem cells represent the most extensively used organoid model in endometrial studies (Gu et al., 2020), with initial protocols outlined in 2017 (Boretto et al., 2017; Turco et al., 2017). EEOs replicated essential biological characteristics of the endometrial epithelium, such as the expression of specific markers (e.g., *FOXA2* and *PAX8*) and glandular-type organization. EEOs also responded similarly to hormones compared to the endometrium when mimicking the menstrual cycle, expressing markers like thyrotropin-releasing hormone (THR) following E_2 treatment and PAEP. Additionally, EEOs downregulate ERα expression after P_4 treatment. Notably, the withdrawal of hormones disrupts EEO structure (Boretto et al., 2017); therefore, human endometrial organoids offer a robust method to investigate the fundamental mechanisms driving endometrial biology (**Figure 7**).

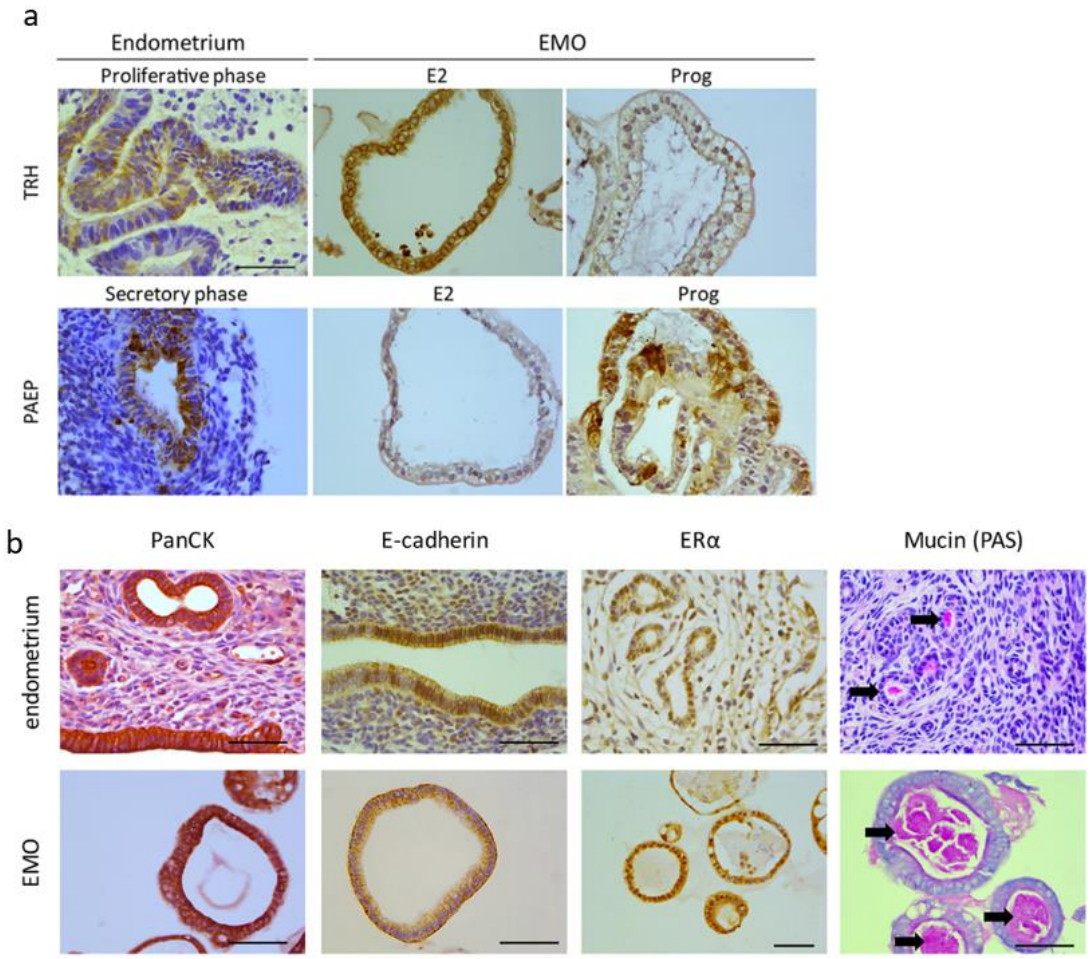

Figure 7. Characterization of endometrial epithelial organoids. a) Immunostaining of phase-specific markers in human endometrium and hormone-treated endometrial epithelial organoids (EEOs). The proliferative phase marker TRH is expressed in the EEOs after E_2 exposure, whereas the secretory phase marker PAEP is expressed after P_4 treatment. b) EEOs reproducing endometrial epithelial phenotype. Immunohistochemical staining for PanCK, E-cadherin, and Erα, and PAS staining of mucin (arrows) are shown in the endometrium (upper images) and organoids (lower images). Figure reproduced with permission from Boretto et al. (2017).

EEOs have been developed using samples of diverse characteristics, including those obtained during menstrual cycle phases (Boretto et al., 2017; Fitzgerald et al., 2019; Garcia-Alonso et al., 2021; Turco et al., 2017) and decidualization and menopause (Haider et al., 2019; Turco et al., 2017) and from menstrual flow samples (Cindrova-Davies et al., 2021). Their characterization via scRNA-seq revealed a heterogeneous cell composition, including ciliated and secretory cells (Cochrane et al., 2020), along with distinct hormone-responsive subpopulations (Fitzgerald et al., 2019). scRNA-seq

analysis, conducted following hormonal treatment to replicate the WOI, using E_2 and P_4, revealed cell grouping based on predicted cell types. The analysis unveiled five distinct endometrial cell types in untreated and E_2-treated EEOs, encompassing epithelial, ciliated, proliferative, unciliated, and stem cells. Moreover, six cell types emerged with the introduction of medroxyprogesterone acetate (MPA) to continue mimicking the human hormonal cycle. Notably, the administration of P_4 led to a new glandular secretory cluster (Fitzgerald et al., 2019). In addition, E_2+MPA treatment prompted a reduction in the proportion of putative endometrial stem cells (expressing previously described stem cell markers), accompanied by an increase in the proportions of epithelial and secretory cell populations. Differential gene expression analysis revealed the upregulation of genes like *OLFM4* by E_2 in stem and ciliated cells, mirroring the vivo endometrial environment. Additionally, PAEP exhibited upregulation by P4 effect (E2+MPA) in ciliated, proliferative, secretory, and epithelial stem cells (Fitzgerald et al., 2019). These insights, derived from EEO-based investigations, contribute to our understanding of the hormonal regulation of endometrial cell differentiation throughout the menstrual cycle.

As an instrument, EEOs have played a role in identifying pathways associated with differentiating secretory and ciliated endometrial cells and serve as a validation method for evaluating the outcomes derived from scRNA-seq of fresh human cells (Garcia-Alonso et al., 2021). Organoid cultures featuring NOTCH and WNT drug inhibitors helped assess their impact on cell development throughout the menstrual cycle. The findings revealed a correlation between the NOTCH pathway and the maturation into secretory cells, whereas the WNT pathway was associated with the maturation into ciliated cells. This substantiates the presence of a putative stem cell that gives rise to both cell populations.

Importantly, organoids derived from stem cells play a crucial role in identifying and characterizing the mechanisms of endometrial regeneration. Indeed, organoid scRNA-seq profiling revealed that the most prominent cell population within endometrial organoids aligns with MUC5B$^+$ epithelial cells observed in primary tissue, potentially unveiling a novel candidate population of endometrial stem cells capable of tissue renewal (Tan et al., 2022). In addition, organoids derived from menstrual flow exhibit a

transcriptional signature abundant in stem cell markers (Cindrova-Davies et al., 2021). EEOs have been employed to explore various medical conditions, such as endometrial cancer (Cochrane et al., 2020) and endometriosis (Boretto et al., 2019) and screen drugs (Bi et al., 2021).

5. Asherman syndrome

Asherman syndrome (AS) is an acquired condition characterized by the existence of intrauterine adhesions (IUAs) (located within the upper and lower uterine tract). Injury to the *stratum basalis* within the endometrium frequently triggers the formation of fibrotic tissues, resulting in functional impairment as normal endometrial tissue becomes substituted by non-functional fibrotic tissue, leading to adhesions within the uterine wall (**Figure 8**) (Smikle et al., 2023). AS is regarded as an iatrogenic condition, a term encompassing ailments stemming from diagnostic/therapeutic interventions performed by medical professionals on patients (Krishnan & Kasthuri, 2005). Procedures associated with AS comprise cesarean section, surgery, and repeated dilation and curettage (Conforti et al., 2013); however, instances of AS lacking prior trauma (triggered by infections or chronic endometriosis) have also been reported (Stillman & Asarkof, 1985) while congenital abnormalities of the uterine cavity (e.g., malformations in the Müllerian ducts) can worsen disease outcomes (Dmowski & Greenblatt, 1969; Sharma et al., 2008).

AS was named after Joseph G. Asherman, an Austro-Hungarian gynecologist who extensively researched the clinical histories of 29 women experiencing diverse complications during labor, abortions, or cervical obstructions leading to traumatic amenorrhea (Asherman, 1948). While Asherman was describing what would be recognized as Asherman syndrome, Heinrich Fritsch described IUAs in a patient experiencing amenorrhea following postpartum curettage in 1894 (Fritsch, 1894), while Bass and Stamer also reported correlations between cervical obstructions and IUAs in patients who had undergone abortions (Bruno Bass, 1927; Stamer, 1946).

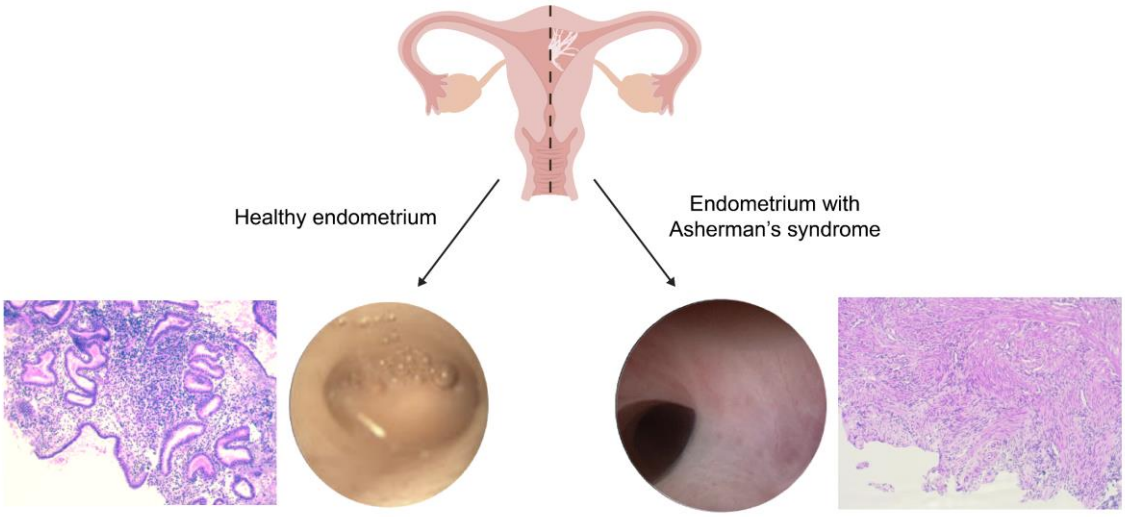

Figure 8. Schematic illustrations of the differences between healthy and Asherman syndrome-affected endometria. Hysteroscopy images and hematoxylin and eosin (H&E) staining highlight the micro- and macro-anatomy of this condition. Images reproduced with permission from Santamaria et al. 2016.

5.1. Clinical features of Asherman Syndrome

AS prevalence varies depending on the population under study. Due to its iatrogenic nature, countries with less advanced gynecological medicine or where illegal interventions (such as abortions) tend to have higher incidence rates. The European Medicines Agency (EMA) has established a prevalence of 4.4 cases per 10,000 individuals in the European Union. As this prevalence falls below the threshold defining pathologies as rare diseases (below 5 cases per 10,000 individuals), AS has been classified as a rare disease and is listed in the Orphanet database (under the code ORPHA137686) (*Committee for Orphan Medicinal Products (COMP) | European Medicines Agency*, n.d.).

The emergence of IUAs represents the main symptom of AS; their development involves the transformation of the stroma into fibrotic tissue and the glandular epithelium into inactive cubo-columnar epithelium (**Figure 8**). Consequently, both layers of the *strata* (*stratum basalis* and *stratum functionalis*) become indistinguishable and unresponsive to hormones (Schenker & Yaffe, 1978). In severe cases, different layers of the uterus (endometrium, myometrium, and/or connective tissue) become involved in IUA formation, with fibrous strips, collagen bundles, or muscle as part of the adhesions.

Patients with IUAs suffer from an endometrium containing 50–80% fibrous tissue (compared to 13–20% in a healthy endometrium), which leads to atrophic patches and the lack of a functional uterine cavity (Schenker & Yaffe, 1978). Due to the expansion of IUAs through the uterine cavity, endometrial fibrosis leads to the onset of clinical symptoms (Conforti et al., 2013).

Persistent inflammation (may participate in onset and recurrent formation of IUAs) (Chen et al., 2017), macrophage polarization (Lv et al., 2023; Song et al., 2021; Yao et al., 2023), endoplasmic reticulum stress, and ferroptosis (Bao et al., 2023; Zhu et al., 2023) all induce the expansion of IUAs. Furthermore, alterations in autophagy have been noted in the endometrium of patients with IUAs, which increases EMT (Zhao et al., 2020; Zhou et al., 2022) and upregulated ΔNp63 expression, leading to endometrial quiescence (Song et al., 2021; Zhao et al., 2017).

In this scenario of increasing IUAs and endometrial fibrosis, minor AS symptoms such as pelvic pain or changes in menstruation may arise, often remaining unnoticed until the patient seeks conception. At this stage, infertility as the primary AS symptom becomes apparent (D. Yu et al., 2008); the prevalence of AS in women experiencing fertility issues varies depending on the disease subgroup (from 2% to 6%). Significantly, procedures such as removing placental remnants or repeated curettage notably elevate the prevalence of infertility to 40% (Dreisler & Kjer, 2019).

5.2. Disease classifications

Numerous efforts have been undertaken to categorize severity into distinct stages since the first description of AS. Initial classifications relied on hysterosalpingography; however, this once valuable approach is now entirely outdated. Classifications based on hysteroscopy (with or without clinical data) have since gained prominence in clinical settings, facilitating effective comparisons of treatment techniques and outcomes (Manchanda et al., 2021). The initial hysteroscopy-based classification of IUAs established in 1978 evaluated the severity of IUAs by examining the extent and occlusion in the uterine cavity (March et al., 1978). IUA categorization into three groups depended

on the uterine cavity area presenting adhesion: minimal (a quarter of the cavity), moderate (from one to three-quarters of the cavity), and severe (more than three-quarters of the cavity). While the simplicity of this classification has led to common use, this approach lacks consideration of clinical symptoms (Manchanda et al., 2021).

The American Fertility Society (AFS) devised a comparable classification of IUAs, which not only assessed the area occupied by IUAs but also considered the type of adhesion, clinical symptoms, and menstrual patterns as indicators of severity (Buttram et al., 1988). This classification categorizes adhesions as mild, moderate, and severe and offers a prognostic score with information such as, for example, that moderate and severe cases can cause hypomenorrhea or amenorrhea (Buttram et al., 1988). The European Society of Hysteroscopy (ESH) also devised a grading system; however, its complex nature and absence of critical clinical details (such as previous deliveries) have led to decreased prominence (Sutton & Diamon, 1995).

Interestingly, a research group put forward a novel system integrating hysteroscopy findings with clinical information from patients, including symptoms, menstrual patterns, and reproductive outcomes, to enhance AS diagnosis (Aboul Nasr et al., 2000). Under this system, the pathological classification of adhesions encompasses three types: filmy, dense, and tubular. Tubular adhesions represent the most severe cases, distinguished by their density and the total occlusion of the uterine cavity that obscures both tubal ostia. Additionally, the classification identifies isthmic fibrosis as a separate entity, emphasizing the capacity of this condition capacity to trigger a neuroendocrine reflex that induces endometrial deactivation and amenorrhea, even if the remainder of the cavity lacks adhesions (Aboul Nasr et al., 2000; Manchanda et al., 2021). Despite recent efforts to establish a more complete classification of AS severity, the classification developed by the AFH remains the most widely used.

5.3. Clinical management and obstetrical challenges

As for diagnosis, hysteroscopy currently represents the gold standard for AS treatment. This technique offers a real-time view of the uterine cavity and allows for the characterization and immediate treatment of adhesions by removing IUAs

(hysteroscopic adhesiolysis), often restoring the uterine cavity to its standard shape and size (March 2011). This approach can restore fertility in some patients, although factors such as menstrual patterns or the severity/recurrence of IUAs heavily influence success (Capella-Allouc et al., 1999). Despite this success, hysteroscopic adhesiolysis often encounters restricted long-term clinical outcomes, primarily due to the tendency for IUA recurrence (Gharibeh et al., 2022). Thus, preventive strategies (e.g., hyaluronic acid gels, hormonal treatments, or intrauterine devices) are often used to avoid the occurrence of new IUAs; however, cases with a high recurrence rate or a severe nature require multiple procedures (Lekovich et al., 2017). The average pregnancy rate after IUA removal is from 40% to 60%; however, specific obstetrical challenges must be addressed even in the event of achieving pregnancy (Pistofidis et al., 1996).

Recurrent pregnancy loss represents a common condition in AS patients who have undergone hysteroscopic adhesiolysis (Carbonnel et al., 2021). An analysis of published reports of AS patients at various stages of pregnancy following hysteroscopic surgery revealed a pregnancy prevalence of 50%, accompanied by an average loss rate of 17.7% (with individual higher values corresponding to severe AS patients, compared to mild cases, even after undergoing adhesiolysis) (Guo et al., 2019). Placental abnormalities have also been identified as common AS symptoms; treated AS patients may exhibit higher incidences of placenta accreta, increta, and previa due to inadequate endometrial decidualization and residual scarring (Tavcar et al., 2023; Zhang et al., 2020). AS also prompts an increase in preterm birth, with figures ranging from 11.6% to 50% (Mára et al., 2023; Wang et al., 2021). Finally, AS also leads to lower birth weights of pregnant women with AS (compared to patients with a normal uterine cavity), with a lower weight ratio related to higher severity (Baradwan et al., 2023; Mára et al., 2023).

Due to the diversity of preventive treatments and potential complications, clinical practice follows a protocol known as PRACTICE (Prevention, Anticipation, Comprehensive therapy, Timely surveillance of pregnancies, Investigation, and Continuing Education), which focuses on ongoing patient monitoring and selecting optimal treatment options (March 2011).

5.4. Regenerative therapies

The development of alternative therapies represents a significant current focus in AS research. Since the absence of functional endometrium due to injury of the *stratum basalis* characterizes AS, stem cell-based therapies focused on the endometrial niche to enhance endometrial function present a hopeful prospect for addressing this pathology by contributing to endometrial regeneration (Baraniak & McDevitt, 2010). One exciting strategy focuses on paracrine-acting factors secreted by stem cells, such as extracellular vesicles (EVs) (Baraniak & McDevitt, 2010), although current evaluations use animal models, as the lack of protocol standardization for EV manipulation hinders their translation into clinical applications (Saribas et al., 2020; Zeng et al., 2022). Advancements in AS treatment have seen breakthroughs with therapies using artificially engineered scaffolds (Cao et al., 2018; Singh et al., 2020; Zhang et al., 2021). Several studies have showcased the efficacy of transplantation of BMDSCs (Zhu et al., 2024), MenSCs (Tan et al., 2016), or human umbilical cord-derived mesenchymal stem cells (UC-MSCs) (Cao et al., 2018) via scaffolds in AS patients. The results of clinical trials suggest higher rates of ongoing pregnancies and live births among AS patients undergoing treatment. Despite promising outcomes, tissue-engineered therapies comprise a minor proportion of ongoing clinical trials; conversely, cell therapies represent a more established approach and constitute the largest category of ongoing phase II trials (*Regenerative Medicine: The Pipeline Momentum Builds H1*, 2022).

A range of stem cell types have been explored for AS treatment, including MenSCs and adipose-derived stem cells (Azizi et al., 2018), amniotic fluid-derived stem cells (Bai et al., 2020; Gan et al., 2017), mesenchymal stem cells (MSCs) (Saribas et al., 2020), and UC-MSCs (Gao et al., 2021); however, BMDSCs hold the most significant promise due to their multipotent nature (Taylor, 2004). BMDSCs can migrate to the endometrium and effectively treat the damaged endometrium in mouse models (Alawadhi et al., 2014), highlighting their therapeutic capability. Our research group developed a prospective, experimental, non-controlled, open-labeled study and a phase II clinical trial using BMDSCs to treat AS patients (Cervelló et al., 2015; Santamaria et al., 2016). This study treated AS patients with previous hysteroscopic adhesiolysis and hormone replacement

therapy cycles with no improvement with autologous $CD133^+$ BDMSCs (isolated from peripheral blood after artificially stimulating BMDSC mobilization). The injection of the isolated $CD133^+$ cells into uterine spiral arterioles improved all patient disease scores (reducing their severity by 1 or 2 FDA stages, some even reaching a normal endometrial cavity state) and endometrial thickness. Of eleven AS patients, three achieved pregnancies spontaneously, and seven after embryo transfers. As a result of these findings, the EMA and the FDA have recognized $CD133^+$ BMDSCs as the first orphan-designed therapy for AS treatment, classifying it as an Advanced Therapy Medicinal Product.

We hypothesize that this treatment depends on the release of paracrine factors, which trigger cell division in neighboring cells to initiate endometrial regeneration (Cervelló et al., 2015; Santamaria et al., 2016); however, the molecular mechanisms underlying AS and the restoration of endometrial function through $CD133^+$ BMDSC therapy remain unknown.

This doctoral thesis offers the first insight into the gene expression of different cell types within the endometrium of patients with AS before and after treatment with $CD133^+$ cells. To better characterize this disease, this thesis describes the development of EEOs from AS patient samples to establish a 3D culture model for this pathology. EEOs developed using samples from AS patients before and after receiving cell therapy will also be used to analyze therapeutic responses and the recovery of endometrial regenerative capacity.

II. Hypothesis

II. Hypothesis

Asherman syndrome (AS) is an acquired condition characterized by the presence of intrauterine adhesions (IUAs) within the upper and lower uterine tract. The development of AS leads to the formation of fibrotic tissue and impaired epithelial function.

We hypothesize that the fibrotic tissue is the result of previous interventions that triggered it, suggesting the existence of an underlying pathogenesis in AS. We aim to investigate this through analyzing transcriptomic profiles at the single-cell level in the endometrium affected by AS, combined with developing an *in vitro* culture model of organoids, both before and after receiving cell therapy, within the context of a phase 1/2 clinical trial authorized by the AEMPS (*Agencia Española de Medicamentos y Productos Sanitarios*) and EMA (European Medicines Agency).

III. Objectives

III. Objectives

The primary objective of this thesis is to elucidate the cellular environment within the endometrium affected by Asherman syndrome through the establishment of cell transcriptomic profiles. Furthermore, it aims to analyze the potential therapeutic effects of an advanced cell therapy developed by our team on the recovery of this condition.

Specific objectives

1. To develop a comprehensive atlas of endometrial cellular transcriptomic profiles in Asherman syndrome and to investigate the differences in cellular composition and gene expression among the identified cell types.
2. To develop an organoid culture model derived from patients with Asherman syndrome to evaluate its capability to accurately represent the disease characteristics.
3. To evaluate the impact of $CD133^{+}$ bone marrow-derived stem cell (BDMSC) based therapy developed by our group on the transcriptomics of endometrial tissue and the developed organoid model to elucidate possible mechanisms of action.

IV. Materials and methods

IV. Materials and methods

1. Experimental design and patient recruitment

1.1. Experimental design

A biomedical study was performed to elucidate endometrial transcriptomic alterations in Asherman syndrome (AS), develop an AS disease model, and analyze the effects of autologous $CD133^+$ bone marrow-derived stem cell (BDMSC) administration on both the endometrium and endometrial epithelial organoids (EEOs) generated from biopsies of the healthy and AS-affected endometrium. The study design included the analysis of various parameters in endometrial biopsy samples/organoid cultures, incorporating samples from healthy control donors, AS patients, and AS patients receiving $CD133^+$ cell therapy treatment. As shown in **Figure 9**, the first part of the study involved processing AS and control biopsies and conducting single-cell RNA sequencing (scRNA-seq)-based analyses. AS EEOs were developed and characterized in the second part, and the impact of CD133+ BDMSC therapy on the AS endometrium and AS EEOs was analyzed via scRNA-seq in the third part.

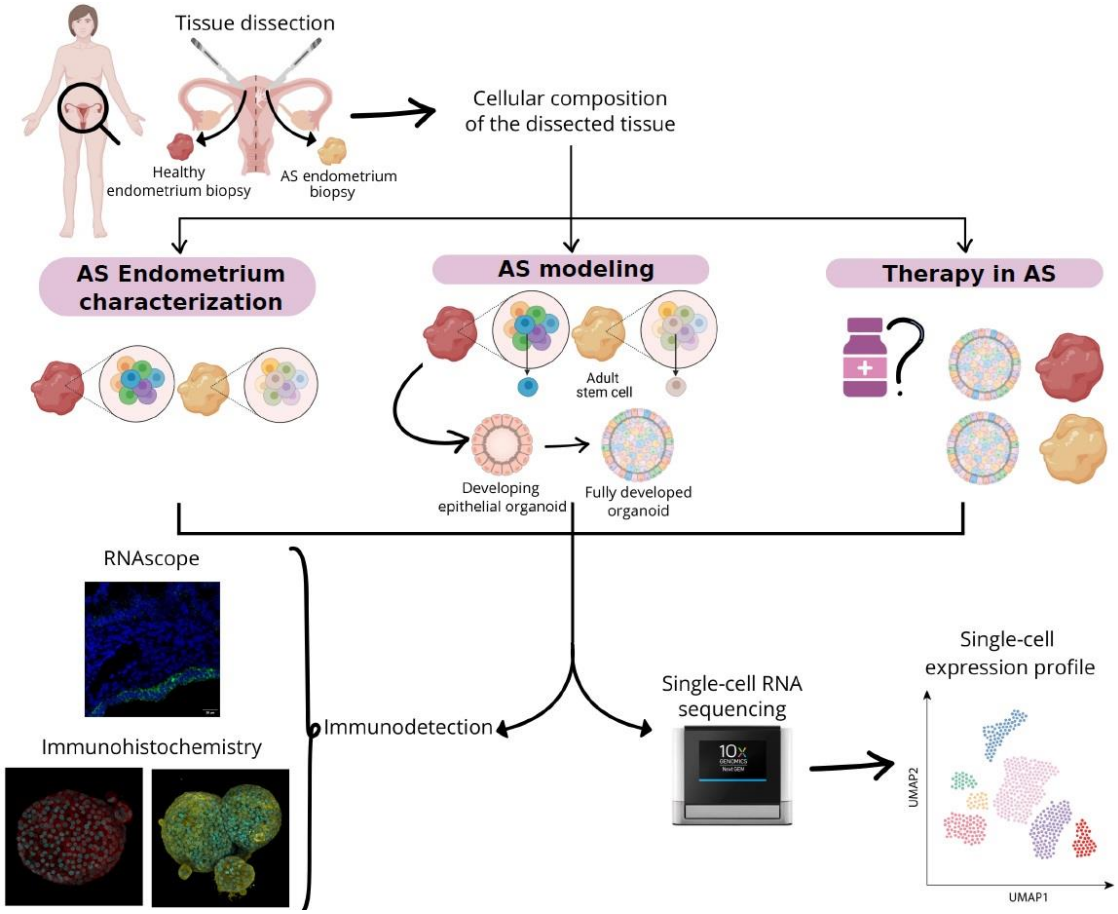

Figure 9. Graphical abstract of the experimental design followed in this thesis.

1.2. Patient recruitment

This study adheres to the guidelines set by the International Conference on Harmonization Good Clinical Practice and the Declaration of Helsinki. All procedures involving human endometrium received approval from the Spanish Agency of Medicines and Medical Devices (Agencia Española de Medicamentos y Productos Sanitarios [AEMPS]) (Annex 1) on April 20, 2020, and the Clinical Research Ethics Committee at Hospital Universitari Vall D'Hebron in Barcelona, Spain, on April 17, 2020. Written informed consent was obtained from all participants. This study is registered with the European Union Clinical Trials Register (EU-CTR) and the Spanish Clinical Studies Registry (Registro Español de Estudios Clínicos [REec]) (EudraCT Number: 2016-003975-23; Registration date: April 21 (2021). The Investigational Medical Product (IMP) was

designed as an Orphan Drug (OD) by the Food and Drug Administration (FDA) on February 1 (2019) (designation request number: DRU-2017-6131) and by the European Medicines Agency (EMA) on April 20 (2017) (EMA/OD/313/16). AEMPS and EMA Scientific Advice and Protocol Assistance were conducted on February 10 and September 1, 2017.

Endometrial biopsies were acquired from non-pregnant women aged between 18 and 44 years, with body mass index (BMI) values between 18-30 kg/m^2 and a commitment to completing the study. Every participant needed to have normal heart, kidney, and liver function and should be free from Hepatitis B or C, HIV, syphilis, and any psychiatric disorder. Sample acquisitions were made through hysteroscopic vision (Betocchi 5mm, Karl-Storz, Germany) with semi-rigid double-action biopsy forceps (Kalr-Storz, Germany) on the posterior wall, at least 1 cm away from any intrauterine adhesion (IUA) under vision. Since active endometritis can influence endometrial tissue composition, a microbiome assay was conducted on patients to eliminate this confounding variable. All specimens were anonymized after sample collection, and for AS patients, diagnosis and severity stage were confirmed by a certified gynecologist based on the American Fertility Society (AFS) classification system.

Nine patients, aged between 34 and 42 years, diagnosed with moderate or severe AS were included in this study. They underwent endometrial biopsies before treatment with $CD133^+$ BMDSCs and again one month afterward. All patients received hormone replacement therapy (HRT) to synchronize cycles and treatments. Hysteroscopies were consistently performed during the window of implantation (WOI), which was determined by identifying endometrial receptivity transcriptomic profile in individual AS patients using a commercially available endometrial receptivity analysis (ERA) test. Hormonal treatment consisted of 6 mg estradiol valerate daily from the second day of menstruation for 10 to 12 days, followed by 400 mg natural micronized progesterone every 12 h for an additional 4 to 6 days.

$CD133^+$ BMDSCs were mobilized using granulocyte-CSF (G-CSF) injections at 10 mcg/kg, collected, and then isolated via peripheral blood apheresis. To ensure consistency and

avoid additional confounding variables, new patient exclusion criteria were implemented, including mobilization of fewer than 30 million cells with a purity of at least 70% and viability of 50%, refusal of a central venous catheter when medically necessary, or unstable medical condition. Following the isolation of $CD133^+$ BMDSCs, a minimally invasive radiology intervention was performed through the left brachial artery to deliver cells into the spiral arterioles of the endometrium, using a microcatheter to reach the uterine arteries.

Endometrial biopsies from AS patients before and after $CD133^+$ BMDSC treatment were used for scRNA-seq analysis and EEO development. Additionally, $CD133^+$ BMDSCs isolated from one sample were characterized by scRNA-seq. **Table 3** summarizes the clinical data of AS patients included in the study, also described in **Supplementary information 1** (Supplementary info (online)).

Table 3. Clinical features of the Asherman syndrome patients involved in this study

Study subject	Age	BMI	Ethnicity	Obstetric formula (GTPAL)	AS predisposing factor	AS grade	Outcome after BMDSC therapy	Change in Endometrial thickness after BMDSC therapy (mm)
Ent-5	40	20.8	Caucasian	11000	Curettage after placental remnants	Severe Stage III	No pregnancy	4.0 - 5.6
Ent-7	34	21.0	Caucasian	30030	Curettage after miscarriage	Moderate Stage II	Live birth	4.5 - 5.7
Ent-8	36	29.7	Caucasian	10010	Curettage after miscarriage	Severe Stage III	Miscarriage	3.6 - 5.1

Ent-9	39	19.8	Caucasian	30030	Curettage after voluntary abortion	Moderate Stage II	Live birth	4.3 - 6.5
Ent-10	39	22.3	Caucasian	11001	Curettage after placental remnants	Severe Stage III	No pregnancy	3.0 - 4.5
Ent-12	43	29.7	Arabic	20020	Curettage after voluntary abortion	Moderate Stage II	No pregnancy	4.3 - 5.5
Ent-13	39	20.0	Caucasian	30030	Curettage after placental remnants	Severe Stage III	Miscarriage	4.2 - 5.6
Ent-14	40	25.9	Caucasian	30030	Curettage after miscarriage	Moderate Stage II	No pregnancy	3.0 - 5.7
Ent-15	41	22.7	Caucasian	31021	Curettage after placental remnants	Moderate Stage II	Ongoing pregnancy	3.6 - 4.1

Abbreviations - AS (Asherman Syndrome), BMDSC (Bone marrow-derived stem cell), BMI (Body Mass Index), GTPAL (Gravidia, Term, Preterm, Abortions, Live birth).

1.3. Control sample recruitment

Transcriptomic profiles of endometrial cells from 10 fertile women in the secretory phase were collected from a previous study (Wang et al., 2020); the data in the GSE111976 GEO dataset were used as "secretory controls". Transcriptomic profiles of endometrial cells from 6 fertile women in the WOI were also collected from the GSE111976 GEO dataset and used as "WOI controls." Transcriptomic profiles of 6 newly processed

endometrial cell samples collected during the WOI from healthy donors were also used as "WOI controls." Control sample collection was conducted under the ethical approval of the Research Ethics Committee of the University of Tartu (ref: 302/T-4), and informed consent was obtained from every participant. All samples were obtained from fertile and asymptomatic women during the WOI, following previously published clinical protocols and sample collection procedures (Wang et al., 2020). These samples were used for scRNA-seq analysis, EEO development, or fixed with paraformaldehyde and embedded in paraffin for tissue section hematoxylin and eosin staining (H&E) or other immunohistochemical analysis. **Table 4** describes the metadata from healthy control samples within the WOI, also described in **Supplementary information 1** (Supplementary info (online)).

Table 4. Metadata of healthy endometrial biopsy donors

Study subject	Age	BMI	Ethnicity	Obstetric formula (GTPAL)	Assay
EST-5-021-G2	26	23.5	Caucasian	31021	Tissue transcriptomics
EST-5-032-G2	27	23.9	Caucasian	31021	Tissue transcriptomics
EST-5-034-G2	33	22.0	Caucasian	22002	Tissue transcriptomics
EST-5-035-G2	40	23.0	Caucasian	22002	Tissue transcriptomics
EST-5-036-G2	27	23.9	Caucasian	11001	Tissue transcriptomics
EST-5-043-G2	32	21.0	Caucasian	31021	Tissue transcriptomics
CO 8	30	19.8	Caucasian	00000	Organoid experiments
CO 9	36	NA	Caucasian	00000	Organoid experiments
CO 14	29	21.9	Caucasian	00000	Organoid experiments

Abbreviations - BMI (Body Mass Index), GTPAL (Gravidia, Term, Preterm, Abortions, Live birth), NA (Not available).

2. Single-cell transcriptomics of endometrial tissue

2.1. Sample description

For the scRNA-seq study of endometrial tissue, 9 AS endometrial biopsies before, 9 after $CD133^+$ BMDSC treatment, and 6 control biopsies from the WOI were processed and analyzed (**Table 3** and **Table 4**). Additionally, transcriptomic data from 10 endometrial biopsy samples collected during the secretory phase were included in our dataset (Wang

et al., 2020). The transcriptomic profiles of 18 AS patient samples, 12 healthy controls within the WOI, and 10 controls within the secretory phase were analyzed.

2.2. Biopsy processing

Endometrial biopsies were disassociated into single cells using a two-stage protocol that separates tissue into epithelial-enriched and stromal fibroblast cell suspensions. Following this protocol, endometrial biopsy fragments were rinsed with phosphate-buffered saline (PBS) in a petri dish to eliminate any blood and mucus that may be present. After removing the remaining PBS, tissue fragments were subjected to mechanical disaggregation, mincing them into small pieces using scalpels. Then minced biopsies were digested enzymatically using a 3 ml collagenase mix, which includes collagenase [1 mg/ml] (Collagenase V, Sigma) in RPMI medium supplemented with fetal bovine serum (FBS) [10%] and DNase I (Sigma), at 37ºC and shaking continuously at 175 rpm for 20-40 mins in a 15 ml Falcon tube. During this digestion, the Falcon tube was sealed with parafilm (Sigma) and placed horizontally to facilitate enzyme action. After 20 mins, digestion status was evaluated, and digestion time was extended in 5-min increments if necessary. This first enzymatic digestion step primarily dissociates stromal fibroblasts into single cells, leaving the epithelial glands and lumen undigested. Once this digestion was completed, the reaction was stopped by adding 10 ml of RPMI supplemented with FBS [10%], and the resulting solution was filtered (through a 100 µm cell strainer) into a 50 ml Falcon tube, leaving single fibroblasts in the tube and epithelial glands retained in the strainer. These glands were recovered from the strainer by pipetting 10 ml of PBS through it, and the resulting solution was centrifuged to remove PBS.

A second digestion was performed by incubating tissue glands in 3 ml Trypsin medium (Trypsin-EDTA [0.25%] with DNase I) for 10 mins at 37ºC and shaking (175 rpm). After stopping the second enzymatic digestion with 10 ml RPM medium supplemented with FBS [10%], the two resulting cell solutions were filtered through a 100 µm cell strainer into new 50 ml Falcon tubes, centrifuged, and resuspended in 1 ml RPMI medium.

The MACS dead cell removal kit (Miltenyi Biotec) was used to remove dead cells. Approximately 2 million stromal cells (65% viability) and 1 million epithelial cells (40% viability) were obtained from each biopsy.

2.3. Single-cell transcriptomics library preparation

Around 18,000 cells were loaded into a Chromium Next GEM Chip G (10x Genomics) and run in a Chromium Controller (10x Genomics), a process which encapsulates each cell in a GEM (Gel Beads-in-emulsion) containing the necessary reagents for the reaction to synthesize cDNA library from cells mRNA. cDNA synthesis and amplification were performed using the Single Cell 3' Reagent Kit v3.1 (10x Genomics). 25% of the resulting cDNA was used for enzymatic fragmentation, end repair, A-tailing, adapter ligation, and amplification, (with an expected yield of 0.1 ng/µl and a peak size between 200 and 9000 bp as determined in a TapeStation using HSD1000 assay reagents) serving as a quality control. Finally, libraries were quantified in a TapeStation using HSD1000 assay reagents. After this quantification, which should show a peak of around 400 bp, libraries were sequenced in a NovaSeq System 6000 (Illumina) according to the manufacturer's instructions.

2.4. Data preprocessing

2.4.1. Gene-to-cell count matrices alignment and quantification

Cell Ranger suite software (version 3.1.0) (Lange et al., 2022) was used to process single-cell transcriptomic data. BCL files from the Illumina NovaSeq 6000 were demultiplexed using the CellRanger *mkfastq* wrapper command of *bcl2fastq* (Illumina). Libraries FASTQ files were then mapped using the human reference genome (GRCh38-3.0.0) provided by 10X Genomics. The gene expression count matrices per cell were computed using the count pipeline. This pipeline includes read alignment using the STAR mapping tool, unique molecular identifier (UMI) counting, cell barcode calling, and filtering of empty droplets. The filtering step uses a simple Good-Turning smoothing model of background gene expression profiles to distinguish low RNA content cells from ambient RNA.

2.4.2. Cell quality control filtering and doublet detection

Cells with low quality within each sample were filtered based on observed gene number, count number, and the percentage of mitochondrial read counts. Cells deviating by 1 median absolute deviation (MAD) in two or more conditions were removed from the sample. R version 4.1 was used for these quality control and downstream analyses. Two methods were used to detect doublets: *DoubletFinder* (2.0.3) and *scds* (1.6.0) packages. The expected doublet formation rate was set for each sample based on the cells recovered by Cell Ranger. A hybrid approach (from the scds package) was used to avoid removing false-positive doublets. Only cells identified as doublets by both algorithms were removed from the samples. Quality control metrics are included in **Supplementary information 1** (Supplementary info (online)).

Assessing the extent to which the expression of WOI genes originated from ambient RNA and identifying these genes in cell populations outside the epithelial compartment used the CellBender (0.2.2) tool on the raw count matrices generated by the CellRanger pipeline. Examining Cell Ranger's Barcode Rank Plot for each sample enabled the configuration of CellBender (Fleming et al., 2022) to account for barcodes associated with empty droplets containing ambient RNA. The ambient plateau was selected, consisting of barcodes below the plot knee (that present relatively low counts) for each sample. A false discovery rate (FDR) threshold was also established at 0.05. The remaining counts obtained from the difference between corrected and uncorrected represent contaminating counts that were subsequently employed to analyze the comparison between AS and WOI control samples. This process led to the identification of a specific gene set signature related to ambient RNA, represented by the percentage of ambient RNA contamination reads present in each gene (filtered out by CellBender).

2.5. Data integration, cell clustering, and annotation

2.5.1. Integration across conditions and cell clustering

Seurat package v.4.0.1 (Hao et al., 2021) was used to aggregate, process, and integrate individual samples. Firstly, the *merge* function was used to perform sample-to-sample

aggregation for each condition dataset, which resulted in four aggregated datasets: 1) AS endometrium, 2) patient-matched AS endometrium after CD133$^+$ BDMSC treatment, 3) secretory control endometrium from a previous dataset (GSE111976) (Wang et al., 2020), and 4) control WOI endometrium (GA#874867). Cells with fewer than 750 detected genes and more than 25% mitochondrial content were excluded from the resulting count matrices due to failing the quality control criteria. Then, the *SCTransform* function was used to process each aggregated dataset to integrate them with the dataset of contrast for two integration analyses: 1) AS endometrium samples collapsed with control endometrium samples, and 2) AS endometrium samples collapsed with CD133$^+$ BDMSC-treated endometrium samples (described below in sections V.1 and V.3). This function pipeline integrates the different conditions by applying a regularized negative binomial regression, enabling the identification of condition-to-condition shared cell identities and the conduction of differential expression analysis.

Cell cycle phase and mitochondrial ratios were regressed out from the integrating datasets. Variable genes for integration were selected using *SelectIntegrationFeatures*. The anchoring vectors were identified across datasets by applying *PrepSCTIntegration* and *FindIntegrationAnchors*, while *integrateData* was used for integration steps (with the normalization method set to SCT). Principal component analysis (PCA) and uniform manifold approximation and projection for dimension reduction (UMAP) were used for dimensionality reduction and to visualize cell clustering. Using an anchor integration protocol, cell populations identified in the AS endometrium were used to transfer cell labels to the CD133$^+$ BDMSC-treated AS endometrium dataset to detect cell types and uncover unique cell types present in AS.

2.5.2. Integration by the dataset of origin: Asherman syndrome mapping

The Seurat integration protocol was applied to integrate the cell populations detected in AS and secretory control endometrial samples; the secretory control dataset was derived from the 10X Single-cell 3'v3.1 dataset (GSE111976). After integration, the AS and secretory control endometrial samples were separated into two objects (to ensure proper integration) and normalized with the *SCTransform* function. *IntegrateData* was

applied using the 3000 most variable genes from the initial dataset as the integration factor, and the conservation of canonical markers was evaluated in both study conditions to validate the integration set. Canonical marker genes used for cell type identification were previously published (Alsaigh et al., 2022; Bister et al., 2021; Björklund et al., 2016; Buechler et al., 2021; Garcia-Alonso et al., 2021; Kirkwood et al., 2022; Ren et al., 2022; Saichi et al., 2021; Schupp et al., 2021; Tan et al., 2022; Vento-Tormo et al., 2018; Wang et al., 2020; Yang et al., 2021), and are available in **Supplementary information 2** (Supplementary info (online)). Canonical marker gene expression profiles across populations are included in Annex 2.

2.5.3. Integration according to treatment: Cartography during cell therapy

Similar processing was performed using the same SCT pipeline to integrate AS endometrial samples before and after $CD133^+$ BDMSC treatment. The Seurat object obtained was split into two, separating the study conditions (pre- and post-treatment).

This study used the *SelectIntegrationFeatures* function and the 4000 most variable genes presented in the combined datasets. In addition, the *FindCluster* function of the *clustree* (0.4.4) package was used to evaluate the optimal resolution number, generating several clusters with a degree of resolution between 0.1-2 (with increments of 0.1). The optimal resolution for labeling the different clusters was determined to be 0.8 after a manual review of the generated UMAPs and *clustree* output. The integration was validated by evaluating the conservation of the canonical markers (**Supplementary information 2**) (Supplementary info (online)) in pre- and post-treatment AS endometrial samples.

2.5.4. Cell type annotation in single-cell datasets

To study the differential expression of each cluster, the Wilcoxon Rank Sum test was used, and the p-values were adjusted using the FDR method. Differentially expressed genes in each cluster were compared with other clusters to identify the major constitutive cell types. Two different approaches were used to annotate the clusters. The first was already described and contrasted with the biological information available in the databases. The second approach was applied only to the main annotated cell types

and their descriptive gene markers (**Supplementary information 2**) (Supplementary info (online)) (Annex 3) to annotate the cell subtypes of the WOI with higher resolution. To accomplish this annotation, the Seurat anchor transfer tag protocol was employed, with the most detailed identities propagated from two recently published endometrial atlases (Garcia-Alonso et al., 2021; Tan et al., 2022) and only identities with a score higher than 0.7 were selected for further annotation. Next, cell types were re-evaluated, and clusters were manually reannotated with new consistent transferred labels and marker profile expression.

2.6. Differential cell abundance analysis

The nb.glm function (edgeR v3.34.0 package) was employed to analyze the cell ratio across the different experimental groups. This resulted in a count matrix for each sample, where each matrix contains the several cell types detected in the sample. This count matrix was then used as input to compute the differential abundance (DA) test across cell types, and the FDR p-value adjustment method was applied. Before performing differential abundance analysis, all cells scored as cycling were removed.

2.7. Differential gene expression and gene signature score

The differential expression analysis across the treatment stages and the different cell types was performed using the *FindMarkers* function of the *Seurat* package. The Wilcoxon Rank Sum test was performed, and the FDR method was used to correct the p-values; all the genes with an FDR of less than 0.05 were considered significant. Then, the *escape* (v1.6.0) R package (Borcherding et al., 2021) was used in the gene cluster to assess endometrial function in the secretory phase between treatment groups. The score for each cell in the data set was then calculated using the *enrichIt* function, with the *UCell* method employed to determine the scores. Finally, scoring differences between the different phases of treatment were studied along cell types stromal, perivascular (PV), epithelium, AS epithelium, and endothelium. A Wilcoxon test (getSignificance function) was performed to evaluate statistical differences, and p-values were corrected with the FDR method. The gene set used for endometrial function in the

secretory phase included *SCGB1D2, MT1F, MT1X, MT1E, MT1G CXCL14, WNT5A, SFRP1, ZFYVE21, CILP, SLF2, MATN2,* and *S100A4*.

2.8. Cell-to-cell communication network analysis

To study the possible signaling interactions between cells, total interaction probabilities and communication information flows were determined with the *CellChat* v1.1.3 package (Jin et al., 2021). The first measure indicates the probability of communication between two cell types; the total probability of interaction is split into two parts: the probability of interaction between the sender and receiver cell, considering the number of interactions (ligand-receptor or L-R pairs expressed) and the level of expression (strength of the interaction). A database of 229 families of signaling pathways was used to obtain information regarding interactions; this curated list of molecules considers the known structure of L-R pairs, including multimeric complexes, soluble agonists and antagonists, stimulators, and inhibitory co-receptors. The second measure, the communication information flow, assesses the amount of information exchanged between several cells through various interactions. A higher value of communication information flow between cell populations indicates a more complex communication network. The *population.size* argument in the *computeCommunProb* function was used to correct the influence of each cell population and remove cycling cells from the downstream analysis. The cell-to-cell communication (CCC) networks were filtered to exclude those with fewer than ten cells. The *ranknet* function with a significance threshold of 0.05 was used to test for network differences between AS and control endometrial samples and between AS endometrial samples pre- and post-treatment with $CD133^+$ BMDSCs. These comparisons included only common cell types. Significantly altered signaling pathways between groups are highlighted in the bar graphs of the flow of information. To explore these plots further, interaction probability scatter plots can be used to identify the receiving and sending cells. The contribution of each L-R pair to a pathway is also shown in interaction probability plots.

3. Histological immunohistochemistry

3.1. Histological sections preparation for hematoxylin and eosin staining

Tissue samples for immunohistochemistry were fixed in 4% paraformaldehyde (PFA) overnight at 4ºC in a rotating platform. After the fixing process, tissue samples were embedded in warm paraffin and allowed to dry while attached to a metal mold. After drying, multiple sections were obtained using a microtome (MRP2015, LUPETEC), with 3 to 4 sections on each slide. For H&E staining, sections were deparaffinized and rehydrated with several incubation and washing steps using xylene (3 times x 3 min), 100% ethanol (3 times x 3 min), 95% ethanol (1 time x 3 min), 80% ethanol (1 time x 3 min) and deionized H_2O (1 time x 5 min). Then, excess water was removed, and slides were incubated with hematoxylin (Poly Scientific, Cat. No. s212A) for 3 min, rinsed with deionized H_2O, and incubated for 5 min. Slides were dipped in acidified ethanol (8-12x) to destain and then washed with tap water (2 times x 1 min) and deionized water (1 time x 2 min). Excess water was blotted, and slides were incubated with eosin (Poly Scientific, Cat. No. s176) (1 x 30 s) and incubated in 95% ethanol (3 times x 5 min), 100% ethanol (3 x 5 min), and xylene (3 x 15 min). Finally, a coverslip was placed over sections using a droplet of Permount (FisherScientific, Cat. No. SP15-100) and left to dry overnight.

3.2. In-situ RNA hybridization using RNAscope

The Advanced Cell Diagnostics RNAscope® Multiplex Fluorescent Detection Kit v2 (Bio-techne) was used according to the manufacturer's instructions for situ RNA hybridization. Briefly, to dry and ensure adhesion of the human endometrial samples to the SuperFrost Plus slides (VWR), 5 µm of formalin-fixed paraffin-embedded (FFPE) samples were applied to the slide and placed in the HybEZ hybridization oven (Advanced Cell Diagnostics) at 60°C for 1 h. The samples were then rinsed twice for 5 min at room temperature (RT), first in Histo-Clear I and then in Histo-Clear II, followed by washing in fresh absolute ethanol at RT and drying at 60ºC for 5 min to deparaffinize FFPE sections. Next, samples were incubated for 10 mins at RT in RNAscope® hydrogen peroxide and immediately washed with distilled water. Slides were pre-warmed in a steamer at 95°C

before incubation in 1X RNAscope Target Retrieval Reagent for 15 mins, then washed with distilled water and incubated in absolute ethanol for 3 mins; slides were then allowed to dry at RT. Slides were incubated with protease solution (RNAscope® protease plus) in the HybEZ hybridization oven at 40ºC for 30 min. The target probes for HS-SLPI-C1 (*Homo sapiens* SLPI) were added to the sections and incubated for 2 h at 40ºC. After incubation, the slides were washed twice for 2 min with wash buffer before amplification. Multiplexv2 AMP1, AMP2, and AMP3 amplifier probes were then applied sequentially, incubating at 40ºC for 30 min for the first two probes and 15 min for the third probe. For detection, the slides were incubated with RNAscope® Multiplex FLv2 HRP-C1 for 15 min, then with a 1:750 dilution of the appropriate fluorophore (SLPI combined with the TSA Vivid™ Fluorophore kit 520 nm, Cat. #7523) and finally with RNAScope Multiplex FL v2 HRP Blocker for 15 min. Finally, the slides were incubated with 4',6-diamidino-2-phenylindole (DAPI) for 30 s to stain nuclei and mounted with Prolong® Gold Antifade Reagent (Life Technologies, Cat. No. P36934). In these assays, RNAscope 3-Plex Negative Control Probe (Cat. No. PN320871) and RNAscope 3-Plex Positive Control Probe (Cat. No. PN320861) were used as controls to image the target probe and quantify the background signal. Images were captured on a Leica TCS-SP2-AOBS confocal microscope using the 63x oil objective, with images showing single or clustered dots considered positive and those showing no fluorescence for the target RNA considered negative.

4. Development of endometrial epithelial organoids

4.1. Sample description

EEOs were developed from samples isolated from 3 AS patients (Ent-13, Ent-14, and Ent-15, **Table 3**) pre- and post-treatment with CD133+BDMSCs and three new WOI controls (CO8, CO9, and CO14, (**Table 4**)) and used for every performed analysis between passages 0 and 4. Since all previous analyses on endometrial biopsies focused on the secretory phase and the WOI, EEOs were subjected to hormonal treatments that mimicked the menstrual cycle, focusing on the WOI (Section 4.3).

4.2. Tissue processing and endometrial epithelial organoid culture

Generating EEOs employed a protocol described by Boretto et al. with minor modifications (Boretto et al. (2017)). Endometrial biopsies were enzymatically digested (Section 2.2) to obtain a suspension of cells for culture and embedding in an artificial extracellular matrix in microwell plates. The total number of cells in this suspension was quantified using the EVE automatic cell counter (NanoEntek), and the necessary volume to achieve 20,000 cells per drop was calculated. The determined volume was centrifuged at 300 x g for 5 min, and the pellet was resuspended in a mix of 70% Matrigel (Corning, Cat. No. 356231) and 30% DMEM/F12 (Thermo Fisher Scientific, Cat. No. 11330032) complemented with 2 µM rho-associated protein kinase inhibitor Y-27632 (Merck, Cat. No. SCM075). In pre-warmed 48-well plates, 20 µL of the cell suspension (25,000 cells/drop) was cultured and incubated at 37ºC in 5% CO_2 for 30 min. After this time, the Matrigel droplets formed a gel, and the organoid culture medium (composition described in **Table 5**) was added and incubated. The first pass (P0) lasted 12-14 days, with medium changes every 48 h. Once EEOs had formed, passages were carried out every seven days, with medium changes every 48 h.

Table 5. Endometrial epithelial organoid culture medium

Reagent	Final concentration	Commercial brand	Reference
DMEM F12 (+ Glutamine + HEPES)	1x	ThermoFisher Scientific	31331028
Noggin	100 ng/ml	R&D Systems	6057-NG-100
RSPO-1 (R-spondin 1)	200 ng/ml	Peprotech	120-38
Insulin-Transferrin-Selenium (ITS)	1%	Life Technologies	41400045
Penicillin/streptomycin	1%	Life Technologies	15140122
N2 supplement	1%	Life Technologies	17502048
B27 supplement	2%	Life Technologies	12587010
N-acetyl L-cysteine	1.25 mM	Merck	A7250-50G
Nicotinamide	1 mM	Merck	72340-100G
A83-01	0.5 µM	Merck	SML0788-5MG
p38 inhibitor (SB202190)	10 µM	Merck	S7067
EGF (epidermal growth factor)	50 ng/ml	R&D Systems	236-EG-01M
b-FGF (basic fibroblast growth factor)	2 ng/ml	Thermo Fisher Scientific	PHG0264
FGF10 (fibroblast growth factor 10)	50 ng/ml	Peprotech	100-26
Rock Inhibitor (Y-27632)	9 µM	Merck	SCM075

For passaging, Matrigel drops containing EEOS were dissolved by pipetting with cold DMEM/F12 (lacking enzymes, serum, and growth factors) to ensure maximum recovery. EEOs were then incubated with TrypLE (ThermoFisher) and 1 µM Y-27632 for 5 min at 37°C, followed by mechanical trituration to achieve complete dissociation. The resulting cell homogenate was centrifugated for 5 min at 300 x g, and the cell pellet was resuspended in 70% Matrigel and 30% DMEM/F12 supplemented with Y-27632 [2µM]. The droplets were seeded in pre-warmed 48-well plates, and a culture medium was added after 30 min of incubation at 37ºC.

4.3. Hormonal treatment

For hormonal treatment after organoid generation, 20,000 EEO cells were seeded in 48-well plates, incubated with an organoid culture medium for 48 h, and treated with steroid hormones as described in the literature (Kagawa et al., 2022). Briefly, organoids were cultured with 10 nM 17β-estradiol (E_2) (Sigma Aldrich, Cat. No. E2758) for 48 h, followed by the mixture of 10 nM E2, 1 µM 17-medroxyprogesterone acetate (MPA) (Sigma Aldrich, Cat. No. M1629), 0.25 mM sodium 8-bromoadenosine 3', 5'-cyclophosphate (cAMP) (Merck, Cat. No. E2758), and 10 µM XAV939 Tankyrase Inhibitor (Deltaclon, Cat. No S1180) for a further four days.

4.4. Endometrial epithelial organoid counting and diameter measurement

Multiple microscopic images were taken to count the number of EEOs forming in each Matrigel drop (Thermo Fisher, EVOS M5000), providing a reliable representation of the total number of EEOs. Each droplet was split into two depth sections, and four regions were imaged. EEOs were counted in two diagonal images of each section to obtain an average of these images. To infer the total number of EEOs per drop, the average was multiplied by the number of sections (2) and the number of divisions in each section (4), with three experimental replicates per condition.

Four random images were taken in two depth sections from three drops in three independent experiments to measure EEO diameter. The end-to-end diameter of EEOs was measured using ImageJ (1.54). The mean and standard deviation for the number of

EEOs and their diameter were plotted in corresponding figures. An unpaired Student t-test with Welch's correction was used for statistical analysis between conditions.

4.5. Statistical analysis

All statistical tests were performed using the GraphPad Prism Software (v9.4). Data were first analyzed for normality, and then analyses of significant differences between EEO variables were carried out using the unpaired or paired two-tailed Student t-test. P-values lower than 0.05 were considered statistically different and referred to as * $p < 0.05$, ** $p < 0.01$, and *** $p < 0.001$. Data are presented as the mean ± standard deviation (SD) in all the presented cases or else included in the figure legends. The number of experiments carried out with biologically independent samples is listed in corresponding figure legends.

5. Immunohistochemical analyses of endometrial epithelial organoids

5.1. Whole endometrial epithelial organoid immunohistochemistry

EEOs cultured on Matrigel droplets were harvested using a Cell Recovery Solution (Corning, Cat. No. 354253). The medium was removed from each well, and 1 ml of Cell Recovery solution was added and incubated for 1 h with agitation at 4ºC. Following incubation, EEOs were recovered using wide-bore tips (Axygen, Cat. No. TF-1005-WB-R-S) and centrifuged at 300 x g for 5 min. The resulting pellet was resuspended with 4% PFA for 1 h at 4ºC for cell fixation. Then, PFA was removed after centrifugation (300 x g for 5 min), and three washing steps (with PBT 0.1%) were performed. Samples were stored for future staining in 70% ethanol for up to one month.

For antibody incubation, stored samples were centrifuged (300 x g for 5 min) to remove ethanol. Pellets were resuspended in PBT [0.5%] and incubated for 30 min under agitation at RT. PBT was removed after centrifugation (300 x g for 5 min), and cells were incubated with a blocking solution (PBT [0.1%] + BSA [2%]) for 30 min under agitation at RT. EEO samples were washed twice with PBT [0.1%] for 10 min under agitation and incubated with the specific primary antibody (**Table 6**) overnight under agitation at 4ºC.

Samples were washed three times with PBT [0.1%] under agitation for 10 min at RT and incubated with specific secondary antibodies (**Table 6**) under agitation for 4 h at RT. After incubation, samples were incubated with DAPI [200 ng/µl] for 30 min under agitation at RT and washed three times with PBT [0.1%]. Washed EEOs were pipetted in glass bottom well plates (Ibidi, Cat. No. 80827), and images were acquired using a Stellaris 5 confocal microscope (LEICA).

Table 6. List of antibodies used in the immunohistochemical analysis of endometrial epithelial organoids

Type	Antigen	Dilution	Brand	Catalog #
Primary Ab	Rabbit anti-E-cadherin	1:200	Cell Signaling Technology	3195T
Primary Ab	Rabbit anti-Pan-Cytokeratin	1:400	Abcam	ab217916
Primary Ab	F-actin AF 488	1:200	ThermoFisher	A12379
Primary Ab	Mouse anti-Ki67	1:200	BD Biosciences	556003
Primary Ab	COL1A2	1:200	ThermoFisher	PA5-29569
Secondary Ab	Goat anti-rabbit AF 555	1:400	ThermoFisher	A21428
Secondary Ab	Goat anti-mouse AF 488	1:400	ThermoFisher	A11001

Abbreviations - Ab (antibody), AF (Alexa fluor)

Statistical analyses for Ki67 image measurements were performed as described in section 4.5. When representative images are displayed without an associated quantification graph, immunostainings were performed in at least three biological samples obtained from independent samples.

5.2. Immunohistochemical analysis of endometrial epithelial organoid sections

For sections, EEOs were fixed according to the protocol detailed in the previous section (5.1). Subsequently, 70% ethanol was removed by centrifugation (300 x g for 5 min), followed by two washes with PBS. Samples were then embedded in hot paraffin using a metal mold and a plastic support. Once paraffin was dried at 4ºC, the metal mold was separated, and sections were made using an ultramicrotome (EM UC6 Leica) device, plated onto glass slides, and dried. The protocol outlined in section 3.1 for tissue slides was followed for deparaffinization and H&E staining of EEO sections.

6. Single-cell transcriptomics of endometrial epithelial organoids

6.1. Sample description

EEOs were dissociated according to the passage protocol (described in section 4.2) with an additional cell count (10X Genomics, as previously described). Cell suspensions from each condition were loaded onto 10X chips for library preparation and sequencing, as described in section 2.3. Data preprocessing and integration were performed as described for biopsy data in sections 2.4 and 2.5.1. Differential abundance and gene expression analysis were also performed for biopsy data in sections 2.6 and 2.7.

6.2. Identifying endometrial epithelial organoid cells using machine learning

Following an approach similar to that described by La Manno et al. (2016), in vivo cell subtypes were utilized to infer the transcriptomic identity of EEO cells. Previously described genetic markers (Garcia-Alonso et al., 2021; Wang et al., 2020) were used to label different subpopulations of epithelial cells in the GSE111976 dataset.

The most representative genes were selected before training the model. Briefly, the Seurat *FindMarker* function was used with the 4,000 most variable genes. Then, the genetic markers specific to each cell type were calculated with the previously selected gene set. Finally, three cell type specificity metrics were applied: fold-increase*fraction-positive^0.5, fold-increase*fraction-positive, and fold-increase and the best-ranked 1,000 genes were selected considering all three. The identity of EEO cells was then predicted by machine learning logistic regression modeling using the R packages *caret* (v6.0-92) and *glmnet* (v4.1-4) (Kuhn, 2008). 70% of EEO cells in the dataset were used to train the model, and the remaining 30% were used to evaluate the model in the testing phase, with the selection of both groups being random. In logistic regression, the hyperparameters were fine-tuned by performing a cross-validation of 10 iterations, in each of which the lambda value was changed by 0.01 by stepping through the threshold from 0.001 to 0.01. In contrast, the value of alpha remained at 1. The result obtained in the test phase was an optimal lambda value of 0.001 with an accuracy of 0.9446 (0.9402,

0.9488 95% CI). Finally, a polygonal representation was used to represent the probabilities of the cell types inferred from the organoids.

Then, Dunn's multiple comparison test was performed, followed by Kruskal-Wallis's test to study the differences between the probabilities of cell types in the different experimental groups, and the Bonferroni method was used to correct the p-values. The next step was to evaluate the differential expression in the cells forming the organoids using the Wilcoxon rank sum test (FDR<0.05) as described above. The transcriptomic similarity between cells from biopsies and EEO cells was performed using the R *Harmony* (version 0.1.1) (Korsunsky et al., 2019) and *scPred* (version 1.9.2) (Alquicira-Hernandez et al., 2019) packages.

The transcriptomic similarity of AS EEOs and control EEOs treated with CD133+ BMDSCs to their in vivo biopsy samples was then determined. First, only in vivo epithelial cells were included, and the 1,000 most representative variables were selected from the in vivo dataset. The effects of the cell cycle phase, the number of genes detected, and the mitochondrial ratio were then removed by linear regression analysis after applying the *ScaleData* function, and the first 30 principal components were calculated. The data was then integrated by the epithelial cell subtype rather than the experimental group using the *RunHarmony* function. The transcriptomic signal corresponding to the experimental groups, pre- and post-treatment with $CD133^{+}$ BMDSCs, AS, and control, were obtained by this approach. The *scPred* software was used to build a predictive model for the EEO dataset. Using the 10-nfold cross-validation method, a support vector machine was trained with the radial basis function kernel (svmRadilal). The optimal value for the constant C was 1, with values of 0.25 and 0.5 also evaluated. Finally, the EEO group probabilities were derived in a triangular representation.

V. Results

V. Results

1. Cellular characterization of the endometrium from patients with Asherman syndrome at single-cell resolution

We explored the endometrium's cellular complexity and diversity to better understand the origins of intrauterine adhesions (IUA) and endometrial dysfunction in AS patients. For this purpose, we employed endometrial biopsy samples from AS patients and healthy donors (representing the control group for comparisons) to discover the main cell types and molecular mechanisms behind the disease. As another potential contributor to infertility, we explored the displacement of the window of implantation (WOI) in AS patients (including those with a hormone replacement therapy (HRT) cycle).

In all cases, we characterized the transcriptomic landscape of the AS endometrium through scRNA-seq of endometrial samples from AS patients and compared said profiles with healthy donor samples within the secretory phase and the WOI. After applying quality control filters and batch correction (section IV.2.4.2), we included 128,503 single-cell transcriptomes in our dataset, comprising 69,202 healthy controls in the secretory phase from 10 donors from a previous study (Wang et al., 2020), 66,064 controls within the WOI from 12 healthy biopsies (including 6 samples from previous secretory phase controls), and 40,336 from 9 AS biopsies. From these data, we complied a comparative cellular atlas of the AS endometrium by exploring marker gene expression in clusters and then comparing these data against previously published endometrial atlases (Garcia-Alonso et al., 2021; Wang et al., 2020) (section I.3).

1.1. Single-cell atlas of the Asherman syndrome secretory endometrium

Clustering single-cell transcriptomes from the AS endometrium compared to previously published secretory phase controls identified 18 cell types (**Figure 10**). These populations include a large proportion of stromal fibroblasts and epithelial cells and minor proportions of endothelial cells, perivascular (PV) cells, and immune subpopulations (such as B cells, natural killer (NK) cells, cytotoxic NK cells, dendritic cells, mast cells, macrophages, $CD8^+$ T cells, and double-negative (DN) T cells). Immune cells

also included a distinct subset of T cells characterized by the expression of the semi-invariant αβ T cell receptor (TCR), which we identified as mucosal-associated invariant T (MAIT) cells. In an initial comparison, we identified three distinct populations in AS samples: smooth muscle cells (SMC), contractile PV cells, and a stressed epithelium, which we designated AS-epithelium. Additionally, we observed a lower density in epithelium and ciliated epithelium clusters (we provide a detailed analysis of all identified populations through a differential abundance analysis below).

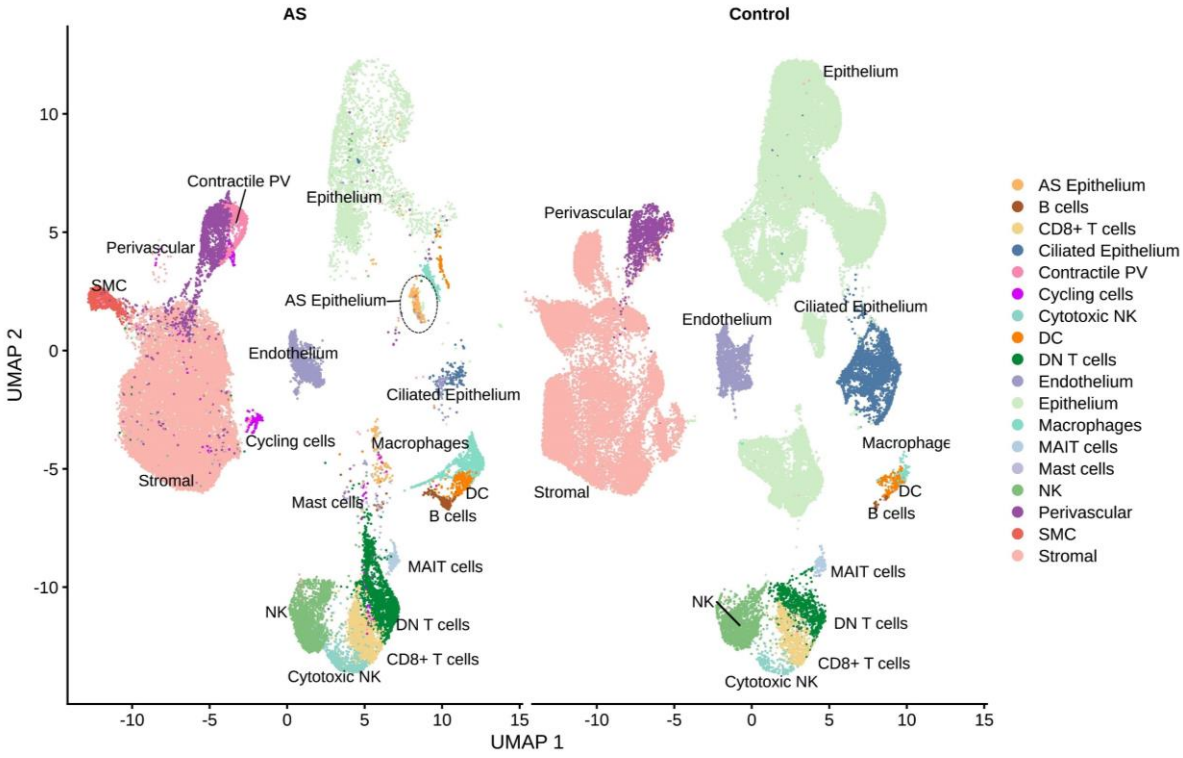

Figure 10. UMAP of cell clustering based on single-cell RNA sequencing from the Asherman Syndrome and healthy endometrium. Integration includes 40,336 biopsied cells from AS patients and 69,202 cells from healthy donors in the secretory phase. The dashed line highlights the AS-epithelium population. Abbreviations - AS (Asherman syndrome), DC (dendritic cells), DN (double negative), MAIT (mucosal-associated invariant T), NK (natural killer), PV (perivascular), SMC (smooth muscle cell).

In addition to the expression of canonical markers commonly used for cell type characterization, we described cell populations according to their top five differentially expressed genes (**Figure 11**). Based on this gene expression, we described two PV populations: i) those expressing G protein signaling 5 (*RGS5*), which we defined as pericytes/mural cells, and ii) those expressing genes related to contractile functions (such as *MYH11, TAGLN, MYL9,* or *ACTA2*) shared with SMCs, which we defined as

contractile PV cells. Notably, contractile PV cell and SMC populations displayed significant enrichment in AS samples compared to the healthy secretory phase endometrium.

We differentiated observed immune populations between myeloid and lymphoid lineages. Myeloid lineage cell clusters included dendritic cells expressing HLA II class genes (*HLA-DRA*, *HLA-DPA2*, *HLA-DPB1*, *HLA-DRB1*, and *CD74*), and macrophages characterized by the expression of *LYZ*, *IL1B*, and genes encoding for S100 calcium-binding proteins (*S100A8*, *S100A9*, and *S100A12*). Lymphoid lineage cell clusters included NK cells expressing *NKG7*, which we subdivided into a cluster of cytotoxic NK cells expressing the cytolytic-related gene *PRF1* and serine protease genes (*GZMB* and *GZMH*). We classified T cells into $CD8^+$ T cells (expressing *IL32, CCL5, IFNG,* and *TRBC2*) and DN T cells (expressing *CD3D, CD52, IL7R,* and *LTB*). In addition, we identified the MAIT cell population subcluster through their characteristic expression pattern (genes such as *LTB, KLRB1, IL23R,* and *IL4I1*), indicating an inherent ability to react to specific ligands without expansion and maturation of memory T cells (**Figure 10 and Figure 11**). Overall, we observed the overrepresentation of all these immune cell clusters in AS samples compared to healthy secretory phase controls.

We also observed significant alterations in epithelial cells in AS samples compared to healthy secretory phase controls, indicative of progressive fibrosis. Epithelial cells expressed canonical markers (such as *EPCAM, CLDN4,* and *WFDC2*) and metallothionein family genes (*MT1G, MT1H, MT1M,* and *MT1X*). We differentiated between a broader population of epithelial cells expressing *PAEP* and a smaller subset of ciliated cells identified by the expression of *CAPS*, a gene involved in cilium assembly (both with smaller cell clusters in AS samples as compared to the healthy secretory phase control (**Figure 10 and Figure 11**). Interestingly, we also discovered another cluster of epithelial cells only presented in the AS endometrium (cells enclosed by a dashed line in **Figure 10**), which does not express epithelial marker genes such as *PAEP* and *CAPS* but instead overexpresses cell stress-related genes, such as HSPA1A or *SOCS3*, the long non-coding RNA *SNHG9*, and the inflammatory serine protease inhibitor *SLPI*.

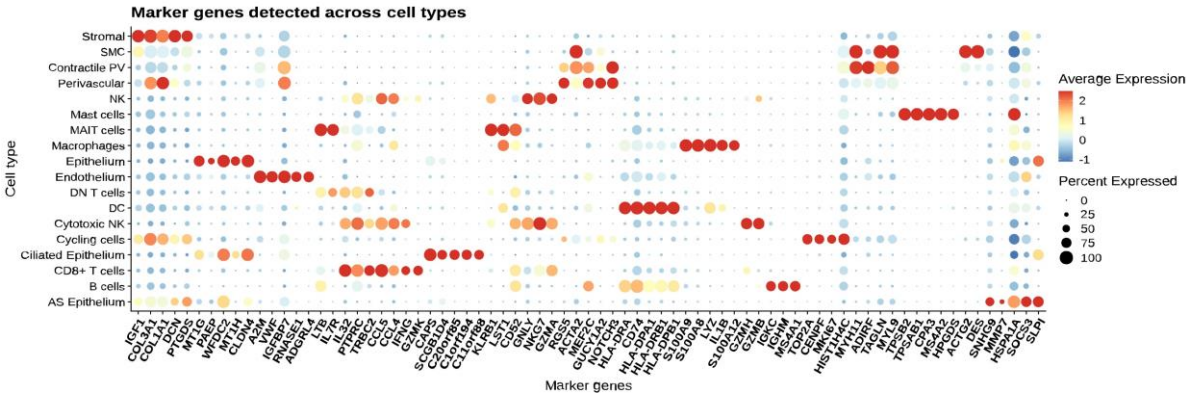

Figure 11. Dot plot indicating the top five differentially expressed genes in the main cell types identified in Asherman syndrome endometrium. Abbreviations - AS (Asherman syndrome) DC (dendritic cells) DN (double negative), MAIT (mucosal-associated invariant T), NK (natural killer), PV (perivascular), SMC (smooth muscle cell).

A comparison of the differential cell abundance between AS and healthy secretory phase control samples, using a Negative Binomial Generalized Linear Model (NB-GLM), revealed significant differences in cellular composition (**Figure 12**). Epithelial clusters presented the most significant differences in cell ratios; the proportion of epithelium and ciliated epithelium in the total cell count was significantly higher in control than in AS samples, with a False Discovery Rate (FDR) of less than 0.05 and 0.01 respectively. Conversely, SMCs, AS-epithelium cells, and contractile PV cells presented a higher number of cells (significance <0.001 for all). All immune clusters displayed a greater representation in AS samples (macrophages, B cells, mast cells, and DC; significance <0.05, and DN T and cytotoxic NK cells; significance <0.1). (**Figure 12**). Notably, these data support the loss of epithelium and an increase in the proportion of immune and contractile cells in the AS endometrium; these data suggest an endometrial composition consistent with the nature of the disease (section I.5) where the endometrium is highly damaged. In addition, the identification of the AS-epithelium population paves the way for discovering a potential biomarker for disease detection.

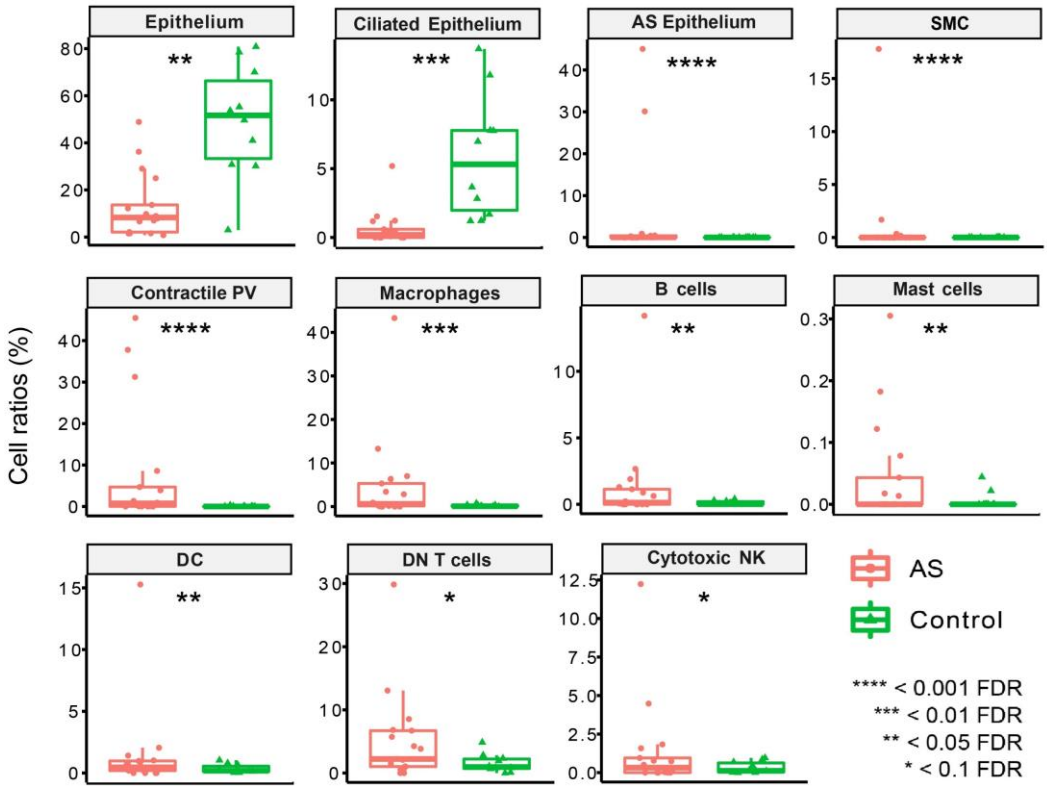

*Figure 12. Comparison of cell ratios in healthy secretory phase endometrial samples (control) and Asherman syndrome-affected endometrial samples. (NB-GLM statistical test, **** = FDR<0.0001, *** = FDR<0.01, ** = FDR<0.05, * = FDR<0.1). Abbreviations - AS (Asherman syndrome), DC (dendritic cells), DN (double negative), NK (natural killer), PV (perivascular), SMC (smooth muscle cell).*

Transcriptomic profiles of the distinct cell types revealed differential gene expression patterns when comparing the expression of the different cell clusters from AS and healthy secretory-phase control endometrial samples (**Figure 13)**. In the **epithelium**, secretoglobin genes (such as *SCGB1D2* and *SCGB2A1*), receptivity-related (such as *PAEP* and *CLDN4*), anti-inflammatory (*ANXA1*) and *MT* family genes became downregulated in AS compared to controls, suggesting decreased secretory and receptive activity in epithelial cells. The ciliated epithelium underexpressed epithelial markers (*WFDC2*), tumor suppressor (*ATF3*), and proliferative (*CXCL8*) genes, suggesting a diminished development activity. The **stroma** overexpressed *FN1* (related to the fibronectin and collagen fibers of the extracellular matrix (ECM)) and growth (*EGR1*) genes; furthermore, the **stroma** also highly overexpressed collagen genes (*COL1A1* or *COL3A1*). **Endothelium** underexpressed apoptosis regulatory genes (*GADD45B* and *IER3*), while **PV** cells showed higher levels of angiogenesis suppressor (*IGFBP5*) and RPL genes (such as *RPL37A* or

RPL31), indicating a constrain in this population growth. While **contractile PV** cells showed similarities with PV cells in their transcriptomic profiles (such as RPL family gene expression), their development was higher in AS (as they presented a lower expression of anti-angiogenic (*IGFBP7*) and cell migration (*TMSB4X*) genes, while presenting a more muscular profile (with overexpression of *MHY11*) (**Figure 13**). Our results revealed an affected epithelium and a proliferating stroma with high ECM production; additionally, we observed a decline in endothelial populations accompanied by an increasing muscle-like profile in one endothelial population, which aligns with the fibrotic and avascular tissue characteristics of AS (**Figure 12**). In the immune compartment, NK cells, DN T cells, and $CD8^+$ T cells overexpressed *GNLY* (cytotoxic granulysin), while macrophages upregulated the expression of genes related to inflammation and immune activation, such as the long non-coding RNA *NEAT1* and S100 family genes (*S100A8, S100A9,* and *S100A12*). Furthermore, all immune populations exhibited increased expression of *MTRNR2L12* (an anti-apoptotic lncRNA) and *JUNB* (a regulator of immune cell differentiation). Overall, these gene expression profiles suggested a pro-inflammatory and stressed cell environment of the AS endometrium consistent with previous observations in patients (Annex 4).

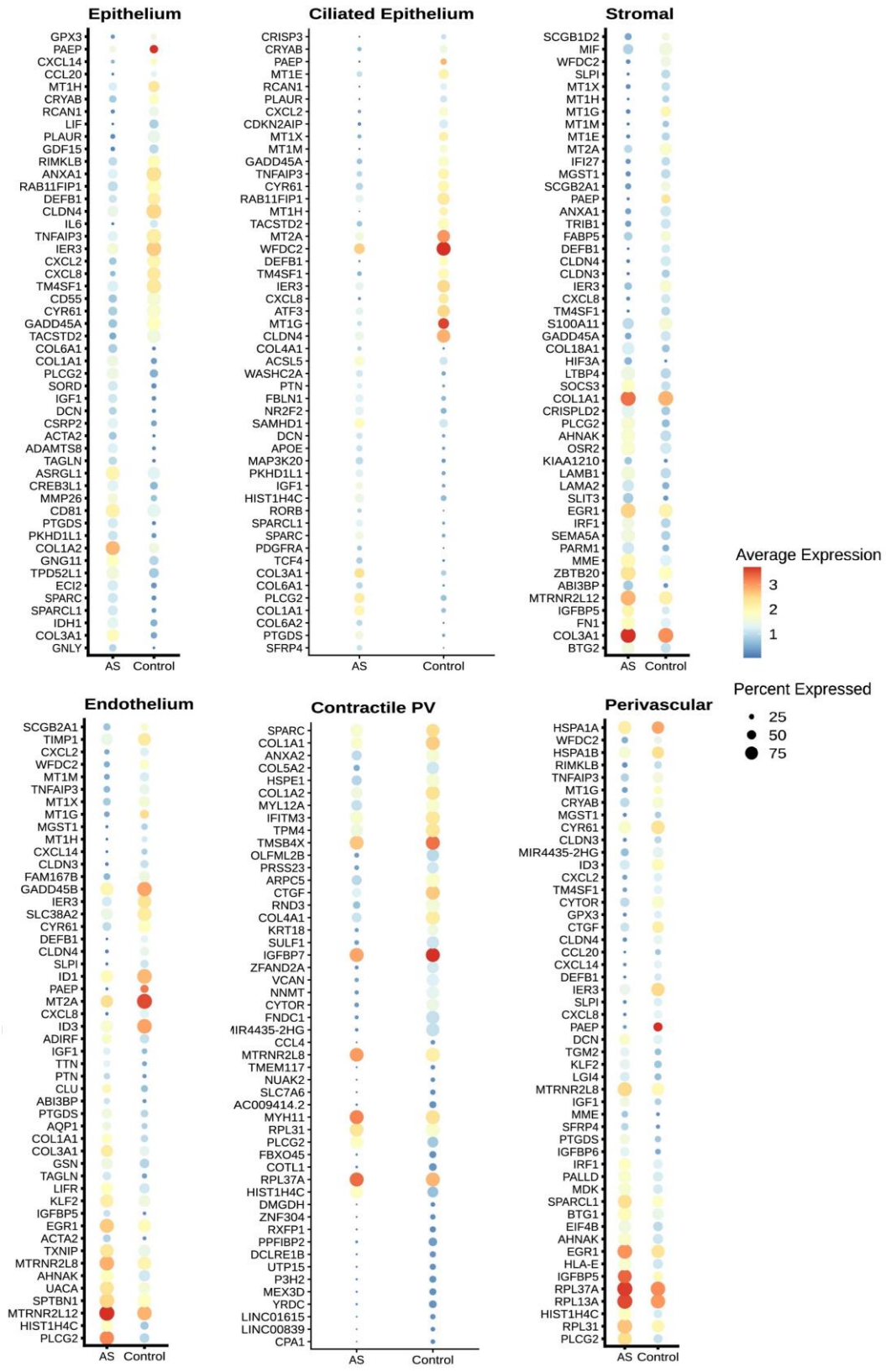

Figure 13. Differential gene expression comparing Asherman syndrome-affected and healthy secretory-phase control endometrial samples divided by cell type (Wilcoxon Rank Sum test, FDR<0.05). Abbreviations - AS (Asherman syndrome), PV (perivascular).

Overall, by creating this scRNA-seq “atlas” of the AS endometrium (and the healthy secretory phase control endometrium), we illustrated our ability to monitor alterations in cell composition and transcriptomic profiles, allowing us to elucidate the previously unknown tissue environment associated with AS.

1.2. Transcriptomic landscape during the window of implantation in the Asherman syndrome endometrium

The WOI is the specific period when the endometrium is receptive to the embryo. Thus, the more accurate assessment of endometrial dysfunction in AS, potentially associated with altered receptivity, requires comparison of AS and healthy control samples within the WOI. We performed a new clustering and cellular annotation, focusing on providing a more detailed description of the cells within the epithelial and stromal clusters most impacted by AS (**Figure 14**). We achieved this description by adding supportive canonical marker genes, whose expression associates with a more specific cell type within the same cell cluster, enabling more precise identification of cellular identities.

This new clustering maintained the ciliated epithelium and AS epithelium clusters, while the broader epithelium cluster became subdivided into luminal epithelium (expressing *LGR5, PTGS1,* and *MSLN*), glandular epithelium (expressing *SCGB2A2, SLC18A2, SPP1,* and *SMAD9*), and glandular-secretory epithelium (which differs from the glandular cluster due to high expression of *PAEP, CXCL14, DPP4,* and *GPX3*) (**Figure 14**-**A** and **Figure 15**). In addition, we observed the presence of two new populations in the AS samples: i) "epithelial-PDGFRA" expressing a mixed combination of epithelial and stromal markers in both AS and WOI control samples, and ii) "epithelium-SOX9" expressing epithelial markers (*EPCAM* and *WFDC2*) together with *SOX9* and *MMP7* in only the WOI control samples. The epithelial-PDGFRA cluster could represent an intermediate state in between the mesenchymal-epithelial transition (MET) and epithelial-mesenchymal transition (EMT), processes involving cellular changes necessary for both endometrial regeneration and embryo implantation (Owusu-Akyaw et al., 2019). The absence of the epithelium-SOX9 population in the AS endometrium might explain the lack of regeneration, given that *SOX9* is related to stem-cell function and regenerative capacity in different tissues (Aggarwal et al., 2024; Chen et al., 2021; Gonzalez et al., 2016).

In the stromal clustering, we observed the preservation of a large cluster of stromal cells that expressed marker genes such as *LUM, DCN,* and *IGF1* and a subcluster of cycling stroma co-expressing stromal markers and cell cycle-related genes such as *TOP2A*, *HMGB2* or *KI67* both in AS and WOI control endometria (**Figure 14 B** and **Figure 15**). PV cells were clustered in supporting-PV cells (expressing *STEAP4* or *MHY11)* and PV cells expressing cycle-related genes, also in both conditions. Additionally, we identified a cell cluster expressing stromal gene markers (such as *LUM* and *DCN*) and the intermediate expression of SMC-related genes (*ACTA2, MYL9,* and *MGP*); we identified this cell cluster as myofibroblasts, which was mainly represented in WOI control samples. In the AS samples, we observed SMCs in the place of myofibroblasts. These two clusters were similar and may indicate how these cells were identified in WOI control samples as fibroblasts expressing some muscle-related genes, and as SMCs in AS with significantly more muscular identity.

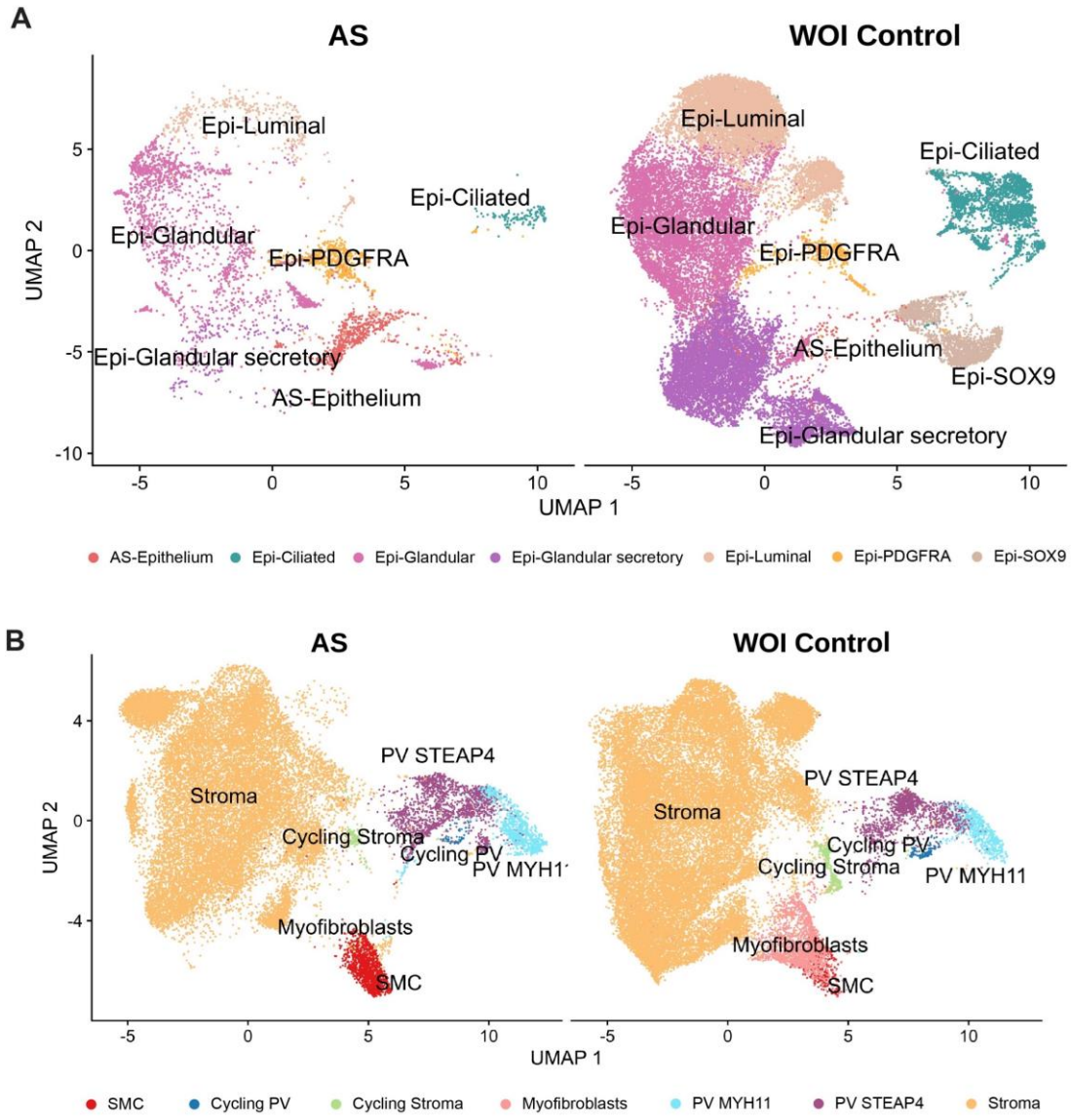

Figure 14. scRNA-seq mediated fine-clustering of epithelial and stromal subpopulations from Asherman syndrome (AS) patient samples (40,336 cells) compared to healthy controls during the window of implantation (66,064 cells). A) UMAP of specific epithelial cell clusters. B) UMAP of specific stromal and perivascular cell clusters. Abbreviations - AS (Asherman syndrome), Epi (epithelium), PV (perivascular), SMC (smooth muscle cell).

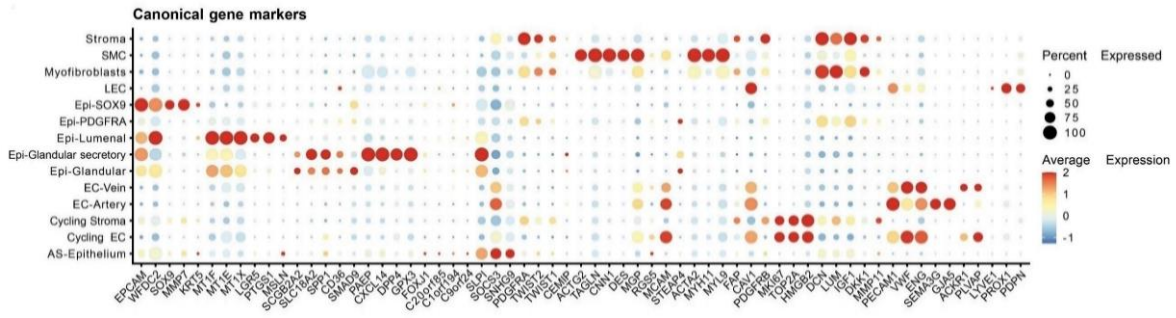

Figure 15. Dot plot of marker gene expression in Asherman syndrome and window of implantation control endometrial samples. A larger-sized image is available in Annex 3. Abbreviations - AS (Asherman syndrome), EC (endothelial cell), Epi (epithelium), PV (perivascular), SMC (smooth muscle cell).

The subsequent analysis of epithelial cell ratios, when comparing AS and healthy WOI control endometrial samples, revealed a statistically significant (FDR <0.05) higher number of ciliated epithelium and glandular secretory epithelium in WOI control samples (**Figure 16**). Although we detected the previously identified SLPI^{+} AS-epithelium cluster (**Figure 10**) in both AS and WOI control samples in this analysis, we found a significantly higher number of SLPI^{+} AS-epithelium cells in AS samples (FDR <0.05). We also detected a significantly higher number of myofibroblast cells in the WOI control epithelium (FDR <0.001). The ratios of various major immune cell populations (cytotoxic NK, DC, and DN T cells) exhibited a significant increase in cell number in AS endometrial samples (all FDR <0.05), NK and mast cells increased but to a lesser degree (FDR <0.1), and macrophages displayed the most significant increase (FDR <0.01). These findings align with the prior analysis comparing against secretory controls, indicating a damaged epithelium (mainly glandular and ciliated epithelium) and the increased number of several immune cell types in the AS endometrium (**Figure 12**).

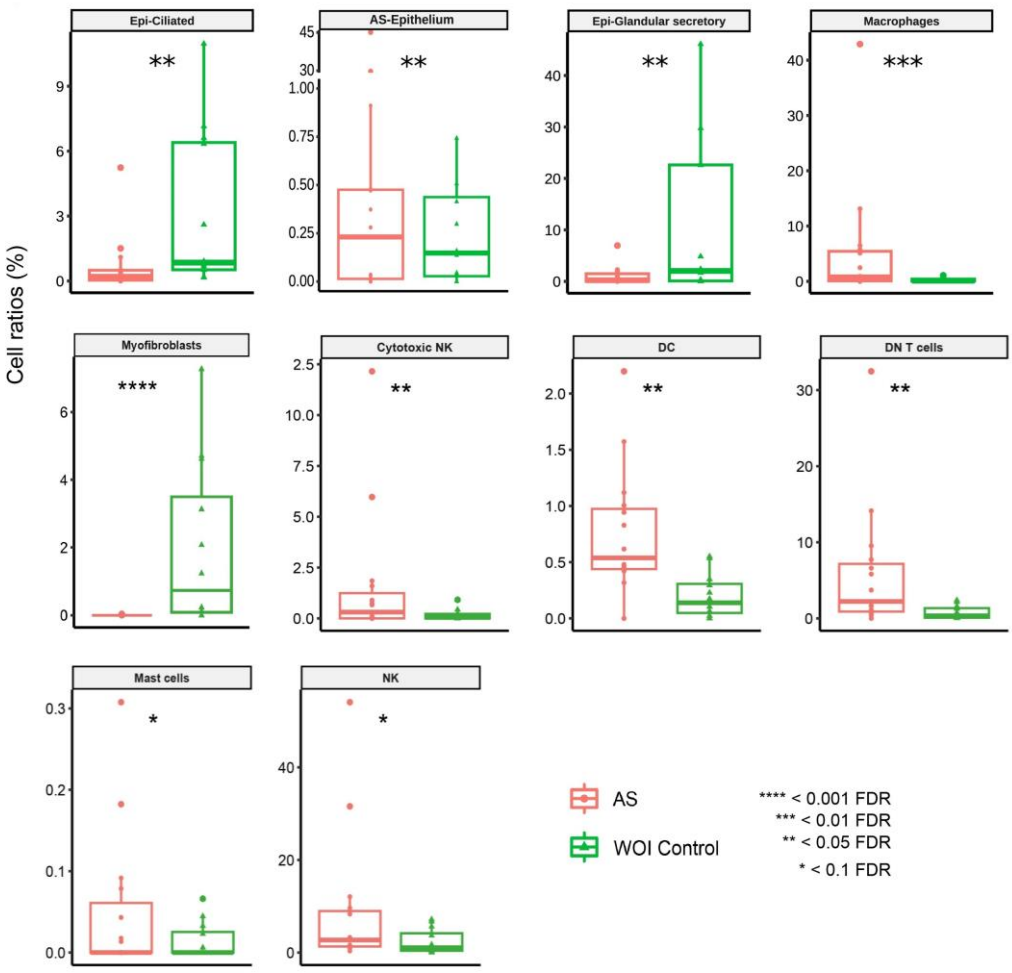

*Figure 16. Cell ratios of cell types comparing Asherman syndrome with the window of implantation control endometrial samples (NB-GLM statistical test, **** = FDR<0.0001, *** = FDR<0.01, ** = FDR<0.05, * = FDR<0.1). Abbreviations - AS (Asherman syndrome), Epi (epithelium), DC (dendritic cells), DN (double negative), NK (natural killer), PV (perivascular).*

Differential gene expression analysis of epithelial clusters (ciliated, luminal, glandular, and glandular secretory revealed the downregulated expression of endometrial receptivity genes (e.g., *GPX3, PAEP, CXCL8*, and *CLDN4*) and *MT* family genes (e.g., *MT2A, MT1G*, and *MT1H*) in AS patient endometrial samples, which may explain the lost epithelial function observed in the AS endometrium (**Figure 17**). By contrast, epithelial clusters also displayed the upregulated expression of ECM-associated genes (such as *COL1A2* and *COL3A1*), which may explain the fibrotic profile observed in the epithelium of AS patients (**Figure 16**). In addition, differential gene expression analysis suggested more significant immune activity in the AS endometrium, suggested by the increased expression of *NEAT1, S100A8, S100A9*, and *IL7R* in macrophages and/or MAIT cells and

more significant stromal growth and vascular restriction, as suggested by the overexpression of *IGF1, COL3A1,* and *IGFBP5* in the stromal cluster.

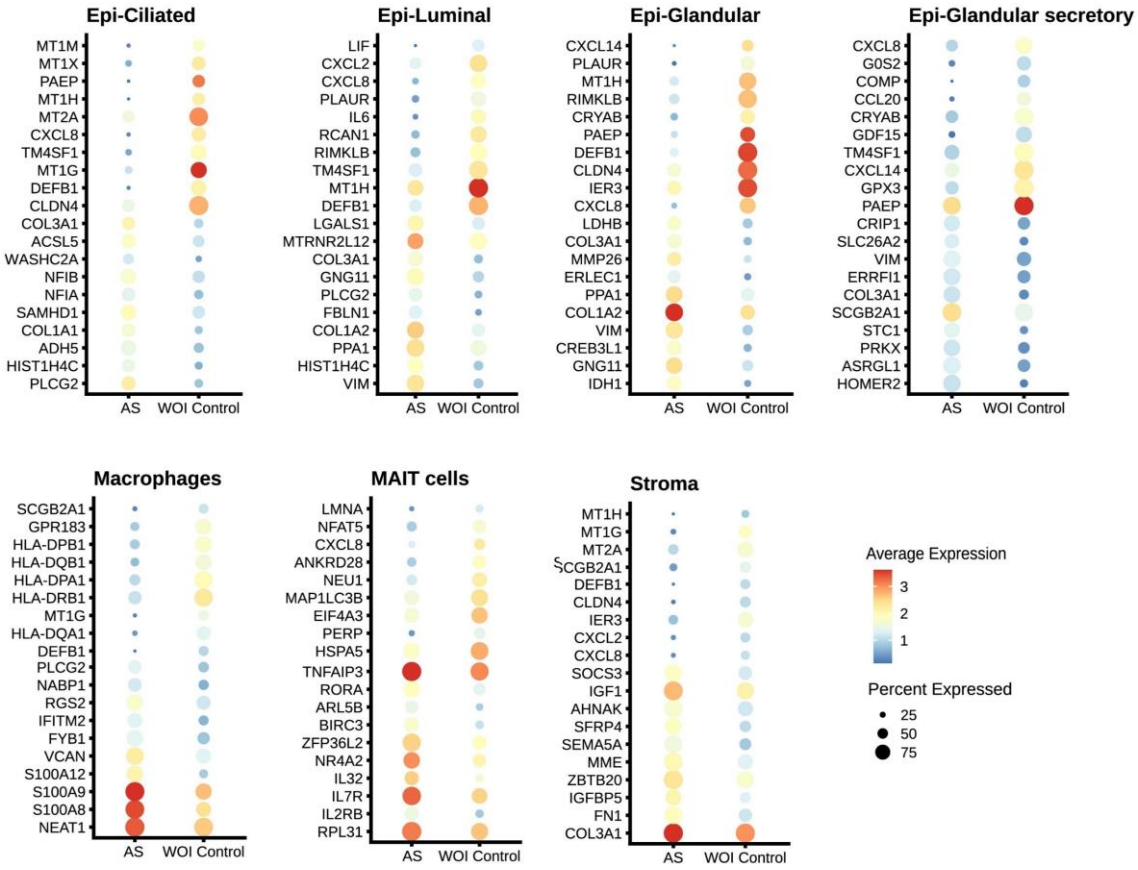

Figure 17. Differential gene expression dot plots for main clusters identified when comparing Asherman syndrome and window of implantation control endometrial samples (Wilcoxon Rank Sum test, FDR<0.05). Abbreviations - AS (Asherman syndrome), EC (endothelial cells), Epi (epithelium), MAIT (mucosal-associated invariant T).

The relative expression of *ESR1* and *PGR* genes in AS and WOI control endometrial samples also showed significant differences (**Figure 18**). We found elevated *ESR1* and *PGR* expression levels in epithelial clusters (luminal, glandular, and glandular-secretory epithelia) and stromal subclusters in AS compared to WOI control endometria (all FDR <0.05). These results agree with previous studies indicating increased *ESR1* and *PGR* expression in the endometrium of patients with IUAs (Ge et al., 2021; Sun et al., 2022; Zhou et al., 2018), considering that PGR studies were conducted on samples during the secretory phase.

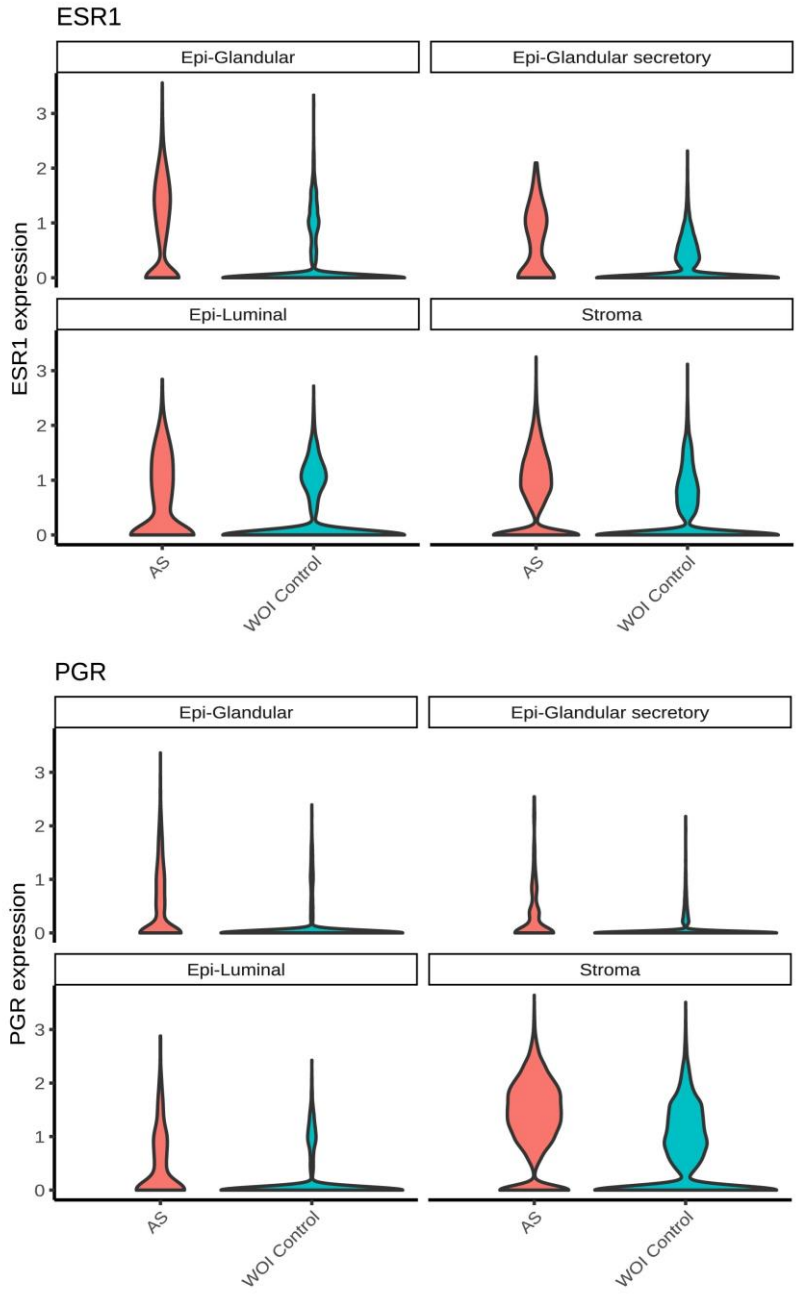

Figure 18. ESR1 and PGR gene expression levels in epithelial and stromal clusters in Asherman syndrome and window of implantation control endometrial samples. (Wilcoxon test; FDR <0.05). Abbreviations - AS (Asherman syndrome), Epi (epithelium).

1.3. SLPI as a cell marker in AS-epithelium

As noted in the preceding section, we described a particularly abundant population present only in the AS endometrium thanks to transcriptomic data comparisons: the "AS-epithelium." Cells in this cluster expressed genes associated with cell stress (**Figure 11**

and **Figure 15**); therefore, we sought to validate our results by analyzing fixed endometrial tissue samples.

After evaluating gene expression values and the number of cells expressing genes of interest within and outside the AS-epithelium cluster, we chose the *SLPI* gene as a marker for this population. We aimed to detect its presence using RNAscope, a technique performed in fixed tissue slides that allows the identification of RNAs by *in situ* hybridization of probes designed for specific genes (**Figure 19**).

We first assessed the condition of our tissue sections by staining them with hematoxylin and eosin; the resulting images revealed that AS endometrial tissue samples exhibited a total lack of glandular epithelium and predominantly comprised fibrotic tissue (**Figure 19-A**). We then evaluated the presence of *SLPI* RNA in endometrial tissue samples isolated from AS patients and healthy WOI donors, observing the presence of *SLPI* exclusively in the luminal and glandular epithelium of AS samples (**Figure 19-B**). We aimed to validate the presence of this population in endometrial tissue; however, we could not detect *SLPI* in the control samples even though we identified the population in scRNA-seq cell annotation. This result may arise to the minimal amount of $SLPI^+$ cells and the difficulty locating epithelium in AS tissue.

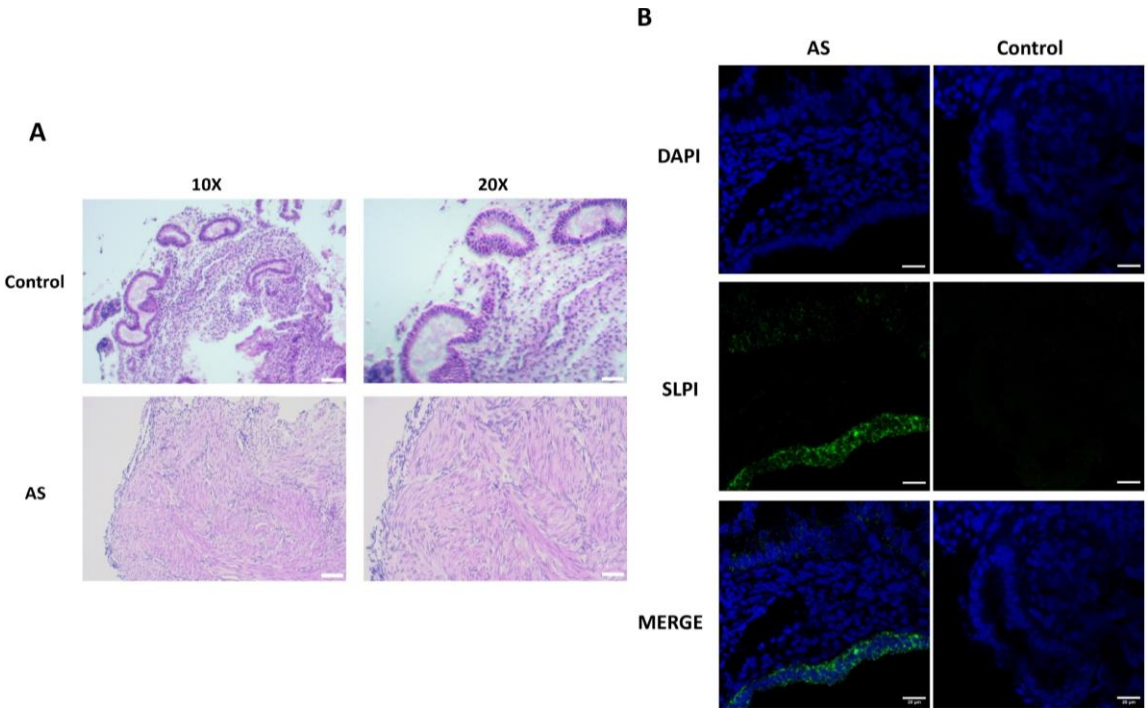

Figure 19. Analysis of histological sections of endometrial tissues isolated from Asherman syndrome patients and healthy controls. A) Hematoxylin and eosin staining to reveal the cellular structure of the tissue. B) Representative images of RNAscope-mediated analysis of SLIP gene expression in the AS-epithelium cell cluster. From top to bottom, images show cell nuclei in blue (stained with DAPI), SLPI gene expression in green, and the merge. Scale bar = 20µm.

1.4. An increasingly pro-inflammatory environment correlates with increasing Asherman syndrome severity

To better understand AS progression, we investigated discernible differences between the endometrium of moderate (stage II) and severe (stage III) levels of AS patients by comparing scRNA-seq data from samples in our dataset that differ in severity status (four severe AS and five moderate AS cases) (**Figure 20**). Following the finer resolution settings developed for the AS vs. WOI control endometrial sample comparison, we performed cell clustering and annotation. With these parameters, the cellular distribution reported in a UMAP (**Figure 20**) displayed a broad decrease in the proportion of SMCs, PV cells, and epithelial when the endometrium transits from moderate to severe disease conditions.

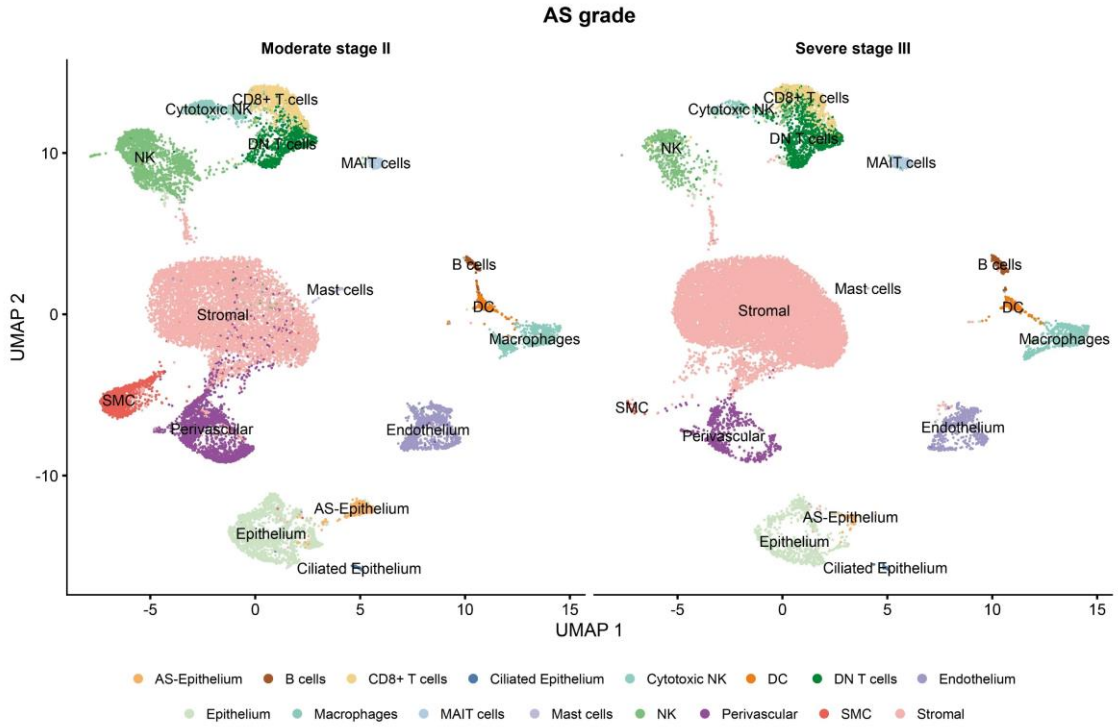

Figure 20. UMAP indicates the main cell populations in endometrial samples from patients with moderate (stage II) and severe (stage III) Asherman syndrome identified by single-cell RNA-sequencing data. Abbreviations - AS (Asherman syndrome) DC (dendritic cells), DN (double negative), MAIT (mucosal-associated invariant T), NK (natural killer), PV (perivascular), SMC (smooth muscle cell).

When analyzing differential gene expression between endometrial cell types in moderate and severe disease stages, we identified a notable upregulation in genes related to stress response, such as *JUND* and *SOCS3*, when transiting from moderate to severe AS cases (**Figure 21**). We observed a general increase in the expression of *JUND* and *SOCS3* (FDR <0.05) in luminal and PDGFRA epithelial populations, the stroma, and several pericyte populations in severe AS.

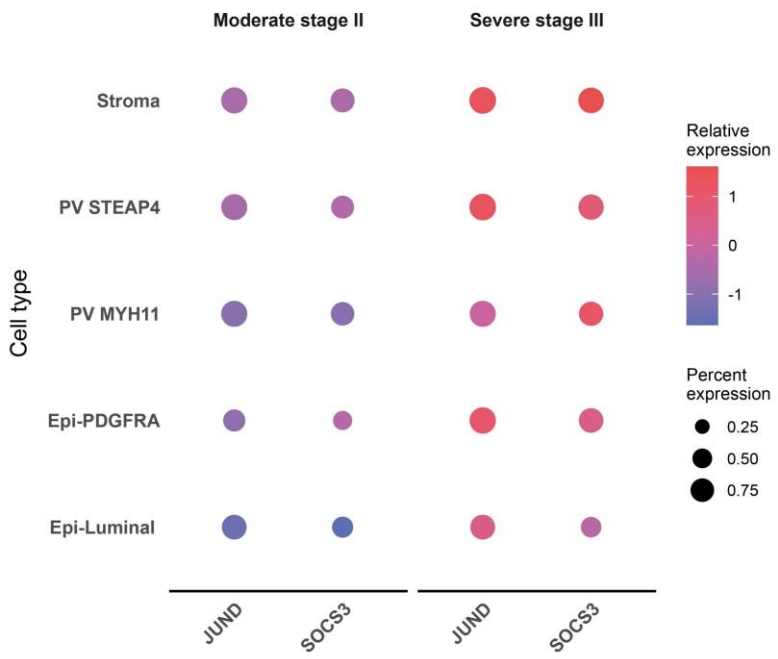

Figure 21. Dot plots of differential JUND and SOCS3 gene expression between the Asherman syndrome endometrium at stage II (moderate) and stage III (severe) disease severity. Statistical analysis used the Wilcoxon Rank Sum test (FDR < 0.05). Abbreviations - AS (Asherman syndrome), Epi (epithelium), PV (perivascular).

The cell composition and gene expression findings regarding differences in the endometrium of AS patients during the WOI and across various severity stages describe a dysfunctional tissue marked by the loss of the glandular secretory epithelium and its transcriptomic receptivity profile alongside the emergence of a stressed epithelial cluster (SLPI^{+} AS-epithelium). The increased expression of stress-response genes marking the transition from moderate to severe AS.

1.5. Cell-to-cell communication in the Asherman syndrome endometrium

Communication between the different cell types and the environment is critical for the proper functioning of the endometrium. Thus, one potential reason behind the endometrial tissue dysfunction observed in AS patients may arise from cell-to-cell communication (CCC) disruption, which encompasses signaling crosstalk through membrane-bound and soluble factors between cells to maintain tissue homeostasis. To address CCC in the AS endometrium, we used a bioinformatic tool called CellChat that quantitatively infers and analyzes ligand-receptor pair activity from scRNA-seq data (Jin

et al., 2021) (section IV.2.8). Using this tool, we computed crosstalk information flows, total communication probability in the inferred network of cell populations in our AS atlas, the contribution differences of the ligand-receptor pairs involved, and changes in cell populations or the intensity of interactions among cell populations.

1.5.1. Altered epithelial-stromal cell-to-cell communication and signaling pathways in Asherman syndrome

The CCC network comparing AS and secretory-phase control endometrial samples revealed robust interactions between the epithelium and stroma in the control endometrium and less robust interactions between the epithelium and other clusters such as the ciliated epithelium, endothelium, PV cells, various immune populations, and itself (**Figure 22**). The AS endometrium CCC network analysis revealed the substantial disappearance of epithelial interactions (mainly with stromal cells), replaced by robust stromal self-stimulation and interactions of stromal cells with immune and PV clusters (**Figure 22**).

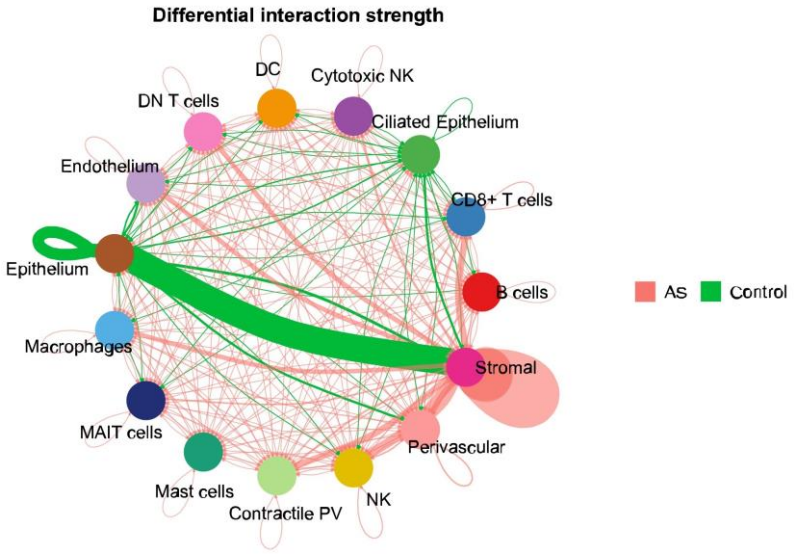

Figure 22. Chord plot representing differential cell-to-cell communication between Asherman syndrome and healthy secretory-phase control endometrial samples. Arrows around chord cell types determine the direction of interactions. Expression-based interactions represented as relative thicknesses of green (control) and red (AS) arrow lines. Abbreviations – AS (Asherman syndrome), DC (dendritic cells), DN (double negative), MAIT (mucosal-associated invariant T), NK (natural killer), PV (perivascular), SMC (smooth muscle cell).

Our analysis identified 59 disrupted signaling pathways in terms of information flow. In agreement with the pro-fibrotic nature of the AS endometrium, ECM and fiber generation pathways emerged as particularly active in the AS endometrium (mainly laminin, collagen, and FN1 components) (**Figure 23**). Pathway networks analysis of these components between AS and control endometrial samples revealed diminished CCC between epithelial and stromal cell clusters, alongside heightened CCC among stromal cells, with stromal populations as the main emitter population (**Figure 24**). **Table 7 and Table 8** show the main ligand-receptor pairs contributing to the loss of CCC with epithelium and the self-stimulation of stroma in AS endometrial samples.

In addition, we observed several enriched immune signaling pathways in AS endometrial samples (such as MHC-I and MHC-II, LIGHT, IL4, NCAM, RESISTIN, CCL, and ICAM), suggesting the activation of distinct immune processes (**Figure 23**). Among these signaling pathways, we further investigated leukocyte/myeloid trans-endothelial migration (ICAM) and C-C motif chemokine ligand (CCL) signaling (**Figure 25**). The CCC chord plots of the ICAM and CCL pathways revealed increased interactions between distinct immune cell clusters (with NK cells, macrophages, and CD8+ T cells as the principal emitter populations). We also encountered heightened interactions between immune cells such as macrophages or $CD8^+$ T cells and the endothelium, indicating more pronounced pro-inflammatory activity and the potential recruitment of immune cells through blood vessels. The CCL5-ACKR1 ligand-receptor pair represents the main contributor in AS and secretory-phase control networks in CCL, with CCL5-CCR1, CCL3-CCR1, and CCL3L1-CCR1 contributing to CCL network differences in AS endometrial samples (Annex 5).

Table 7. Main ligand-receptor pairs activity alteration in COLLAGEN signaling pathway in AS endometrium.

Ligand-receptor pairs	Related CCC clusters	Alteration
COL1A1 (ITGA2+ITGB1)	*Stromal → Epithelium*	*Absent*
COL1A1 (CD44)	*Stromal → Epithelium*	*Absent*
COL1A2 (CD44)	*Stromal → Epithelium*	*Absent*
COL6A1 (CD44)	*Stromal → Epithelium*	*Absent*
COL1A1 (ITGA1+ITGB1)	*Stromal → Stromal*	*Emerged*
COL1A2 (ITGA1+ITGB1)	*Stromal → Stromal*	*Emerged*
COL4A1 (ITGA1+ITGB1)	*Stromal → Stromal*	*Emerged*
COL4A2 (ITGA1+ITGB1)	*Stromal → Stromal*	*Emerged*
COL6A1 (ITGA1+ITGB1)	*Stromal → Stromal*	*Emerged*
COL6A2 (ITGA1+ITGB1)	*Stromal → Stromal*	*Emerged*
COL6A3 (ITGA1+ITGB1)	*Stromal → Stromal*	*Emerged*

Table 8. Main ligand-receptor pairs activity alteration in FN1 and LAMININ pathways in AS endometrium.

Ligand-receptor pairs	Related CCC clusters	Alteration
FN1 (CD44)	*Stromal → Epithelium*	*Absent*
	Stromal → Stromal	*Increased*
FN1 (ITGAV+ITGB1)	*Stromal → Stromal*	*Increased*
FN1 (ITGA8+ITGB1)	*Stromal → Stromal*	*Increased*
LAMB1 (CD44)	*Stromal → Epithelium*	*Absent*
	Stromal → Stromal	*Increased*
LAMA2 (ITGA1+ITGB1)	*Stromal → Stromal*	*Emerged*
LAMA2 (ITGAV+ITGB8)	*Stromal → Stromal*	*Increased*
LAMA2 (CD44)	*Stromal → Stromal*	*Increased*
LAMB1 (ITGA1+ITGB1)	*Stromal → Stromal*	*Emerged*

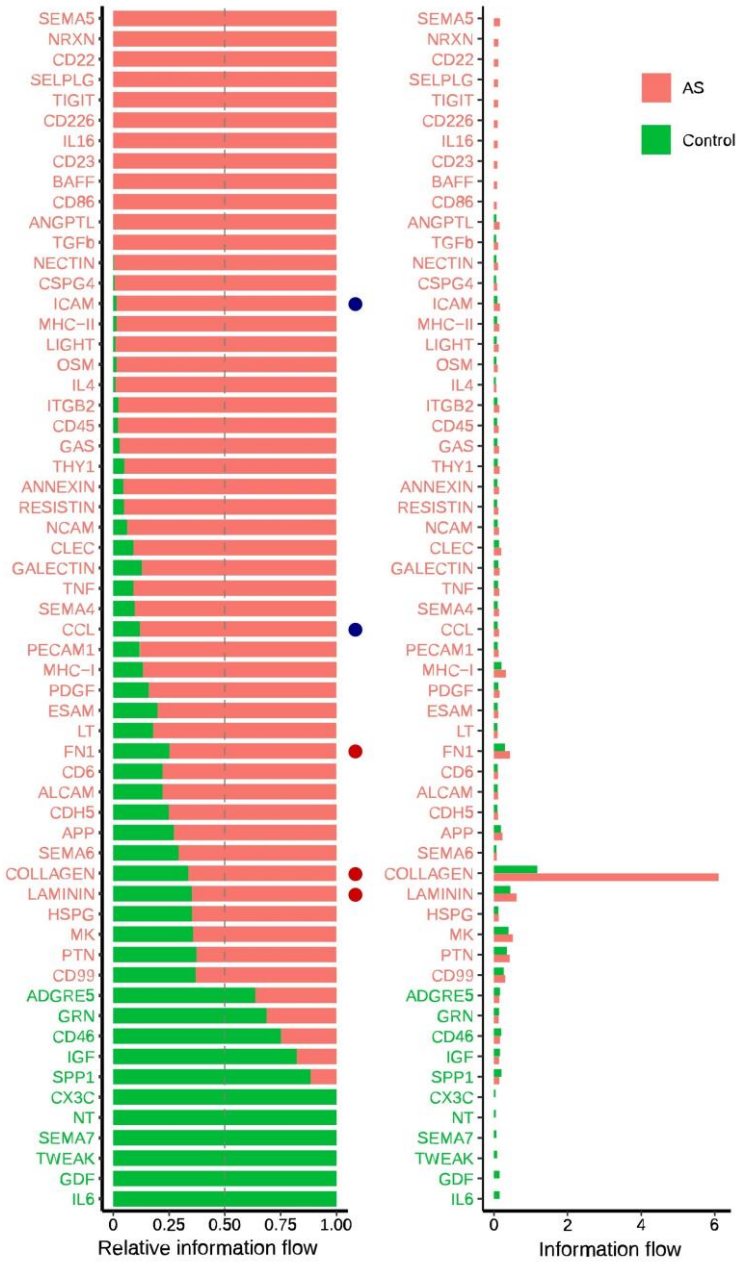

Figure 23. Differentially active signaling pathways between Asherman syndrome and secretory-phase control endometrial samples. Relative (left) and absolute (right) flows of signaling pathways (Wilcoxon test; FDR < 0.05). Red dots: pathways related to fiber and ECM generation. Blue dots: pathways related to inflammation and immune cell recruitment.

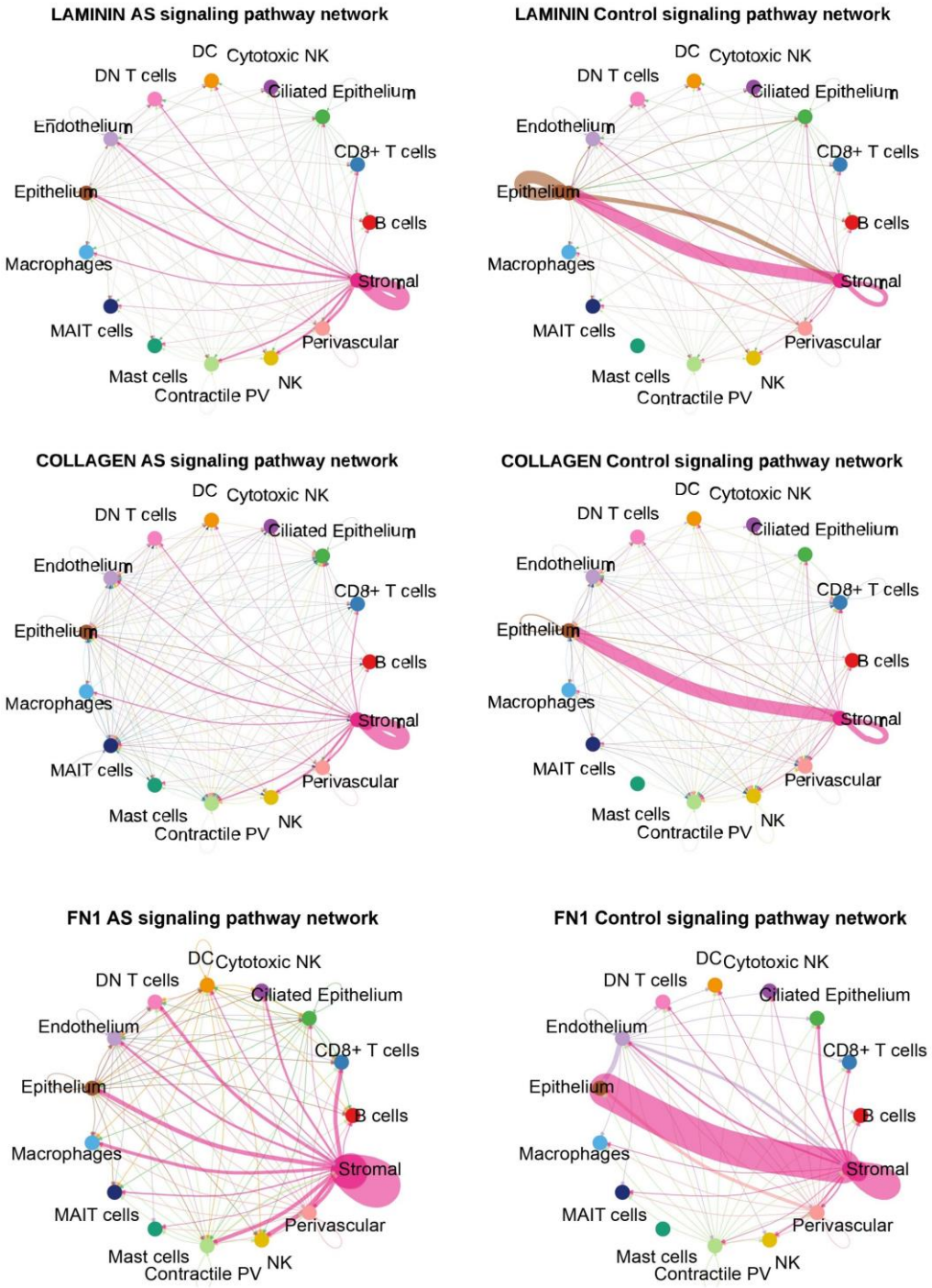

Figure 24. CCC chord plots of LAMININ, COLLAGEN, and FN1 signaling pathways between Asherman syndrome and secretory-phase control endometrial samples. The line's color corresponds to the cluster expressing the ligand (emitter), while its destination indicates the cluster expressing the receptor. The relative thickness of each line depicts the expression-based strength of the interaction between cell types. Abbreviations - AS (Asherman syndrome), DC (dendritic cells), DN (double negative), MAIT (mucosal-associated invariant T), NK (natural killer), PV (perivascular), SMC (smooth muscle cell).

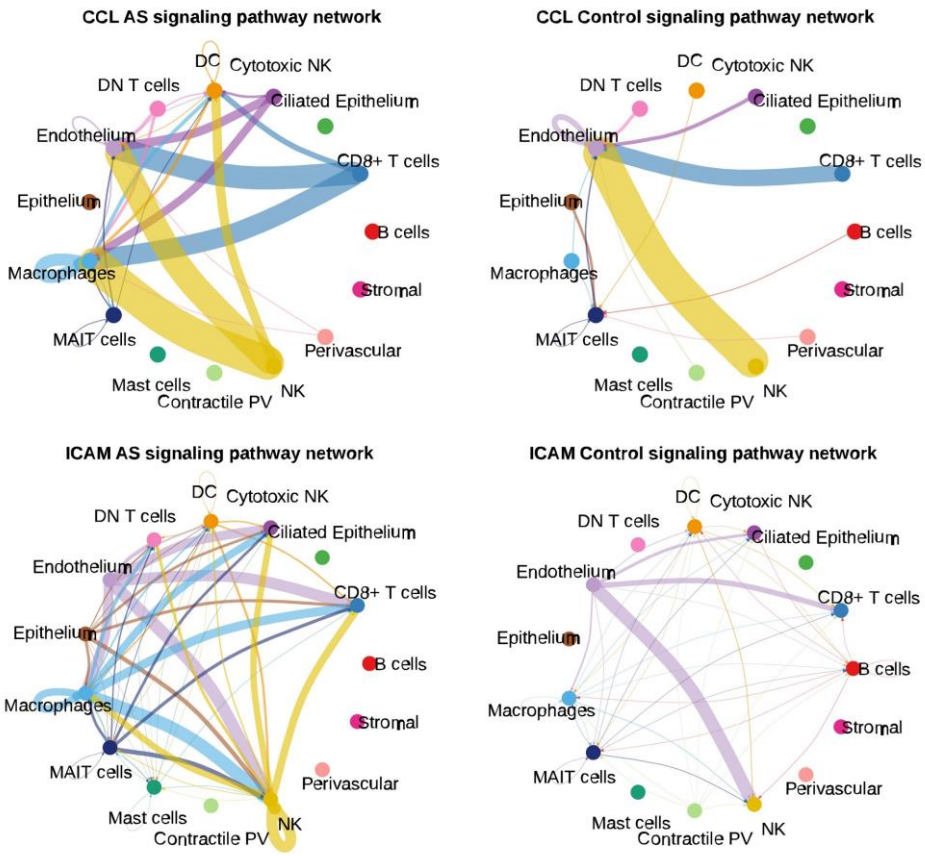

Figure 25. CCC chord plots of ICAM and CCL signaling pathways in AS and healthy control endometria. The line's color corresponds to the cluster expressing the ligand (emitter), while its destination indicates the cluster expressing the receptor. The relative thickness of each line depicts the expression-based strength of the interaction between cell types. Abbreviations - AS (Asherman syndrome), DC (dendritic cells), DN (double negative), MAIT (mucosal-associated invariant T), NK (natural killer), PV (perivascular), SMC (smooth muscle cell).

1.5.2. Abnormal cell-to-cell communication highlights a pro-fibrotic and inflammatory microenvironment in the window of implantation

We performed a subsequent analysis of CCC differences focused on the WOI, using previously refined clustering and annotations from the AS and WOI control sample endometrial atlases (**Figure 26**). The results encompassed 74 disrupted signaling pathways that cover pathways shared with the previous analysis, such as those related to ECM and immune cell communication, alongside 30 signaling pathways specific to this WOI-based analysis. Our analysis also revealed signaling pathways exclusive to the control samples, suggesting their complete loss in the AS endometrium. Such pathways include the IL6 pathway, a recognized epithelial hallmark for establishing and maintaining pregnancy.

Other pathways with very low information flow in AS samples include SPP1 and CDH1 (**Figure 27**). The SPP1 protein plays a role in the ECM (mainly associated with cell attachment) and remains crucial to stromal decidualization. CCC network analysis revealed that almost every cell cluster communicates through the SPP1 pathway under physiological conditions (WOI control endometrial samples), presenting two robust interactions between the glandular epithelium and the stroma and between the stroma and the glandular secretory epithelium (**Figure 27**). We observed the disruption of most signals in the AS endometrial samples (including interactions between stroma and glandular epithelium), indicating SPP1 dysregulation via the SPP1-(ITGA5+ITGB1) and SPP1-CD44 pairs as the main contributors (Annex 5).

The CDH1 protein mediates cell-to-cell epithelial adhesions. As depicted in the CCC chord plot, the WOI control endometrial samples use the CDH1 pathway to signal between epithelial clusters, with notable emanating signals from the glandular and secretory glandular epithelium (**Figure 27**). Conversely, CDH1 signaling from the glandular, secretory glandular, and luminal epithelia primarily occur with immune cells (NK cells and $CD8^+$ T cells) in the AS endometrial samples, inducing a pro-inflammatory microenvironment near these epithelia mediated through the CDH1-KLRG1 pair (**Figure 27**).

Additional pathways with low information flow suggest the loss of epithelial structural integrity in the AS endometrium, such as impaired JAM and DESMOSOME signaling between different epithelial clusters (luminal, glandular, glandular secretory, and ciliated) (**Figure 26**). We observed a similar scenario when viewing the fibroblast growth factor (FGF) signaling pathway (**Figure 27**), which suffers from a downregulation of all interactions between stroma and epithelial clusters, and the absence of interactions between myofibroblasts and epithelial clusters in the AS endometrium, indicating the modification of stromal growth through a decrease in the activity of the FGF7-FGFR1 pair and the activation of the FGF2-FGFR1 pair (Annex 5).

Remarkably, we found that the main overrepresented pathways in the AS endometrium related to interactions between different immune cell clusters and glandular epithelium (including ICOS, CD86, IL4, ALCAM, LCK, CD6, SELPLG, CD226, and TIGIT) and to immune

cell recruitment (such as ICAM, VCAM or PECAM1) (**Figure 26**). This result suggests the continuous attraction of immune cells to the AS endometrium, which then go on to interact with epithelial cells, the most damaged cell type in AS.

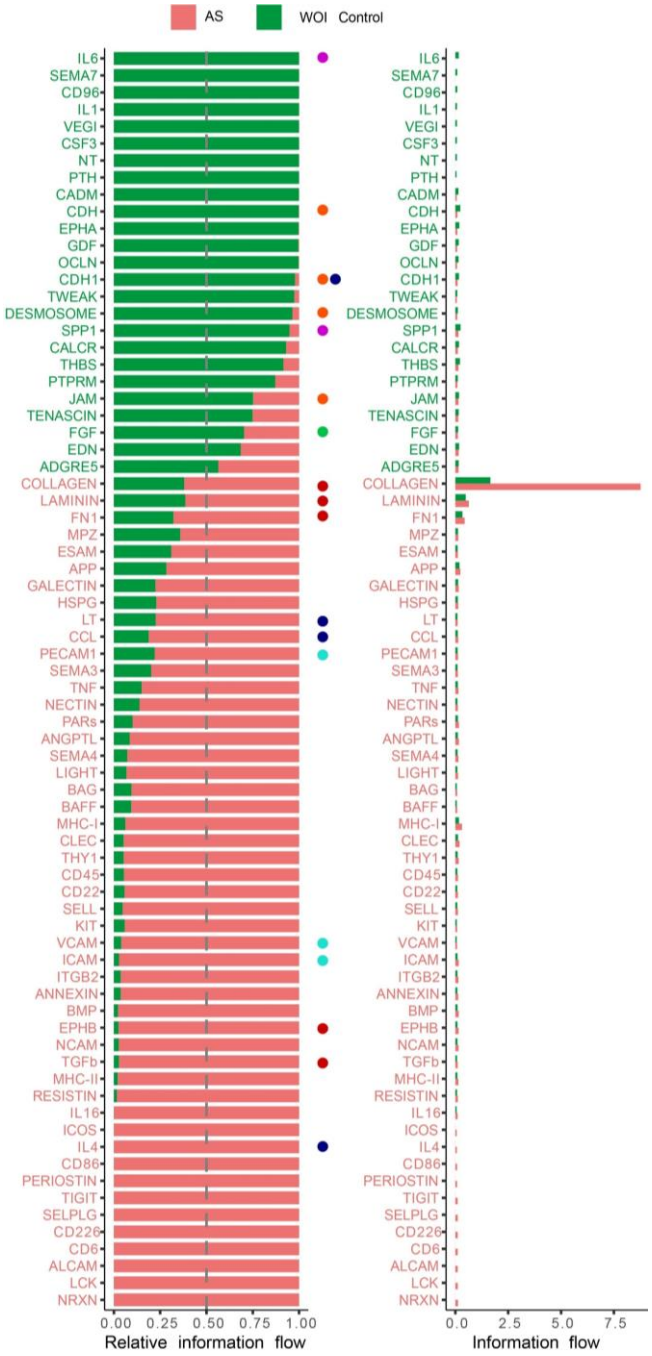

Figure 26. Differentially active signaling pathways between Asherman syndrome and window of implantation control endometrial samples. Relative (left) and absolute (right) flows of signaling pathways (Wilcoxon test; FDR < 0.05). Red dots: pathways related to fiber and ECM generation. Blue dots: pathways related to the immune system. Cyan dots: pathways related to immune cell recruitment. Green dots: pathways related to epithelial development. Orange dots: pathways related to cellular unions and cell junctions. Purple dots: pathways related to WOI and decidualization processes

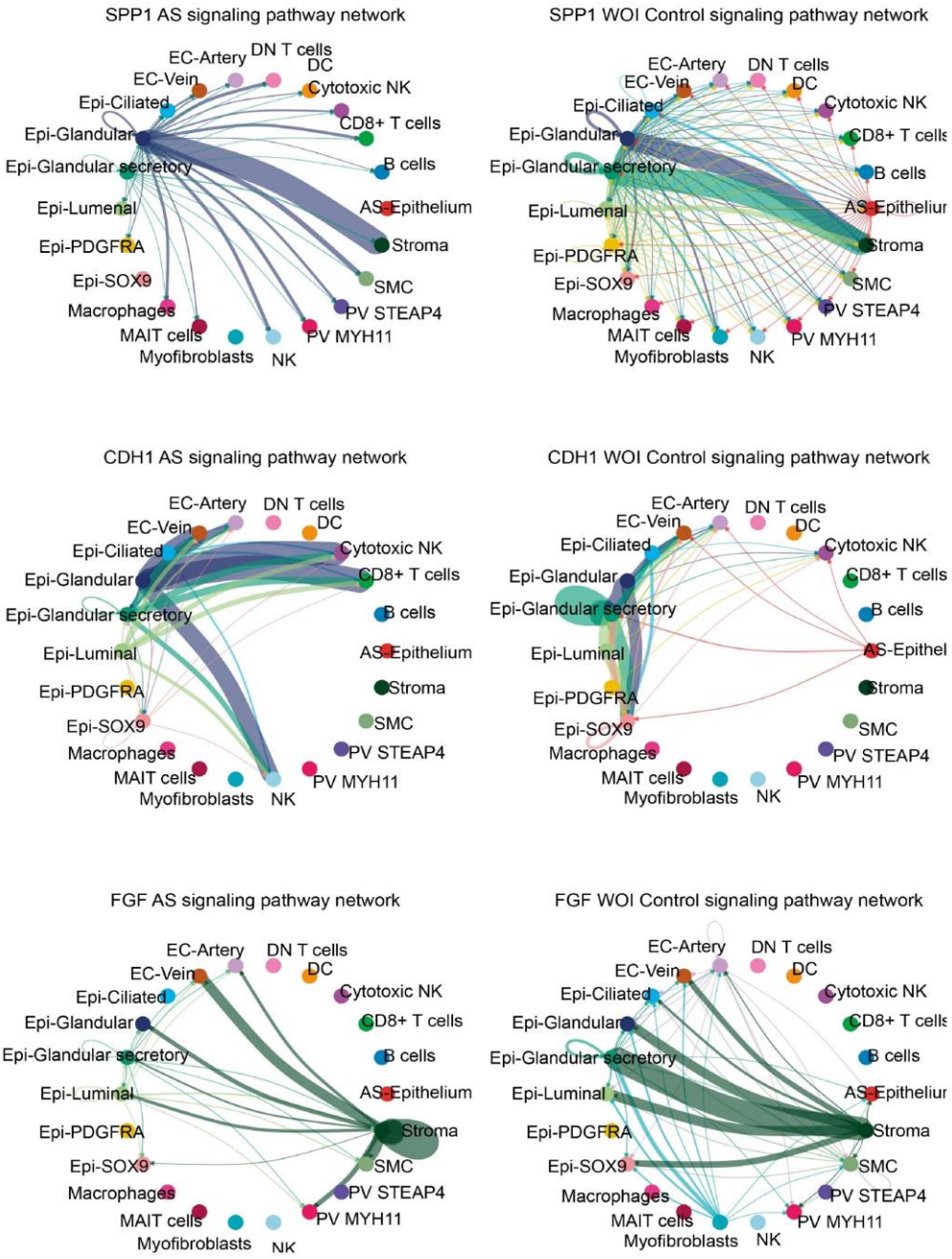

Figure 27. CCC chord plots of SPP1, CDH1, and FGF signaling pathways. The line's color corresponds to the cluster expressing the ligand (emitter), while its destination indicates the cluster expressing the receptor The relative thickness of each line depicts the expression-based strength of the interaction between cell types. Abbreviations - AS (Asherman syndrome), DC (dendritic cells), DN (double negative), EC (endothelial cells), Epi (epithelium), MAIT (mucosal-associated invariant T), NK (natural killer), PV (perivascular), SMC (smooth muscle cell).

We also decided to explore two additional signaling pathways that, although not within the established significant limit (FDR <0.05), had been previously involved in endometrial regeneration (Xue et al., 2022) and differentiation (Garcia-Alonso et al., 2021): the WNT (covering canonical and non-canonical [nc]) and NOTCH pathways, (**Figure 28**). The WNT pathway demonstrated downregulated CCC in AS endometrial samples, as suggested by the loss of the WNT5A-FZD6 interaction between luminal and stromal cells and the loss of the WNT7A-FZD6/LRP6 interaction between stroma and the SOX9-epithelium. NOTCH signaling experienced a notable decline between cells of the luminal, glandular, and glandular secretory clusters, mainly through the JAG1-NOTCH2 pair (**Figure 28**) (Annex 5). These alterations might play a role in the dysregulation of luminal (WNT) and glandular (NOTCH) epithelial differentiation observed in the endometrium of AS patients.

Our findings suggest significant impairments in cell-to-cell interactions between stromal and epithelial cell clusters in AS, which results in a pro-fibrotic environment and altered epithelial differentiation accompanied by dysregulated WNT/NOTCH signaling pathways in the WOI. Simultaneously, alterations to immune CCC lead to the heightened recruitment of leukocytes/myeloid cells through the chemokine-enriched pro-inflammatory environment observed in the endometrium of AS patients.

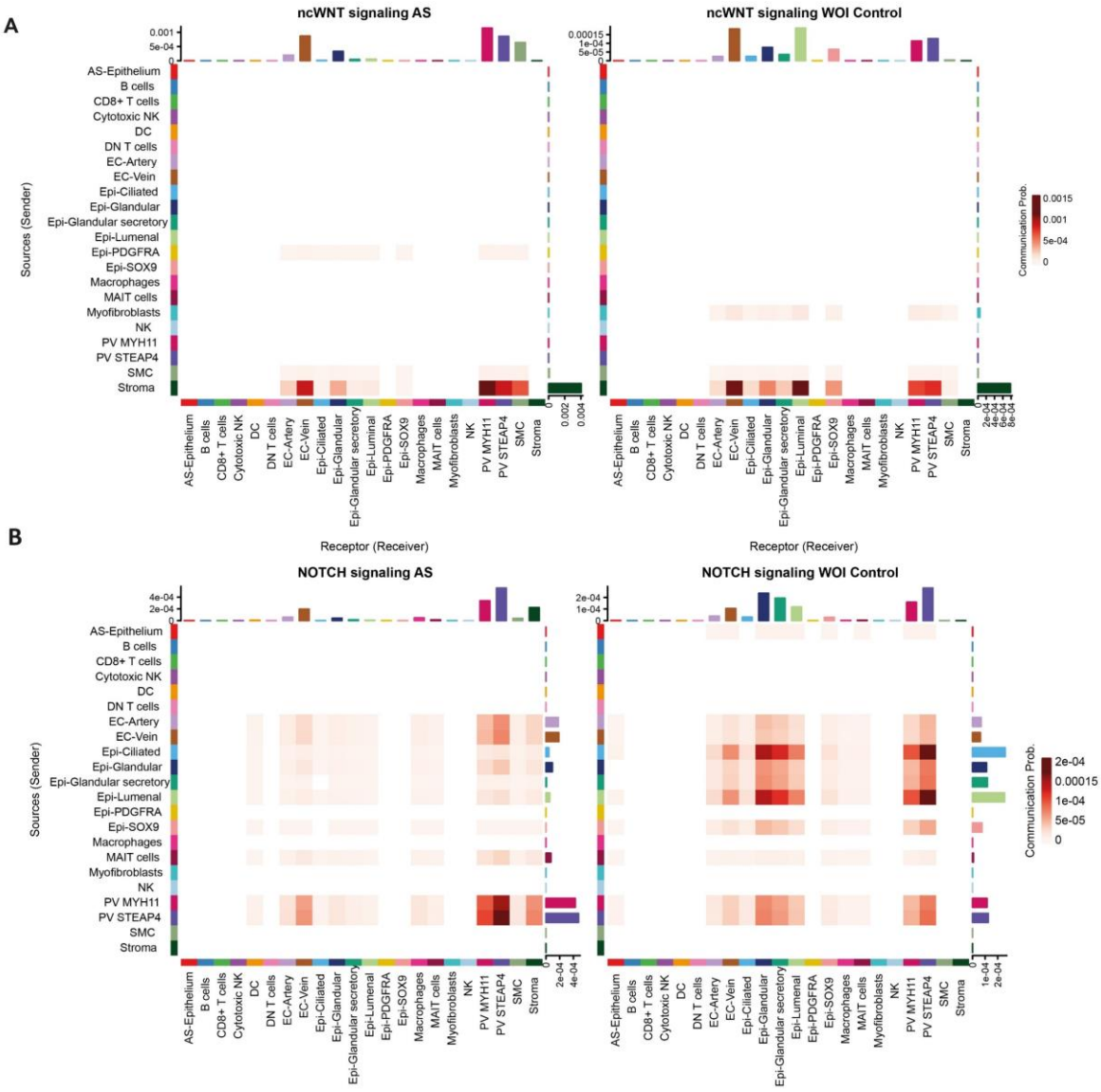

Figure 28. Heatmaps displaying the cell-to-cell communication probabilities in the A) ncWNT and B) NOTCH pathways in Asherman syndrome and window of implantation control endometria. Abbreviations - AS (Asherman syndrome), DC (dendritic cells), DN (double negative), EC (endothelial cells), Epi (epithelium), MAIT (mucosal-associated invariant T), NK (natural killer), PV (perivascular), SMC (smooth muscle cell).

The results from biopsied endometrial samples should be considered in light of certain limitations, including the need for precise timing during sampling and challenges in monitoring endometrial behavior over time; hence, we developed three-dimensional patient-derived organoids (which avoids inherent limitations of two-dimensional culture models) that mimic the endometrial epithelial behavior to investigate their capacity to replicate the characteristics of AS.

2. In vitro model of organoids for Asherman syndrome

As section I.4 outlines, studies focused on the endometrium have widely employed 3D organoid cell culture models. Originally derived from healthy endometrial tissue, organoid culture techniques have evolved to support the representation of various disease states, such as endometriosis or endometrial cancer (Boretto et al., 2019; Katcher et al., 2023). In this doctoral thesis, we describe our efforts to develop an organoid cell culture model for AS and, as such, enable a comprehensive exploration of AS pathology and potential treatments.

2.1. The development of endometrial epithelial organoids

The laboratories of Vankelecom and Turco first reported the development of endometrial epithelial organoids (EEOs) in 2017 via differing but comparable protocols (Boretto et al., 2017; Turco et al., 2017). We based our AS organoid model on the Vankelecom protocol through a scientific collaboration in which I had the pleasure of spending three months in the Vankelecom laboratory in Leuven (Belgium), which provided us with the knowledge to develop, optimize, and manage EEOs and, subsequently, develop the first AS EEO model using biopsies collected from AS patients and WOI control patients (healthy controls).

2.1.1. Differential development between Asherman syndrome and control endometrial epithelial organoids

We applied the conditions used to develop EEOs from healthy donor samples to generate EEOs from AS and healthy control biopsy samples (**Figure 29**). These conditions included Matrigel ® as an artificial ECM source, a culture medium containing several growth and differentiation factors, and incubation at 37ºC and 5% CO_2 (section IV.4). As a result, AS EEOs could be cryopreserved in liquid nitrogen and expanded in the long term, similarly to control EEOs. We also treated EEOs with steroid hormones that mimic estradiol and progesterone impulses in the menstrual cycle and the tissue conditions during the WOI to maintain the culture conditions comparable to the previous biopsy sample analysis (section IV.4.3).

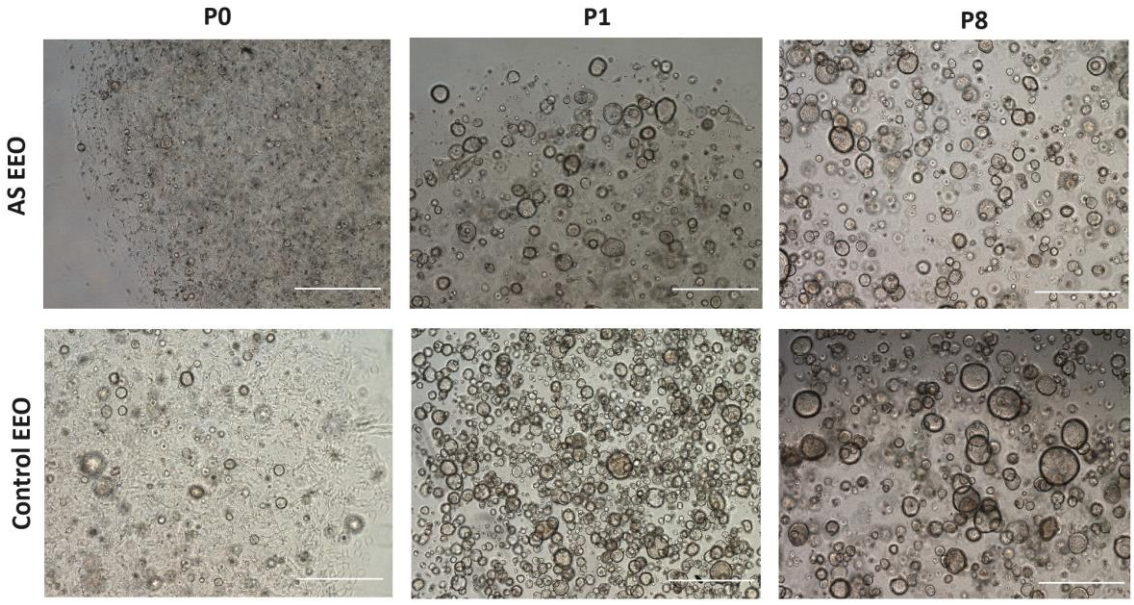

Figure 29. Representative images of endometrial epithelial organoids derived from both Asherman syndrome (AS EEO) (n=3) and window-of-implantation control (Control EEO) (n=3) endometrial biopsies expanded at different passages (P0= Passage 0, P1= Passage 1, P8= Passage 8). Scale bars = 500 µm.

To compare the growth of AS and healthy control EEOs, we quantified the number of EEOs formed from an identical number of cells (evaluates the regenerative capacity of the endometrium of origin) and assessed the diameter of EEOs at different times during development (evaluates cell growth capacity). For the first approach, we seeded 20,000 cells per well, counted the total number of EEOs that formed over seven days, and then averaged measurements across different samples and passages (**Figure 30**). Results revealed a significantly number of organoids generated from AS patient samples than healthy donors at passages 0 and 1. This result suggests that AS patient samples have a lower EEO generation capacity or contain fewer stem cells capable of generating EEOs.

Of note, these differences diminished with successive passages, becoming non-significant at passage 2, which suggests the positive selection of organoid-generating cells during ongoing culture.

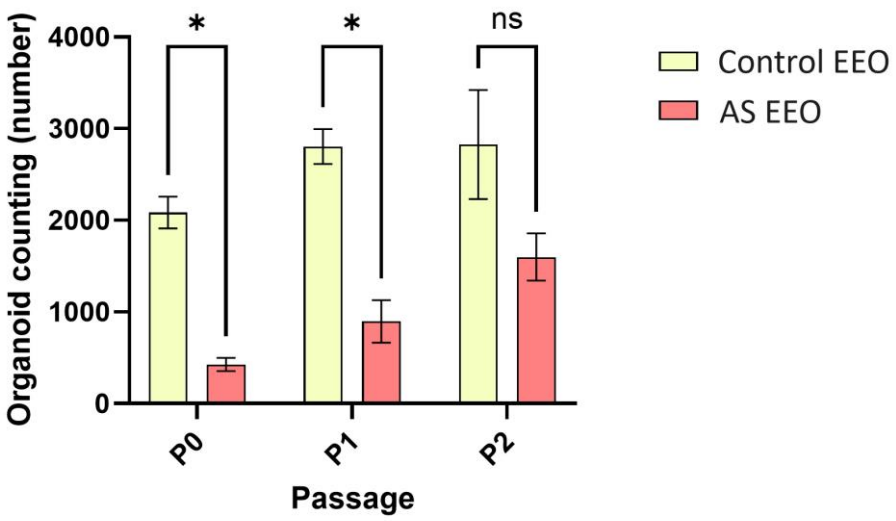

*Figure 30. Average number of Asherman syndrome (AS EEO) and window-of-implantation control (Control EEO) endometrial epithelial organoids measured over three passages (unpaired T test with Welch correction, * p<0.05).*

We used comparable conditions to measure EEO diameter; we used EEOs from higher passages (3 and 4) which we evaluated over seven days. Data from initial days of growth revealed no significant differences in EEO diameters (**Figure 31**), likely due to the overall slow growth during this period; however, we observed a significantly greater diameter of healthy control EEOs compared to AS EEOs at day seven, suggesting a reduced capacity for growth and cell division in the AS endometrium (**Figure 31**).

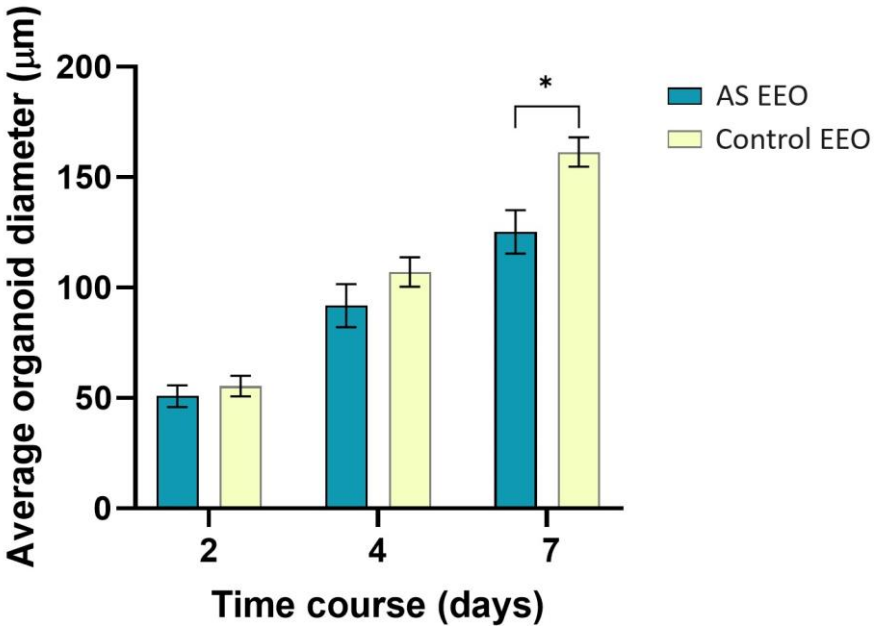

*Figure 31. Average diameter of Asherman syndrome (AS EEO) and window-of-implantation control (Control EEO) endometrial epithelial organoids measured over seven days (unpaired T test with Welch correction, * p<0.05).*

These results proved our ability to generate EEOs under previously described conditions (Boretto et al., 2017; Turco et al., 2017). The culture of AS EEOs presents a more significant challenge, which may relate to poorer tissue/cell microenvironmental conditions or a lower stem cell number/quantity in the AS endometrium; however, the positive selection of organoid-forming cells following multiple passages may mitigate this effect. AS EEOs exhibited a reduced capacity for cell growth and/or division, resulting in significantly smaller organoids, thus retaining specific characteristics of AS pathology. These results suggest that, despite the intrinsic growth-inducing effects of organoid culture, AS EEOs exhibit disease-related characteristics, supporting their use as a 3D cell-based disease model.

2.2. Single-cell transcriptomic analysis of endometrial epithelial organoids

We next profiled the transcriptome of single cells from AS EEOs (compared to control EEOs) using single-cell RNA-sequencing (scRNA-seq) to deeply characterize this model and support a comparison to in vivo data. We employed six biopsy samples (three AS and three WOI healthy controls) to generate EEOs (**Table 3 and Table 4**). In the initial EEO passages, we observed a high number of primary stromal cells from the biopsy, which

were eliminated after two passages (**Figure 32**). While these cells did not pose an issue when counting EEOs, they did represent a problem for scRNA-seq as they would be processed, decreasing the number of analyzed organoid cells; for this reason, we passaged AS and control EEOs twice before processing them for scRNA-seq).

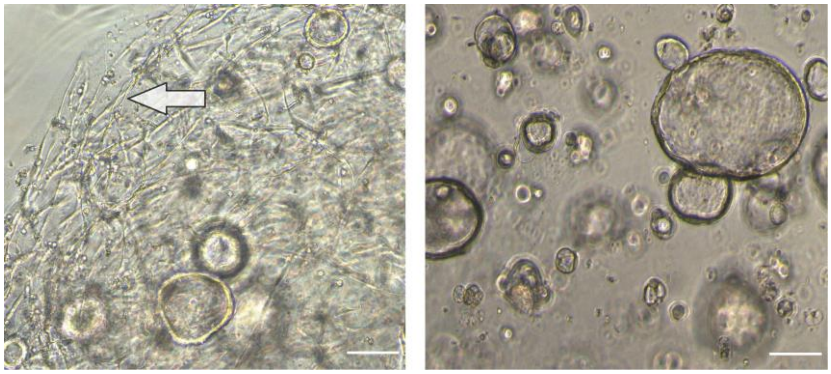

Figure 32. Representative images of endometrial epithelial organoid cultures at passages 0 (left) and 2 (right). The white arrow indicates stromal cells. Scale bars = 50µm.

We acquired transcriptomic profiles of 30,053 cells from hormone-treated EEOs, including 14,459 cells from AS EEOs and 15,594 cells from control EEOs. We characterized cell identities by inferring transcriptomic profiles from our *in vivo* data and utilizing a logistic regression prediction model (section IV.2.5.4). As shown in the recovered cells projection (**Figure 33**), we characterized seven main cell clusters from AS and control EEOS. Specific clusters corresponded with populations previously reported in the literature for EEOs (Garcia-Alonso et al., 2021) validating our identity detection. We named these seven epithelial cell populations as ciliated, cycling organoids (cycling org.), glandular, glandular secretory, KRT17^{+}, proliferative EMT and proliferative KRT19^{+}. Having obtained a similar number of cells in both conditions, we can infer that the AS EEOs had a higher number of glandular and cycling cells and lower number of secretory glandular cells than controls. The following analysis focuses on the transcriptomic description of the different populations and their contribution to the total number of cells.

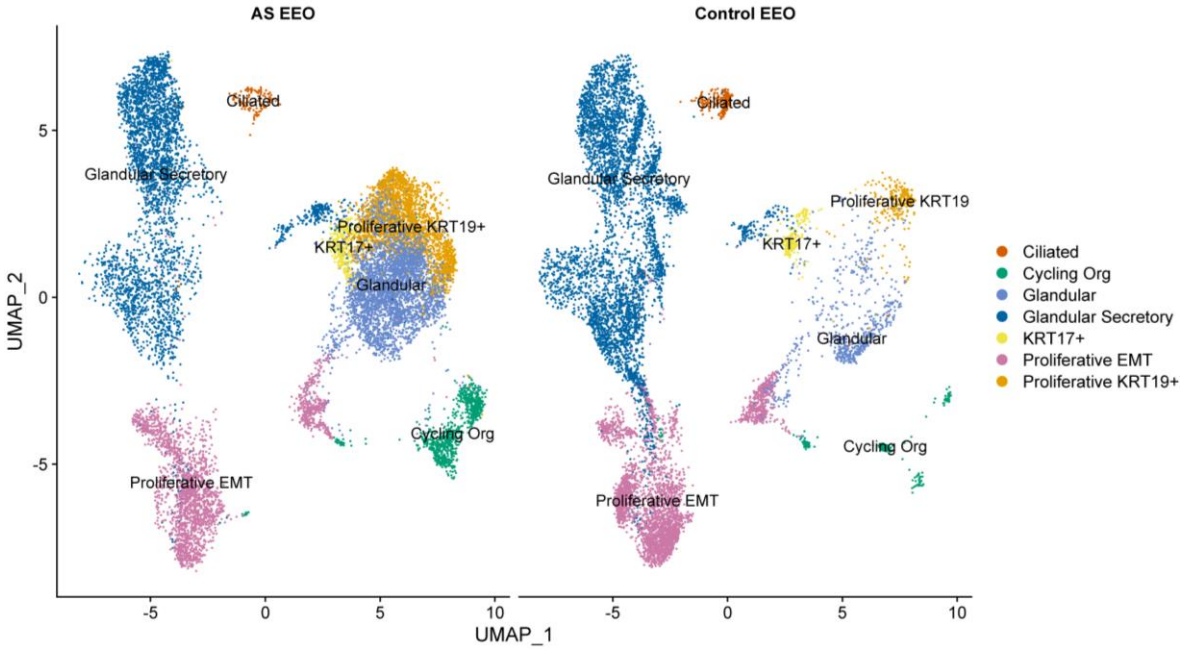

Figure 33. Uniform manifold approximation and projection integration of the main cell clusters identified through single-cell RNA sequencing analysis of Asherman syndrome (AS EEO; 14,459 cells) and window-of-implantation healthy control EEOs (Control EEO; 15,594 cells).

In addition to the markers used to classify common populations, such as *TPP3* for ciliated epithelial cells, *SCGB1D2* for glandular epithelial cells, or *TOP2A* for cycling epithelial cells, specific genes characterize remaining epithelial cell populations (**Figure 34**). The KRT17^{+} epithelial cell population (previously described in EEOs (Garcia-Alonso et al., 2021)) is characterized by the expression of *KRT17* and *KRT19* (related to cell growth and differentiation through WNT/NOTCH crosstalk (Kumar et al., 2018)), *MMP7* (associated with ECM breakdown and tissue remodeling), *TFF1* (an ER-regulated gene), and genes representative of glandular epithelium with lower expression levels. The proliferative KRT19^{+} epithelial cell expressed *KRT19*, *FGFBP1* (associated with proliferation), and *CYP1B1* (a key player in estrogen metabolism that presents elevated levels in estrogen-mediated diseases) (Gajjar et al., 2012). The proliferative EMT epithelial cell population expressed high levels of genes related to cell proliferation and epithelial-mesenchymal transition (e.g., *NEAT1*, *KCNQ1OT1*, and *MALAT1*). Similar to biopsy clustering, the secretory glandular cluster is distinguished from the glandular cluster based on the expression of WOI and receptivity-associated genes.

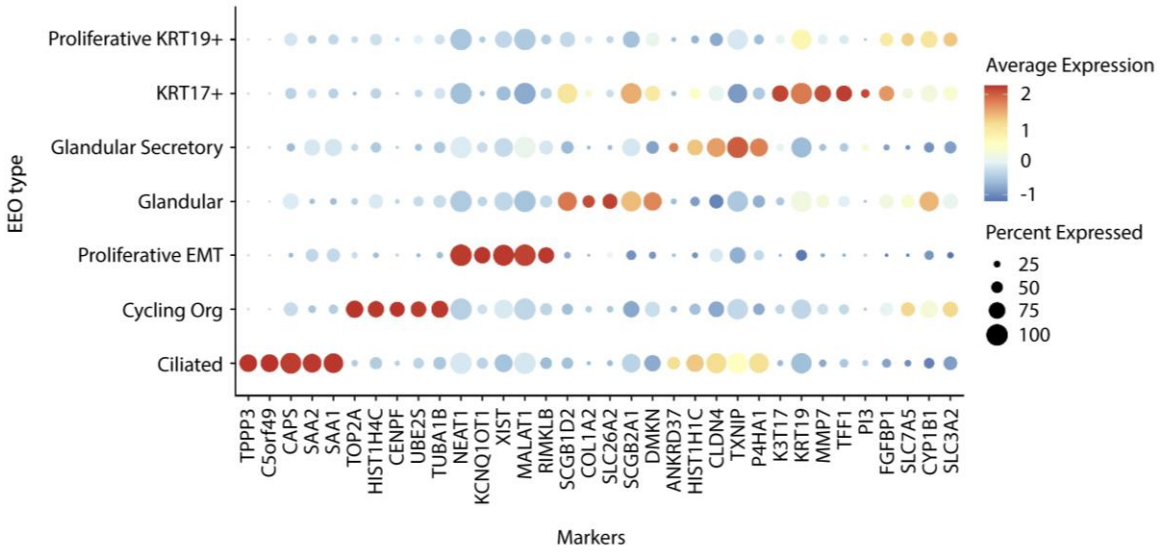

Figure 34. Dot plot displaying maker gene expression profiles used for cell clustering derived from the single-cell RNA-sequencing-based analysis of endometrial epithelial organoid populations.

Cell composition in AS and control EEOs presented notable differences (**Figure 35**). We did not identify the "AS-epithelium" cluster of cells identified in AS biopsies, likely due to the absence of immune cells and the simpler *in vitro* conditions in EEO cultures. Similar to the *in vivo* situation, we observed a smaller proportion of ciliated (0.93% vs 2.65%) and glandular secretory epithelial cells (26.58% vs 49.42%) in AS EEOs than control EEOs, similar to what occurs in tissue samples. The predominance of glandular epithelial cells in AS EEOs compared to control EEOs (29.04% vs 6.54%) agrees with a less responsive epithelial transcriptomic profile, potentially indicating incomplete differentiation after hormonal stimulation and increased induction of ECM growth, as is the cluster with higher COL1A2 gene expression (**Figure 34**), two features associated with AS. The remaining four populations relate to cell division and/or growth. The "Cycling Org." population expresses genes identifying cells as passing through the cell cycle, while the proliferative EMT population overexpresses genes related to cell proliferation regulation and EMT. AS EEOs contain a slightly higher proportion of Cycling Org. epithelial cells (6.84% vs 2.27%), whereas control EEOs contain a slightly higher proportion of proliferative EMT epithelial cells (17.35% vs 34.01%), which may indicate differential growth patterns of these EEOs. The two remaining proliferative populations express genes associated with ECM remodeling (MMP7) or cell differentiation (KRT19);

we observed a similar representation of KRT17^{+} epithelial cells (2.48% vs 2.55%) in both EEO types and a noticeable overrepresentation of proliferative KRT19^{+} epithelial cells (16.76% vs 2.53%) in AS EEOs. The proliferative KRT19^{+} population expressed the estrogen metabolism and estrogen-mediated disease gene *CYP1B1*, which may relate to the higher expression of ERs observed in biopsy transcriptomics. Although these populations differences are not statistically significant, the observed trends align with previous results from AS and control biopsies (**Figure 12** and **Figure 16**), suggesting the AS EEOs ability to replicate the epithelium in AS pathology.

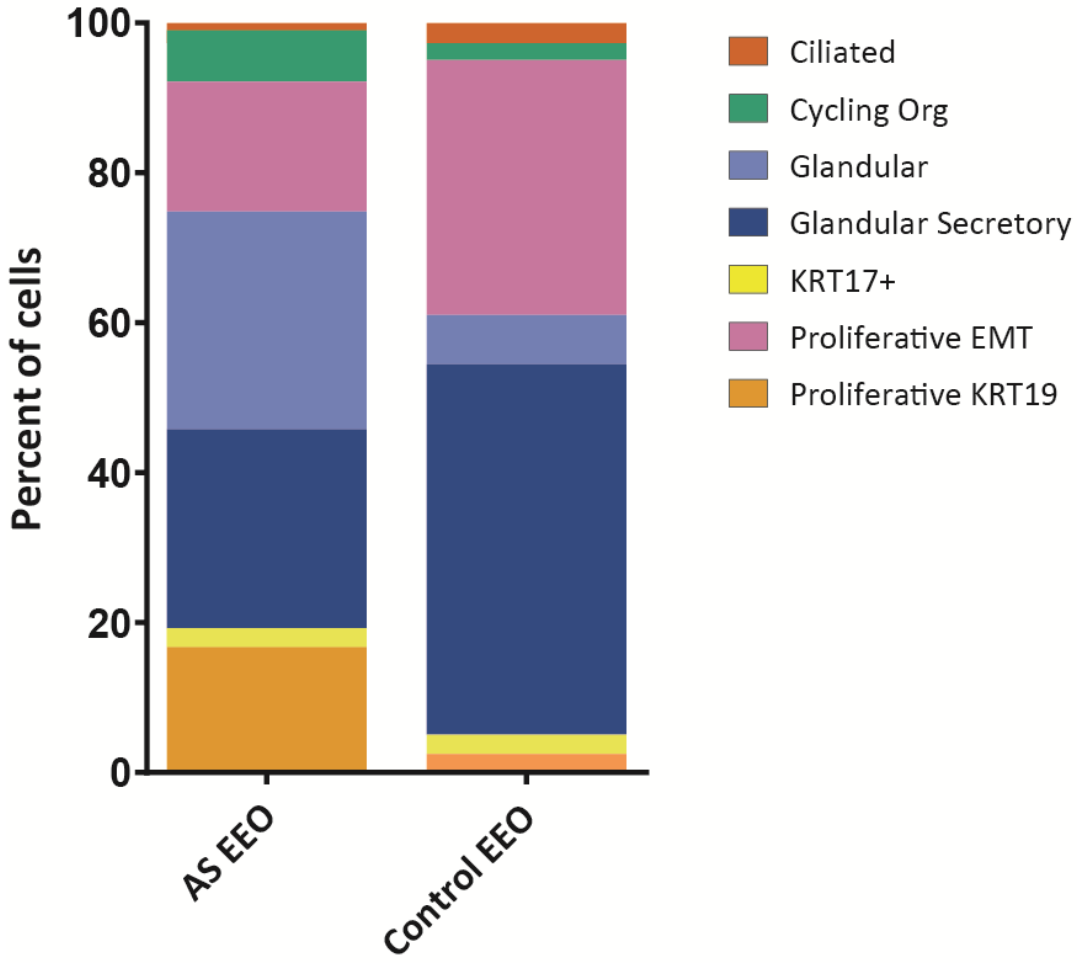

Figure 35. Histogram comparing the proportion of epithelial cell types in Asherman syndrome (AS EEO) and healthy control (control EEO) endometrial epithelial organoids.

To compare the transcriptomic data of our EEOs with *in vivo* tissue, we measured the distance (a measure of similarity between populations) of each cell population identified

in AS and control EEOs to those identified in WOI biopsy controls (**Figure 14**), calculating a similarity score between conditions. The resultant polygonal plot (**Figure 36**) demonstrates that cells of AS and control EEOs present the highest similarity scores for glandular and glandular secretory epithelial cell clusters. As indicated by the previous cell type classification (**Figure 35**), control EEO cells (in green) display a closer relation to glandular and glandular secretory epithelium than AS EEO cells, while both EEO types contain cells that resemble ciliated epithelial cells (although at a much lower rate) (**Figure 36**). Furthermore, none of the analyzed EEO cells seemed to associate with luminal epithelium, with only a few resembling the SOX9^{+} population. Therefore, we continued analyzing the glandular and glandular secretory epithelium.

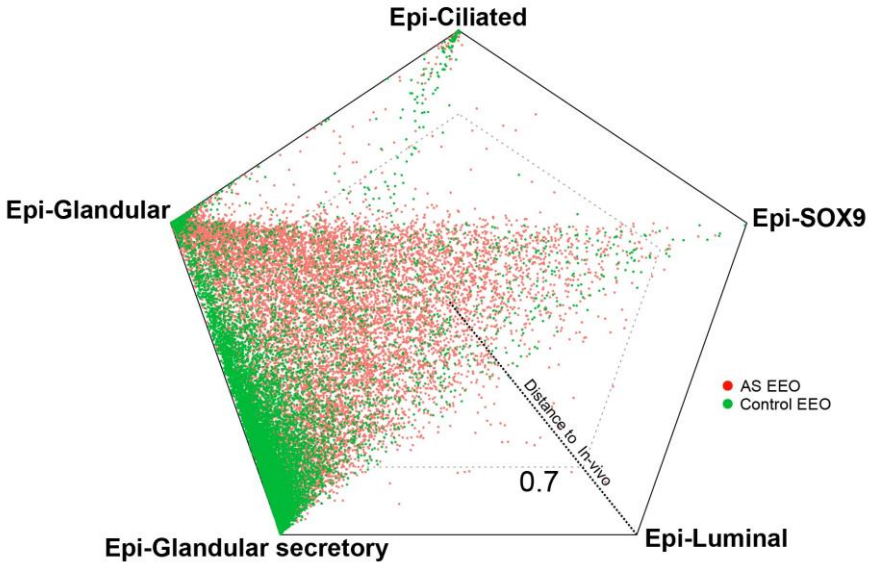

Figure 36. A polygonal plot representing predicted probabilities of endometrial epithelial organoid cell type identity using a logistic model trained on epithelial tissue clustering from window-of-implantation control biopsies. Cell types at vertices correspond to the epithelia identified in control tissue biopsies, while colored points correlate with individual cells from endometrial epithelial organoids (both Asherman syndrome and window-of-implantation healthy controls). The dashed line forming the interior polygon indicates a 0.7 score value, and points outside this line indicate higher score values. The dashed straight line from the center to a vertex exemplifies the distance to in vivo cell identities; the greater the distance from the vertex, the less similar they are.

After stratifying calculated scores as box plots (**Figure 37**), we observed a significant difference in the transcriptomic profiles of AS EEOs (p<0.001) from those found in control

EEOs and WOI control biopsies when comparing the glandular and glandular secretory epithelial cells.

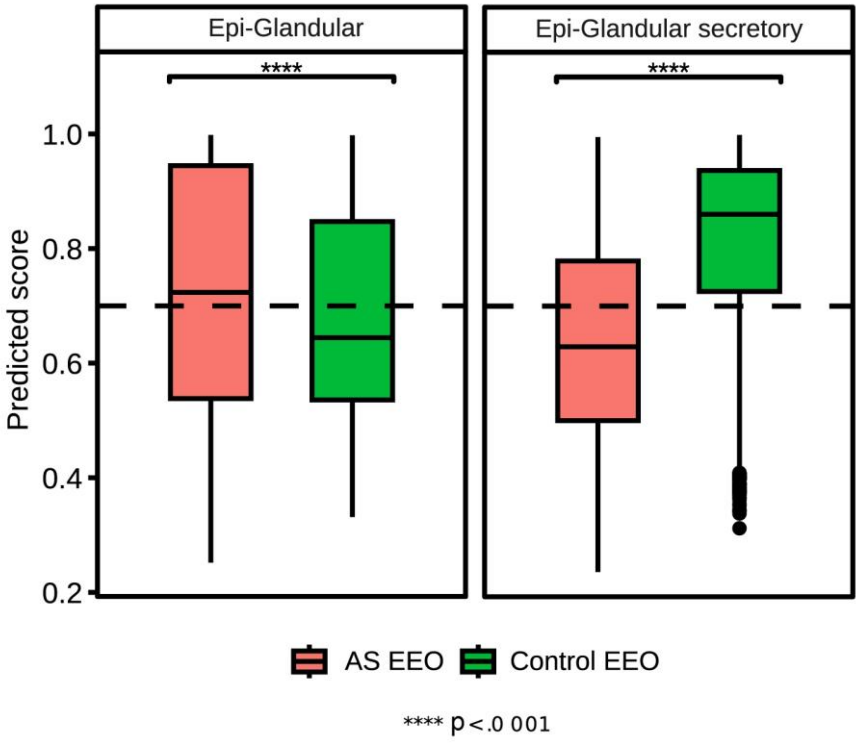

*Figure 37. Box plot representing prediction scores for the similarity of glandular and glandular secretory epithelial cells (from Asherman syndrome and window-of-implantation healthy control endometrial biopsies) and endometrial epithelial organoid cells. A two-sided Dunn test was applied to evaluate differences between groups; p-values adjusted through Bonferroni method; ****p<0.001. The dashed line marks a 0.7 score value, the same line forming a pentagon in image Figure 36.*

Differential gene expression analysis comparing AS and healthy control EEOs (**Figure 38**) revealed that the glandular epithelial cells upregulated the expression of *SCGB2A1*, *SCGB1D2*, and *CYP1B1* (estradiol regulation or metabolism) and *DMKN* and *ANXA1* (anti-inflammatory) and downregulated the expression of *GOS2* (apoptosis promoter), MT-ND2 (mitochondrial respiratory chain), SOD2 (antioxidant), and *CXCL14* (a characteristic WOI gene) in AS EEOs compared to control EEOs. The glandular secretory epithelial cells expressed lower levels of genes such as *MT-ATP6* (ATP production in the mitochondria) and *GOS2* and higher levels of *SCGB2A1* (which is related to the estrogen and progesterone receptor pathway) in AS EEOs compared to control EEOs. These gene expression differences suggest the more significant implication of the glandular

epithelium in AS EEOs in inflammatory processes, the response to estradiol, and reduced apoptotic and mitochondrial activity. Overall, these results agree well with the characteristics of the AS endometrial tissue described previously (section I.5.1).

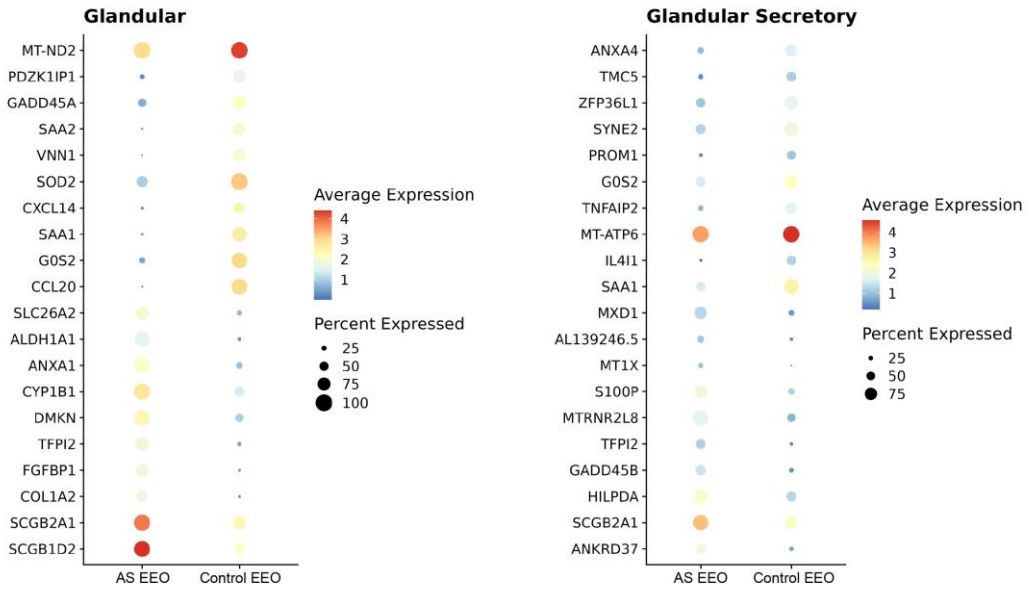

Figure 38. Dot plots of differential gene expression for glandular and glandular secretory cell populations identified in Asherman syndrome (AS EEO) and healthy control (Control EEOs) endometrial epithelial organoids (two-sided Wilcoxon Rank Sum test; FDR<0.05).

These data suggest that AS EEOs recapitulate specific characteristics found in the AS epithelium, such as a less prevalent glandular secretory epithelium, an inflammatory response profile with high predicted reactivity to estradiol, and lower proliferative-related gene expression.

2.3. Immunohistochemical characterization of endometrial epithelial organoids

To further characterize our AS EEO model, we explored aspects such as proliferation, morphology, and the presence of specific cellular markers (via immunohistochemical approaches).

We performed immunohistochemistry to identify critical features associated with AS EEOs (**Figure 39)** and control EEOs (**Figure 40**). We detected the epithelial cell markers E-cadherin (a cell adhesion glycoprotein essential for epithelial cell adhesion and polarity) and Pan-cytokeratin (PANCK; an epithelial cell cytoskeleton filament protein) in AS and

control EEOs at seven days of *in vitro* culture, confirming the differentiation of adult stem cells into epithelium cell-containing organoids. We stained individual Z-stack images of organoids with phalloidin to label F-actin; this approach revealed the presence of a solid F-actin positive boundary, which demonstrates the apicobasal polarity of the epithelium in the interior of AS and control EEOs. The 2D sections also confirmed the presence of a hollow lumen within EEOs. This approach also identified the glandular structure of AS and control EEOs, verifying the polarization of epithelial cells within EEOs (a characteristic not observed in traditional 2D cultures), as observed previously in EEOs generated from healthy endometrial samples (Boretto et al., 2017; Turco et al., 2017).

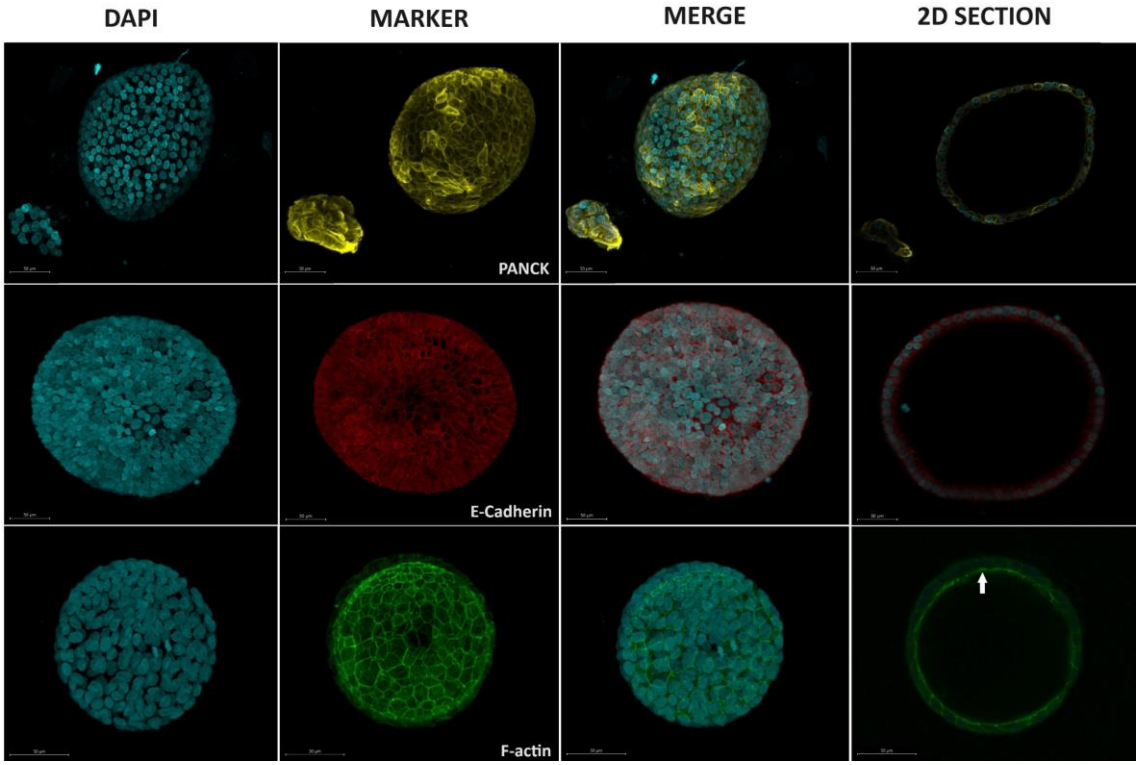

Figure 39. Immunohistochemical analysis of window-of-implantation healthy control endometrial epithelial organoids. Cell nuclei are stained in blue, pan-cytokeratin in yellow (PANCK), E-cadherin in red, and F-actin in green. White arrows indicate F-actin label accumulation. Scale bar = 50 µm.

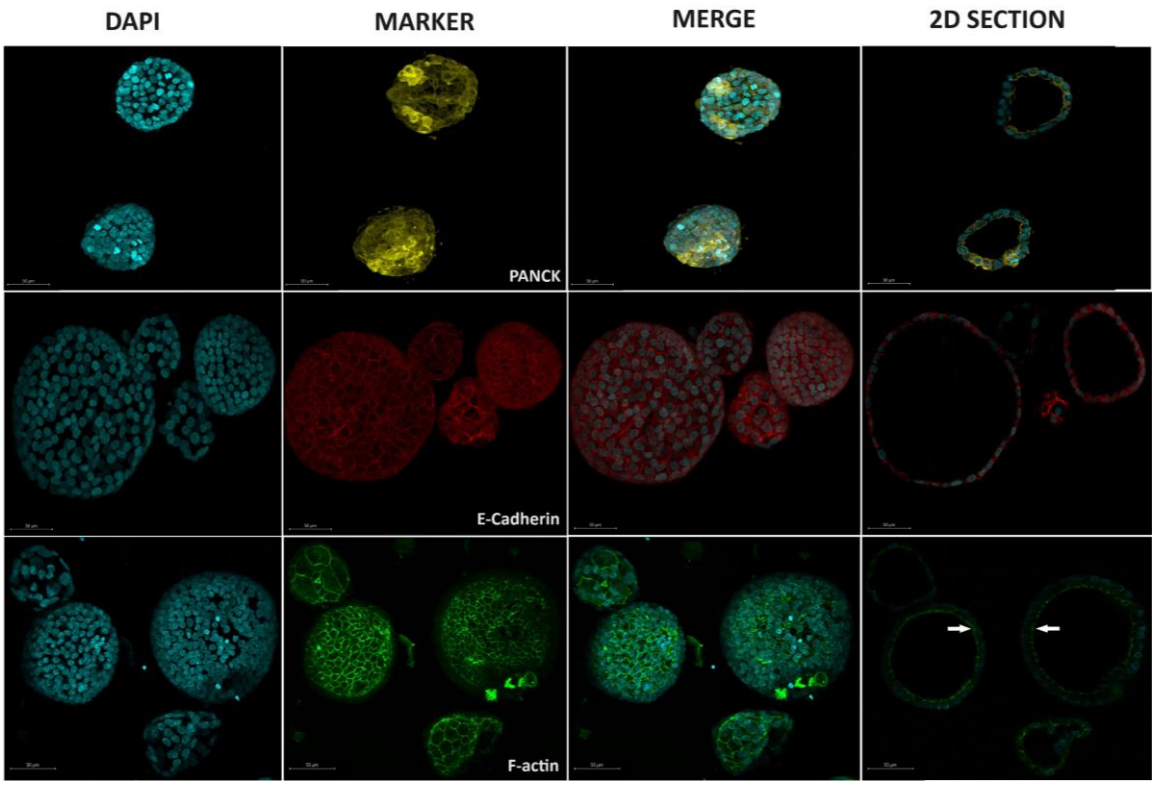

Figure 40. Immunohistochemical analysis of Asherman syndrome endometrial epithelial organoids. Cell nuclei are stained in blue, pan-cytokeratin in yellow (PANCK), E-cadherin in red, and F-actin in green. White arrows indicate F-actin label accumulation. Scale bar = 50 µm.

Utilizing fixed organoids, we conducted additional measurements to assess cell proliferation across the two EEO types. We stained the samples with Ki67 antibody, a well-known proliferation marker, and DAPI for nuclei detection to analyze the number of Ki67-positive cells relative to the total cell count. We determined the proliferation ratio by confocal microscopy (**Figure 41**) by measuring the number of $Ki67^{+}$ cells relative to the total cell count. This analysis revealed a significant difference in the proliferation of organoids from AS biopsies compared to control samples (**Figure 42**), with the pathological model exhibiting lower proliferation.

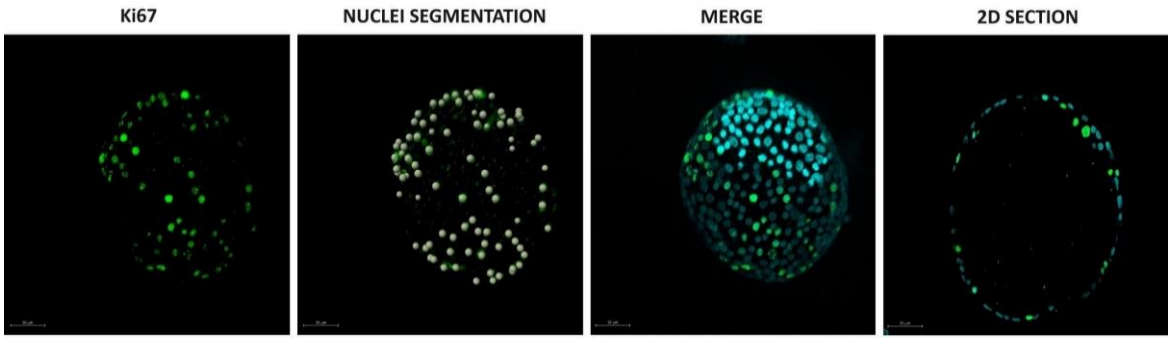

Figure 41. Representative confocal images of Ki67 positive (green) showing the Ki67⁺ cells, their nuclei segmentation, and merging with nuclei (blue) in 3D and 2D. 4,6-diamidino-2-phenylindole (DAPI) was used for nuclear staining. Scale bar = 50 µm.

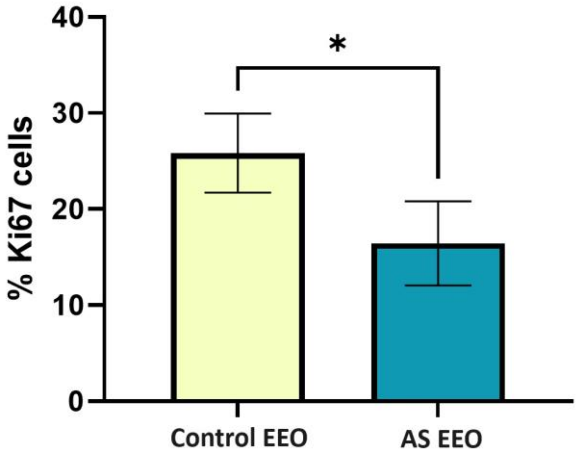

Figure 42. Ki67⁺ cells quantification in endometrial epithelial organoids three independent donors. One-way analysis of variance with post-hoc Tukey test (ANOVA) (p-value<0.05).

In conclusion, EEOs developed from AS samples partially recapitulate the characteristics of this disease. AS EEOs exhibit lower proliferation and smaller sizes and are composed of epithelial cells that present a transcriptomic profile more closely related to AS epithelium than healthy WOI epithelium. Similarly, AS EEOs represent polarized glandular epithelium in the same manner as control EEOs; however, we did not detect the characteristic tissue population named "AS-epithelium" (with overexpressed SLPI marker) nor represent the remaining cell types not part of the epithelium. Despite these limitations, we suggest that AS EEOs represent a useful *in vitro* model for studying this pathology and a starting point for the development of even more complex models.

3. Effect of autologous cell therapy in the Asherman syndrome endometrium

In this concluding chapter, we aimed to evaluate the effects of a therapeutic approach developed by our group on the endometrium of (AS) patients. This therapy, comprising the application of autologous $CD133^+$ bone marrow-derived stem cells (BMDSCs) to regenerate the fibrotic endometrium, has been approved by the European Medicines Agency and the United States Food and Drug Administration as an orphan drug for AS treatment (section IV.1) and is currently in phase I/II trials (EudraCT Number: 2016-003975-23). We performed single-cell transcriptomics in biopsies from nine AS patients one month after treatment to analyze the impact on the diseased endometrium using our single-cell atlas to achieve this objective.

3.1. Tissue transcriptomics

3.1.1. Partial recovery of transcriptomic profiles in Asherman syndrome patients after patient-specific autologous cell therapy

We included nine patients who participated in the clinical study in the transcriptomic analysis. To determine therapeutic responses, we analyzed endometrial biopsies for each patient before and after $CD133^+$ BMDSC administration. We analyzed 123,250 cells from these biopsies - 40,336 pre-treatment and 82,914 post-treatment (patient contribution available in Annex 6). We integrated matched pre-treatment (AS) and post-treatment (AS-Post) samples into the same dimensional reduction depiction (**Figure 43**). Overall, we observed smaller epithelium, ciliated epithelium, endothelium and cycling cells clusters before treatment (AS) and a decrease in the size of the AS-epithelium cluster after treatment (AS-Post).

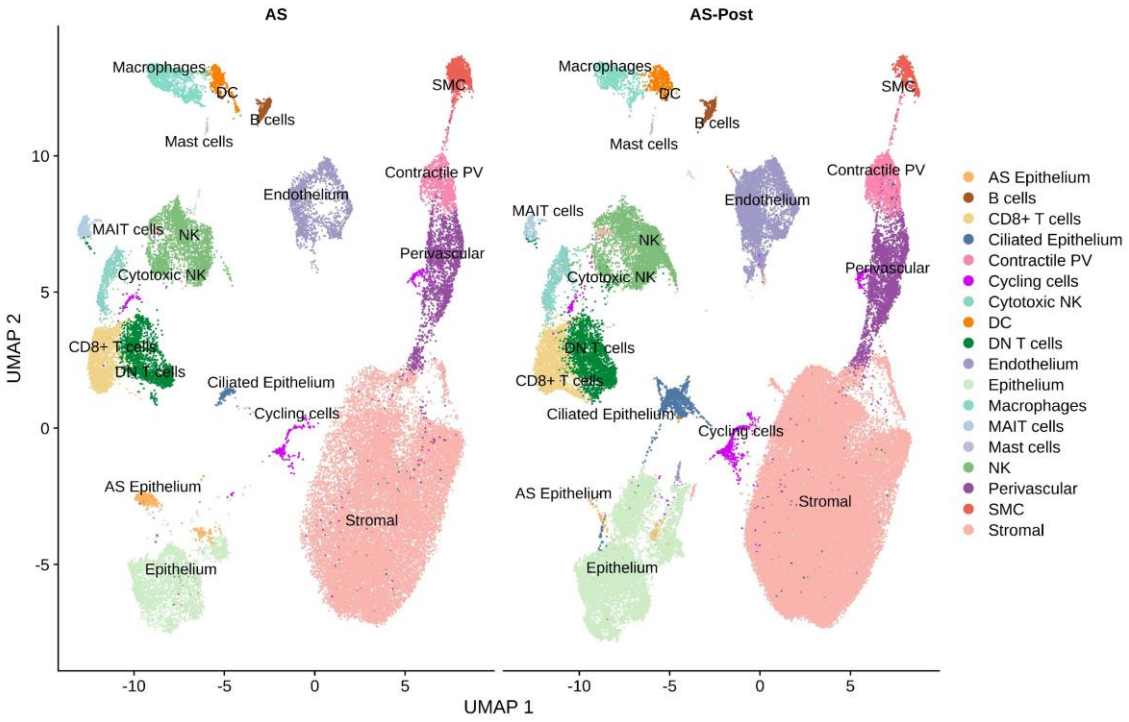

Figure 43. Uniform manifold approximation and projection representing single-cell RNA sequencing results of Asherman syndrome patients before (40,336 cells) and after (82,914 cells) autologous cell therapy administration. Abbreviations - DC (dendritic cells), DN (double negative), MAIT (mucosal-associated invariant T), NK (natural killer), PV (perivascular), SMC (smooth muscle cells).

Despite these findings, only some observations were further supported by comparative cell ratio analysis comparing pre- and post-treatment samples. These populations were the AS-epithelium, which presented a statistically significant (FDR <0.05) reduction from 0.035% to 0.012% of cells (**Figure 44**), and the macrophage population, which showed a reduction in cell number from 0.61% to 0.21% (FDR <0.1). However, although not statistically significant, there is a noticeable trend of an increase in specific populations, such as in the epithelium, which rose from 8.39% to 10.43%, ciliated epithelium, which increased from 0.30% to 1.25%, and endothelium, which rose from 3.26% to 6.31% .

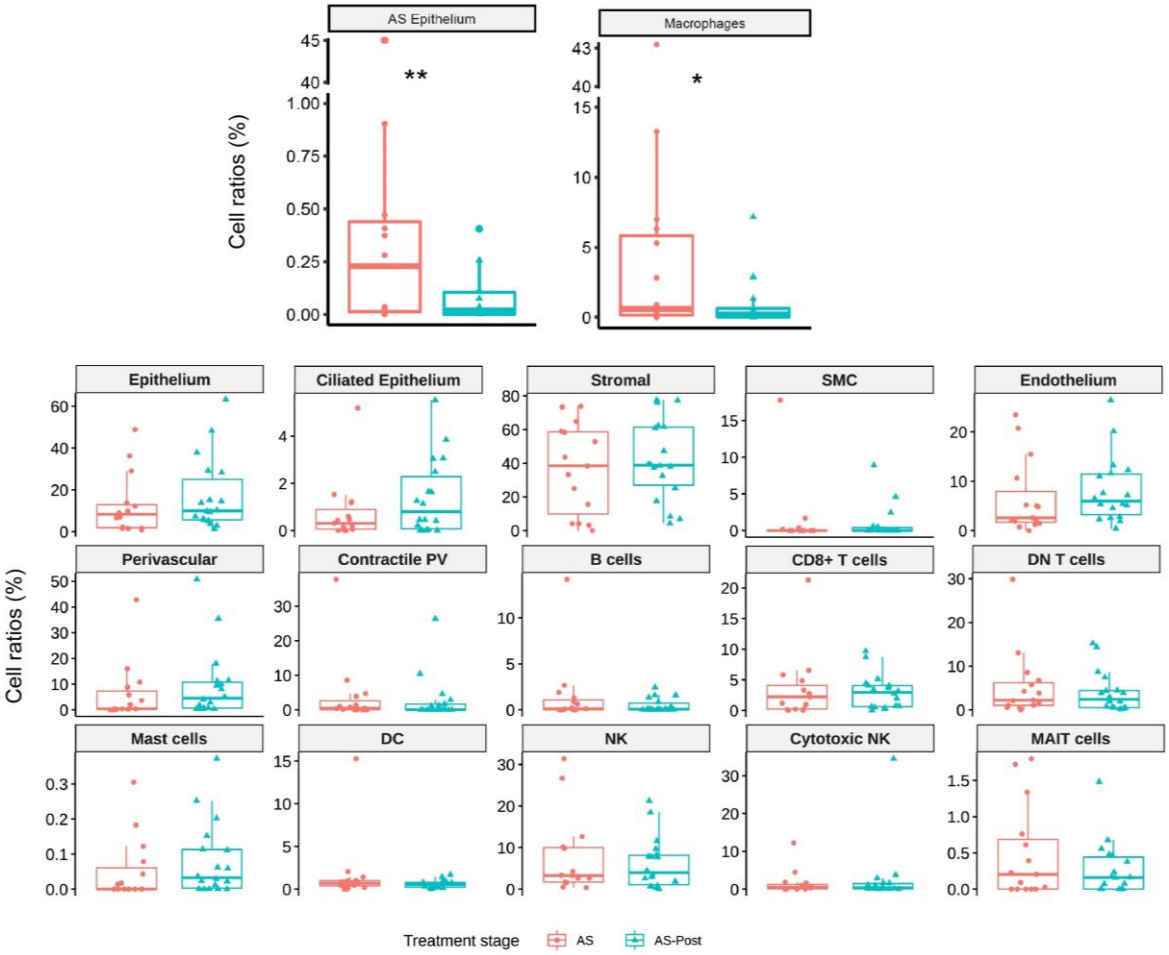

*Figure 44. Box plots of cell type ratios comparing Asherman syndrome endometrium in pre-treatment (AS) and post-treatment (AS-Post) stages. (NB-GLM statistical test** = FDR<0.05, *= FDR<0.1). Abbreviations - DC (dendritic cells), DN (double negative), MAIT (mucosal-associated invariant T), NK (natural killer), PV (perivascular), SMC (smooth muscle cells).*

Next, we determined the expression of a gene set signature related to endometrial function in the secretory phase (the gene set signature is described in section IV.2.7) in endometrial samples before and after CD133⁺ BMDSCs treatment. This analysis provides an overview of endometrial functionality by examining the global expression of specific genes associated with various cellular functions during the secretory phase. We determined the gene set from those previously identified by our group as highly expressed during the early-secretory and mid-secretory (WOI) phases of the menstrual cycle. This set is composed of the following genes: *SCGB1D2*, *MT1F*, *MT1X*, *MT1E*, *MT1G*, *CXCL14*, *WNT5A*, *SFRP1*, *ZFYVE21*, *CILP*, *SLF2*, *MATN2* and *S100A4*. **Figure 45** represents the combined expression of this gene set as a score (UCell score). The results revealed

that epithelial, AS-epithelial, stromal, endothelial, and PV cells presented a higher expression of the gene set after CD133⁺ BMDSCs treatment. This result suggest that cell treatment activates endometrial functionality, enhancing the endometrium's receptivity and its readiness for a potential pregnancy.

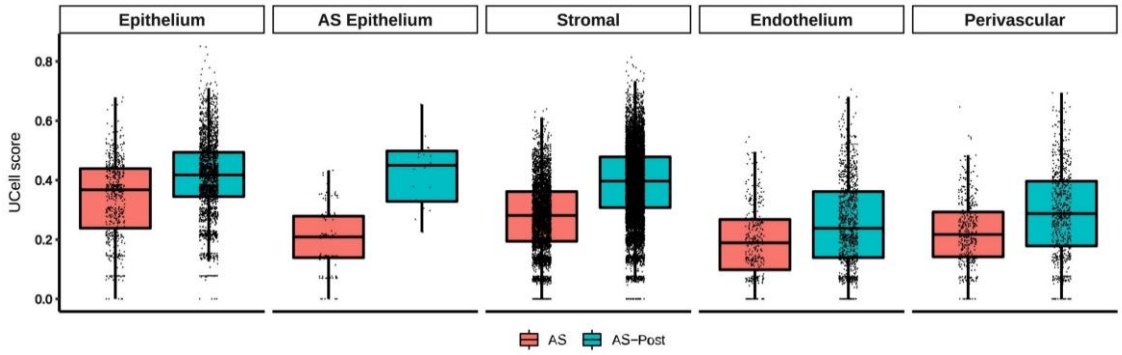

Figure 45. Boxplot of enrichment score results (UCellScore) of gene signature characteristic of the secretory phase in the menstrual cycle.

Differential gene expression evaluation between pre-treatment and post-treatment endometrial samples revealed increased *SCGB1D2* (related to functional secretory activity) (Wang et al., 2020; Zieba et al., 2015), *LGALS1* (which diminishes immune activity) (Chaney et al., 2022), and *PDGFRA* and *IGF1* (associated with extracellular matrix remodeling and regeneration) (Milingos et al., 2011) expression in epithelial cells of post-treatment samples (**Figure 46**). We also observed the reduced expression of *S100A10* (promotes macrophage recruitment) (Lou et al., 2019) and genes related to inflammation and immune response (such as *IL6ST, MIF,* or *DEFB1*) (Prasad et al., 2019) in post-treatment epithelial cells. These gene expression differences suggest that autologous cell therapy in the AS endometrium induces the appearance of an epithelium with reduced immune activity and inflammation and restores secretory and regenerative functions.

The stromal cell cluster in the AS endometrium after autologous cell therapy exhibited the upregulated expression of genes related to angiogenesis and vascular development (such as *IGFBP2* and *PTN*) (Chung et al., 2002; Slater et al., 2019), cell division (*TPM1*) (Poon & Storms, 1991), cell migration and invasion (*PTN, LMO4,* and *SPARCL1*) (Wang et

al., 2016), and EMT reduction via autophagy (*DIO2*) (Zhou et al., 2022) (**Figure 46**). Meanwhile, autologous cell therapy induced downregulated expression of genes related to cell proliferation (*JUN, JUNB, FOS, FOSB, EGR,* or *BTG2*), oxidative stress response (*SOD2*) (Herrlich et al., 1990; Hu et al., 2010; Schlingensiepen et al., 1994), cellular stress (*HSPA1A* and *HSPA1B*) (Radons, 2016), and anti-angiogenic functions under pro-inflammatory environments (*IGFBP3*) (Santamaria et al., 2016) in stromal cells (**Figure 46**). These expression profiles indicate that autologous cell therapy in the AS stroma prompts diminished growth and EMT, enhanced cell migration and invasion, and increased vascularization induction, all within an environment of reduced cellular stress and inflammation, resulting the shift of the AS endometrium to a state more similar to a healthy state.

After $CD133^+$ BMDSC administration, analysis of the endothelial compartment indicated a transcriptomic shift from a pro-inflammatory profile characterized by cell stress to a more homeostatic state (**Figure 46**). We observed the downregulation of genes involved in leukocyte/myeloid trans-endothelial migration (*ICAM*), antigen presentation (*HLA-DRA* and *HLA-DRB5*), cell proliferation (*FOS* and *JUNB*) or heat shock proteins (*HSPH1* and *HSPA1B*) (**Figure 46**). Furthermore, *IGFBP2* overexpression suggest the enhanced formation of new blood vessels, and the expression of different collagen genes (e.g., *COL1A1, COL3A1, COL6A1,* and *COL6A3*) indicate ECM cell adhesion and the development of capillaries from vessel surroundings (Davis & Senger, 2005) (**Figure 46**).

Our transcriptomic analysis also revealed the overexpression of *IGFBP2* and *TMSB10* (related to cytoskeleton organization and cell motility) (Zhang et al., 2017) in PV cells, and *FOSB, JUND,* and *FAU* (a pro-apoptotic gene)(Pickard et al., 2011), *KLF2* (promotes functional differentiation of endothelial cells) (Dekker et al., 2006), and *SPARCL1* in contractile PV cells after $CD133^+$ BMDSC administration (**Figure 46**). Contractile PV cells displayed the reduced expression of the *TPM1* (Poon & Storms, 1991) proliferation-associated gene, while both Contractile PV and PV cells displayed a reduction in the expression of genes related to smooth muscle cells (e.g., *MYH11, MYLK,* and *MYL9*) (Shen et al., 2015). The SMC cluster downregulated genes related to cell proliferation (*SOX4*) (Saegusa et al., 2012), stress response (*PAGE4*) (Kulkarni et al., 2016), and ATP regeneration (*CKB*) following $CD133^+$ BMDSC administration (**Figure 46**). The PV cell,

contractile PV cell, and SMC populations also displayed reduced cellular stress response (with decreased expression of *S100A6* (Wang et al., 2023)) after CD133$^+$ BMDSC administration. Overall, the transcriptomic profiles of these populations suggest that the PV and contractile PV cell populations exhibit a loss of muscular characteristics, which results in increased proliferation of PV cells, differentiation towards endothelial cells, and reduced growth in the contractile PV cell and SMC populations in a background of reduced stress as a result of cell therapy effect.

Lastly, analysis of immune cell populations following CD133$^+$ BMDSC administration confirmed reduced immune activity and cell stress suggested by the gene expression patterns observed in other endometrial cell populations. We observed decreased expression of *MTRNR2L12* (an anti-apoptotic lncRNA) (Li et al., 2023) in almost every analyzed immune cell population, *S100A* family genes (*S100A8, S100A9, S100A11,* and *S100A12*) and *IL32* in NK cells, and *HSPA1A* in MAIT cells (Annex 7).

These results indicate that administering CD133$^+$ BMDSCs to the AS endometrium partially reverts the diseased state of the epithelium and macrophage cell compartment. CD133$^+$ BMDSCs also partly restore the transcriptomic profiles of critical endometrial cell populations to decrease oxidative stress and inflammation, increase angiogenesis, and induce the proliferation of stromal cells and SMCs.

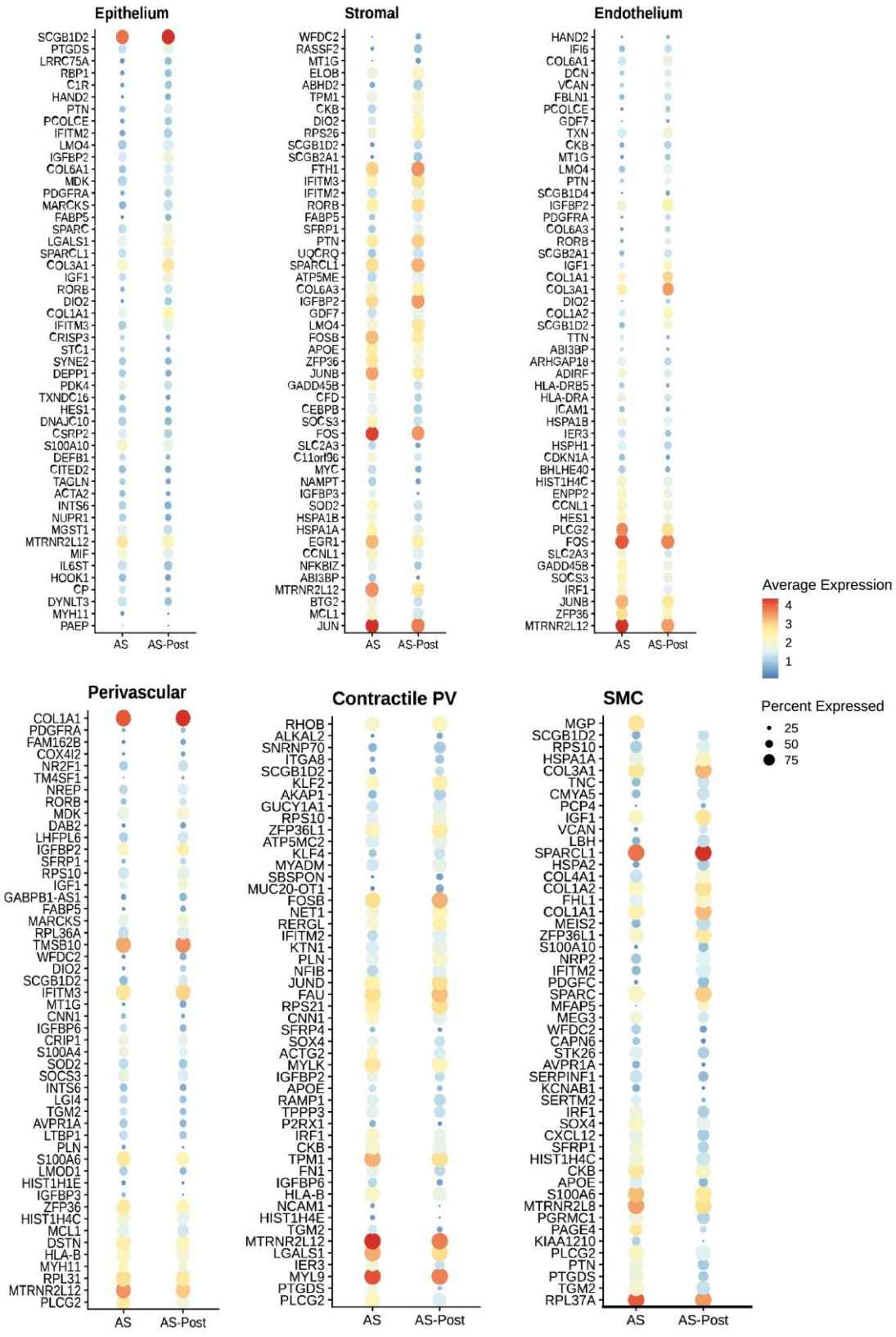

Figure 46. Differential gene expression between pre-treatment and post-treatment Asherman syndrome cell types (Wilcoxon Rank Sum test, FDR <0.05). Abbreviations - AS (Asherman syndrome), As-Post (Asherman syndrome after treatment), PV (perivascular), SMC (smooth muscle cells).

3.1.2. Cell-to-cell communication modifications after autologous cell therapy

As we observed significant impairment in cell-to-cell interactions between several cell clusters in AS patients compared to healthy controls, we investigated similar alterations in the AS endometrium following CD133$^+$ BMDSC administration. For this purpose, we CCC analysis using transcriptomic data from AS patient cells before and after receiving cell therapy.

Analysis of information flows of differentially detected signaling pathways in AS patients after CD133$^+$ BMDSC administration revealed the enrichment of pathways previously present only in healthy endometrial samples (e.g., TWEAK, CXC3, IGF, and GDF) (**Figure 23** and **Figure 47**). Additionally, AS endometrium-associated signaling pathways related to immune response and pro-inflammatory processes (e.g., CCL, CXCL, MHC-I, MHC-II, LIGHT, SEMA6, NECTIN, CD22, TNF, and RESISTIN) became reduced in strength after CD133$^+$ BMDSC administration (**Figure 47**). In addition, the ITGB2 pathway, an interacting molecule related to fibrosis, suffered from reduced representation after CD133$^+$ BMDSC administration, while epithelial development (CADM) and angiogenesis pathways (e.g., PTPRM and FGF) became enriched. Of note, the ANGPTL and LT signaling pathways displayed enrichment in the AS endometrium; however, CD133$^+$ BMDSC administration prompted their reduction (**Figure 47**), similar to what we observed when comparing AS samples with both healthy secretory and WOI controls (**Figure 23** and **Figure 26**).

These results indicate a recovery of CCC to a state resembling that of healthy samples; overall, CD133$^+$ BMDSC administration restored lost signaling pathways in the AS endometrium and reduced AS-associated pathways, such as those involved in fibrosis and immune responses.

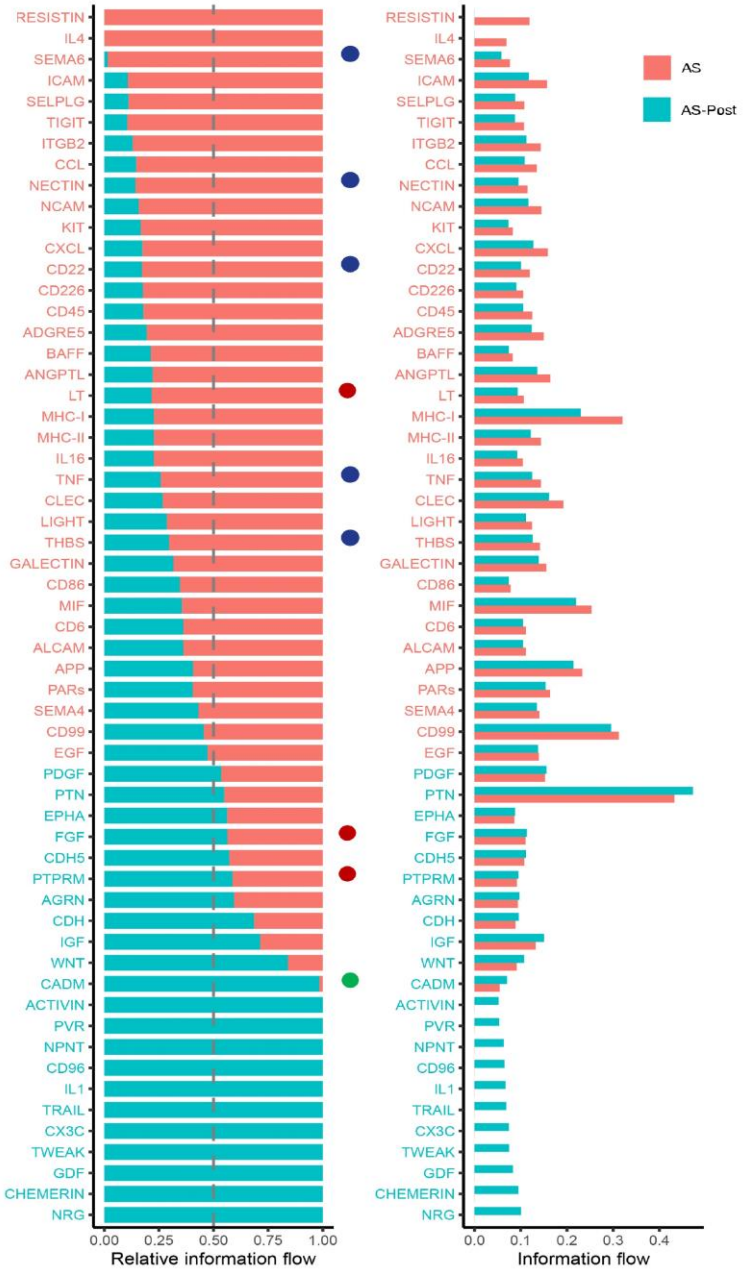

Figure 47. Relative and absolute information flows of differentially detected signaling pathways in Asherman syndrome patient samples before (AS) and after (AS-post) CD133⁺ bone marrow-derived mesenchymal stem cell administration (Wilcoxon; FDR <0.05). Red dots = vascular and angiogenesis processes related pathways. Blue dots = immune system-related signaling pathways. Green dots = Epithelial development signaling pathways.

Some disrupted pathways between pre- and post-treatment AS samples are highlighted due to their association with AS pathology, including the angiogenic, immune system, and epithelial developmental processes (**Figure 47**). Within these pathways, the FGF signaling pathway, related to vascular development and cell proliferation, presents

ligand-receptor pairs that contribute differently to CCC. FGF7 and FGF10 predominated over FGF2 after CD133⁺ BMDSC administration (**Figure 48**), replicating the pattern determined in our previous AS vs secretory control analysis (**Figure 27**). In pre-treatment AS samples, FGF2 represented the only detected ligand. Despite the difference in receptor-ligand interactions, pre- and post-treatment AS endometria display robust CCC via the FGF signaling pathway between stromal cells and the endothelium, epithelium, contractile PV, and SMC (**Figure 48** and **Figure 27**).

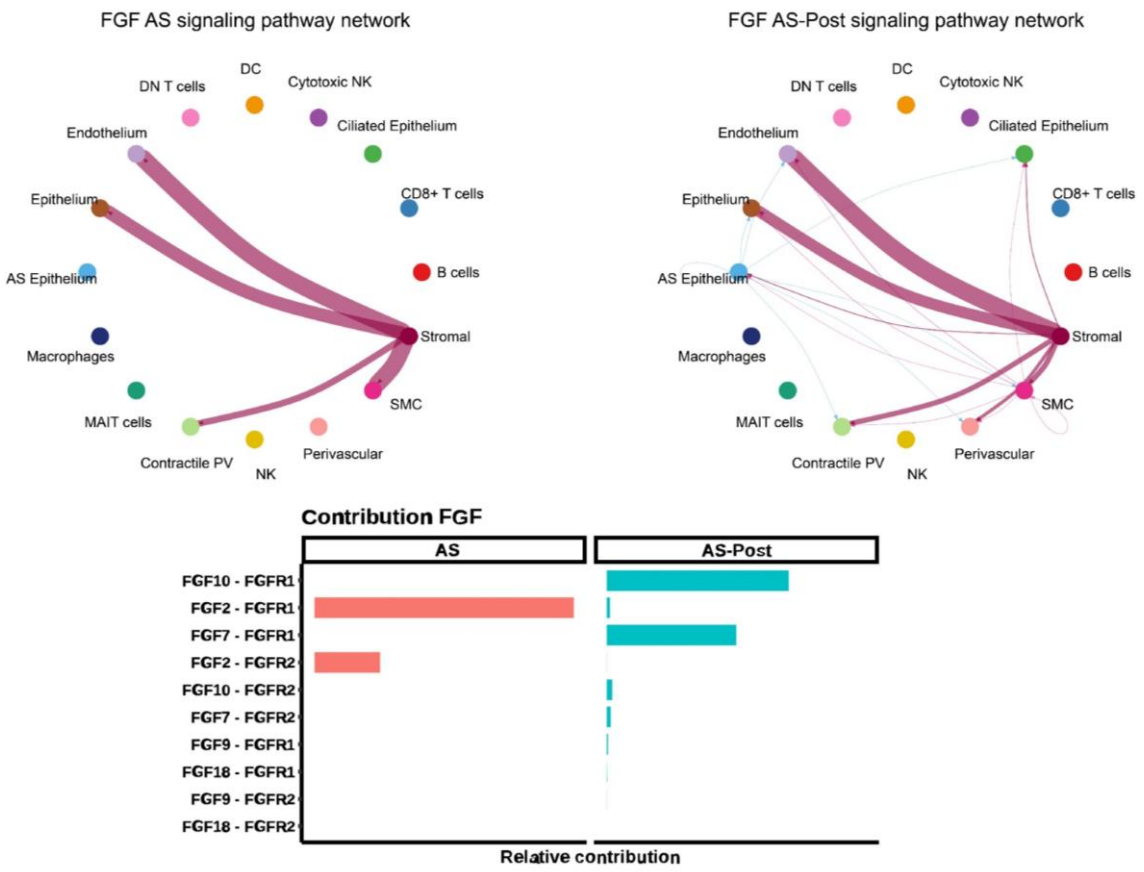

Figure 48. Cell-to-cell communication chord plots (upper images) and contribution diagram (lower image) indicating fibroblast growth factors (FGF) signaling pathway alterations and related ligand-receptor pairs contribution between pre-treated (AS) and treated (AS-Post) Asherman syndrome endometria. Abbreviations - DC (dendritic cells), DN (double negative), MAIT (mucosal-associated invariant T), NK (natural killer), PV (perivascular), SMC (smooth muscle cells).

Within the ICAM pathway, previously involved in immune cell recruitment in AS endometrium (**Figure 25**), we observed reduced interactions between various cell types (**Figure 49**). CD133⁺ BMDSC administration to the AS endometrium led to a decline in

CCC between endothelial cells and macrophages or CD8$^+$ T cells, the almost complete loss of communication from macrophages, MAIT cells, and NK cells to other cell types, and the gain of self-stimulation of macrophages and NK cells.

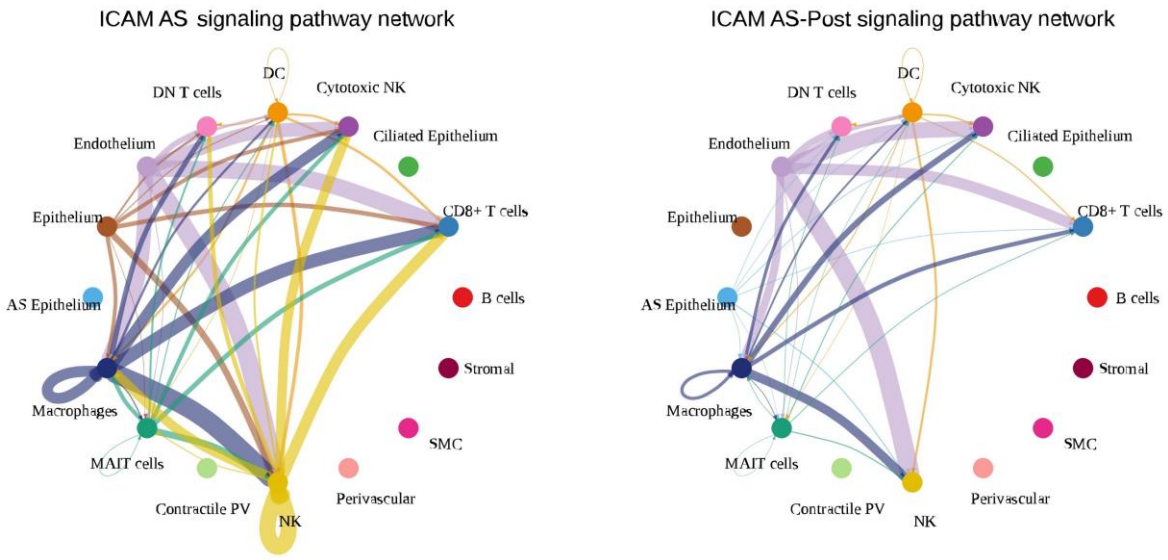

Figure 49. CCC chord plots in pre-treatment (AS) and post-treatment (AS-Post) Asherman syndrome endometria for the ICAM signaling pathway. Abbreviations - DC (dendritic cells), DN (double negative), MAIT (mucosal-associated invariant T), NK (natural killer), PV (perivascular), SMC (smooth muscle cells).

LIGHT signaling (related to chronic inflammation) decreased significantly after CD133$^+$ BMDSC administration (**Figure 50**); we observed a disruption in established CCC between CD8$^+$ T cells and various cell types (including stroma, epithelium, endothelium, PV, and immune cells), which was accompanied by a decline in LIGHT signaling between MAIT and stromal cells.

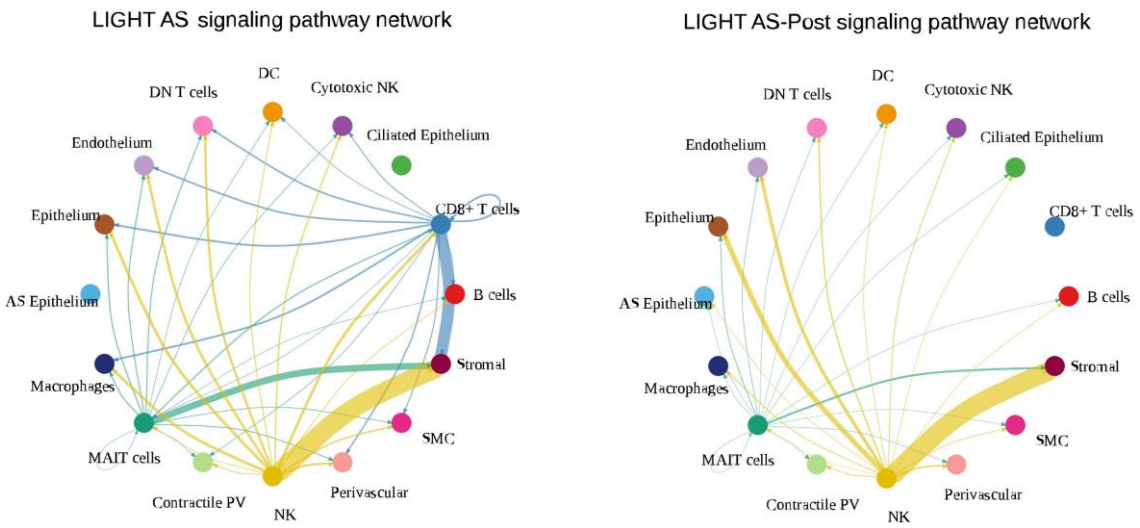

Figure 50. Cell-to-cell communication chord plots in pre-treatment (AS) and post-treatment (AS-Post) Asherman syndrome endometria for the LIGHT signaling pathway. Abbreviations - DC (dendritic cells), DN (double negative), MAIT (mucosal-associated invariant T), NK (natural killer), PV (perivascular), SMC (smooth muscle cells).

Pre-treatment AS samples displayed IL4 (**Figure 51-A**). and RESISTIN (**Figure 51-B**) signaling pathway activation, which is linked to immune activity and involved interactions between MAIT cells (via CSF2-(CSF2RA+CSF2RB) ligands) and macrophages (via RETN-CAP1 and RETN-TLR4 ligands). Importantly, $CD133^{+}$ BMDSC administration prompted the loss of these signaling pathways, contributing to the restoration of a homeostatic environment in the endometrium.

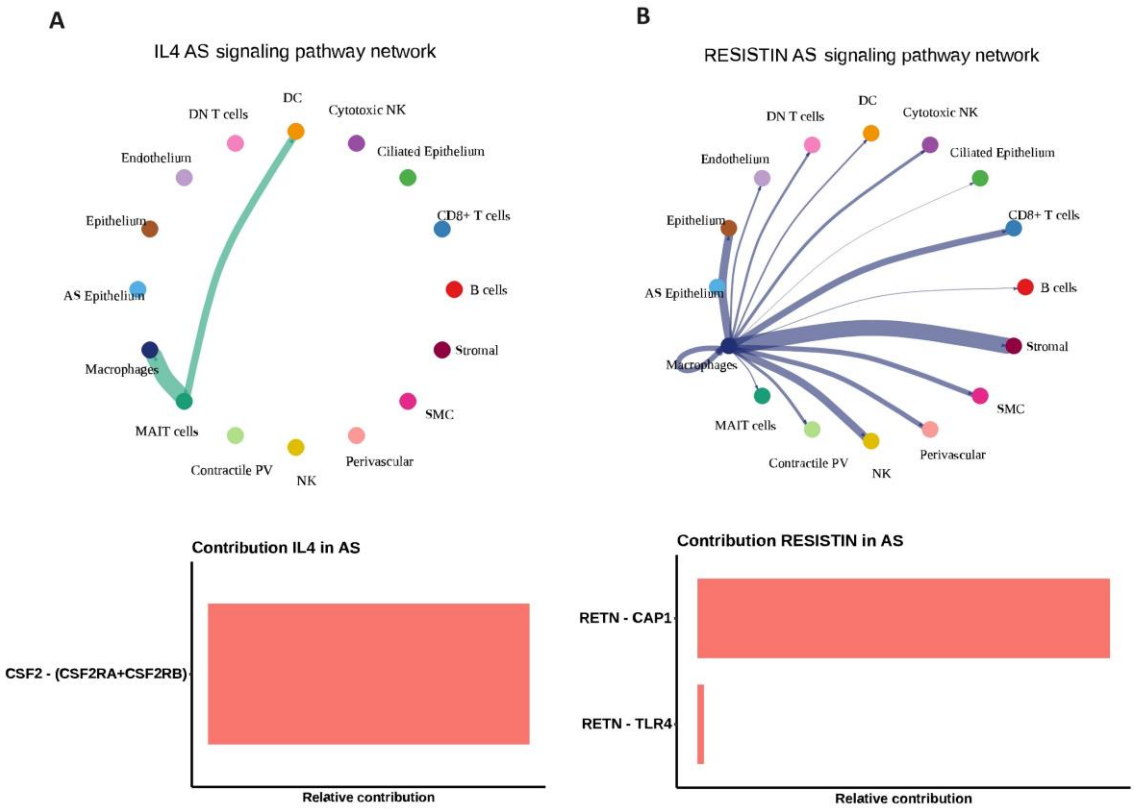

Figure 51. Cell-to-cell communication chord plot (upper panel) and pathway interactor molecules (lower panel) in pre-treatment Asherman syndrome endometria for A) IL4 and B) RESISTIN signaling pathways. Abbreviations - DC (dendritic cells), DN (double negative), MAIT (mucosal-associated invariant T), NK (natural killer), PV (perivascular), SMC (smooth muscle cells).

Following treatment, endometrial regeneration is characterized by the WNT pathway activation. WNT pathway activity initially involved interactions between the stroma and endothelium in the pre-treated AS endometrium; however, $CD133^{+}$ BMDSC administration prompted the recovery of CCC between the stroma, epithelium, and contractile cells (contractile PV and SMC populations) (**Figure 52**). Furthermore, cell therapy-mediated recovery was accompanied by an increase in the number of distinct ligand-receptor pairs involved, which prompted a notable decrease in interactions mediated by WNT4 (FZD5+LRP6) and WNT2 (FZD4/6+LRP6).

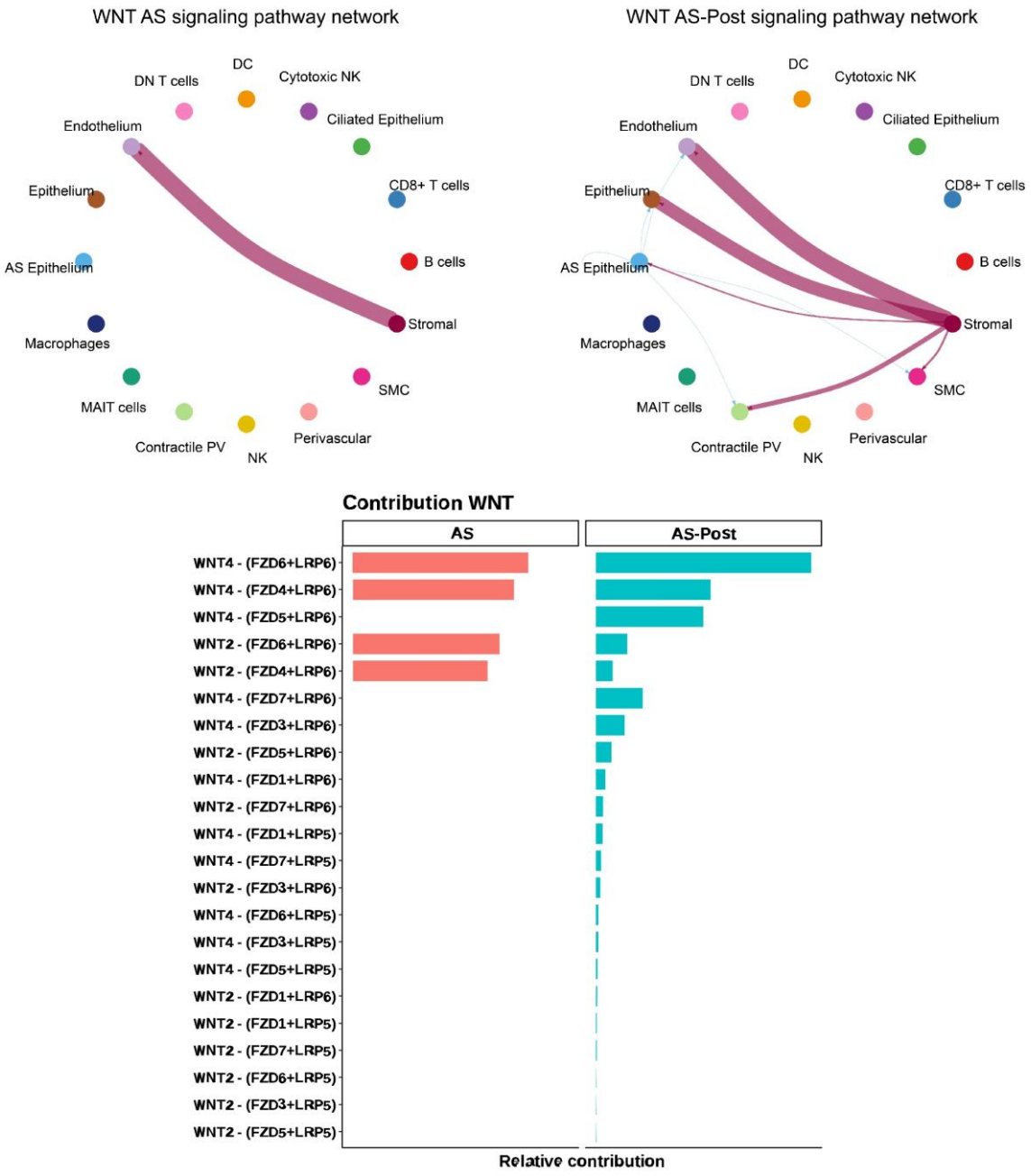

Figure 52. Cell-to-cell communication chord plots (upper images) and contribution diagram (lower image) indicating WNT signaling pathway alterations and related ligand-receptor pairs contribution between pre-treated (AS) and treated (AS-Post) Asherman syndrome endometria. Abbreviations - DC (dendritic cells), DN (double negative), MAIT (mucosal-associated invariant T), NK (natural killer), PV (perivascular), SMC (smooth muscle cells).

In contrast to the IL4 and RESISTIN pathways, CD133^{+} BMDSC administration prompted the recovery of the NRG pathway (related to early precursor proliferation and maturation) (**Figure 53**). NRG signaling becomes established between stromal and

epithelial populations, mainly driven by NRG2-ERBB3 and NRG2-(ERBB2+ERBB3) receptor-ligand pairs, suggesting its involvement in endometrial regeneration.

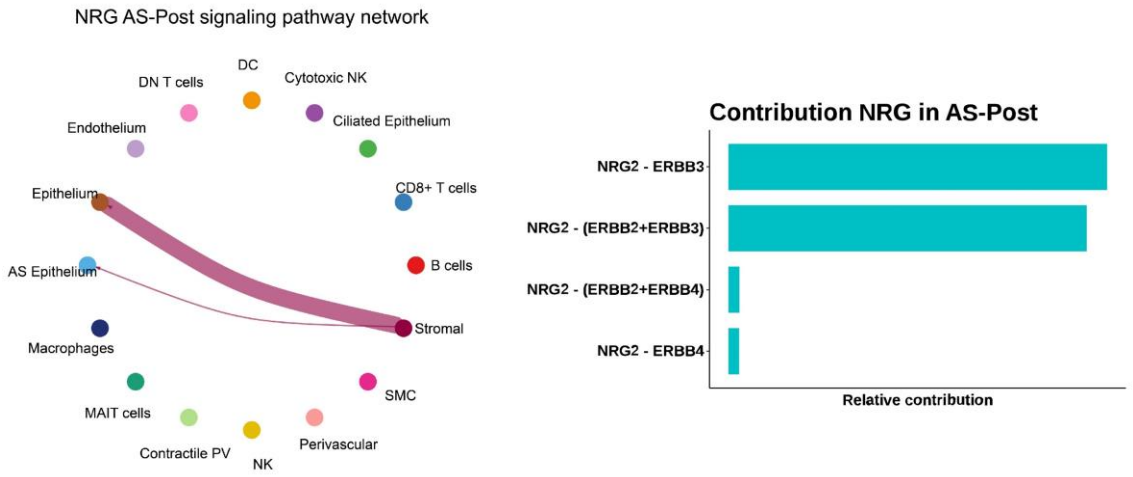

Figure 53. Cell-to-cell communication chord plot (left image) and contribution diagram (right image) indicating NRG signaling pathway alterations and ligand-receptor pairs contribution between pre-treated (AS) and treated (AS-Post) Asherman syndrome endometria. Abbreviations - DC (dendritic cells), DN (double negative), MAIT (mucosal-associated invariant T), NK (natural killer), PV (perivascular), SMC (smooth muscle cells).

Within the ANGPTL pathway, we observed the loss of several CCC interactions after $CD133^+$ BMDSC administration (such as between stroma and epithelium, NK, or PV cells) (**Figure 54**). We observed an interesting prevalence of ANGPTL2 ligand after $CD133^+$ BMDSC administration, as the co-existence and balanced activity of ANGPTL1 and 2 remain essential for angiogenesis and vascular regeneration regulation (**Figure 54**).

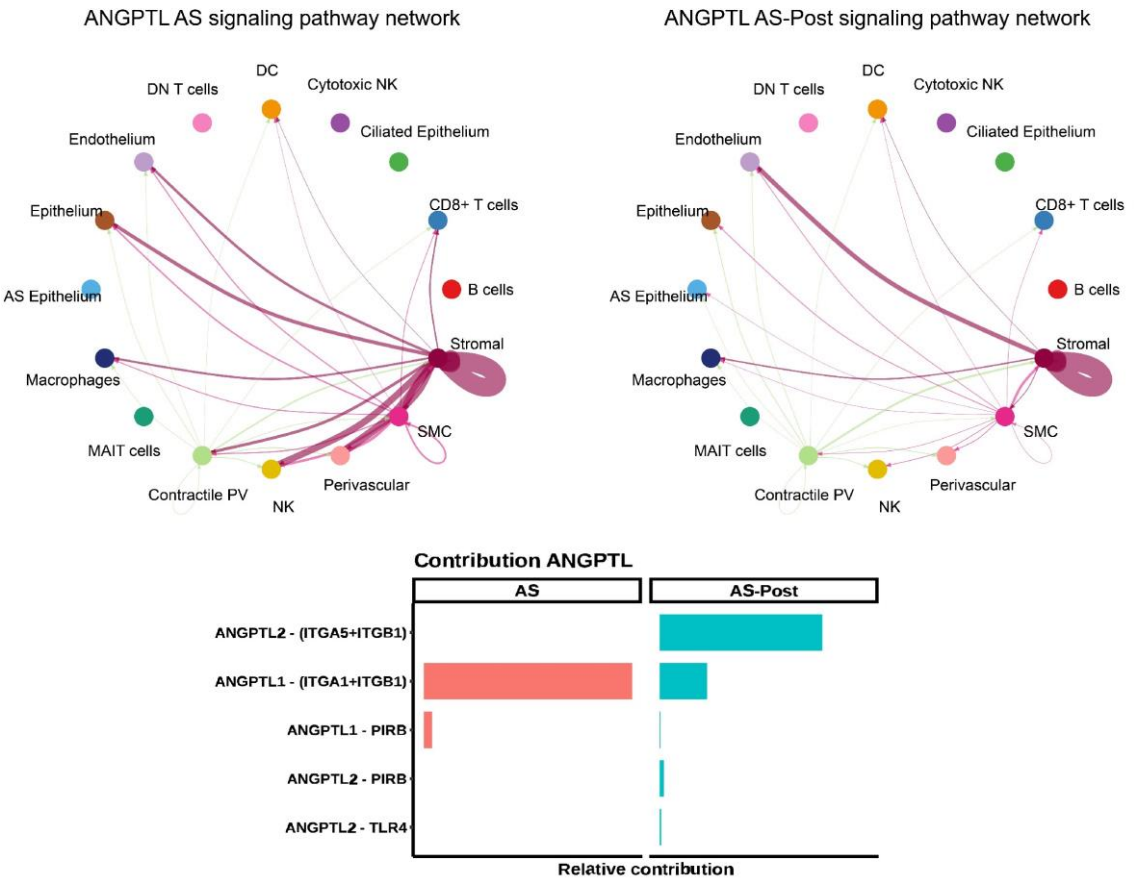

Figure 54. Cell-to-cell communication chord plots (upper images) and contribution diagram (lower image) indicating ANGPTL signaling pathway alterations and ligand-receptor pairs contribution between pre-treated (AS) and treated (AS-Post) Asherman syndrome endometria. Abbreviations – DC (dendritic cells), DN (double negative), MAIT (mucosal-associated invariant T), NK (natural killer), PV (perivascular), SMC (smooth muscle cells).

These findings suggest that administering CD133⁺ BMDSCs to the AS endometrium modulates CCC networks by activating signaling pathways related to angiogenesis, proliferation, and cell differentiation. Specific pathways recover healthy interaction patterns (e.g., GDF, TWEAK, CXC3, or IGF), indicating that CD133⁺ BMDSC helps to transition the AS endometrium towards a healthier state.

3.1.3. Impact of cell therapy on Asherman syndrome endometrium: A more detailed resolution

To gain a more detailed understanding of the alterations to endometrial cell populations after CD133⁺ BMDSC administration, we re-examined pre- and post-treatment samples from AS patients, with a focus on those cells that present canonical gene markers for

epithelial, stromal, and PV subpopulations previously used in AS and healthy control comparisons (**Figure 14**). This approach enables us to distinguish between cellular subtypes.

Cell clustering and subsequent cellular distribution analysis did not reveal any additional significant differences beyond those found in the AS-epithelium; however, results displayed a clear trend of ciliated epithelium recovery and a slight increase in secretory cells after $CD133^{+}$ BMDSC administration (**Figure 55** and **Figure 56**).

In addition, analysis of enrichment scores for endometrial secretory function revealed higher values in post-treatment AS endometrial samples for the epithelial and secretory epithelial populations, reinforcing the evidence of functional recovery and tissue growth stimulated by autologous cell the therapy (**Figure 57**).

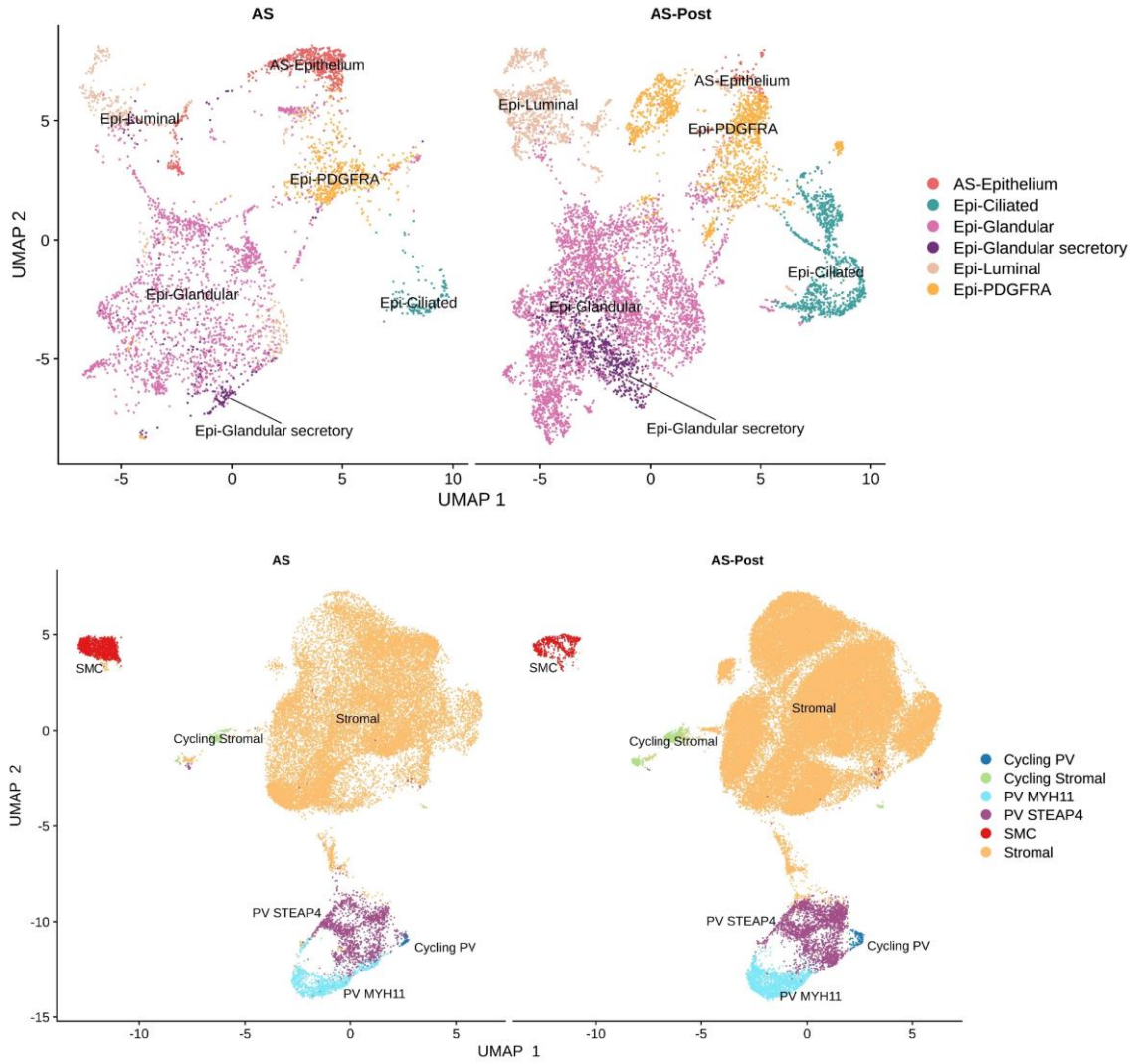

Figure 55. Uniform manifold approximation and projection representing single-cell RNA sequencing data-based fine-grain comparison of epithelial (upper image) and stromal (lower image) populations in pre-treatment (AS) and post-treatment (AS-Post) Asherman syndrome endometria. Abbreviations - PV (perivascular), SMC (smooth muscle cells).

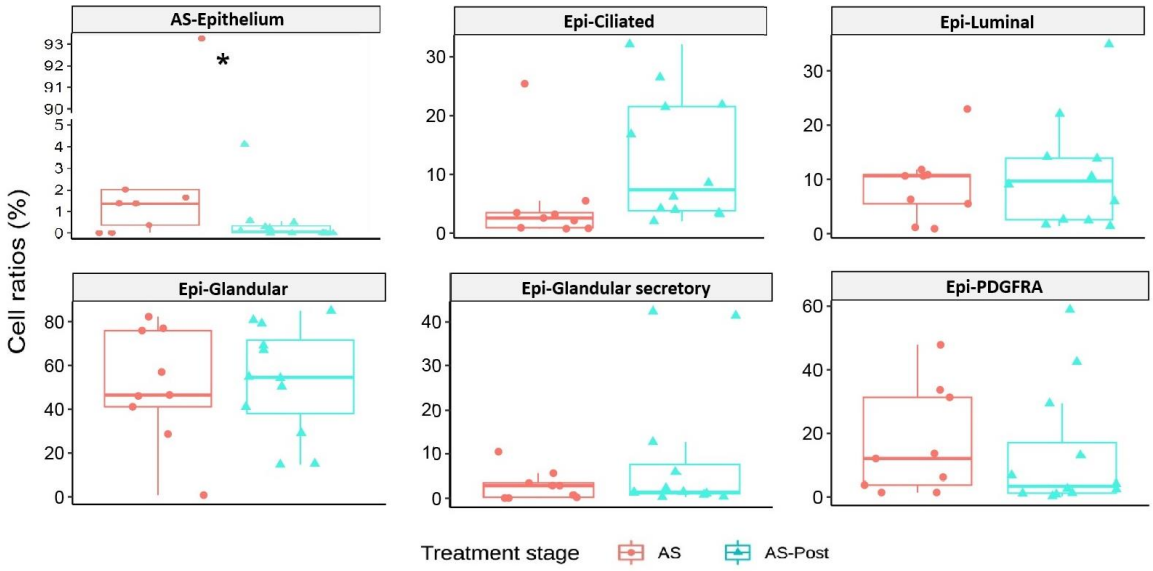

*Figure 56. Box plots of epithelial cell subtype ratios comparing Asherman syndrome endometrium in pre-treatment (AS) and post-treatment (AS-Post) stages. (NB-GLM statistical test * = FDR<0.05).*

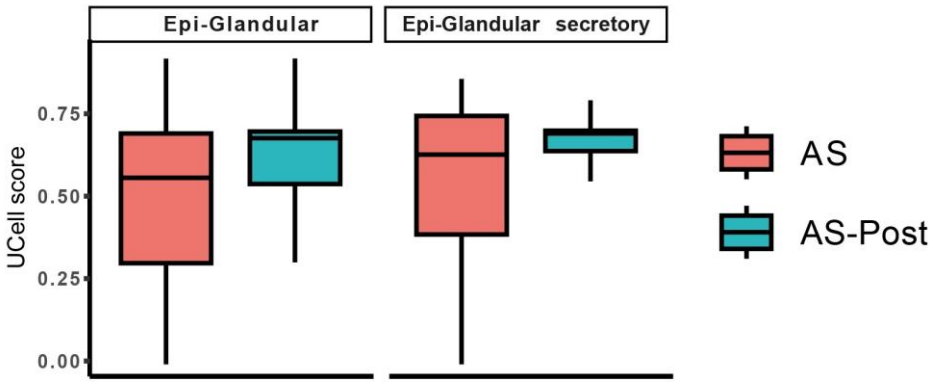

Figure 57. Enrichment score (UCellScore) results box plot of a characteristic gene signature of the secretory phase within the menstrual cycle (Wilcoxon test; FDR <0.05).

We also analyzed CCC within detailed clustering, and the results indicated that specific signaling pathways became restored after cell therapy (**Figure 58**, **Figure 59** and **Figure 60**).

The IL6 pathway (completely absent in the AS endometrium) recovered following CD133^{+} BMDSC administration (**Figure 58**), facilitating interactions between the luminal epithelium and other populations (secretory glandular epithelium, DCs, SMCs, and macrophages) via the IL6-(IL6R+IL6ST) ligand-receptor pair (Annex 8). Similarly, CD133^{+}

BMDSC administration prompted the recovery of NRG pathway interactions (completely absent in the AS endometria) between the stromal population and the glandular and glandular secretory epithelia (**Figure 58**) (via NRG2-(ERBB2+ERBB3) and the luminal epithelium (via NRG2-(ERBB2+ERBB4) (Annex 8), leading to CCC networks more akin to those observed in healthy endometrium.

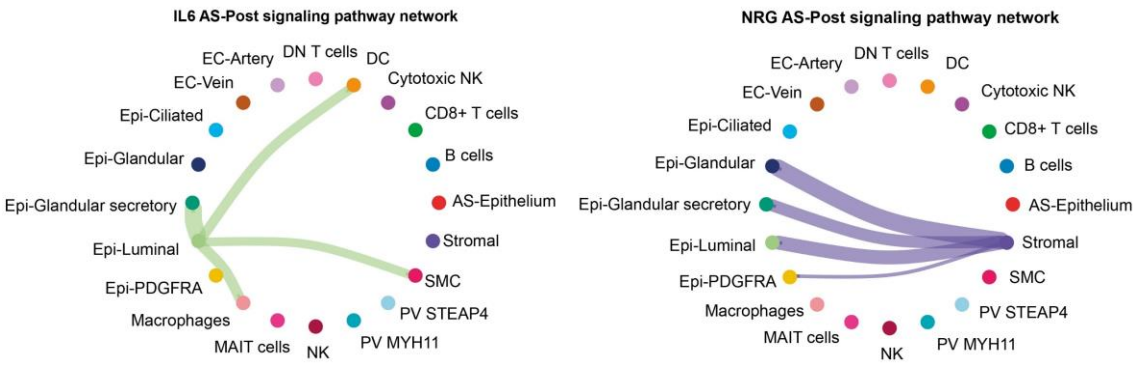

Figure 58. Cell-to-cell communication chord plots for IL6 (left image) and NRG (right image) signaling pathway exclusively present in post-treatment (AS-Post) Asherman syndrome endometrial populations in detailed resolution. Abbreviations - DC (dendritic cells), DN (double negative), EC (endothelial cell), MAIT (mucosal-associated invariant T), NK (natural killer), PV (perivascular), SMC (smooth muscle cells).

The GDF signaling pathway functioned in pre-treatment AS endometrial samples via interactions between the luminal epithelium and cell populations such as $CD8^+$ T, PV, or epithelial cells (**Figure 59**); however, $CD133^+$ BMDSC administration induced the appearance of novel interactions between luminal epithelium and glandular secretory epithelium and the stroma and between stromal and EC-artery cells. The GDF15-TGFBR2 receptor-ligand pair primarily drove these interactions, which could relate to the restoration of homeostasis in these cell populations (Annex 8).

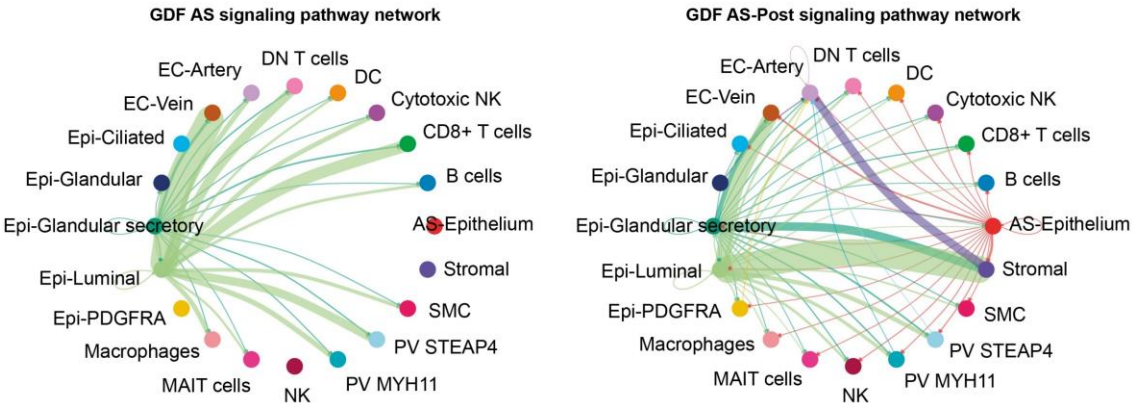

Figure 59. Cell-to-cell communication chord plots in pre-treatment (AS) and post-treatment (AS-Post) Asherman syndrome endometria for GDF signaling pathway within populations in detailed resolution. Abbreviations - DC (dendritic cells), DN (double negative), EC (endothelial cell), MAIT (mucosal-associated invariant T), NK (natural killer), PV (perivascular), SMC (smooth muscle cells).

ICAM and ITGB2 signaling pathways also undergo modifications following $CD133^+$ BMDSC administration (**Figure 60**). The ICAM pathway experienced a loss of signaling between NK cells, macrophages, and other immune cells and self-stimulation within NK and macrophage populations. ITGB2 signaling pathway underwent similar changes, including decreased interactions between $CD8^+$ T cells and NK and MAIT cells. Both signaling pathways also displayed an increase in the number of interactions between the EC-vein population and NK cells (**Figure 60**).

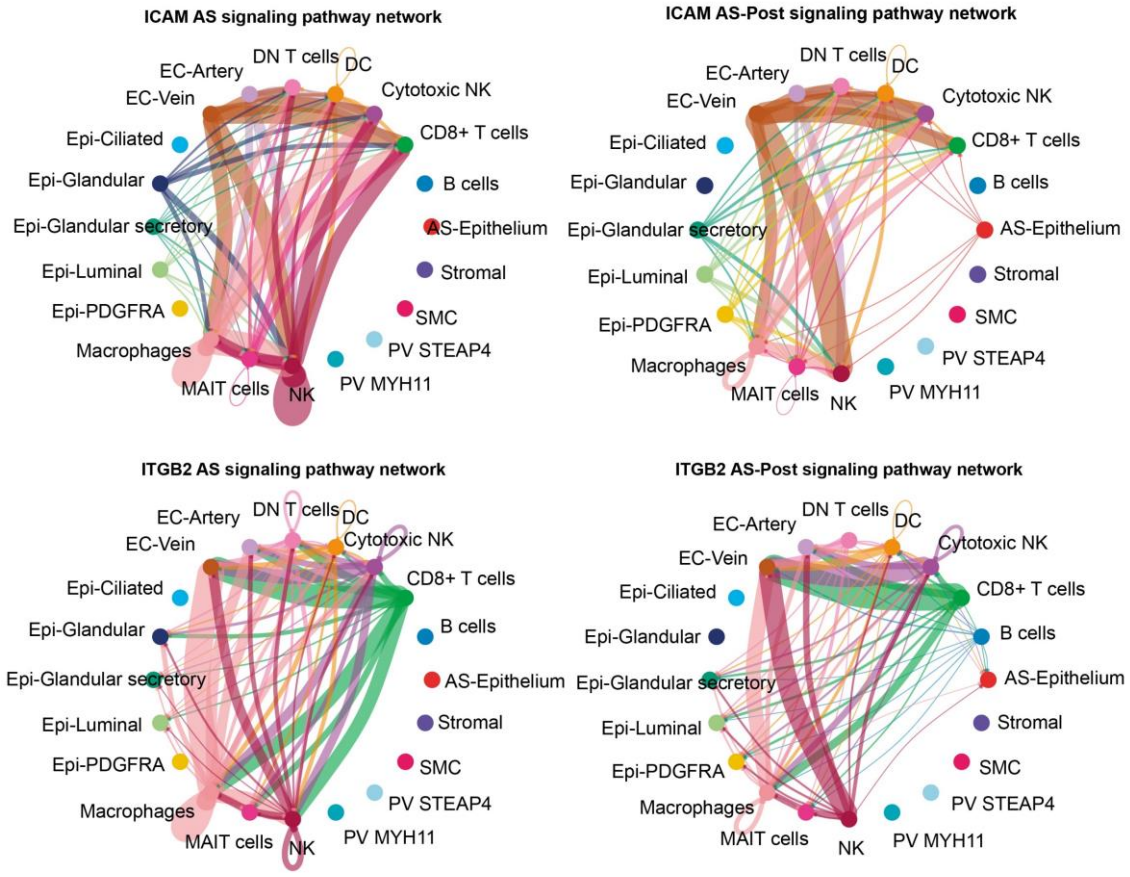

Figure 60. Cell-to-cell communication chord plots in pre-treatment (AS) and post-treatment (AS-Post) Asherman syndrome endometria for ICAM (upper image) and ITGB2 (lower image) signaling pathways within populations in detailed resolution. Abbreviations - DC (dendritic cells), DN (double negative), EC (endothelial cell), MAIT (mucosal-associated invariant T), NK (natural killer), PV (perivascular), SMC (smooth muscle cells).

Based on these findings, we suggest that CD133^{+} BMDSC treatment induces the recovery of epithelium, increasing their functional capacity. Moreover, CD133^{+} BMDSC treatment recovers CCC networks between epithelial, stromal, and endothelial populations, including signaling pathways lost in the AS endometrium, and reduces the pro-inflammatory activity of immune cell populations.

3.2. SLPI as a cell marker in the epithelium of the Asherman syndrome endometrium after patient-specific autologous cell therapy

Next, we explored the relevance of the AS-epithelium cell population following autologous cell therapy using *SLPI* as a marker. *SLPI* was previously detected in the AS-epithelium of AS endometrium but was undetectable in healthy control samples. As

scRNA-seq results of the AS endometria before and after CD133^{+} BMDSC treatment revealed a significant reduction in the AS-epithelium, we evaluated if *SLPI* mRNAs detection in fixed samples also showed this decrease and could serve as an indicator of improvement.

RNAscope analysis revealed the complete loss of *SLPI* mRNAs in the AS endometria after CD133^{+} BMDSC treatment (**Figure 61**), rather than a diminished detection. We may attribute the lack of detection to the significantly reduced number of AS-epithelial cells due to cell therapy, making *SLPI* mRNAs visualization by fluorescent microscopy impractical. This result, closely mirroring the analysis of pretreated AS samples versus healthy controls, suggests that *SLPI* could be used as a marker for detecting endometrial recovery after cell therapy.

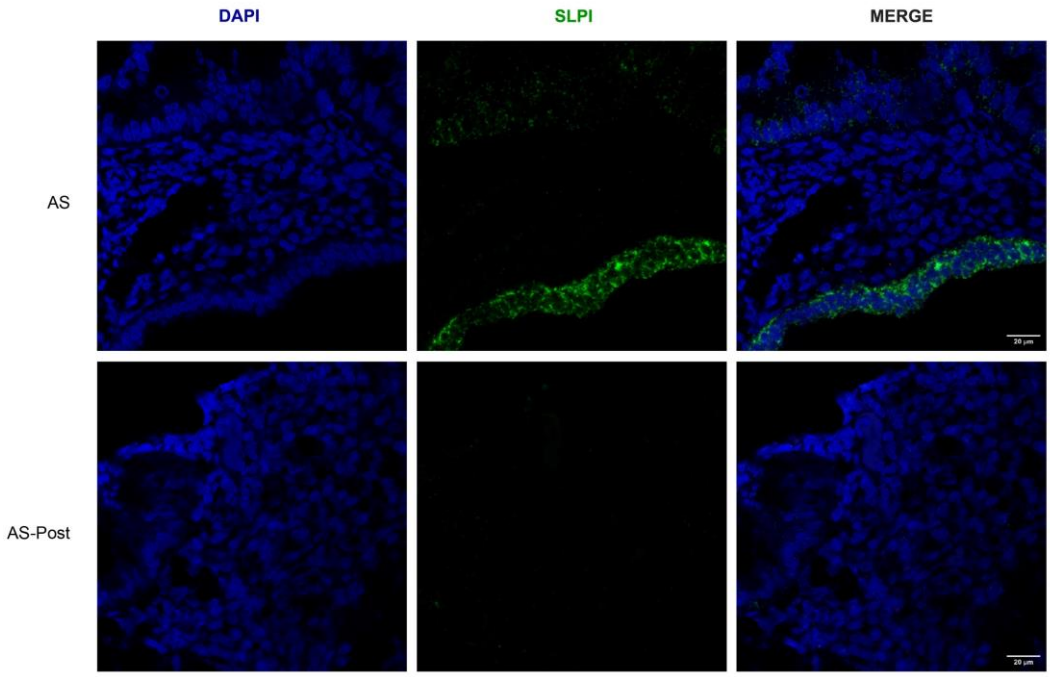

Figure 61. RNAscope representative images of SLPI gene expression present in the AS-epithelium cluster in histological sections of Asherman syndrome patient endometria before (AS) and after (AS-Post) cell therapy administration. Cell nuclei are stained in blue (DAPI), and the SLPI gene expression in green. Scale bar = 20 µm.

3.3. Recapitulation of cell therapy-mediated effects in Asherman syndrome endometrial epithelial organoids

We next sought to explore the impact of CD133$^+$ BMDSC treatment on the generation of EEOs from AS endometrial biopsies taken after treatment by comparing the results with our *in vivo* data. We analyzed the parameters we previously measured during EEO development: AS EEO formation (in terms of quantity and size), transcriptomic alterations, and diverse cell marker expression through immunofluorescence, consistently mimicking a WOI-like state through hormone treatment (section IV.4.3).

3.3.1. Endometrial epithelial organoid development from Asherman syndrome pre- and post-cell therapy

We isolated biopsy samples after administration of CD133$^+$ BMDSC therapy to the AS endometrium and developed EEOs (from the same three patients previously analyzed in section 2.2). We quantified EEO formation by counting the total number of EEOs from an identical number of cells over time to measure the regenerative capacity of the original tissue. Interestingly, we observed improvements in EEO formation after CD133$^+$ BMDSC treatment (**Figure 62**); specifically, we found significant improvements at passages 0 and 1 (both with $p<0.05$). By passage 2 (P2), the organoid-forming capacity of pre-treatment and post-treatment biopsied cells displayed no significant differences, suggesting the positive selection of organoid-forming cells.

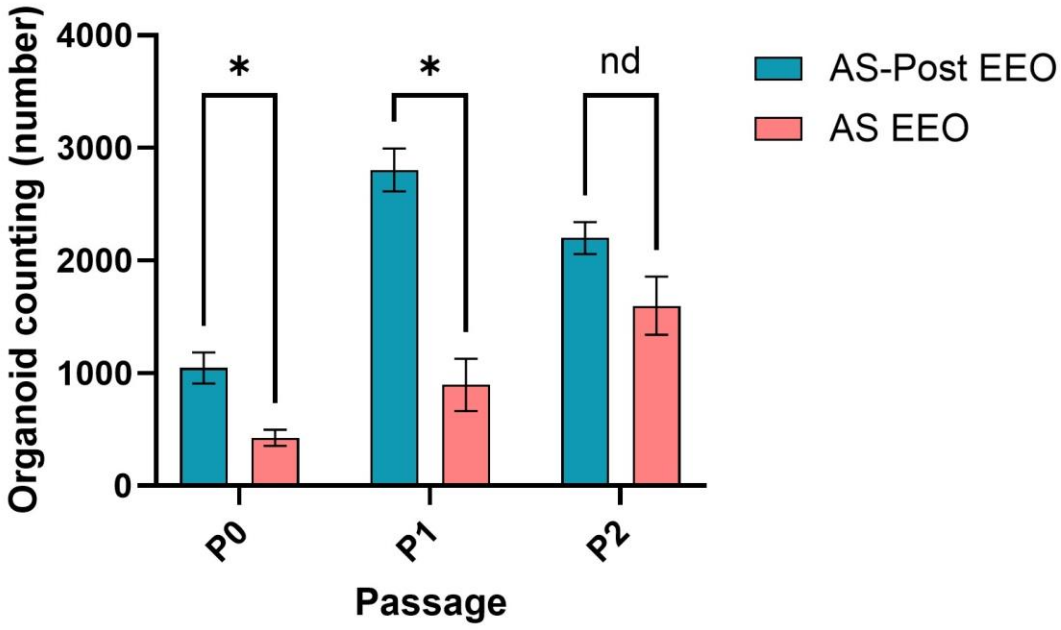

*Figure 62. The average number of Asherman syndrome endometrial epithelial organoids at different passages (P0-P2) developed from pre-treatment (AS EEO) and post-treatment (AS-Post EEO) endometrial samples. An unpaired T-test with Welch correction was applied to test for differences between groups (*p<0.05). Abbreviations - P0 (Passage 0), P1 (Passage 1), P2 (Passage 2).*

Next, we measured EEO diameter to evaluate epithelial cell growth and development after $CD133^+$ BMDSC treatment. We discovered that EEOs generated from biopsied cells isolated from the AS endometrium after treatment (AS-Post EEO) had significantly larger diameters after seven days of growth than AS EEOs, suggesting a higher growth rate (**Figure 63**). When comparing results from $CD133^+$ BMDSC-treated AS EEOs and AS EEOs to previous healthy control EEOs, we observed no significant differences at day seven between $CD133^+$ BMDSC-treated AS EEOs and healthy control EEOs, suggesting that $CD133^+$ BMDSC treatment helps AS EEOs to recover cell growth, reaching values similar to those observed in the healthy situation.

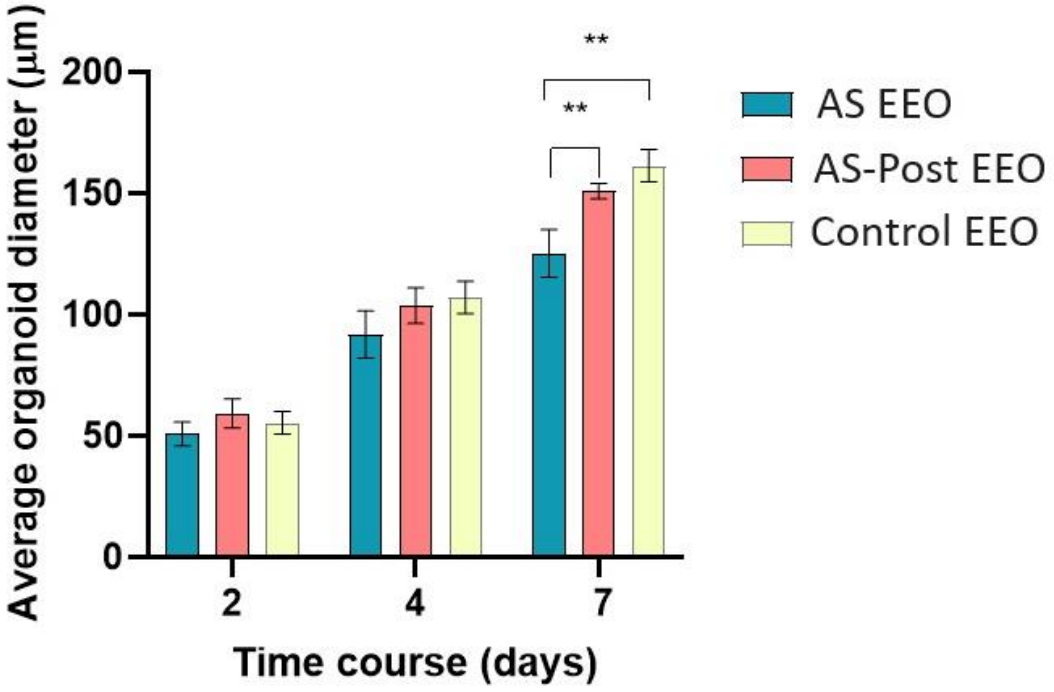

*Figure 63. Average Asherman syndrome endometrial epithelial organoid diameter at different days through their development from pre-treatment (AS EEO), post-treatment (AS-Post EEO), and healthy (Control EEO) endometrial samples (unpaired T test with Welch correction,** p<0.005).*

These results suggest that AS EEOs can function as a model for the recovery of epithelial cell proliferative capacity following autologous cell therapy. Although the difference in the number of organoids between AS EEOs and $CD133^+$ BMDSC-treated AS EEOs decreased in latter passages, EEO diameter remained larger in $CD133^+$ BMDSC-treated AS EEOs, suggesting a positive effect of $CD133^+$ BMDSCs on the AS-affected epithelium.

3.3.2. Transcriptomic analysis of endometrial epithelial organoids pre- and post-cell therapy

Next, we transcriptomically profiled AS EEOs from $CD133^+$ BMDSC-treated patients by scRNA-seq. We processed 49,609 cells and analyzed the single-cell transcriptomic data, comparing $CD133^+$ BMDSC-treated AS EEOs (AS-Post EEO; 9,556 cells) with previously reported pre-treatment AS EEOs (AS EEO; 14,459 cells) and healthy WOI control EEOs (Control EEO; 15,594 cells) (**Figure 64**). We identified the same cell identities from AS and WOI control characterization in section 2.2 in this analysis based on canonical marker gene expression.

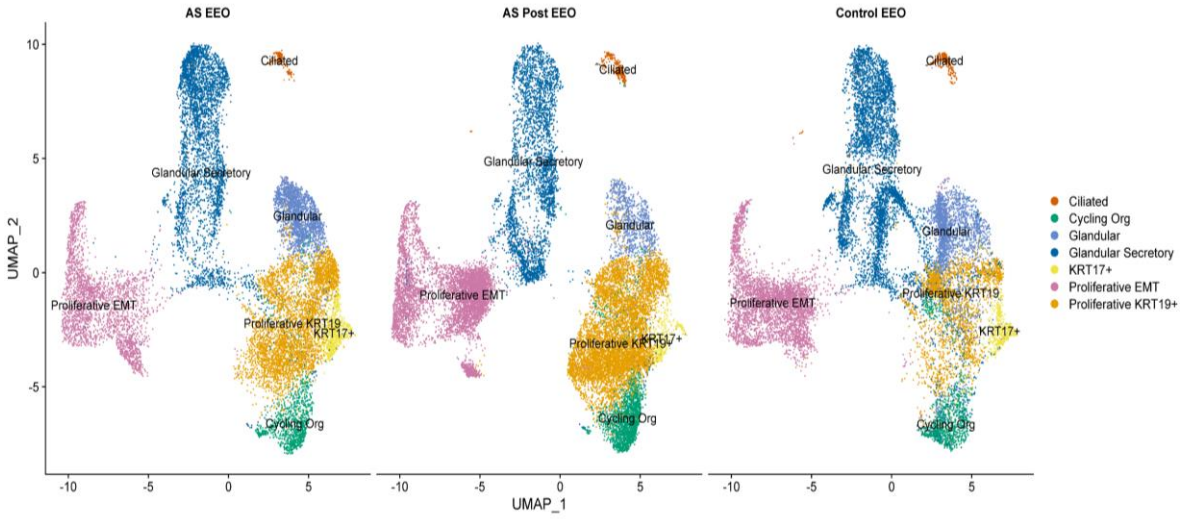

Figure 64. Uniform manifold approximation and projection integration of main cell types identified in endometrial epithelial organoids from healthy window-of-implantation control (Control EEO, 15,695 cells), Asherman syndrome pre-treatment (AS EEO, 14,482 cells), and Asherman syndrome post-treatment with CD133⁺ BMDSCs (AS-Post, 19,619 cells) samples.

Analysis of cell type distribution revealed a higher representation of ciliated (1.38% vs 0.89%) and proliferative EMT (27.81% vs 17.53%) cell clusters in post-treatment AS EEOs than in pre-treatment AS EEOs (**Figure 65**), similar to the distribution of control EEOs and with previous results where an increasing trend in ciliated cells was observed (**Figure 44**). In addition, we observed the lower representation of the KRT17⁺ cell population (highly expresses the ECM remodeling gene *MMP7*) in post-treatment AS EEOs (1.74%) compared to pre-treatment AS EEOs (4.99%) and control EEOs (2.95%). Post-treatment AS EEOs exhibited a more proliferative profile than control EEOs and pre-treatment AS EEOs, as in addition to proliferative KRT19⁺ (26.40% vs 18.82% in pre-treatment AS EEOs and 10.87% in control EEOs) and proliferative EMT populations (27.81% vs 17.53% in pre-treatment AS EEOs and 25.10% in control EEOs), the cycling population was also higher in post-treatment AS EEOs (10.61% vs 7.47 % in pre-treatment AS EEOs and 6.77% in control EEOs). Enhanced proliferation could suggest that CD133⁺ BDMSC treatment induces an endometrial regenerative effect, resulting in an epithelium with increased cell division and potential for tissue regeneration. The two glandular cell clusters are less represented in post-treatment AS EEOs (32.03% vs 50,25% in AS EEOs and 52.78% in control EEOs), since most of the cells in these EEOs constitute proliferative clusters.

However, the glandular secretory population is proportionally much larger than the glandular population in post-treatment AS EEOs (25.21% vs 6.82%), which also occurs in control EEOs (40.50% vs 12.28%), differing from pre-treatment AS EEOs (25.56% vs 24.70%). Although not statistically significant, these results offer insights into the differences in organoid development after treatment, reinforcing the claim of glandular epithelium differentiation towards a more receptive profile after treatment.

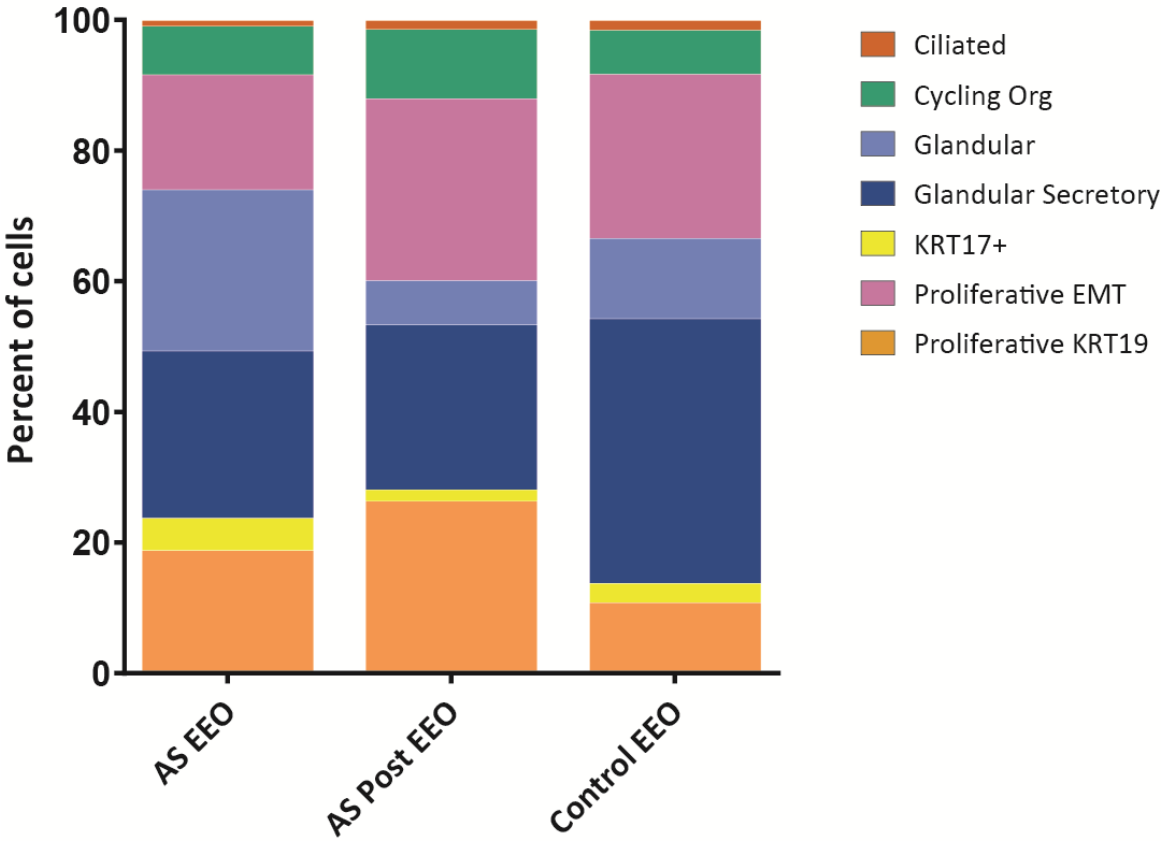

Figure 65. Cell type proportion across Asherman syndrome (AS EEOs), post-treatment Asherman syndrome (AS-Post EEO), and Control (Control EEO) endometrial epithelial organoids.

We calculated a similarity score by measuring the distance of each identified cell population in EEOs to those identified in the in vivo healthy WOI controls, as represented in a pentagonal plot (**Figure 66**). We observed that cells from the three EEO types mainly corresponded to the glandular or glandular secretory epithelia, with some residual cells corresponding to ciliated and SOX9 epithelia. This result suggests that EEO cells primarily represent the glandular epithelium of tissue samples and, to a lesser extent, the ciliated

epithelium. Additionally, we found that luminal epithelium is not represented in this model and that the organoid-generating cells do not correspond to SOX9^{+} epithelial cells. Regarding the different EEO types, control EEOs cluster more within secretory glandular epithelium, whereas pre-treatment AS EEOs seem more associated with glandular epithelium. Post-treatment AS EEOs occupy an intermediate state between pre-treatment AS and Control EEOs.

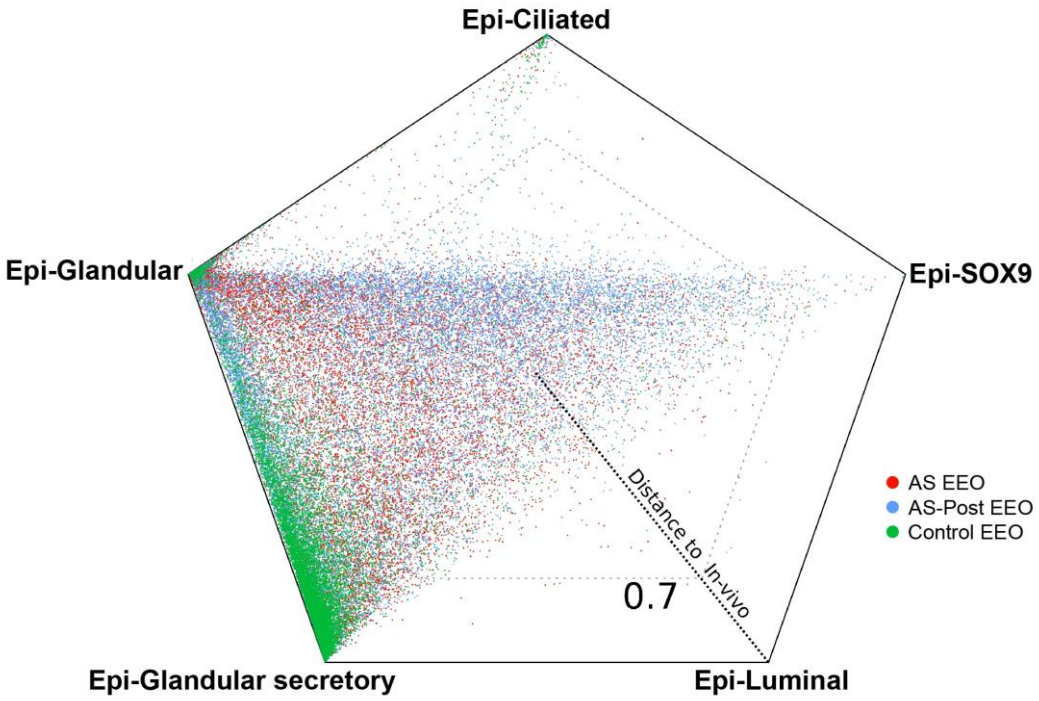

Figure 66. Predicted linear representation of cell type identity probabilities using a logistic model trained with epithelial cell subclusters from healthy window-of-implantation control samples.

We stratified similarity scores in boxplots to verify these results and confirmed the differences between EEO types regarding their clustering within cell identities previously identified for endometrial tissue samples (**Figure 67**). Cells from pre-treatment AS EEOs exhibit a lower similarity score with the secretory glandular epithelium than post-treatment AS EEOs and control EEOs, with the latter having the highest score value. All group comparisons in this cell type were statistically significant ($p<0.001$). Pre-treatment AS EEOs had the highest similarity score for glandular epithelium, showing significant differences from control EEOs and post-treatment AS EEOs ($p<0.001$). We also observed significant differences between post-treatment AS and control EEOs within this cell

identity (p<0.01). For ciliated epithelium, similarity values comparing pre-treatment AS EEOs and control EEOs were similar, but both differed significantly from post-treatment AS EEOs (p<0.001). (**Figure 67**). These results indicate that pre-treatment AS EEO cells do not achieve a transcriptomic profile related to the WOI, remaining in a glandular-like profile characteristic of an early stage in the menstrual cycle. Moreover, they demonstrate that cell therapy alters endometrial cells, enabling them to acquire a more receptive profile without reaching control EEOs similarity levels.

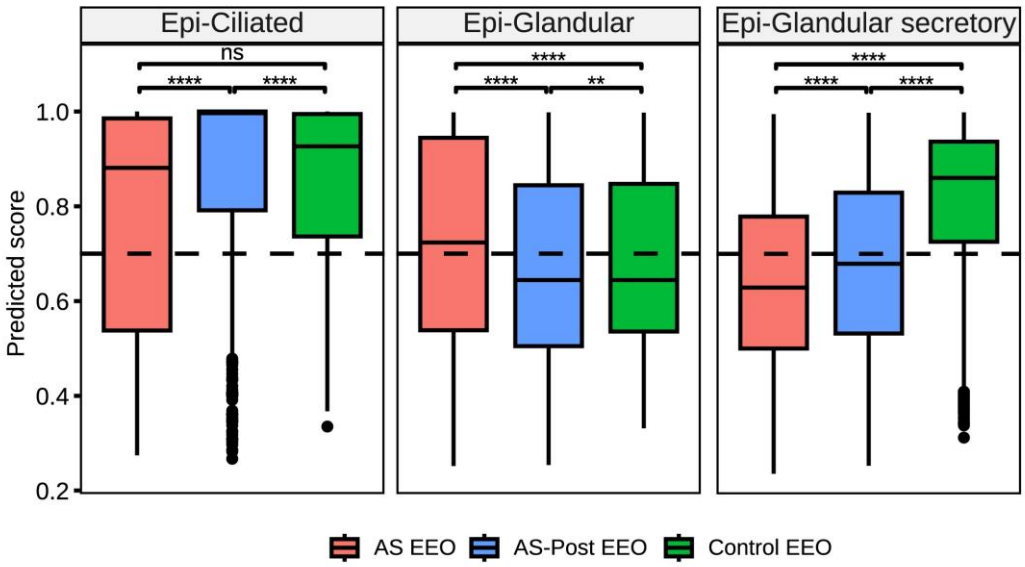

*Figure 67. Box plots prediction for cell types and organoid types. Differences between groups were analyzed using the Dunn test; the Bonferroni method adjusted p-values. (**p<0.01, ****p<0.001).*

We performed a transcriptomic analysis in glandular and glandular secretory EEO cells and identified a set of genes that displayed consistent patterns in pre-treatment and post-treatment AS EEOs, with similar trends observed both *in vitro* and *in vivo*. We found that the glandular cell population downregulated the expression of *TFPI2*, *TMEM101*, and *COL1A2* and upregulated the expression of *LAMB3* in post-treatment AS EEOs and control EEOs compared to pre-treatment AS EEOs. Meanwhile, glandular secretory cells from post-treatment AS EEOs exhibited the reduced expression of *TFPI2* and *PLCG2* and the increased expression of *CXCL14, SYNE2, ANXA4,* and *TMC5* (**Figure 68**). These changes in transcriptomic profiles suggest that $CD133^{+}$ BMDSC administration reduced collagen production and immune responses, enhanced differentiation capacity, and

improved adhesion to the extracellular matrix. Additionally, cell therapy restored the expression of *CXCL14* in glandular secretory cells, a gene associated with the WOI.

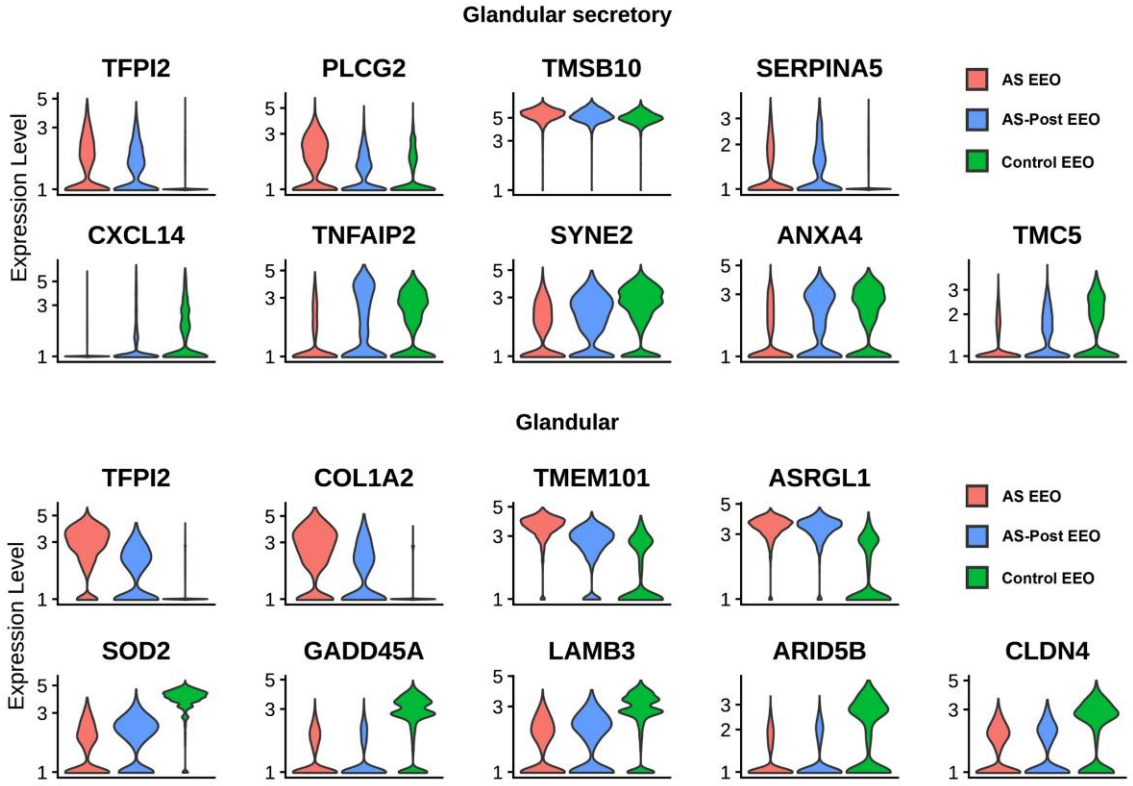

Figure 68. Violin plots represent the differentially expressed genes with the same trends within glandular and glandular secretory populations in single-cell RNA sequencing data from Asherman syndrome (AS EEO), post-treatment Asherman syndrome (AS-Post EEO), and control biopsy (Control EEO) endometrial epithelial organoids.

The transcriptomic analysis of EEOs derived from patients treated with $CD133^{+}$ BDMSCs revealed a positive therapeutic impact. Post-treatment AS EEOs exhibited highly proliferative profiles, with a higher proportion of glandular secretory cells than glandular cells, and displayed similarities to epithelial populations from healthy biopsies. Additionally, the transcriptomic modifications observed in post-treatment AS EEOs remained consistent with a healthy-like state of epithelial cells, indicating the ability of EEOs to reflect the changes produced by the treatment *in vivo*.

3.3.3. Immunohistochemical analysis of endometrial epithelial organoids pre- and post-cell therapy

To further elucidate the effects of CD133^{+} BDMSCs, we analyzed the structural features, proliferation rates, and altered cell markers of EEOs derived from treated AS patient samples.

3.3.3.1. Structural features

We assessed the levels of characteristic epithelial markers for the cell cytoskeleton (Pan cytokeratin; PANCK) and cell adhesion (E-cadherin) in post-treatment AS EEOs. We detected both markers in EEOs at seven days of *in vitro* culture (**Figure 69**); these results agree with the previously observed results for control EEOs (**Figure 39** and **Figure 40**), with EEOs presenting similar glandular structures with a hollow lumen (confirmed by 2D sections). In addition, F-actin staining verifies epithelial cell polarization, which accumulates within the inner part of the organoid near the lumen (**Figure 69**).

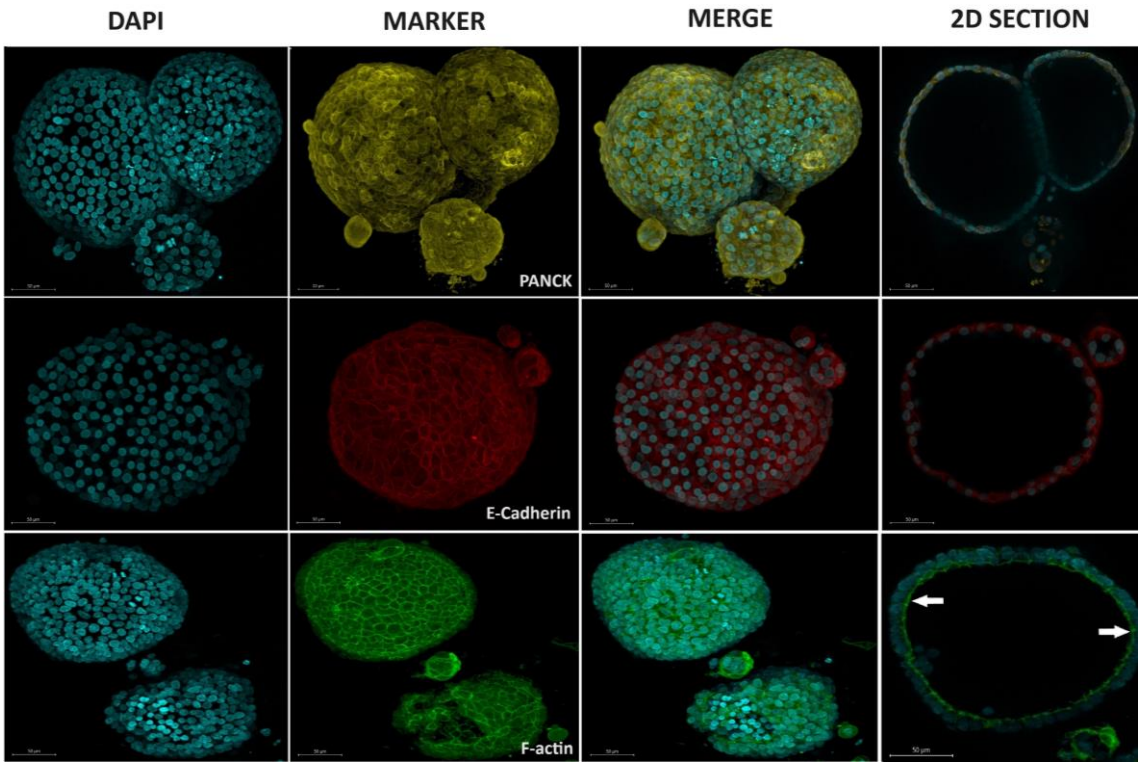

Figure 69. Confocal images of post-treatment Asherman syndrome endometrial epithelial organoids. Cell nuclei are stained in blue, pan-cytokeratin in yellow (PANCK), E-cadherin in red, and F-actin in green. White arrows indicate F-actin label accumulation (zoomed). Scale bar 50 µm.

3.3.3.2. Cell proliferation and cell markers

Utilizing fixed organoids, we conducted additional measurements to assess cell proliferation and levels of the COL1A2 marker across the three EEO types. We stained the samples with Ki67 antibody, a well-known proliferation marker, and DAPI for nuclei detection to analyze the number of Ki67-positive cells relative to the total cell count (as described in section IV.5.1) (**Figure 70**). This analysis indicated minor differences in Ki67 staining, suggesting a non-significant difference in proliferation rates; however, we did see a trend toward lower proliferation in pre-treatment AS EEOs and an increase in proliferation in post-treatment AS EEOs (**Figure 70**). Overall, additional analyses in more EEO samples may reveal small but significant alterations in proliferation rates induced by $CD133^{+}$ BMDSCs in AS EEOs.

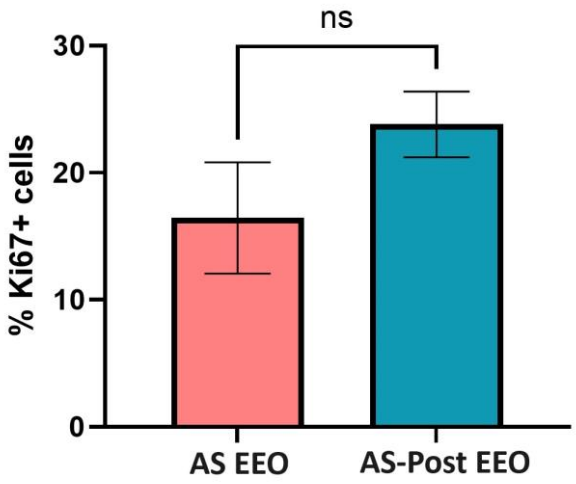

Figure 70. $Ki67^{+}$ cells quantification in endometrial epithelial organoids from three independent donors. One-way analysis of variance with post-hoc Tukey test (ANOVA).

ECM increases in size and extent through the synthesis of its fibers, such as collagen, which is a crucial aspect of AS. Transcriptomic analyses in organoids reveal the overexpression of COL1A2 in pre-treatment AS EEOs compared to control EEOs (**Figure 68**). This overexpression decreases in post-treatment AS EEOs but does not reach the levels observed in control EEOs. Consequently, we selected this marker to validate our transcriptomic findings in fixed organoids.

Confocal microscopy images illustrate how collagen forms accumulations in pre-treatment AS EEO cells but, conversely, displays a dispersed nature in post-treatment AS and control EEOs (**Figure 71**).

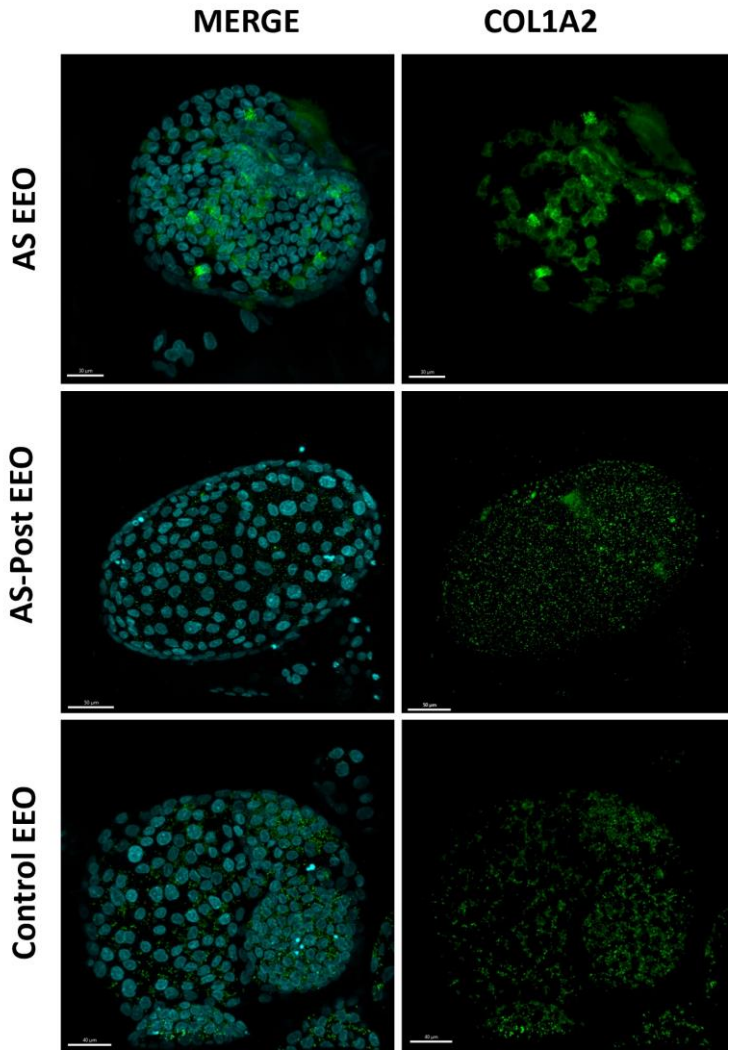

Figure 71. Confocal images of COL1A2 fluorescence in Asherman syndrome (AS EEO), post-treatment Asherman syndrome (AS-Post EEO), and control biopsy (Control EEO) endometrial epithelial organoids. COL1A2 shows the fluorescence of the protein in green, and merge includes nuclei stained in blue (DAPI).

These results are further supported by COL1A2 fluorescence intensity profiles measured along the diameter of organoids (**Figure 72**). These profiles show higher intensity peaks in pre-treatment AS EEOs compared to post-treatment AS and control EEOs. These findings provide insights into the behavior of collagen in the pathology and highlight the effectiveness of cell therapy in promoting recovery of the endometrium in AS patients.

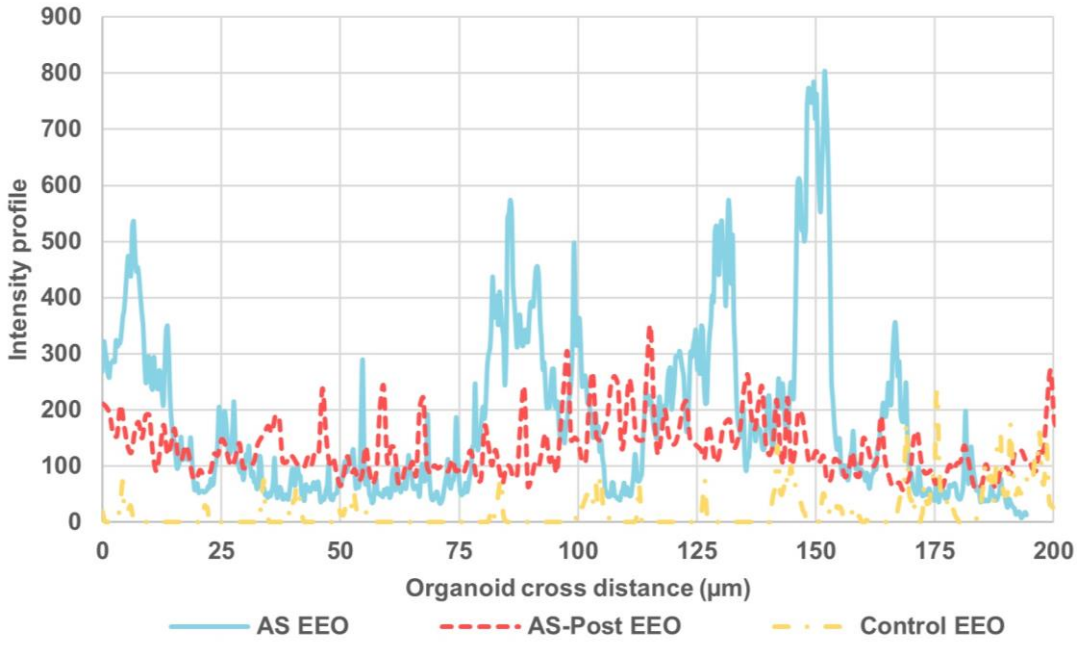

Figure 72. Representative plot of COL1A2 fluorescence intensity profiles along the diameter of Asherman syndrome (AS EEO), post-treatment Asherman syndrome (AS-Post EEO), and control biopsy (Control EEO) endometrial epithelial organoids.

Immunohistochemical analyses of post-treatment AS EEOs revealed a similar structure compared to pre-treatment AS and control EEOs. These analyses also indicated a non-significant trend toward recovery of proliferative capacity following our cell therapy treatment, along with a collagen distribution pattern in post-treatment AS EEOs more similar to that of control EEOs.

VI. Discussion

VI. Discussion

The endometrium - the innermost layer of the uterus - plays critical roles in reproduction (implantation and pregnancy support) and can self-regenerate thanks to the preservation of a fraction of its basal component after menstruation, suggesting the presence of undifferentiated cell types (Critchley et al., 2020). Several pathologies can impact the endometrium and affect its regenerative capabilities, including Asherman syndrome (AS) (Smikle et al., 2023), an iatrogenic condition characterized by endometrial fibrosis and the formation of intrauterine adhesions (IUAs) (Conforti et al., 2013; Smikle et al., 2023).

This thesis focuses on the study of AS, with three main interconnected objectives:

1. The single-cell transcriptomic description of the endometrium of AS patients and a comparison with healthy tissue
2. The generation and characterization of an organoid cell culture model of AS
3. The study of how autologous cell therapy affects AS

The underlying molecular mechanisms and cellular interactions impacted in the AS endometrium remain poorly understood; therefore, our single-cell approach aimed to address this knowledge gap, creating an atlas of the pathological endometrium and laying the groundwork for future research.

Previous advances in AS treatment have mainly been achieved using animal models due to the absence of alternative models and the ethical constraints associated with human studies (de Miguel-Gómez et al., 2021). Developing an AS model that recapitulates specific disease-associated parameters will help to reduce any reliance on animal models, complying with the first objective of the principle of the three Rs ("replacement"), promoted by the European Union within Directive 2010/63/EU (Díaz et al., 2020). Our laboratory has developed a therapeutic approach for AS that involves administering autologous $CD133^+$ bone marrow-derived stem cells (BMDSCs) to the AS endometrium. Examining the changes induced by this autologous cell therapy in tissue samples and within a newly developed organoid model will allow us to understand the

improvements observed in our previous study of BMDSC administration (Santamaria et al., 2016).

Our comprehensive, functional single-cell RNA sequencing (scRNA-seq) atlas of the AS endometrium identified eighteen distinct cell populations, including a disease-specific cell type: the AS-epithelium. Our analysis revealed substantial differences in cell population ratios, gene expression patterns, and cell-to-cell communication (CCC) networks between healthy and AS endometrium. These alterations support the emergence of an AS-associated defective endometrial environment with pro-inflammatory, pro-fibrotic, and anti-angiogenic properties, consistent with previous research (Santamaria, Mas, et al., 2018). By integrating scRNA-seq analysis into our $CD133^{+}$ BMDSC-based phase I/II clinical trial for AS treatment, we discovered that this mode of cell therapy reversed specific AS-associated alterations in the endometrium (related to epithelial cell function and inflammation).

Our transcriptomics data revealed how endometrial cell composition became altered in response to AS-associated pathological alterations (**Figure 10**, **Figure 12**, **Figure 14** and **Figure 16**). AS associated with a significant reduction in the proportion of epithelial cells, primarily affecting the luminal and glandular secretory subpopulations. The AS-induced reduction in the epithelium aligns with the histological phenotype previously observed in AS patients, which Smikle et al. (2023) described as predominantly composed of fibroblast-like cells with the loss of most of the glands.

We also we observed the loss of a potentially endometrial stem cell-containing population in AS endometrial samples – the SOX9-epithelium. SOX9, a recognized stem cell transcriptional regulator (Kadaja et al., 2014), has been detected within cells of the endometrial *basalis* layer (Garcia-Alonso et al., 2021); therefore, *SOX9*-expressing populations may represent a source of undifferentiated stem/progenitor cells that support endometrial regeneration. Thus, the absence of the SOX9-epithelium in the AS endometrium could directly relate to the lack of endometrial regeneration observed in AS patients.

In contrast, other cell populations significantly increased in the AS endometrium, including cell types exhibiting a muscular-related gene profile (such as smooth muscle

cells (SMCs) and contractile perivascular (PV) cells) and myeloid/lymphoid immune cell populations (such as macrophages, mast cells, and double-negative T cells). Immune cell alterations can give rise to a pro-inflammatory environment, while SMC alterations could increase stiffness; of note, both these features arise in the AS endometrium (Schenker & Yaffe, 1978; Smikle et al., 2023). Importantly, we must consider that the relative thinness of the AS endometrium may result in the collection of a higher number of myometrial cells during biopsy acquisition, which could explain their overrepresentation in AS samples. In our research, we utilized published cell annotations from previous transcriptomic studies and successfully identified most of the previously described cell clusters, reinforcing the robustness of analyzed biopsies despite their limited number.

Treating AS patients with autologous $CD133^+$ BMDSCs prompted the reversal of some AS disease-induced alterations (**Figure 43** and **Figure 44**). Overall, $CD133^+$ BMDSC administration increased the percentage of endothelial cells and epithelial subpopulations alongside a drastic decrease in the percentage of AS-epithelium cells. Previous studies demonstrated that BMDSC administration increased endometrial thickness and gland number in rabbit (Yuan et al., 2022) and rat (Cervelló et al., 2015) models of endometrial damage. Additionally, Cervelló et al., (2015) suggested that the regenerative capacity of $CD133^+$ BMDSCs derives from the secretion of paracrine factors, such as thrombospondin I and IGF1 (Insulin-like growth factor 1) (Cervelló et al., 2015), a mechanism through which our therapy could induce human endometrial regeneration.

Of note, studies have highlighted that the reparative/regenerative effects of mesenchymal stem cells (MSCs) and menstrual blood stem cells (MenSCs) on the endometrium occur through exosome secretion (Ebrahim et al., 2018; Zhang et al., 2023). Although not proven for BMDSCs, communication through extracellular vesicles could play a significant role in the induced therapeutic effect in AS endometrium. Cervelló et al. (2015) reported the recruitment of $CD133^+$ BMDSCs from the bone marrow to the damaged endometrium in rats, where they eventually localized around blood vessels. The tropism of $CD133^+$ BMDSCs to the blood vessels combined with their endothelial identity (Urbich & Dimmeler, 2004) suggests that recruited $CD133^+$ BMDSCs may directly give rise to endothelial cells rather than through supporting neighboring cells by releasing paracrine-acting factors. The observed recovery of the proportions of

endometrial cell types after CD133$^+$ BMDSC administration provides an initial indicator of treatment-induced improvement.

Nevertheless, we failed to detect *SOX9*$^+$ cells after CD133$^+$ BMDSC administration, suggesting that the observed regeneration did not occur through the restoration of these cells. The observed regeneration might result from the activation of proliferation in more differentiated *SOX9*$^+$ cells and from changes in the status of endometrial cells, which increased their expression of genes associated with endometrial receptivity (**Figure 45**). The absence of potential SOX9$^+$ stem cells may suggest that this form of cell therapy cannot restore the endometrium's natural regenerative capacity, resulting in only a temporary improvement that fades as CD133$^+$ BMDSCs become naturally depleted. This hypothesis is supported by previous patient treatment results (Santamaria et al., 2016), where the pathological state returned months after the initial application of therapy.

For the first time, we identified a disease-associated stressed cell population we termed "AS-epithelium" in the AS endometrium (**Figure 10** and **Figure 12**). AS-epithelium cells expressed elevated levels of cellular stress-related genes, including *HSPA1A* (Radons, 2016) and *SOCS3*, whose product controls the activation of STAT3-cytokine signaling through JAK inhibition (Carow & Rottenberg, 2014). The AS-epithelium also highly expressed the inflammatory-response gene *SLPI* (Mongkolpathumrat et al., 2024), which we explored as a marker for this population. We validated our results by detecting *SLPI*$^+$ cells by *in situ* hybridization in glands and near the lumen of AS endometrium; however, this population was barely detectable in the healthy endometrium (**Figure 19**). CD133$^+$ BMDSC administration prompted a significant reduction in the size of the *SLPI*$^+$ AS-epithelium to a level undetectable in tissue (**Figure 61**). This decrease in the stressed epithelium could be attributed to a therapeutic effect induced by CD133$^+$ BMDSC administration, as we demonstrated partially reversed stress-related signaling through growth differentiation factor (GDF) signaling pathway, involving GDF15 in cellular stress response following damage (Luan et al., 2019). This homeostatic effect may be mediated by the release of anti-inflammatory cytokines, such as has been observed for FGF-β or IL6 in bone marrow-derived MSCs (Salama et al., 2020).

Ciliated and glandular secretory epithelial cells remain critical to the receptive function of the endometrium during the window of implantation (WOI) (Dmowski & Greenblatt, 1969); interestingly, we observed a pronounced reduction in these specific cell populations in the AS endometrium. The transcriptomic profiles of AS endometrial epithelial cells suggested decreased secretory activity (decreased *SCGB1D2* and *SCGB2A1* expression) and revealed lower expression of WOI-related genes (**Figure 13**), describing a dysfunctional endometrium that would hinder embryo adhesion. These findings agree well with the poor reproductive outcomes generally observed in AS patients (Guo et al., 2019).

We observed robust cell-to-cell communication (CCC) both between distinct epithelial cell populations and between these epithelial cells and other cell types, such as stromal, endothelial, or perivascular (PV) cells, in the healthy endometrium; however, the loss of this CCC profile provided further evidence of impaired epithelial activity in the AS endometrium. We observed the complete absence of IL6 signaling, previously related to establishing and maintaining pregnancy (Yoo et al., 2017), in the AS endometrium, while we observed the notable disruption of the SPP1 pathway, which functions in epithelial cell adhesion and stromal decidualization (Wang et al., 2018), and the CHD1, JAM, and DESMOSOME pathways, which function in epithelial cell adhesion and cell differentiation (Grund & Grümmer, 2018; Reardon et al., 2012). Said alterations to CCC profiles could prompt the detachment of epithelial cells and alter epithelial differentiation, partially explaining the thin epithelial lining and the lack of structural integrity described in AS patients (Smikle et al., 2023).

After treatment with $CD133^+$ BMDSCs, the AS-affected endometrial epithelium underwent significant alterations that suggested partial recovery toward a healthy-like state. We observed the restored expression of genes related to functional and secretory activity (*SCGB1D2* and *LGALS1*) (Koel et al., 2022) and proliferation and stemness (*IGF1* and *PDGFRA*) (Zhang et al., 2023) (**Figure 46**) and of proliferation and development pathways (such as CADM or NRG) (Balko et al., 2012; Kimura et al., 2021). This latter finding reinforces research suggesting that $CD133^+$ BMDSCs induce proliferation in injured tissue to improve endometrial function (Fu et al., 2019; Mohsen et al., 2019). Both results agree with our previous clinical study results following $CD133^+$ BMDSC

administration (Santamaria et al., 2016); we observed increased endometrial thickening (which may be attributed to increased epithelial cell proliferation) and subsequent pregnancies in AS patients (supportive of an improvement in epithelial layer functionality).

Endometrial regeneration after damage has been linked to the activity of the canonical and non-canonical WNT pathways through the role of WNT in stem cell expansion and self-renewal (Boland et al., 2004; Ling et al., 2009). In this study, we observed the absence of WNT-mediated CCC in the SOX9-epithelium (WNT7a interactions) and CCC between luminal epithelium and stromal cells (WNT5a interactions) (**Figure 28**). This contradicts the findings of Xue et al., (2022), who reported *WNT7a* and *WNT5a* overexpression in the endometria of AS patients (Xue et al., 2022) and subsequent AS progression through the hyperactivation of WNT signaling. Our results suggest a link between decreased WNT signaling and the AS-associated loss of endometrial regeneration. The loss of *WNT7a* might cause the disappearance of the *SOX9*$^{+}$ population by limiting cell self-renewal; similarly, the absence of *WNT5a* could hinder the expansion of undifferentiated cells, leading to the loss of cells essential for endometrial regeneration.

A balance between WNT and NOTCH signaling participates in endometrial cell differentiation into distinct epithelial subtypes. WNT pathway inhibition prompts differentiation into glandular epithelial cells, while NOTCH pathway inhibition prompts differentiation into ciliated epithelial cells (Garcia-Alonso et al., 2021). We observed a notable decline in NOTCH pathway signaling in luminal and glandular epithelial subclusters in the AS endometrium (**Figure 28**), which hinders epithelial differentiation. CD133^{+} BMDSC administration prompted the restoration of WNT-promoted cell differentiation signaling between the stroma and epithelium involving both canonical (*WNT2*) and non-canonical (*WNT4*) pathways (Qin et al., 2024). This suggests WNT-based stem cell regulation and epithelial differentiation controlled by stromal cells (**Figure 52**). These results may imply the reactivation of stem cell expansion and self-renewal activities and could explain the absence of the *SOX9*$^{+}$ epithelium after cell therapy; this may occur due to the lack of *WNT7a*, which appears to regulate *SOX9*$^{+}$ renewal in healthy samples or the inability of this pathway to restore a lost cell type.

Fibrosis - a crucial consequence of AS that leads to IUA formation – impairs the reproductive function of the uterus (Smikle et al., 2023). Fibrosis arises as a response to epithelial injury and inflammation and involves fibroblast proliferation and the synthesis of substantial amounts of proteoglycans and collagens, which prompts increased tissue stiffness. Our analysis of the AS endometrium suggested increased proliferation (IGF and IGFBP5) (Hu et al., 2006; Rajski et al., 2010) and elevated production of the extracellular matrix (ECM) components fibronectin and collagen (COL1/3 and FN1) (Yoshida et al., 2021) by endometrial fibroblasts (**Figure 13**). This pro-fibrotic profile of AS fibroblasts agrees well with results obtained in AS animal models (Salama et al., 2020) and human histological characteristics (Smikle et al., 2023). CCC analysis demonstrated how the AS-induced loss of epithelial-stroma interactions altered, leading to the self-stimulation of stromal cells and the activation of ECM fiber production (**Figure 23** and **Figure 24**). Furthermore, we observed the upregulation of additional pro-fibrotic networks - FGF2 and periostin (O'Dwyer & Moore, 2017) - in the AS endometrium. Our results suggest that *FGF* gene expression and ECM accumulation could drive tissue fibrosis and the onset of tissue adhesion and rigidity, which could relate to altered cell differentiation mediated by ECM alterations (Smith et al., 2018) and influence the invasion phase during abnormal placentation (Dmowski & Greenblatt, 1969).

$CD133^+$ BMDSC administration in AS patients also leads to the upregulation of genes involved in ECM stabilization (*TPM1*) (Irungu et al., 2019), cell migration and invasion (*PTN* and *SPARCL1*) (Wang et al., 2016), and decreased epithelial-mesenchymal transition (EMT) (*DIO2*) in stromal cells (Zhou et al., 2022) (**Figure 46**), as well as to a less proliferative transcriptome (Hu et al., 2010; Radons, 2016). This reorganization and limited expansion of the ECM suggest the regression of fibrosis required for recovery in AS patients (Santamaria et al., 2016).

Concurrently, $CD133^+$ BMDSC administration induced the decreased expression of proliferative (*SOX4*) and contractile (*MYL9*) genes in PV contractile and SMC cells (**Figure 46**). The *MYL9* product participates in myometrial fibrosis, a process in which SMCs display an increase in contractility, collagen production, and myofibroblastic differentiation through RhoA/ROCK1/MYL9 pathway signaling (Qin et al., 2024). The reduced expression of these genes indicates a loss of muscle-like characteristics, leading

to reduced fibrosis and decreased tissue stiffness. In addition, $CD133^+$ BMDSCs decreased CCC via fibrosis-related ligands (ITGB2 and FGF2) (Tan et al., 2020) and replacement with signaling via molecules with robust homeostatic functions (FGF7 and FGF10) (Lessey & Young, 2014; Wang et al., 2005) (**Figure 48** and **Figure 60**), indicating a more flexible and dynamic tissue environment. Differentiation induced by the previously discussed restoration of epithelial-stromal CCC (through WNT and NRG pathways) may also affect fibrosis prevention. Lin et al. (2023) discovered that MSC-derived exosomes could impact fibrosis marker expression (such as collagen), reducing fibrosis in a rat IUA model (Lin et al., 2023). Notably, collagen gene overexpression remained in most endometrial cell populations after $CD133^+$ BMDSC administration, suggesting that their mechanism of action does not coincide with the therapeutic impact described for MSC-derived exosomes. This could relate to the limited duration of the previously described cell therapy effect (Santamaria et al., 2016), as sustained collagen expression could cause the AS phenotype to persist several months after treatment.

A pro-inflammatory state in the endometrium represents another characteristic of AS. Our results revealed the expansion of myeloid and lymphoid cell populations and a shift in transcriptomic profiles in the AS endometrium (Annex 4). Various immune populations, including macrophages and natural killer (NK) cells, displayed inflammatory/immune activation profiles (expressing *S100A8/9/12* or cytokines). Meanwhile, the expression of a cytokine receptor (*CCR1*), and the heightened permeability of venous endothelial cells to leukocyte trans-endothelial migration (ICAM, VCAM, and PECAM1 pathways) by immune cells supports cell recruitment and an active immune pattern (P. J. Murray & Wynn, 2011). CCC data also revealed heightened interactions between epithelial and immune cells in the AS endometrium, indicating an increased pro-inflammatory epithelial environment. We observed increased estrogen and progesterone receptor expression (*ESR1* and *PGR*) in the epithelial and stromal subclusters in the AS endometrium, which agrees with the gene expression levels observed in the endometrium of patients with IUAs (Kovats, 2015). This finding implies that these receptors could be involved in immune cell inflammatory response regulation.

$CD133^+$ BMDSC administration significantly reduced pro-inflammatory profile in the AS endometrium, decreasing the expression of immune response and chronic

inflammation-related genes (e.g., *IL6ST*, *MIF,* and *DEFB1*) in epithelial cells, genes related to migration (*ICAM*), antigen presentation (*HLADR*), and heat shock (*HSPH1* and *HSPA1B*) in endothelial cells, and *IL32* and the anti-apoptotic lncRNA gene *MTRNR2L12* in immune cells (**Figure 46**). We also observed a general reduction in the expression of the endometrial fibrosis-related *S100A* family of genes across all cell types initially expressing said genes (Xin et al., 2024) and reduced activity of signaling pathways related to the immune response and pro-inflammatory processes. These results support our hypothesis that administering $CD133^+$ BMDSCs promotes homeostatic recovery of the AS endometrium, reducing oxidative stress and inflammation. Although the mechanisms of action that induce said changes remain unknown, Su et al. (2019) reported that bone marrow-derived MSCs secrete anti-inflammatory cytokines when applied to damaged lung tissue; therefore, we hypothesize that $CD133^+$ BMDSCs function similarly in the damaged AS endometrium, potentially secreting anti-inflammatory cytokines (such as IL6) to inhibit signaling via the NF-κB pathway.

The avascular nature of endometrial tissue in AS patients contributes to the lack of menstruation. Avascularity, which also prompts increased fibrosis due to tissue hypoxia (Santamaria et al., 2018), can be attributed to the anti-angiogenic signals identified in the transcriptomic analysis of the AS endometrium; specifically, endothelial, stromal, and PV cells overexpressed known anti-angiogenic factors (*IGFBP3/5/6*) (Lala & Nandi, 2016) (**Figure 13**). Interestingly, we discovered that $CD133^+$ BMDSCs reversed this anti-angiogenic effect, decreasing the expression of *IGFBP3* and increasing the expression of pro-angiogenic genes (*IGFBP2* and *PTN*) (Chung et al., 2002; Slater et al., 2019), and endothelial differentiation genes (*KLF2*) (Dekker et al., 2006) (**Figure 46**). The ANGPTL1 (angiogenesis inhibitor) and ANGPTL2 (angiogenesis promoter) ligands exhibited altered profiles in stromal-endothelial CCC before and after $CD133^+$ BMDSC administration. The emergence of ANGPTL2 as the dominant ligand after treatment (**Figure 54**) represents a significant change, as the balance of these interacting molecules plays a crucial role in modulating vascular regeneration and angiogenesis (Carbone et al., 2018). (Davis & Senger, 2005). These findings agree with the clinical improvements observed in our previous study, which reported recovered menstruation and increased endometrial vascularization (Santamaria et al., 2016). Nevertheless, we note the apparent transient

nature of vascular growth promotion, as patients experience decreased menstrual volume and regularity six months post-treatment, although the underlying reasons for this decline remain unclear.

We collected endometrial samples for our single-cell analysis via hysteroscopic visualization, allowing the selection of areas free of IUAs. This approach revealed that moderate and severe AS cases associate with endometrial dysfunction, suggesting that IUAs are a consequence of the underlying disease rather than its primary cause. Several stress-associated marker genes increase their expression when the endometrium transitions from moderate to severe AS (Tsuji, 2005), linked to epithelial inflammatory diseases, including inflammatory bowel disease (Li et al., 2012).

Despite the significant progress in understanding disease pathology, the intrinsic limitations of animal experimental models and human biopsy samples have constrained AS research. To facilitate the study of AS from a different perspective, we developed (for the first time) a self-organizing 3D culture model from endometrial adult stem cells isolated from AS patient biopsies. Endometrial epithelial organoids (EEOs) recapitulate the functionality and structure of the epithelium (Clevers, 2016) and have been widely used in the study of healthy endometrium (Boretto et al., 2017; Fitzgerald et al., 2019; Garcia-Alonso et al., 2021; Rawlings et al., 2021) and the modeling of associated diseases such as endometriosis (Boretto et al., 2019) or endometrial cancer (Katcher et al., 2023). We demonstrated the development of AS EEOs using a protocol developed for healthy tissue-derived EEOs (Boretto et al., 2017) and established a WOI-like state using hormonal treatment. Immunohistochemical characterization revealed that AS EEOs comprised differentiated and apicobasal polarized epithelial cells with their apical side facing the inner lumen of the organoid; these findings compare well to control EEOs and those developed by other groups (Boretto et al., 2017; Turco et al., 2017). Despite AS EEOs exhibiting long-term expansion capacity, they developed fewer EEOs than control EEOs, suggesting the lower regenerative capacity of the AS endometrium (**Figure 29** and **Figure 30**). This difference in AS EEO generation capacity diminished after the second passage, possibly due to the positive selection of stem/progenitor cells during passaging; however, individual EEOs exhibited differences in diameter between AS and control, the latter displaying a larger diameter (**Figure 31**), and a lower proliferative capacity in AS

EEOs in more advanced passages. These results suggest a smaller number of adult stem cells (or an impairment in their functionality) in the AS endometrium and lower cell growth and division capacity of AS EEO cells. Overall, AS EEOs retain specific pathological characteristics, underscoring their potential utility in studies on AS endometrium.

To characterize AS EEOs and compare their transcriptomic profiles with *in vivo* tissue, we analyzed EEOs from AS patients and healthy donors using scRNA-seq. We identified populations with profiles associated with ciliated, glandular, and glandular epithelial cells expressing WOI genes (glandular secretory cluster) and several proliferative populations (**Figure 33**). AS EEOs contained fewer ciliated and glandular secretory cells than control EEOs, with a glandular cell cluster exhibiting high *COL1A2* expression as the most prevalent (**Figure 35**), suggesting the increased production of ECM. This population distribution agrees well with the results observed from AS biopsies, which present most epithelial cells in the glandular secretory population.

We did not identify the "AS-epithelium" population previously detected in AS endometrial tissue samples in AS EEOs. The absence of this AS-associated population could be attributed to the lower level of inflammatory environmental pressures present in the cell culture conditions compared to AS endometrium, which may reduce the expression of the characteristic stress-related gene. The prominent proliferative epithelial cell population in AS EEOs expressed estradiol-regulated and ECM remodeling-associated genes, consistent with the overexpression of estradiol receptors in AS biopsies and supporting the hypothesis of estradiol as a regulator of certain aspects of AS. When comparing identified EEO populations with those described from *in vivo* samples (**Figure 36** and **Figure 37**), results support our initial EEO annotation and the transcriptomic resemblance of AS EEO cells to epithelial cells outside the WOI and control EEOs resembling epithelial cells within the WOI. In addition, glandular and glandular secretory AS EEO cells expressed higher levels of inflammatory response genes (*DMKN* and *ANXA1*) and lower levels of proapoptotic (*GOS2*) and WOI (*CXCL14*) genes (**Figure 38**). These results indicate that AS EEOs present an inflammatory, estradiol-responsive profile, suggesting the recapitulation of AS-associated features and supporting their use in future research. Given that all EEOs underwent the same hormonal treatment to mimic the WOI, the gene expression profile of AS EEO cells

indicates the possible resistance of the epithelium to differentiation-inducing factors, leading to the retention of cell states before the WOI that may contribute to the impaired functional capacity of the AS epithelium (Smikle et al., 2023).

Despite the pathological characteristics of AS EEOs, we found that this culture model did not recapitulate many disease-associated parameters. As mentioned earlier, the CCC networks between the distinct cell types of the endometrium remain crucial for a comprehensive understanding of AS pathology. As EEOs only represent the epithelial fraction of the tissue, adding complexity to these models (such as developing assembloids - organoid models that include other cell types) (Cai et al., 2023; Rawlings et al., 2021) may be of use when studying interactions between cell types. Overall, the AS EEOs developed in this thesis may represent a starting point for developing increasingly complex models that more accurately represent AS.

Interestingly, we discovered that the pro-regenerative/reparative effect of $CD133^+$ BMDSC treatment observed *in vivo* was reflected in the characteristics of EEOs generated from biopsies of treated patients. Post-treatment AS EEOs presented a higher growth rate, larger diameter, and more significant proliferation when compared to pre-treatment AS EEOs (**Figure 62** and **Figure 63**). Specific parameters used to assess the regenerative of EEOs have served as indicators for endometrial regeneration when evaluating other therapies. For example, proliferation indicated by the Ki67 marker increases after treatment with UC-MSCs (Aygün & Tümentemur, 2022; Zhang et al., 2018), platelet-rich plasma (de Miguel–Gómez et al., 2021; Jang et al., 2017), collagen scaffolds with growth factors (Li et al., 2011), and BMDSCs (Yi et al., 2019) including our therapy (Cervelló et al., 2015) in animal models. These results suggest that AS EEOs recapitulate the impact of $CD133^+$ BMDSC administration *in vivo*, enhancing this model's value. Combined with control EEO results, we found that post-treatment AS EEOs recovery parameters lay between control EEOs and AS EEOs. This agrees with the results obtained from $CD133^+$ BMDSC administration in human patients, who demonstrated partial recovery with decreased disease severity but not complete restoration to a healthy-like state (Santamaria et al., 2016).

Our transcriptomic analysis revealed that CD133$^+$ BMDSCs altered the cellular composition of EEOs to a state comparable to control EEOs. Ciliated and proliferative cells expressing EMT-associated genes increased in number, with the glandular cluster proportionally lower than the glandular secretory cluster, indicating enhanced cell proliferation and differentiation (**Figure 65**). The expression of EMT genes may represent a side effect of using a WNT pathway inhibitor during EEO hormonal treatment, which has been used previously to decrease the proliferation and increase the differentiation of epithelial cells, as occurs during the WOI (Kagawa et al., 2022). However, WNT pathway signaling has also been linked to decreased EMT (Yuan et al., 2022); therefore, inhibition may have the opposite effect. Nonetheless, post-treatment AS EEOs displayed increased proliferation, which could be explained by the induction of the proliferative epithelium with regenerative capacity by CD133$^+$ BMDSCs.

The comparison between *in vivo* and *in vitro* results after cell therapy confirmed that post-treatment AS EEO cells resembled control EEO cells compared to AS EEOs and biopsy secretory glandular cells compared to biopsy glandular cells (**Figure 66** and **Figure 67**). Interestingly, post-treatment AS EEOs displayed more similarity to cells from control biopsies than post-treatment AS biopsy cells, which may be attributed to the less pro-inflammatory conditions associated with *in vitro* culture. Finally, gene expression analysis revealed that the post-treatment AS EEOs displayed reduced collagen production and immune responses, together with increased cell differentiation as an effect of the cell therapy. These findings revealed how our AS EEO model reflected disease improvement, recapitulating the changes observed in endometrial tissues and validating EEOs as a valuable *in vitro* model for studying AS and the mechanisms that regulate endometrial epithelial regeneration in AS patients following cell therapy. This model may also be applied to study the effects of different therapies by direct application to EEOs, allowing researchers to observe whether modifications indicative of endometrial regeneration occur before applying them in humans. Of note, the EEO culture medium contains growth factors such as FGF, EGF, and R-spondin (a WNT pathway ligand), which can induce cell growth and development and may mask the effects of a given therapeutic approach. These factors may also explain the decreased collagen gene expression observed in EEOs. Therefore, studying the specific factors

secreted by CD133$^+$ BMDSCs and the effect of organoid culture medium growth factors in AS endometrium may be valuable to assess if supplementing CD133$^+$ BMDSC with specific factors could achieve a more prolonged regenerative effect.

We observed the elevated expression of *SLPI* in the AS endometrium but not for AS-EEOs; therefore, we selected *COL1A2* as a gene marker since the transcriptomic landscape revealed significant expression differences between EEO types. AS EEOs present high levels of *COL1A2* expression, while control EEOs mainly lacked *COL1A2* expression, and post-treatment AS EEOs showed mild expression levels. Salama et al., (2020) previously associated reduced *COL1A2* expression with endometrial regeneration when treating an AS mouse model with MSCs; this agrees with our EEO results, suggesting the recovery of the endometrial epithelium after stem cell treatment.

The results described in this thesis allowed for the description of the cellular state of the AS endometrium, thus creating an "atlas" via scRNA-seq data. Our data suggest a pro-inflammatory, pro-fibrotic, and anti-angiogenic environment associated with epithelial dysfunction. We identified a disease-associated population, the absence of previously described endometrial epithelial stem cells, and CCC that maintains pathological phenotypes mainly due to stromal self-stimulation, precluding the typical reproductive function of the uterus. Moreover, our findings suggest that patient-specific autologous CD133$^+$ BMDSC therapy can partially reverse AS pathology. The transcriptomic and CCC alteration observed following CD133$^+$ BMDSC therapy indicated the recovery of the epithelium's secretory and regenerative functions, enhancing cell proliferation and differentiation and decreasing the presence of pro-inflammatory factors, tissue fibrosis, and contractility. These modifications, which could be accomplished through the secretion of paracrine growth factors and WNT pathway regulators, resulted in the transition of the endometrium to a healthier state that may improve AS symptoms such as recurrent pregnancy loss or implantation failure (Moreno et al., 2023). In addition, we reproduced the pathological profile of the AS epithelium in an EEO model, which also recapitulated alterations observed following cell therapy. These findings support the ongoing use of EEOs in future research; however, EEOs provided more definitive regenerative effects, probably due to the specific model culture conditions.

By achieving these objectives, we have improved our understanding of AS, establishing a cell atlas that will be referenced for numerous future studies. Including this data in a phase I/II clinical trial protocol authorized by the European Medicines Agency supports the functionality of the cell atlas, which may help develop novel therapies for AS. We also demonstrated the positive therapeutic impact of cell therapy on AS. The combined effect of cell therapy on various disease-associated factors appears crucial for improving gestational outcomes, as previous studies focusing on one factor (such as blood vessel growth via vasoactive treatments (de Miguel-Gómez et al., 2021) or cell therapy (Kaczynski & Rzepka, 2022)) did not report significant improvements. Although we do not yet understand the process by which $CD133^{+}$ BMDSCs support endometrial regeneration, nor whether they do so under normal conditions or only after damage, our data has allowed us to hypothesize about their potential secretory and regulatory roles in the growth and differentiation pathways of different cell types. This paves the way for research focused on understanding the mechanisms of action, simplifying treatments, and improving treatment efficacy.

Additionally, our characterization of a novel EEO culture model for AS disease broadens avenues for the investigation of novel therapies or combined treatments (e.g., platelet-rich plasma (de Miguel–Gómez et al., 2021), mitomycin C (Xu et al., 2020), or PDGFBB (Zhang et al., 2023)). This initial description of AS EEOs will support the future incorporation of additional cell types into organoids to enhance complexity. This approach facilitates not only transcriptomic studies but also the exploration of other layers of information, including the proteome involved in disease progression or possible genetic or epigenetic predisposing factors (Santamaria et al., 2018). Future studies would be enhanced by supplementing the information in this thesis with a more significant number of samples, encompassing both the secretory and proliferative phases, to capture a more comprehensive range of disease progression.

VII. Conclusions

VII. Conclusions

1. Our single-cell study of the endometrium in patients with AS demonstrates the existence of 5 cellular populations, which include 18 transcriptomically defined cell subtypes.
2. The endometrium in AS displays a reduction in secretory glandular and ciliated epithelium compared to healthy endometrium. Additionally, the decreased secretory activity and a loss of epithelial-stroma communication mediated by the CDH1 and SPP1 signaling pathways, likely affect endometrial receptivity.
3. In the endometrium of AS patients, we identified a new epithelial cell population (AS-epithelium) that expresses genes related to cellular stress and inflammatory response. This population associates with AS and significantly decreases after therapy with $CD133^+$ BMDSCs, making the AS-epithelium a potential diagnostic and prognostic marker through the *SLPI* marker.
4. The endometrium in AS lacks $SOX9^+$ epithelial cells - characterized as a progenitor cell population in normal endometrium - likely due to the loss of communication via WNT7a and WNT5a. This mechanism may represent a cause of impaired endometrial regeneration in AS.
5. This endometrial pathology induces a pro-inflammatory profile characterized by an increase in various immune populations that overexpress different inflammatory genes such as *NEAT1* and *S100A8/9/12*, cytokines *CCL5/3* and *CCL3L1*, and the attraction of immune cells through ICAM, PECAM1, and VCAM signaling pathways.
6. Additionally, endometrial fibrosis occurs in AS due to paracrine stimuli from the pro-fibrotic FGF and PERIOSTIN pathways in stromal cells, leading to an increase in collagen production and the expansion of contractile populations (smooth muscle cells and contractile perivascular cells) that cause extracellular matrix expansion and increased rigidity.

7. The AS endometrium exhibits an anti-angiogenic profile, characterized by a loss of endometrial vasculature due to the overexpression of anti-angiogenic factors such as IGFBP3 and IGFBP5 by stromal, endothelial, and perivascular cells.
8. Cell therapy - the administration of autologous $CD133^+$ BMDSCs - induces partial recovery of the endometrium's pro-inflammatory, pro-fibrotic, and anti-angiogenic profile in AS patients.
9. Cell therapy increases endometrial secretory capacity and reduces the expression of pro-inflammatory genes. Cell therapy also decreases the pro-fibrotic profile in the endometrium by reducing the expression of genes such as *MYL9*, *ITGB2*, or *TPM1* in stromal and/or contractile cells. Finally, cell therapy induces angiogenesis by expressing *PTN*, *IGFBP2*, *KLF2*, and communication via the ANGPTL pathway.
10. The development of endometrial epithelial organoids from endometrial biopsies of AS patients partially replicates the epithelium's characteristics and the partial recovery after treatment with this cell therapy, allowing their use as an *in vitro* model for studying AS.

VIII. Annexes

VIII. Annexes

Annex 1. Favorable opinion of the Ethics Committee of "Agencia Española de medicamentos y productos sanitarios" for the biomedical study that includes this thesis.

MINISTERIO DE SANIDAD

agencia española de medicamentos y productos sanitarios

DEPARTAMENTO DE MEDICAMENTOS DE USO HUMANO

Área de Ensayos Clínicos

ASUNTO: Respuesta a Condiciones en la Resolución de Autorización del EC nº EudraCT: 2016-003975-23, fecha 07 de agosto de 2020

DESTINATARIO: **Experior S.L.**
C/ Vicente Galmés 1 A
46139 La Pobla de Farnals,
Valencia

Promotor: **Asherman Therapy S.L.U.**
Ronda Narciso Monturiol, 11 B.
Parque Tecnológico de Paterna
46980 Paterna, Valencia

En relación a las respuestas recibidas en fecha 06-08-2020 para las condiciones que se detallaban en la Resolución de Autorización del ensayo clínico titulado: **Eficacia y seguridad de células CD133+ autólogas, movilizadas, no expandidas para tratar pacientes con Síndrome de Asherman: Ensayo clínico prospectivo, multicéntrico, fase I/II.**

Tras evaluar la respuesta a las condiciones de autorización de este ensayo, la AEMPS comunica que se puede iniciar, teniendo en cuenta las siguientes

OBSERVACIONES:

Los compromisos son aceptables y se puede iniciar el ensayo.

JEFE DEL DEPARTAMENTO DE MEDICAMENTOS DE USO HUMANO
P.D. (Resolución de 27 de julio de 2020)
Jefe de la División de Farmacología y Evaluación Clínica de la AEMPS

agencia española de medicamentos y productos sanitarios

Mª Luisa Suárez Gea

Agencia Española de Medicamentos y Productos Sanitarios (AEMPS)
Fecha de la firma: 07/08/2020
Puede comprobar la autenticidad del documento en la sede de la AEMPS:https://localizador.aemps.es
CSV: G28P587D7F

CORREO ELECTRÓNICO
smhaem@aemps.es

Página 1 de 1

C/ CAMPEZO, 1 - EDIFICIO 8
28022 MADRID
Tel.: 918225073
Fax: 918225043

Annex 2. Dot plot of canonical marker gene expression in A) main identified populations, and B) immune populations in AS atlas. Abbreviations – DN (double negative), MAIT (mucosal-associated invariant T), NK (natural killer), PV (perivascular), SMC (smooth muscle cells).

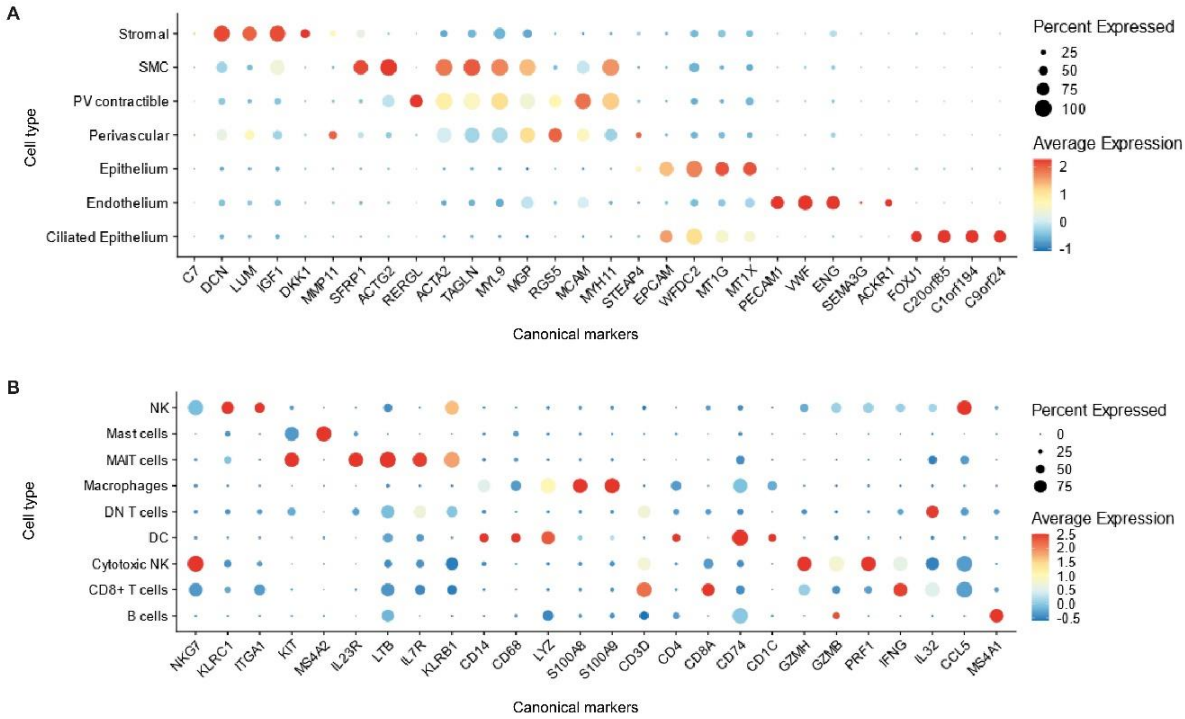

Annex 3. Dot plot of marker gene expression in Asherman syndrome-affected and window of implantation control endometrial samples. Abbreviations - AS (Asherman syndrome), EC (endothelial), Epi (epithelium), PV (perivascular), SMC (smooth muscle cell).

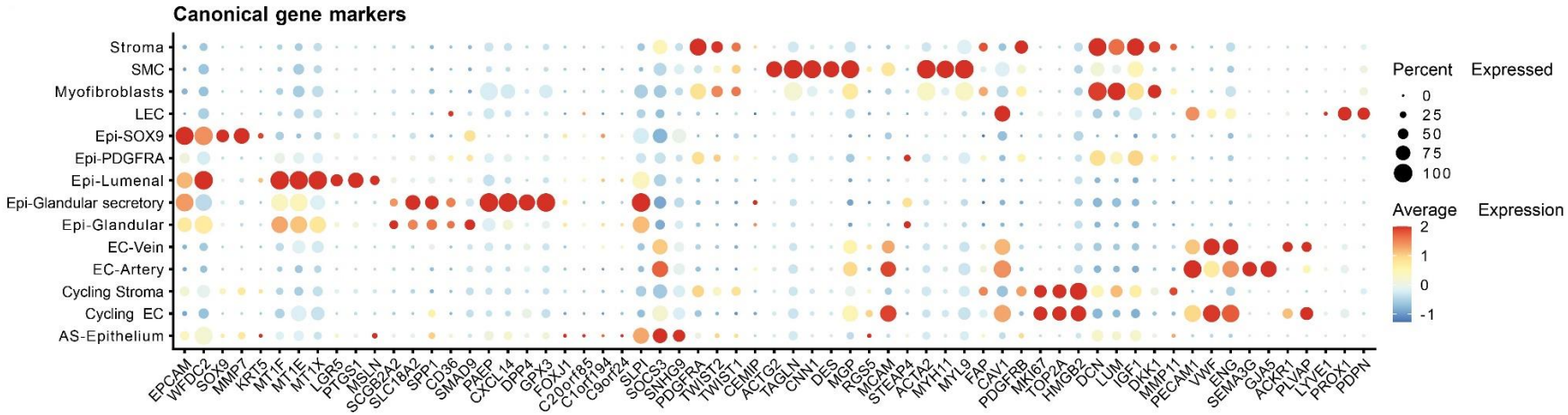

Annex 4. Differential gene expression between AS and secretory phase controls immune cell types (Wilcoxon Rank Sum test, FDR<0.05). Abbreviations – DC (Dendritic cell), DN (Double negative), MAIT (Mucosal-associated invariant T), NK (Natural killer).

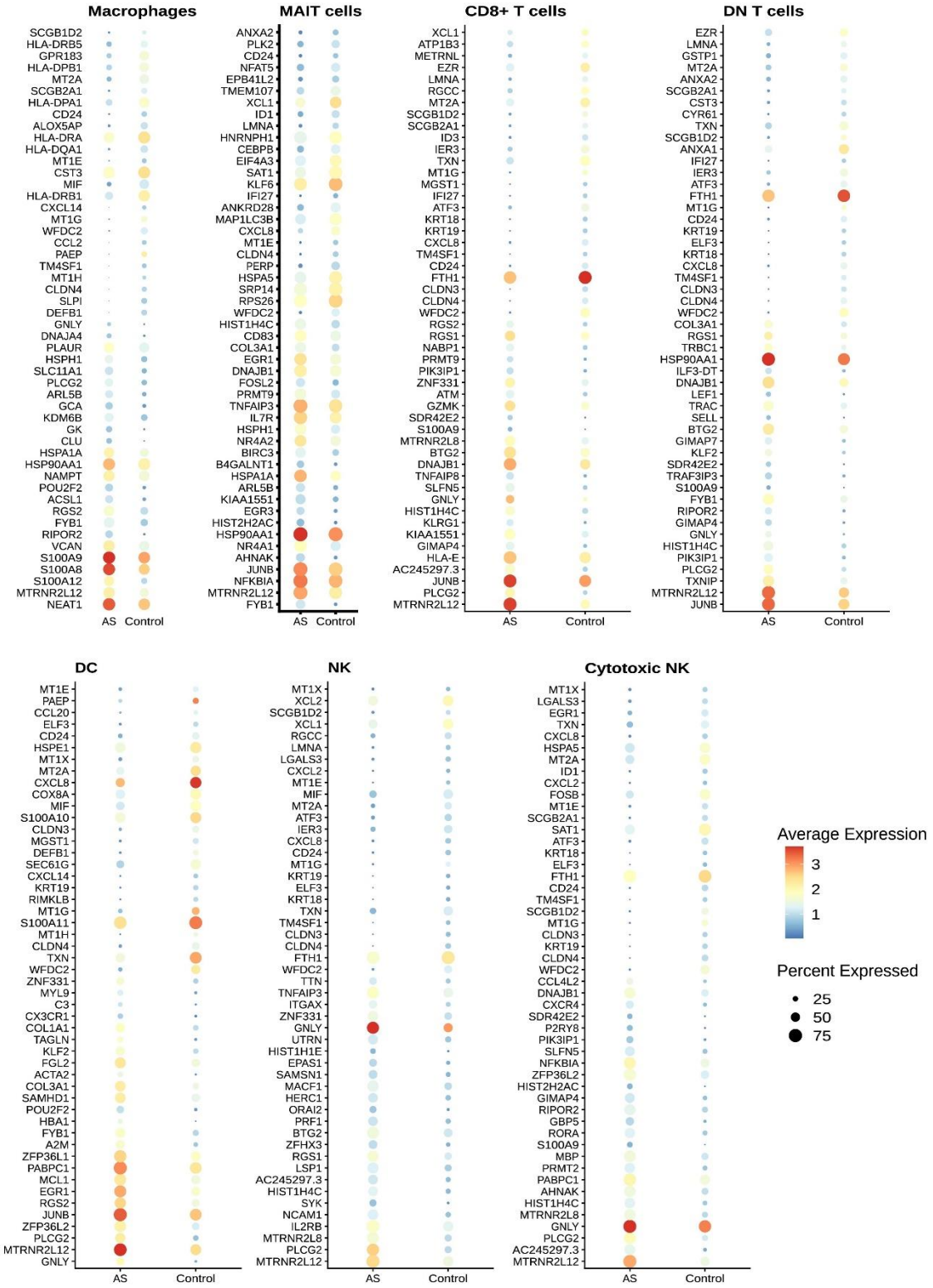

Annex 5. Dot plots of cell-to-cell communication results for the A) CCL, B) SPP1, C) FGF, D) WNT, and E) NOTCH signalling pathways (Wilcoxon test). AS in red labels, control in green labels). Abbreviations – AS (Asherman syndrome), DC (dendritic cell), EC (endothelial), MAIT (mucosal-associated invariant T).

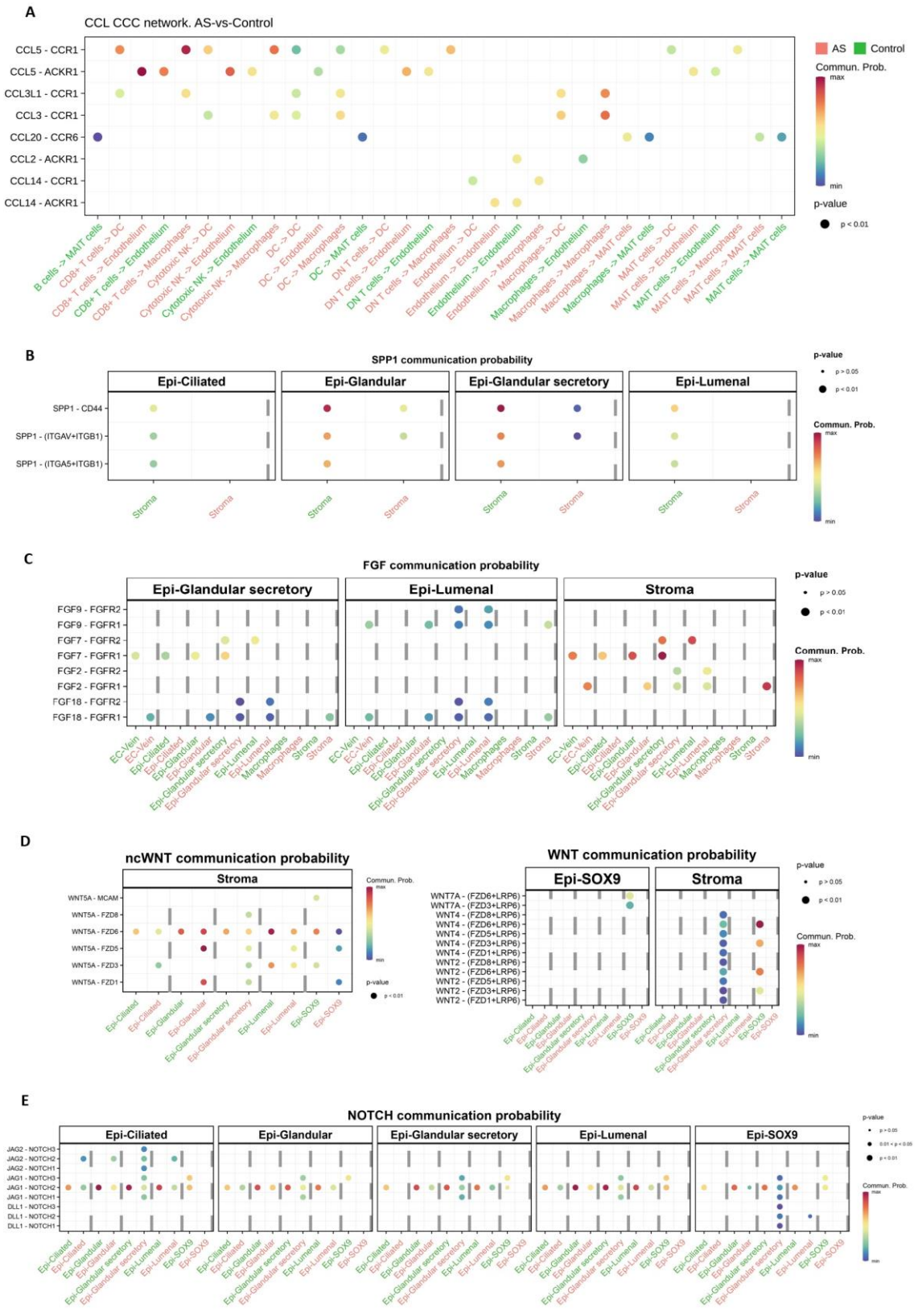

Annex 6. Yield of endometrial cells per AS patient before (AS) and after cell (AS-Post) therapy administration.

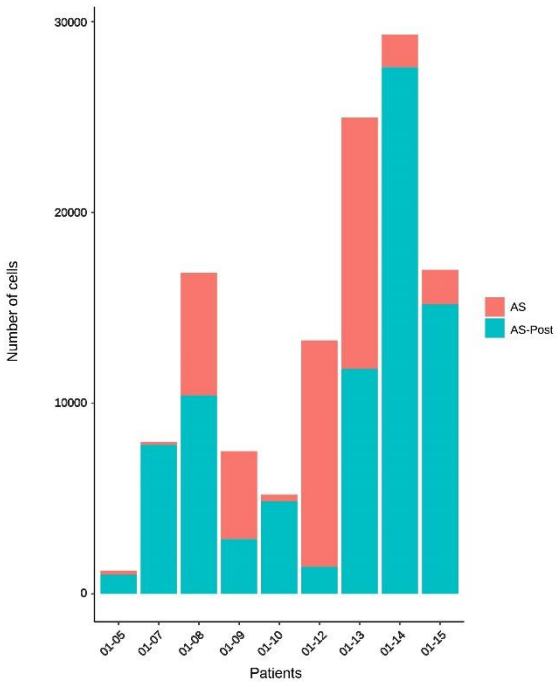

Annex 7. Differential gene expression between pre-treatment and post-treatment AS immune cell types (Wilcoxon Rank Sum test, FDR<0.05). Abbreviations – DC (dendritic cells), DN (double negative), MAIT (mucosal-associated invariant T), NK (natural killer).

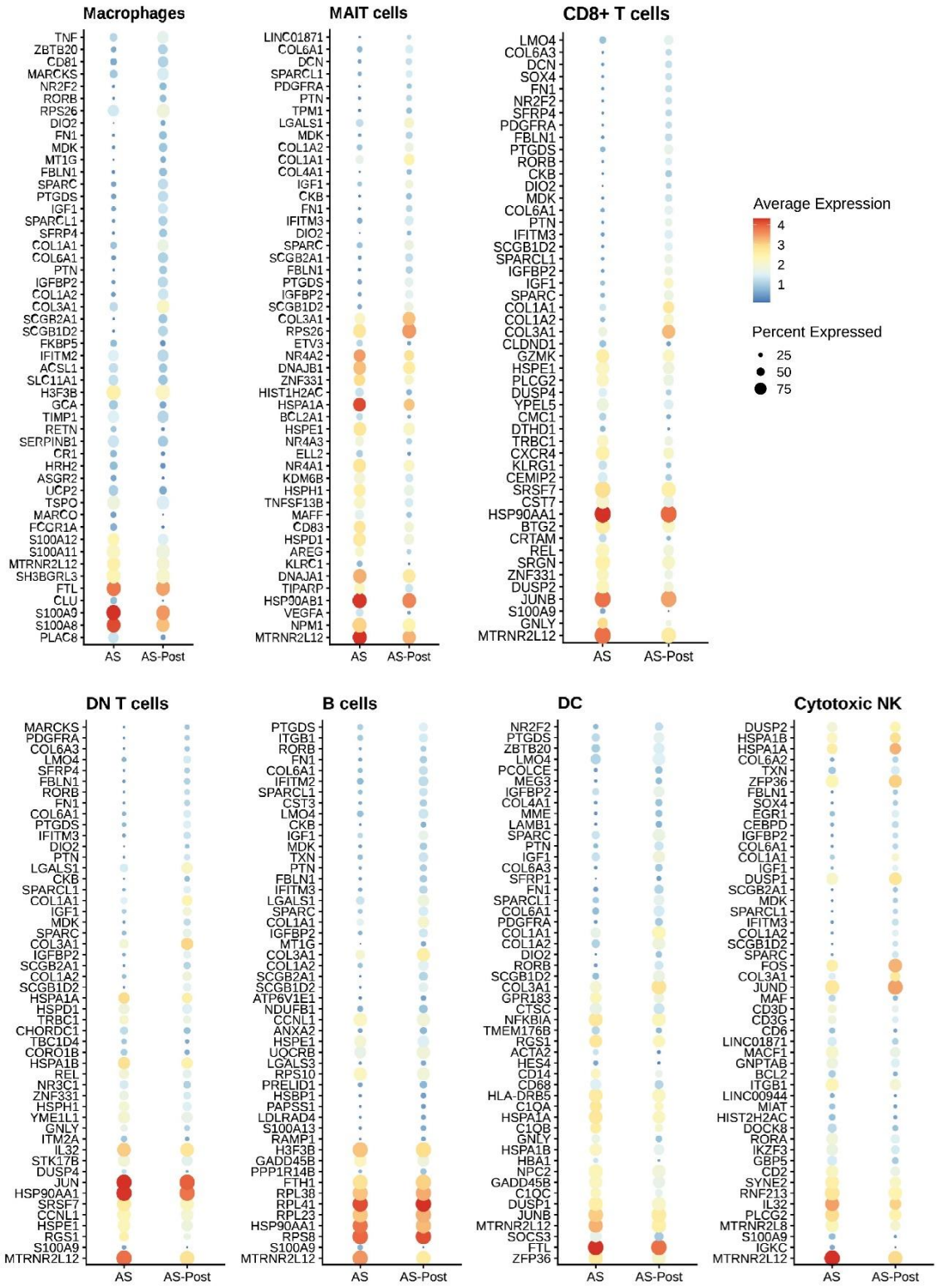

Annex 8. Dot plots of cell-to-cell communication results for the A) NRG, B) IL6, and C) GDF signalling pathways (Wilcoxon test). Pre-treatment AS in red labels, post-treatment AS in blue labels). Abbreviations – AS (Asherman syndrome), DC (dendritic cells), EC (endothelial), MAIT (mucosal-associated invariant T), SMC (smooth muscle cells).

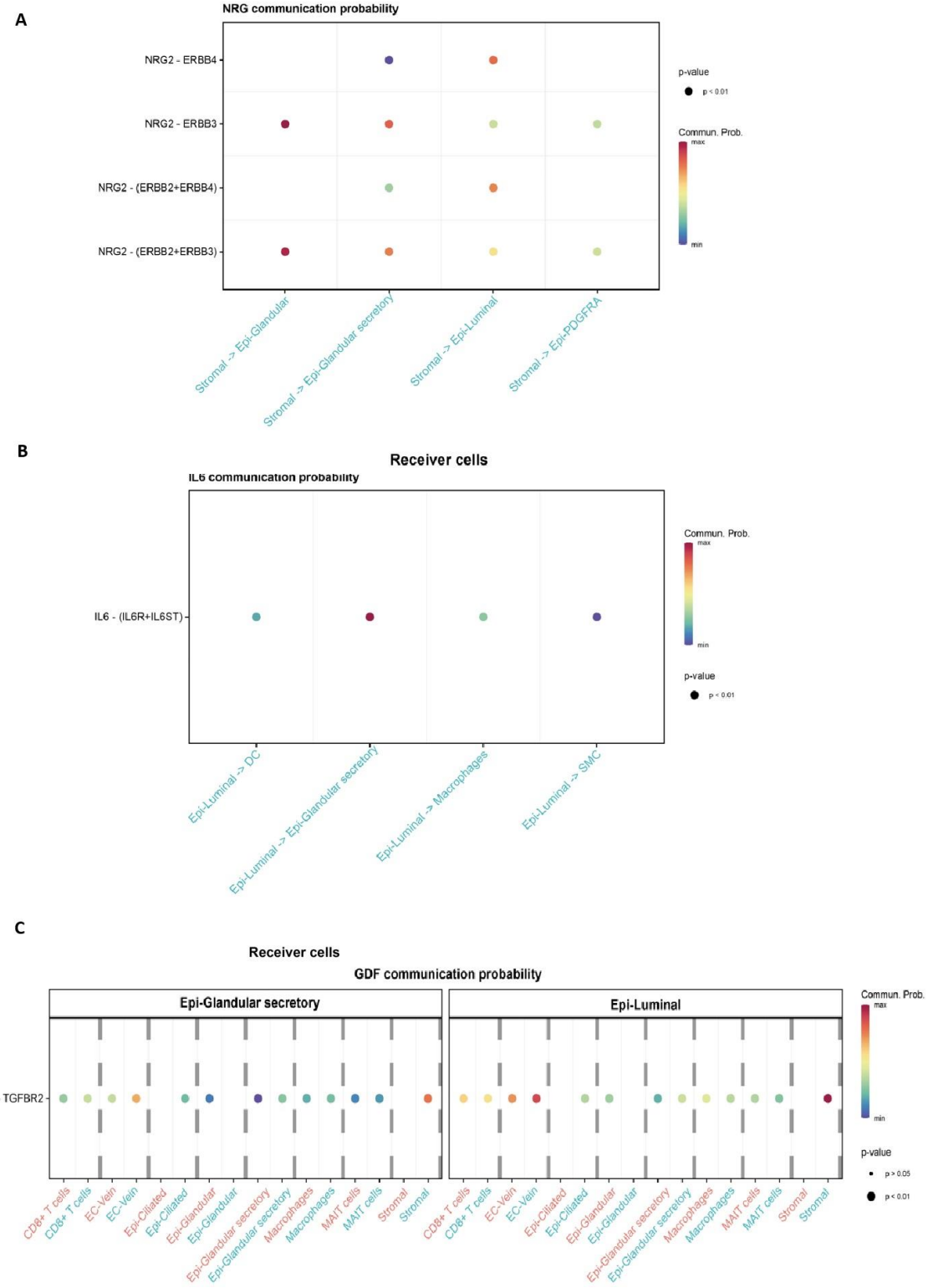

IX. References

IX. References

Aboul Nasr, A. L., Al-Inany, H. G., Thabet, S. M., & Aboulghar, M. (2000). A clinicohysteroscopic scoring system of intrauterine adhesions. *Gynecologic and Obstetric Investigation*, *50*(3), 178–181. https://doi.org/10.1159/000010305

Abrahamsohn, P. A., & Zorn, T. M. T. (1993). Implantation and decidualization in rodents. *The Journal of Experimental Zoology*, *266*(6), 603–628. https://doi.org/10.1002/JEZ.1402660610

Aggarwal, S., Wang, Z., Pacheco, D. R. F., Rinaldi, A., Rajewski, A., Callemeyn, J., Van Loon, E., Lamarthée, B., Covarrubias, A. E., Hou, J., Yamashita, M., Akiyama, H., Karumanchi, S. A., Svendsen, C. N., Noble, P. W., Jordan, S. C., Breunig, J. J., Naesens, M., Cippà, P. E., & Kumar, S. (2024). SOX9 switch links regeneration to fibrosis at the single-cell level in mammalian kidneys. *Science (New York, N.Y.)*, *383*(6685), 1–14. https://doi.org/10.1126/SCIENCE.ADD6371

Aghajanova, L., Hamilton, A. E., & Giudice, L. C. (2008). Uterine Receptivity to Human Embryonic Implantation: Histology, Biomarkers, and Transcriptomics. *Seminars in Cell & Developmental Biology*, *19*(2), 204. https://doi.org/10.1016/J.SEMCDB.2007.10.008

Aikawa, S., Kano, K., Inoue, A., Wang, J., Saigusa, D., Nagamatsu, T., Hirota, Y., Fujii, T., Tsuchiya, S., Taketomi, Y., Sugimoto, Y., Murakami, M., Arita, M., Kurano, M., Ikeda, H., Yatomi, Y., Chun, J., & Aoki, J. (2017). Autotaxin–lysophosphatidic acid– LPA 3 signaling at the embryo-epithelial boundary controls decidualization pathways . *The EMBO Journal*, *36*(14), 2146–2160. https://doi.org/10.15252/EMBJ.201696290/SUPPL_FILE/EMBJ201696290-SUP-0002-EVFIGS.PDF

Alawadhi, F., Du, H., Cakmak, H., & Taylor, H. S. (2014a). Bone Marrow-Derived Stem Cell (BMDSC) transplantation improves fertility in a murine model of Asherman's syndrome. *PloS One*, *9*(5). https://doi.org/10.1371/JOURNAL.PONE.0096662

Alquicira-Hernandez, J., Sathe, A., Ji, H. P., Nguyen, Q., & Powell, J. E. (2019). ScPred: Accurate supervised method for cell-type classification from single-cell RNA-seq data. *Genome Biology*, *20*(1), 1–17. https://doi.org/10.1186/S13059-019-1862-5/FIGURES/6

Alsaigh, T., Evans, D., Frankel, D., & Torkamani, A. (2022). Decoding the transcriptome of calcified atherosclerotic plaque at single-cell resolution. *Communications Biology 2022 5:1*, *5*(1), 1–17. https://doi.org/10.1038/s42003-022-04056-7

Altmäe, S., Esteban, F. J., Stavreus-Evers, A., Simón, C., Giudice, L., Lessey, B. A., Horcajadas, J. A., Macklon, N. S., D'Hooghe, T., Campoy, C., Fauser, B. C., Salamonsen, L. A., & Salumets, A. (2014). Guidelines for the design, analysis and interpretation of 'omics' data: focus on human endometrium. *Human Reproduction Update*, *20*(1), 12. https://doi.org/10.1093/HUMUPD/DMT048

Aplin, J. D., Charlton, A. K., & Ayad, S. (1988). An immunohistochemical study of human endometrial extracellular matrix during the menstrual cycle and first trimester of pregnancy. *Cell and Tissue Research*, *253*(1), 231–240. https://doi.org/10.1007/BF00221758

IX. References

Aplin, J. D., Hey, N. A., & Li, T. C. (1996). MUC1 as a cell surface and secretory component of endometrial epithelium: reduced levels in recurrent miscarriage. *American Journal of Reproductive Immunology (New York, N.Y. : 1989)*, *35*(3), 261–266. https://doi.org/10.1111/J.1600-0897.1996.TB00042.X

Armstrong, G. M., Maybin, J. A., Murray, A. A., Nicol, M., Walker, C., Saunders, P. T. K., Rossi, A. G., & Critchley, H. O. D. (2017). Endometrial apoptosis and neutrophil infiltration during menstruation exhibits spatial and temporal dynamics that are recapitulated in a mouse model. *Scientific Reports*, *7*(1). https://doi.org/10.1038/S41598-017-17565-X

Asherman, J. G. (1948). Amenorrhoea Traumatica (Atretica). *BJOG: An International Journal of Obstetrics & Gynaecology*, *55*(1), 23–30. https://doi.org/10.1111/J.1471-0528.1948.TB07045.X

Aygün, E. G., & Tümentemur, G. (2022). Effects of stem cells and amniotic fluid on uterus and ovaries in a rat model of abdominal adhesions: a controlled study. *Journal of the Turkish German Gynecological Association*, *23*(3), 154. https://doi.org/10.4274/JTGGA.GALENOS.2022.2022-1-14

Azizi, R., Aghebati-Maleki, L., Nouri, M., Marofi, F., Negargar, S., & Yousefi, M. (2018). Stem cell therapy in Asherman syndrome and thin endometrium: Stem cell- based therapy. *Biomedicine & Pharmacotherapy = Biomedecine & Pharmacotherapie*, *102*, 333–343. https://doi.org/10.1016/J.BIOPHA.2018.03.091

Bai, X., Liu, J., Yuan, W., Liu, Y., Li, W., Cao, S., Yu, L., & Wang, L. (2020). Therapeutic Effect of Human Amniotic Epithelial Cells in Rat Models of Intrauterine Adhesions. *Cell Transplantation*, *29*. https://doi.org/10.1177/0963689720908495

Balko, J. M., Miller, T. W., Morrison, M. M., Hutchinson, K., Young, C., Rinehart, C., Sańchez, V., Jee, D., Polyak, K., Prat, A., Perou, C. M., Arteaga, C. L., & Cook, R. S. (2012). The receptor tyrosine kinase ErbB3 maintains the balance between luminal and basal breast epithelium. *Proceedings of the National Academy of Sciences of the United States of America*, *109*(1), 221–226. https://doi.org/10.1073/PNAS.1115802109/-/DCSUPPLEMENTAL

Bao, M., Feng, Q., Zou, L., Huang, J., Zhu, C., & Xia, W. (2023). Endoplasmic reticulum stress promotes endometrial fibrosis through the TGF-β/SMAD pathway. *Reproduction (Cambridge, England)*, *165*(2), 171–182. https://doi.org/10.1530/REP-22-0294

Baradwan, S., Alharbi, D., Bashir, M. S., Saleh, A., & Al-Jaroudi, D. (2023). Short and long-term reproductive outcomes after hysteroscopic adhesiolysis for infertile women. *JBRA Assisted Reproduction*, *27*(2), 191–196. https://doi.org/10.5935/1518-0557.20220016

Baraniak, P. R., & McDevitt, T. C. (2010). Stem cell paracrine actions and tissue regeneration. *Regenerative Medicine*, *5*(1), 121–143. https://doi.org/10.2217/RME.09.74

Bergeron, C. (2006). Histología y fisiología del endometrio normal. *EMC - Ginecología-Obstetricia*, *42*(4), 1–8. https://doi.org/10.1016/s1283-081x(06)47901-7

Bhurke, A. S., Bagchi, I. C., & Bagchi, M. K. (2016). Progesterone-Regulated Endometrial Factors Controlling Implantation. *American Journal of Reproductive Immunology*, *75*(3), 237–245. https://doi.org/10.1111/AJI.12473

Bi, J., Dixit, G., Zhang, Y., Devor, E. J., Losh, H. A., Newtson, A. M., Coleman, K. L., Santillan, D. A., Maretzky, T., Thiel, K. W., & Leslie, K. K. (2021). Advantages of tyrosine kinase anti-angiogenic cediranib over bevacizumab: Cell cycle

abrogation and synergy with chemotherapy. *Pharmaceuticals*, *14*(7), 682. https://doi.org/10.3390/PH14070682/S1

Bister, J., Crona Guterstam, Y., Strunz, B., Dumitrescu, B., Haij Bhattarai, K., Özenci, V., Brännström, M., Ivarsson, M. A., Gidlöf, S., & Björkström, N. K. (2021). Human endometrial MAIT cells are transiently tissue resident and respond to Neisseria gonorrhoeae. *Mucosal Immunology*, *14*(2), 357–365. https://doi.org/10.1038/S41385-020-0331-5

Björklund, A. K., Forkel, M., Picelli, S., Konya, V., Theorell, J., Friberg, D., Sandberg, R., & Mjösberg, J. (2016). The heterogeneity of human CD127(+) innate lymphoid cells revealed by single-cell RNA sequencing. *Nature Immunology*, *17*(4), 451–460. https://doi.org/10.1038/NI.3368

Blanpain, C., & Fuchs, E. (2014). Stem cell plasticity. Plasticity of epithelial stem cells in tissue regeneration. *Science (New York, N.Y.)*, *344*(6189). https://doi.org/10.1126/SCIENCE.1242281

Blau, H. M., Brazelton, T. R., & Weimann, J. M. (2001). The evolving concept of a stem cell: entity or function? *Cell*, *105*(7), 829–841. https://doi.org/10.1016/S0092-8674(01)00409-3

Boland, G. M., Perkins, G., Hall, D. J., & Tuan, R. S. (2004). Wnt 3a promotes proliferation and suppresses osteogenic differentiation of adult human mesenchymal stem cells. *Journal of Cellular Biochemistry*, *93*(6), 1210–1230. https://doi.org/10.1002/JCB.20284

Borcherding, N., Vishwakarma, A., Voigt, A. P., Bellizzi, A., Kaplan, J., Nepple, K., Salem, A. K., Jenkins, R. W., Zakharia, Y., & Zhang, W. (2021). Mapping the immune environment in clear cell renal carcinoma by single-cell genomics. *Communications Biology*, *4*(1). https://doi.org/10.1038/S42003-020-01625-6

Boretto, M., Cox, B., Noben, M., Hendriks, N., Fassbender, A., Roose, H., Amant, F., Timmerman, D., Tomassetti, C., Vanhie, A., Meuleman, C., Ferrante, M., & Vankelecom, H. (2017). Development of organoids from mouse and human endometrium showing endometrial epithelium physiology and long-term expandability. *Development (Cambridge, England)*, *144*(10), 1775–1786. https://doi.org/10.1242/DEV.148478

Boretto, M., Maenhoudt, N., Luo, X., Hennes, A., Boeckx, B., Bui, B., Heremans, R., Perneel, L., Kobayashi, H., Van Zundert, I., Brems, H., Cox, B., Ferrante, M., Uji-i, H., Koh, K. P., D'Hooghe, T., Vanhie, A., Vergote, I., Meuleman, C., … Vankelecom, H. (2019). Patient-derived organoids from endometrial disease capture clinical heterogeneity and are amenable to drug screening. *Nature Cell Biology*, *21*(8), 1041–1051. https://doi.org/10.1038/S41556-019-0360-Z

Bozorgmehr, M., Gurung, S., Darzi, S., Nikoo, S., Kazemnejad, S., Zarnani, A. H., & Gargett, C. E. (2020). Endometrial and Menstrual Blood Mesenchymal Stem/Stromal Cells: Biological Properties and Clinical Application. *Frontiers in Cell and Developmental Biology*, *8*. https://doi.org/10.3389/FCELL.2020.00497

Brighton, P. J., Maruyama, Y., Fishwick, K., Vrljicak, P., Tewary, S., Fujihara, R., Muter, J., Lucas, E. S., Yamada, T., Woods, L., Lucciola, R., Hou Lee, Y., Takeda, S., Ott, S., Hemberger, M., Quenby, S., & Brosens, J. J. (2017). Clearance of senescent decidual cells by uterine natural killer cells in cycling human endometrium. *ELife*, *6*. https://doi.org/10.7554/ELIFE.31274

Brosens, I., Muter, J., Ewington, L., Puttemans, P., Petraglia, F., Brosens, J. J., & Benagiano, G. (2019). Adolescent Preeclampsia: Pathological Drivers and Clinical Prevention. *Reproductive Sciences (Thousand Oaks, Calif.)*, *26*(2), 159–171. https://doi.org/10.1177/1933719118804412

IX. References

Brosens, I., Muter, J., Gargett, C. E., Puttemans, P., Benagiano, G., & Brosens, J. J. (2017). The impact of uterine immaturity on obstetrical syndromes during adolescence. *American Journal of Obstetrics and Gynecology*, *217*(5), 546–555. https://doi.org/10.1016/J.AJOG.2017.05.059

Brosens, J. J., Hayashi, N., & White, J. O. (1999). Progesterone receptor regulates decidual prolactin expression in differentiating human endometrial stromal cells. *Endocrinology*, *140*(10), 4809–4820. https://doi.org/10.1210/ENDO.140.10.7070

Bruno Bass. (1927). Ueber die Verwachsungen in der cervix uteri nach curettagen. *Zentralbl Gynakol*, *51*, 223.

Buechler, M. B., Pradhan, R. N., Krishnamurty, A. T., Cox, C., Calviello, A. K., Wang, A. W., Yang, Y. A., Tam, L., Caothien, R., Roose-Girma, M., Modrusan, Z., Arron, J. R., Bourgon, R., Müller, S., & Turley, S. J. (2021). Cross-tissue organization of the fibroblast lineage. *Nature 2021 593:7860*, *593*(7860), 575–579. https://doi.org/10.1038/s41586-021-03549-5

Buttram, V. C., Gomel, V., Siegler, A., DeCherney, A., Gibbons, W., & March, C. (1988). The American Fertility Society classifications of adnexal adhesions, distal tubal occlusion, tubal occlusion secondary to tubal ligation, tubal pregnancies, müllerian anomalies and intrauterine adhesions. *Fertility and Sterility*, *49*(6), 944–955. https://doi.org/10.1016/S0015-0282(16)59942-7

Cai, Y., Li, N., & Li, H. (2023). Combining Endometrial Assembloids and Blastoids to Delineate the Molecular Roadmap of Implantation. *Stem Cell Reviews and Reports*, *19*(5), 1268–1282. https://doi.org/10.1007/S12015-023-10527-Z

Cao, Y., Sun, H., Zhu, H., Zhu, X., Tang, X., Yan, G., Wang, J., Bai, D., Wang, J., Wang, L., Zhou, Q., Wang, H., Dai, C., Ding, L., Xu, B., Zhou, Y., Hao, J., Dai, J., & Hu, Y. (2018). Allogeneic cell therapy using umbilical cord MSCs on collagen scaffolds for patients with recurrent uterine adhesion: a phase I clinical trial. *Stem Cell Research & Therapy*, *9*(1). https://doi.org/10.1186/S13287-018-0904-3

Capella-Allouc, S., Morsad, F., Rongières-Bertrand, C., Taylor, S., & Fernandez, H. (1999). Hysteroscopic treatment of severe Asherman's syndrome and subsequent fertility. *Human Reproduction (Oxford, England)*, *14*(5), 1230–1233. https://doi.org/10.1093/HUMREP/14.5.1230

Carbone, C., Piro, G., Merz, V., Simionato, F., Santoro, R., Zecchetto, C., Tortora, G., & Melisi, D. (2018). Angiopoietin-Like Proteins in Angiogenesis, Inflammation and Cancer. *International Journal of Molecular Sciences*, *19*(2). https://doi.org/10.3390/IJMS19020431

Carbonnel, M., Pirtea, P., de Ziegler, D., & Ayoubi, J. M. (2021). Uterine factors in recurrent pregnancy losses. *Fertility and Sterility*, *115*(3), 538–545. https://doi.org/10.1016/J.FERTNSTERT.2020.12.003

Carow, B., & Rottenberg, M. E. (2014). SOCS3, a Major Regulator of Infection and Inflammation. *Frontiers in Immunology*, *5*(FEB). https://doi.org/10.3389/FIMMU.2014.00058

Carson, D. D., Lagow, E., Thathiah, A., Al-Shami, R., Farach-Carson, M. C., Vernon, M., Yuan, L., Fritz, M. A., & Lessey, B. (2002). Changes in gene expression during the early to mid-luteal (receptive phase) transition in human endometrium detected by high-density microarray screening. *Molecular Human Reproduction*, *8*(9), 871–879. https://doi.org/10.1093/MOLEHR/8.9.871

Cervelló, I., Gil-Sanchis, C., Mas, A., Faus, A., Sanz, J., Moscardó, F., Higueras, G., Sanz, M. A., Pellicer, A., & Simón, C. (2012). Bone marrow-derived cells from male donors do not contribute to the endometrial side population of the recipient. *PloS One*, *7*(1). https://doi.org/10.1371/JOURNAL.PONE.0030260

Cervelló, I., Gil-Sanchis, C., Santamaría, X., Cabanillas, S., Díaz, A., Faus, A., Pellicer, A., & Simón, C. (2015). Human CD133(+) bone marrow-derived stem cells promote endometrial proliferation in a murine model of Asherman syndrome. *Fertility and Sterility*, *104*(6), 1552-1560.e3. https://doi.org/10.1016/J.FERTNSTERT.2015.08.032

Chaney, H. L., Grose, L. F., Labarbara, J. M., Sirk, A. W., Blancke, A. M., Sánchez, J. M., Passaro, C., Lonergan, P., & Mathew, D. J. (2022). Galectin-1 induces gene and protein expression related to maternal-conceptus immune tolerance in bovine endometrium†. *Biology of Reproduction*, *106*(3), 487–502. https://doi.org/10.1093/BIOLRE/IOAB215

Chen, S., Li, K., Zhong, X., Wang, G., Wang, X., Cheng, M., Chen, J., Chen, Z., Chen, J., Zhang, C., Xiong, G., Xu, X., Chen, D., Li, H., & Peng, L. (2021). Sox9-expressing cells promote regeneration after radiation-induced lung injury via the PI3K/AKT pathway. *Stem Cell Research and Therapy*, *12*(1), 1–13. https://doi.org/10.1186/S13287-021-02465-9/FIGURES/6

Chen, Y., Liu, L., Luo, Y., Chen, M., Huan, Y., & Fang, R. (2017). Prevalence and Impact of Chronic Endometritis in Patients With Intrauterine Adhesions: A Prospective Cohort Study. *Journal of Minimally Invasive Gynecology*, *24*(1), 74–79. https://doi.org/10.1016/J.JMIG.2016.09.022

Cheng, Y., Wang, H., Shang, J., Wang, J., Yin, J., Zhang, J., Guo, X., Wang, S., Duan, Y. G., Lee, C. L., Chiu, P. C. N., Zhang, J., Yeung, W. S. B., Cao, D., & Yao, Y. (2023). Transcriptomic analysis of mid-secretory endometrium reveals essential immune factors associated with pregnancy after single euploid blastocyst transfer. *American Journal of Reproductive Immunology (New York, N.Y. : 1989)*, *89*(3). https://doi.org/10.1111/AJI.13672

Christian, M., Marangos, P., Mak, I., Mcvey, J., Barker, F., White, J., & Brosens, J. J. (2001). Interferon-γ Modulates Prolactin and Tissue Factor Expression in Differentiating Human Endometrial Stromal Cells. *Endocrinology*, *142*(7), 3142–3151. https://doi.org/10.1210/ENDO.142.7.8231

Chung, H. W., Wen, Y., Choi, E. A., Hao-Li, Moon, H. S., Yu, H. K., & Polan, M. L. (2002). Pleiotrophin (PTN) and midkine (MK) mRNA expression in eutopic and ectopic endometrium in advanced stage endometriosis. *Molecular Human Reproduction*, *8*(4), 350–355. https://doi.org/10.1093/MOLEHR/8.4.350

Cindrova-Davies, T., Zhao, X., Elder, K., Jones, C. J. P., Moffett, A., Burton, G. J., & Turco, M. Y. (2021). Menstrual flow as a non-invasive source of endometrial organoids. *Communications Biology*, *4*(1). https://doi.org/10.1038/S42003-021-02194-Y

Clevers, H. (2016). Modeling Development and Disease with Organoids. *Cell*, *165*(7), 1586–1597. https://doi.org/10.1016/J.CELL.2016.05.082

Clevers, H., Loh, K. M., & Nusse, R. (2014). Stem cell signaling. An integral program for tissue renewal and regeneration: Wnt signaling and stem cell control. *Science (New York, N.Y.)*, *346*(6205). https://doi.org/10.1126/SCIENCE.1248012

Co, E. C., Gormley, M., Kapidzic, M., Rosen, D. B., Scott, M. A., Stolp, H. A. R., McMaster, M., Lanier, L. L., Bárcena, A., & Fisher, S. J. (2013). Maternal decidual macrophages inhibit NK cell killing of invasive cytotrophoblasts during human pregnancy. *Biology of Reproduction*, *88*(6). https://doi.org/10.1095/BIOLREPROD.112.099465

IX. References

Cochrane, D. R., Campbell, K. R., Greening, K., Ho, G. C., Hopkins, J., Bui, M., Douglas, J. M., Sharlandjieva, V., Munzur, A. D., Lai, D., DeGrood, M., Gibbard, E. W., Leung, S., Boyd, N., Cheng, A. S., Chow, C., Lim, J. L. P., Farnell, D. A., Kommoss, S., … Huntsman, D. G. (2020). Single cell transcriptomes of normal endometrial derived organoids uncover novel cell type markers and cryptic differentiation of primary tumours. *The Journal of Pathology*, *252*(2), 201–214. https://doi.org/10.1002/PATH.5511

Committee for Orphan Medicinal Products (COMP) | European Medicines Agency. (n.d.). Retrieved April 15, 2024, from https://www.ema.europa.eu/en/committees/committee-orphan-medicinal-products-comp

Conforti, A., Alviggi, C., Mollo, A., De Placido, G., & Magos, A. (2013). The management of Asherman syndrome: a review of literature. *Reproductive Biology and Endocrinology : RB&E*, *11*(1). https://doi.org/10.1186/1477-7827-11-118

Cousins, F. L., Kirkwood, P. M., Saunders, P. T. K., & Gibson, D. A. (2016). Evidence for a dynamic role for mononuclear phagocytes during endometrial repair and remodelling. *Scientific Reports*, *6*. https://doi.org/10.1038/SREP36748

Cousins, F. L., Murray, A., Esnal, A., Gibson, D. A., Critchley, H. O. D., & Saunders, P. T. K. (2014). Evidence from a mouse model that epithelial cell migration and mesenchymal-epithelial transition contribute to rapid restoration of uterine tissue integrity during menstruation. *PloS One*, *9*(1). https://doi.org/10.1371/JOURNAL.PONE.0086378

Cousins, F. L., Pandoy, R., Jin, S., & Gargett, C. E. (2021). The Elusive Endometrial Epithelial Stem/Progenitor Cells. *Frontiers in Cell and Developmental Biology*, *9*. https://doi.org/10.3389/FCELL.2021.640319

Coutifaris, C., Myers, E. R., Guzick, D. S., Diamond, M. P., Carson, S. A., Legro, R. S., McGovern, P. G., Schlaff, W. D., Carr, B. R., Steinkampf, M. P., Silva, S., Vogel, D. L., & Leppert, P. C. (2004). Histological dating of timed endometrial biopsy tissue is not related to fertility status. *Fertility and Sterility*, *82*(5), 1264–1272. https://doi.org/10.1016/J.FERTNSTERT.2004.03.069

Critchley, H. O. D., Henderson, T. A., Kelly, R. W., Scobie, G. S., Evans, L. R., Groome, N. P., & Saunders, P. T. K. (2002). Wild-type estrogen receptor (ERbeta1) and the splice variant (ERbetacx/beta2) are both expressed within the human endometrium throughout the normal menstrual cycle. *The Journal of Clinical Endocrinology and Metabolism*, *87*(11), 5265–5273. https://doi.org/10.1210/JC.2002-020502

Critchley, H. O. D., Maybin, J. A., Armstrong, G. M., & Williams, A. R. W. (2020). Physiology of the Endometrium and Regulation of Menstruation. *Physiological Reviews*, *100*(3), 1149–1179. https://doi.org/10.1152/PHYSREV.00031.2019

Cullinan, E. B., Abbondanzo, S. J., Anderson, P. S., Pollard, J. W., Lessey, B. A., & Stewart, C. L. (1996). Leukemia inhibitory factor (LIF) and LIF receptor expression in human endometrium suggests a potential autocrine/paracrine function in regulating embryo implantation. *Proceedings of the National Academy of Sciences*, *93*(7), 3115–3120. https://doi.org/10.1073/PNAS.93.7.3115

Dabbs, D. J., Geisinger, K. R., & Norris, H. T. (1986). Intermediate filaments in endometrial and endocervical carcinomas. The diagnostic utility of vimentin patterns. *The American Journal of Surgical Pathology*, *10*(8), 568–576. https://doi.org/10.1097/00000478-198608000-00007

Davis, G. E., & Senger, D. R. (2005). Endothelial extracellular matrix: biosynthesis, remodeling, and functions during vascular morphogenesis and neovessel stabilization. *Circulation Research*, *97*(11), 1093–1107. https://doi.org/10.1161/01.RES.0000191547.64391.E3

de Jolinière, J. B., Ayoubi, J. M., Lesec, G., Validire, P., Goguin, A., Gianaroli, L., Dubuisson, J. B., Feki, A., & Gogusev, J. (2012). Identification of Displaced Endometrial Glands and Embryonic Duct Remnants in Female Fetal Reproductive Tract: Possible Pathogenetic Role in Endometriotic and Pelvic Neoplastic Processes. *Frontiers in Physiology*, *3*. https://doi.org/10.3389/FPHYS.2012.00444

de Miguel–Gómez, L., López-Martínez, S., Campo, H., Francés-Herrero, E., Faus, A., Díaz, A., Pellicer, A., Domínguez, F., & Cervelló, I. (2021). Comparison of different sources of platelet-rich plasma as treatment option for infertility-causing endometrial pathologies. *Fertility and Sterility*, *115*(2), 490–500. https://doi.org/10.1016/j.fertnstert.2020.07.053

de Miguel-Gómez, L., Romeu, M., Pellicer, A., & Cervelló, I. (2021). Strategies for managing Asherman's syndrome and endometrial atrophy: Since the classical experimental models to the new bioengineering approach. *Molecular Reproduction and Development*, *88*(8), 527–543. https://doi.org/10.1002/MRD.23523

Dekker, R. J., Boon, R. A., Rondaij, M. G., Kragt, A., Volger, O. L., Elderkamp, Y. W., Meijers, J. C. M., Voorberg, J., Pannekoek, H., & Horrevoets, A. J. G. (2006). KLF2 provokes a gene expression pattern that establishes functional quiescent differentiation of the endothelium. *Blood*, *107*(11), 4354–4363. https://doi.org/10.1182/BLOOD-2005-08-3465

Díaz, L., Zambrano, E., Flores, M. E., Contreras, M., Crispín, J. C., Alemán, G., Bravo, C., Armenta, A., Valdés, V. J., Tovar, A., Gamba, G., Barrios-Payán, J., & Bobadilla, N. A. (2020). Ethical Considerations in Animal Research: The Principle of 3R's. *Revista de Investigacion Clinica; Organo Del Hospital de Enfermedades de La Nutricion*, *73*(4), 199–209. https://doi.org/10.24875/RIC.20000380

Díaz-Gimeno, P., Horcajadas, J. A., Martínez-Conejero, J. A., Esteban, F. J., Alamá, P., Pellicer, A., & Simón, C. (2011). A genomic diagnostic tool for human endometrial receptivity based on the transcriptomic signature. *Fertility and Sterility*, *95*(1), 50-60.e15. https://doi.org/10.1016/j.fertnstert.2010.04.063

Diniz-da-Costa, M., Kong, C. S., Fishwick, K. J., Rawlings, T., Brighton, P. J., Hawkes, A., Odendaal, J., Quenby, S., Ott, S., Lucas, E. S., Vrljicak, P., & Brosens, J. J. (2021). Characterization of highly proliferative decidual precursor cells during the window of implantation in human endometrium. *Stem Cells (Dayton, Ohio)*, *39*(8), 1067–1080. https://doi.org/10.1002/STEM.3367

Dmowski, W., & Greenblatt, R. (1969). *Asherman's syndrome and risk of placenta accreta* (Vol. 34).

Doll, A., Abal, M., Rigau, M., Monge, M., Gonzalez, M., Demajo, S., Colás, E., Llauradó, M., Alazzouzi, H., Planagumá, J., Lohmann, M. A., Garcia, J., Castellvi, S., Cajal, J. R. y., Gil-Moreno, A., Xercavins, J., Alameda, F., & Reventós, J. (2008). Novel molecular profiles of endometrial cancer-new light through old windows. *The Journal of Steroid Biochemistry and Molecular Biology*, *108*(3–5), 221–229. https://doi.org/10.1016/J.JSBMB.2007.09.020

Dominguez, F., Yáñez-Mó, M., Sanchez-Madrid, F., & Simón, C. (2005). Embryonic implantation and leukocyte transendothelial migration: different processes with similar players? *FASEB Journal : Official Publication of the Federation of American Societies for Experimental Biology*, *19*(9), 1056–1060. https://doi.org/10.1096/FJ.05-3781HYP

IX. References

Dreisler, E., & Kjer, J. J. (2019). Asherman's syndrome: current perspectives on diagnosis and management. *International Journal of Women's Health*, *11*, 191–198. https://doi.org/10.2147/IJWH.S165474

Du, H., Naqvi, H., & Taylor, H. S. (2012). Ischemia/reperfusion injury promotes and granulocyte-colony stimulating factor inhibits migration of bone marrow-derived stem cells to endometrium. *Stem Cells and Development*, *21*(18), 3324–3331. https://doi.org/10.1089/SCD.2011.0193

Ebrahim, N., Mostafa, O., El Dosoky, R. E., Ahmed, I. A., Saad, A. S., Mostafa, A., Sabry, D., Ibrahim, K. A., & Farid, A. S. (2018). Human mesenchymal stem cell-derived extracellular vesicles/estrogen combined therapy safely ameliorates experimentally induced intrauterine adhesions in a female rat model. *Stem Cell Research & Therapy*, *9*(1). https://doi.org/10.1186/S13287-018-0924-Z

Einspanier, A., Lieder, K., Husen, B., Ebert, K., Lier, S., Einspanier, R., Unemori, E., & Kemper, M. (2009). Relaxin Supports Implantation and Early Pregnancy in the Marmoset Monkey. *Annals of the New York Academy of Sciences*, *1160*(1), 140–146. https://doi.org/10.1111/J.1749-6632.2009.03947.X

Evans, G. E., Martínez-Conejero, J. A., Phillipson, G. T. M., Simón, C., McNoe, L. A., Sykes, P. H., Horcajadas, J. A., Lam, E. Y. N., Print, C. G., Sin, I. L., & Evans, J. J. (2012). Gene and protein expression signature of endometrial glandular and stromal compartments during the window of implantation. *Fertility and Sterility*, *97*(6). https://doi.org/10.1016/J.FERTNSTERT.2012.03.007

Evans, J., & Salamonsen, L. A. (2014). Decidualized human endometrial stromal cells are sensors of hormone withdrawal in the menstrual inflammatory cascade. *Biology of Reproduction*, *90*(1). https://doi.org/10.1095/BIOLREPROD.113.108175

Fatehullah, A., Tan, S. H., & Barker, N. (2016). Organoids as an in vitro model of human development and disease. *Nature Cell Biology*, *18*(3), 246–254. https://doi.org/10.1038/NCB3312

Fitzgerald, H. C., Dhakal, P., Behura, S. K., Schust, D. J., & Spencer, T. E. (2019). Self-renewing endometrial epithelial organoids of the human uterus. *Proceedings of the National Academy of Sciences of the United States of America*, *116*(46), 23132–23142. https://doi.org/10.1073/PNAS.1915389116

Fleming, S. J., Chaffin, M. D., Arduini, A., Akkad, A.-D., Banks, E., Marioni, J. C., Philippakis, A. A., Ellinor, P. T., & Babadi, M. (2022). Unsupervised removal of systematic background noise from droplet-based single-cell experiments using CellBender. *BioRxiv*, 791699. https://doi.org/10.1101/791699

Fonseca, M. A. S., Haro, M., Wright, K. N., Lin, X., Abbasi, F., Sun, J., Hernandez, L., Orr, N. L., Hong, J., Choi-Kuaea, Y., Maluf, H. M., Balzer, B. L., Fishburn, A., Hickey, R., Cass, I., Goodridge, H. S., Truong, M., Wang, Y., Pisarska, M. D., … Lawrenson, K. (2023). Single-cell transcriptomic analysis of endometriosis. *Nature Genetics*, *55*(2), 255–267. https://doi.org/10.1038/S41588-022-01254-1

Fritsch, H. (1894). Ein Fall von volligen schwund der Gebaumutterhohle nach Auskratzung. *Zentralbl Gynaekol*, *18*, 1337–1342.

Fu, X., Liu, G., Halim, A., Ju, Y., Luo, Q., & Song, G. (2019). Mesenchymal Stem Cell Migration and Tissue Repair. *Cells 2019, Vol. 8, Page 784*, *8*(8), 784. https://doi.org/10.3390/CELLS8080784

Gajjar, K., Martin-Hirsch, P. L., & Martin, F. L. (2012). CYP1B1 and hormone-induced cancer. *Cancer Letters*, *324*(1), 13–30. https://doi.org/10.1016/J.CANLET.2012.04.021

Gan, L., Duan, H., Xu, Q., Tang, Y. Q., Li, J. J., Sun, F. Q., & Wang, S. (2017). Human amniotic mesenchymal stromal cell transplantation improves endometrial regeneration in rodent models of intrauterine adhesions. *Cytotherapy*, *19*(5), 603–616. https://doi.org/10.1016/J.JCYT.2017.02.003

Gao, Y., Wu, G., Xu, Y., Zhao, D., & Zheng, L. (2021). Stem Cell-Based Therapy for Asherman Syndrome: Promises and Challenges. *Cell Transplantation*, *30*. https://doi.org/10.1177/09636897211020734

Garcia-Alonso, L., Handfield, L. F., Roberts, K., Nikolakopoulou, K., Fernando, R. C., Gardner, L., Woodhams, B., Arutyunyan, A., Polanski, K., Hoo, R., Sancho-Serra, C., Li, T., Kwakwa, K., Tuck, E., Lorenzi, V., Massalha, H., Prete, M., Kleshchevnikov, V., Tarkowska, A., … Vento-Tormo, R. (2021). Mapping the temporal and spatial dynamics of the human endometrium in vivo and in vitro. *Nature Genetics*, *53*(12), 1698–1711. https://doi.org/10.1038/S41588-021-00972-2

Gargett, C. E. (2007). Uterine stem cells: what is the evidence? *Human Reproduction Update*, *13*(1), 87–101. https://doi.org/10.1093/HUMUPD/DML045

Gargett, C. E., & Masuda, H. (2010). Adult stem cells in the endometrium. *Molecular Human Reproduction*, *16*(11), 818–834. https://doi.org/10.1093/MOLEHR/GAQ061

Garrido-Gómez, T., Ruiz-Alonso, M., Blesa, D., Diaz-Gimeno, P., Vilella, F., & Simón, C. (2013). Profiling the gene signature of endometrial receptivity: clinical results. *Fertility and Sterility*, *99*(4), 1078–1085. https://doi.org/10.1016/J.FERTNSTERT.2012.12.005

Ge, J., Chen, Y., Yang, H., Zhao, J., Ren, D., & Wu, X. (2021). Expression and significance of estrogen receptor and progesterone receptor in endometrial tissue of patients with intrauterine adhesions. *Gland Surgery*, *10*(4), 1478–1486. https://doi.org/10.21037/GS-21-232

Gellersen, B., Brosens, I. A., & Brosens, J. J. (2007). Decidualization of the human endometrium: mechanisms, functions, and clinical perspectives. *Seminars in Reproductive Medicine*, *25*(6), 445–453. https://doi.org/10.1055/S-2007-991042

Gellersen, B., & Brosens, J. J. (2014). Cyclic decidualization of the human endometrium in reproductive health and failure. In *Endocrine Reviews* (Vol. 35, Issue 6, pp. 851–905). Endocrine Society. https://doi.org/10.1210/er.2014-1045

Gharibeh, N., Aghebati-Maleki, L., Madani, J., Pourakbari, R., Yousefi, M., & Ahmadian Heris, J. (2022). Cell-based therapy in thin endometrium and Asherman syndrome. *Stem Cell Research & Therapy*, *13*(1). https://doi.org/10.1186/S13287-021-02698-8

Giudice, L. C. (2006). Application of functional genomics to primate endometrium: insights into biological processes. *Reproductive Biology and Endocrinology : RB&E*, *4 Suppl 1*(Suppl 1). https://doi.org/10.1186/1477-7827-4-S1-S4

Gonzalez, G., Mehra, S., Wang, Y., Akiyama, H., & Behringer, R. R. (2016). Sox9 overexpression in uterine epithelia induces endometrial gland hyperplasia. *Differentiation; Research in Biological Diversity*, *92*(4), 204–215. https://doi.org/10.1016/J.DIFF.2016.05.006

Grund, S., & Grümmer, R. (2018). Direct Cell–Cell Interactions in the Endometrium and in Endometrial Pathophysiology. *International Journal of Molecular Sciences*, *19*(8). https://doi.org/10.3390/IJMS19082227

Gu, Z. Y., Jia, S. Z., Liu, S., & Leng, J. H. (2020). Endometrial Organoids: A New Model for the Research of Endometrial-Related Diseases. *Biology of Reproduction*, *103*(5), 918. https://doi.org/10.1093/BIOLRE/IOAA124

Guo, E. J., Chung, J. P. W., Poon, L. C. Y., & Li, T. C. (2019). Reproductive outcomes after surgical treatment of asherman syndrome: A systematic review. *Best Practice & Research. Clinical Obstetrics & Gynaecology*, *59*, 98–114. https://doi.org/10.1016/J.BPOBGYN.2018.12.009

Gurung, S., Ulrich, D., Sturm, M., Rosamilia, A., Werkmeister, J. A., & Gargett, C. E. (2020). Comparing the Effect of TGF-β Receptor Inhibition on Human Perivascular Mesenchymal Stromal Cells Derived from Endometrium, Bone Marrow and Adipose Tissues. *Journal of Personalized Medicine*, *10*(4), 1–19. https://doi.org/10.3390/JPM10040261

Habiba, M., Heyn, R., Bianchi, P., Brosens, I., & Benagiano, G. (2021). The development of the human uterus: Morphogenesis to menarche. In *Human Reproduction Update* (Vol. 27, Issue 1, pp. 1–26). Oxford University Press. https://doi.org/10.1093/humupd/dmaa036

Haider, S., Gamperl, M., Burkard, T. R., Kunihs, V., Kaindl, U., Junttila, S., Fiala, C., Schmidt, K., Mendjan, S., Knöfler, M., & Latos, P. A. (2019). Estrogen Signaling Drives Ciliogenesis in Human Endometrial Organoids. *Endocrinology*, *160*(10), 2282–2297. https://doi.org/10.1210/EN.2019-00314

Hao, Y., Hao, S., Andersen-Nissen, E., Mauck, W. M., Zheng, S., Butler, A., Lee, M. J., Wilk, A. J., Darby, C., Zager, M., Hoffman, P., Stoeckius, M., Papalexi, E., Mimitou, E. P., Jain, J., Srivastava, A., Stuart, T., Fleming, L. M., Yeung, B., … Satija, R. (2021). Integrated analysis of multimodal single-cell data. *Cell*, *184*(13), 3573. https://doi.org/10.1016/J.CELL.2021.04.048

Henriet, P., Gaide Chevronnay, H. P., & Marbaix, E. (2012). The endocrine and paracrine control of menstruation. *Molecular and Cellular Endocrinology*, *358*(2), 197–207. https://doi.org/10.1016/J.MCE.2011.07.042

Herrlich, P., Ponta, H., Stein, B., Gebel, S., König, H., Schönthal, A., Büscher, M., & Rahmsdorf, H. J. (1990). The Role of FOS in Gene Regulation. *Activation of Hormone and Growth Factor Receptors*, 77–91. https://doi.org/10.1007/978-94-009-1936-5_9

Hiby, S. E., King, A., Sharkey, A. M., & Loke, Y. W. (1997). Human uterine NK cells have a similar repertoire of killer inhibitory and activatory receptors to those found in blood, as demonstrated by RT-PCR and sequencing. *Molecular Immunology*, *34*(5), 419–430. https://doi.org/10.1016/S0161-5890(97)00032-1

Hong, I. S. (2023). Endometrial stem/progenitor cells: Properties, origins, and functions. *Genes & Diseases*, *10*(3), 931–947. https://doi.org/10.1016/J.GENDIS.2022.08.009

Horcajadas, J. A., Pellicer, A., & Simón, C. (2007). Wide genomic analysis of human endometrial receptivity: new times, new opportunities. *Human Reproduction Update*, *13*(1), 77–86. https://doi.org/10.1093/HUMUPD/DML046

Hu, C. T., Chang, T. Y., Cheng, C. C., Liu, C. S., Wu, J. R., Li, M. C., & Wu, W. S. (2010). Snail associates with EGR-1 and SP-1 to upregulate transcriptional activation of p15INK4b. *The FEBS Journal*, *277*(5), 1202–1218. https://doi.org/10.1111/J.1742-4658.2009.07553.X

Hu, S., Yao, G., Wang, Y., Xu, H., Ji, X., He, Y., Zhu, Q., Chen, Z., & Sun, Y. (2014). Transcriptomic changes during the pre-receptive to receptive transition in human endometrium detected by RNA-Seq. *The Journal of Clinical Endocrinology and Metabolism*, *99*(12), E2744–E2753. https://doi.org/10.1210/JC.2014-2155

Hu, W. P., Sun, K. T., & Zháo, Y. (2006). Endometriosis-Specific Genes Identified by Real-Time Reverse Transcription-Polymerase Chain Reaction Expression Profiling of Endometriosis Versus Autologous Uterine Endometrium. *The Journal of Clinical Endocrinology & Metabolism*, *91*(1), 228–238. https://doi.org/10.1210/JC.2004-1594

Huang, X., Wu, L., Pei, T., Liu, D., Liu, C., Luo, B., Xiao, L., Li, Y., Wang, R., Ouyang, Y., Zhu, H., & Huang, W. (2023). Single-cell transcriptome analysis reveals endometrial immune microenvironment in minimal/mild endometriosis. *Clinical and Experimental Immunology*, *212*(3), 285–295. https://doi.org/10.1093/CEI/UXAD029

Huynh, M.-L. N., Fadok, V. A., & Henson, P. M. (2002). Phosphatidylserine-dependent ingestion of apoptotic cells promotes TGF-beta1 secretion and the resolution of inflammation. *The Journal of Clinical Investigation*, *109*(1), 41–50. https://doi.org/10.1172/JCI11638

Ikoma, T., Kyo, S., Maida, Y., Ozaki, S., Takakura, M., Nakao, S., & Inoue, M. (2009). Bone marrow-derived cells from male donors can compose endometrial glands in female transplant recipients. *American Journal of Obstetrics and Gynecology*, *201*(6), 608.e1-608.e8. https://doi.org/10.1016/J.AJOG.2009.07.026

Irungu, S., Mavrelos, D., Worthington, J., Blyuss, O., Saridogan, E., & Timms, J. F. (2019). Discovery of non-invasive biomarkers for the diagnosis of endometriosis. *Clinical Proteomics*, *16*(1), 14. https://doi.org/10.1186/S12014-019-9235-3

Irwin, J. C., Kirk, D., King, R. J. B., Quigley, M. M., & Gwatkin, R. B. L. (1989). Hormonal regulation of human endometrial stromal cells in culture: an in vitro model for decidualization. *Fertility and Sterility*, *52*(5), 761–768. https://doi.org/10.1016/S0015-0282(16)61028-2

Jang, H. Y., Myoung, S. M., Choe, J. M., Kim, T., Cheon, Y. P., Kim, Y. M., & Park, H. (2017). Effects of Autologous Platelet-Rich Plasma on Regeneration of Damaged Endometrium in Female Rats. *Yonsei Medical Journal*, *58*(6), 1195–1203. https://doi.org/10.3349/YMJ.2017.58.6.1195

Jin, S., Guerrero-Juarez, C. F., Zhang, L., Chang, I., Ramos, R., Kuan, C. H., Myung, P., Plikus, M. V., & Nie, Q. (2021). Inference and analysis of cell-cell communication using CellChat. *Nature Communications*, *12*(1). https://doi.org/10.1038/S41467-021-21246-9

Jones, R. L., Kelly, R. W., & Critchley, H. O. D. (1997). Chemokine and cyclooxygenase-2 expression in human endometrium coincides with leukocyte accumulation. *Human Reproduction (Oxford, England)*, *12*(6), 1300–1306. https://doi.org/10.1093/HUMREP/12.6.1300

Joshi, S. G. (1987). Progestin-dependent human endometrial protein: a marker for monitoring human endometrial function. *Advances in Experimental Medicine and Biology*, *230*, 167–186. https://doi.org/10.1007/978-1-4684-1297-0_10

Kaczynski, J. B., & Rzepka, J. K. (2022). Endometrial regeneration in Asherman's syndrome and endometrial atrophy using Wharton's jelly-derived mesenchymal stem cells. *Ginekologia Polska*, *93*(11), 904–909. https://doi.org/10.5603/GP.A2022.0091

Kadaja, M., Keyes, B. E., Lin, M., Amalia Pasolli, H., Genander, M., Polak, L., Stokes, N., Zheng, D., & Fuchs, E. (2014). SOX9: a stem cell transcriptional regulator of secreted niche signaling factors. *Genes & Development*, *28*(4), 328–341. https://doi.org/10.1101/GAD.233247.113

Kagawa, H., Javali, A., Khoei, H. H., Sommer, T. M., Sestini, G., Novatchkova, M., Scholte op Reimer, Y., Castel, G., Bruneau, A., Maenhoudt, N., Lammers, J., Loubersac, S., Freour, T., Vankelecom, H., David, L., & Rivron, N. (2022). Human blastoids model blastocyst development and implantation. *Nature*, *601*(7894), 600. https://doi.org/10.1038/S41586-021-04267-8

Kao, L. C., Tulac, S., Lobo, S., Imani, B., Yang, J. P., Germeyer, A., Osteen, K., Taylor, R. N., Lessey, B. A., & Giudice, L. C. (2002). Global gene profiling in human endometrium during the window of implantation. *Endocrinology*, *143*(6), 2119–2138. https://doi.org/10.1210/ENDO.143.6.8885

Kastner, P., Krust, A., Turcotte, B., Stropp, U., Tora, L., Gronemeyer, H., & Chambon, P. (1990). Two distinct estrogen-regulated promoters generate transcripts encoding the two functionally different human progesterone receptor forms A and B. *The EMBO Journal*, *9*(5), 1603–1614. https://doi.org/10.1002/J.1460-2075.1990.TB08280.X

Katcher, A., Yueh, B., Ozler, K., Nizam, A., Kredentser, A., Chung, C., Frimer, M., Goldberg, G. L., & Beyaz, S. (2023). Establishing patient-derived organoids from human endometrial cancer and normal endometrium. *Frontiers in Endocrinology*, *14*. https://doi.org/10.3389/FENDO.2023.1059228

Kelly, R. W., King, A. E., & Crithley, H. O. D. (2001). Cytokine control in human endometrium. *Reproduction (Cambridge, England)*, *121*(1), 3–19. https://doi.org/10.1530/REP.0.1210003

Kim, J., Koo, B. K., & Knoblich, J. A. (2020). Human organoids: model systems for human biology and medicine. *Nature Reviews. Molecular Cell Biology*, *21*(10), 571–584. https://doi.org/10.1038/S41580-020-0259-3

Kim, M. R., Park, D. W., Lee, J. H., Choi, D. S., Hwang, K. J., Ryu, H. S., & Min, C. K. (2005). Progesterone-dependent release of transforming growth factor-beta1 from epithelial cells enhances the endometrial decidualization by turning on the Smad signalling in stromal cells. *Molecular Human Reproduction*, *11*(11), 801–808. https://doi.org/10.1093/MOLEHR/GAH240

Kimura, R., Otani, T., Shiraishi, N., Hagiyama, M., Yoneshige, A., Wada, A., Kajiyama, H., Takeuchi, F., Mizuguchi, N., Morishita, K., & Ito, A. (2021). Expression of cell adhesion molecule 1 in human and murine endometrial glandular cells and its increase during the proliferative phase by estrogen and cell density. *Life Sciences*, *283*. https://doi.org/10.1016/J.LFS.2021.119854

King, A. E., Critchley, H. O. D., & Kelly, R. W. (2001). The NF-kappaB pathway in human endometrium and first trimester decidua. *Molecular Human Reproduction*, *7*(2), 175–183. https://doi.org/10.1093/MOLEHR/7.2.175

Kirkwood, P. M., Gibson, D. A., Shaw, I., Dobie, R., Kelepouri, O., Henderson, N. C., & Saunders, P. T. K. (2022). Single-cell RNA sequencing and lineage tracing confirm mesenchyme to epithelial transformation (MET) contributes to repair of the endometrium at menstruation. *ELife*, *11*. https://doi.org/10.7554/ELIFE.77663

Koel, M., Krjutškov, K., Saare, M., Samuel, K., Lubenets, D., Katayama, S., Einarsdottir, E., Vargas, E., Sola-Leyva, A., Lalitkumar, P. G., Gemzell-Danielsson, K., Blesa, D., Simon, C., Lanner, F., Kere, J., Salumets, A., & Altmäe, S. (2022). Human endometrial cell-type-specific RNA sequencing provides new insights into the embryo-endometrium interplay. *Human Reproduction Open*, *2022*(4). https://doi.org/10.1093/HROPEN/HOAC043

Koot, Y. E. M., Teklenburg, G., Salker, M. S., Brosens, J. J., & Macklon, N. S. (2012). Molecular aspects of implantation failure. *Biochimica et Biophysica Acta*, *1822*(12), 1943–1950. https://doi.org/10.1016/J.BBADIS.2012.05.017

Korsunsky, I., Millard, N., Fan, J., Slowikowski, K., Zhang, F., Wei, K., Baglaenko, Y., Brenner, M., Loh, P. ru, & Raychaudhuri, S. (2019). Fast, sensitive and accurate integration of single-cell data with Harmony. *Nature Methods 2019 16:12*, *16*(12), 1289–1296. https://doi.org/10.1038/s41592-019-0619-0

Kovats, S. (2015). Estrogen receptors regulate innate immune cells and signaling pathways. *Cellular Immunology*, *294*(2), 63–69. https://doi.org/10.1016/J.CELLIMM.2015.01.018

Krishnan, N. R., & Kasthuri, A. S. (2005). Iatrogenic Disorders. *Medical Journal, Armed Forces India*, *61*(1), 2. https://doi.org/10.1016/S0377-1237(05)80107-8

Krjutškov, K., Katayama, S., Saare, M., Vera-Rodriguez, M., Lubenets, D., Samuel, K., Laisk-Podar, T., Teder, H., Einarsdottir, E., Salumets, A., & Kere, J. (2016). Single-cell transcriptome analysis of endometrial tissue. *Human Reproduction (Oxford, England)*, *31*(4), 844–853. https://doi.org/10.1093/HUMREP/DEW008

Kuhn, M. (2008). Building Predictive Models in R Using the caret Package. *Journal of Statistical Software*, *28*(5), 1–26. https://doi.org/10.18637/JSS.V028.I05

Kulkarni, P., Dunker, A. K., Weninger, K., & Orban, J. (2016). Prostate-associated gene 4 (PAGE4), an intrinsically disordered cancer/testis antigen, is a novel therapeutic target for prostate cancer. *Asian Journal of Andrology*, *18*(5), 695. https://doi.org/10.4103/1008-682X.181818

Kumar, S., Kim, K., Yang, G.-M., Choi, H. Y., & Cho, S.-G. (2018). Cytokeratin 19 (KRT19) has a Role in the Reprogramming of Cancer Stem Cell-Like Cells to Less Aggressive and More Drug-Sensitive Cells. *Int J Mol Sci*, *19*(5), 1423.

La Manno, G., Gyllborg, D., Codeluppi, S., Nishimura, K., Salto, C., Zeisel, A., Borm, L. E., Stott, S. R. W., Toledo, E. M., Villaescusa, J. C., Lönnerberg, P., Ryge, J., Barker, R. A., Arenas, E., & Linnarsson, S. (2016). Molecular Diversity of Midbrain Development in Mouse, Human, and Stem Cells. *Cell*, *167*(2), 566-580.e19. https://doi.org/10.1016/J.CELL.2016.09.027

Lai, Z. Z., Wang, Y., Zhou, W. J., Liang, Z., Shi, J. W., Yang, H. L., Xie, F., Chen, W. D., Zhu, R., Zhang, C., Mei, J., Zhao, J. Y., Ye, J. F., Zhang, T., & Li, M. Q. (2022). Single-cell transcriptome profiling of the human endometrium of patients with recurrent implantation failure. *Theranostics*, *12*(15), 6527–6547. https://doi.org/10.7150/THNO.74053

Lala, P. K., & Nandi, P. (2016). Mechanisms of trophoblast migration, endometrial angiogenesis in preeclampsia: The role of decorin. *Cell Adhesion & Migration*, *10*(1–2), 111–125. https://doi.org/10.1080/19336918.2015.1106669

Lange, M., Bergen, V., Klein, M., Setty, M., Reuter, B., Bakhti, M., Lickert, H., Ansari, M., Schniering, J., Schiller, H. B., Pe'er, D., & Theis, F. J. (2022). CellRank for directed single-cell fate mapping. *Nature Methods*, *19*(2), 159–170. https://doi.org/10.1038/S41592-021-01346-6

Lee, S. K., Kim, C. J., Kim, D.-J., & Kang, J. (2015). Immune Cells in the Female Reproductive Tract. *Immune Network*, *15*(1), 16. https://doi.org/10.4110/IN.2015.15.1.16

Lekovich, J., Stewart, J., Anderson, S., Niemasik, E., Pereira, N., & Chasen, S. (2017). Placental malperfusion as a possible mechanism of preterm birth in patients with Müllerian anomalies. *Journal of Perinatal Medicine*, *45*(1), 45–49. https://doi.org/10.1515/JPM-2016-0075

IX. References

Lessey, B. A., Killam, A. P., Metzger, D. A., Haney, A. F., Greene, G. L., & McCarty, K. S. (1988). Immunohistochemical analysis of human uterine estrogen and progesterone receptors throughout the menstrual cycle. *The Journal of Clinical Endocrinology and Metabolism*, *67*(2), 334–340. https://doi.org/10.1210/JCEM-67-2-334

Lessey, B. A., & Young, S. L. (2014). Homeostasis imbalance in the endometrium of women with implantation defects: the role of estrogen and progesterone. *Seminars in Reproductive Medicine*, *32*(5), 365–375. https://doi.org/10.1055/S-0034-1376355

Li, J., Huang, F. M., Ma, Q. L., Guo, W., Feng, K. Y., Huang, T., & Cai, Y. D. (2023). Identification of genes related to immune enhancement caused by heterologous ChAdOx1–BNT162b2 vaccines in lymphocytes at single-cell resolution with machine learning methods. *Frontiers in Immunology*, *14*, 1131051. https://doi.org/10.3389/FIMMU.2023.1131051/BIBTEX

Li, Q., Kannan, A., Wang, W., DeMayo, F. J., Taylor, R. N., Bagchi, M. K., & Bagchi, I. C. (2007). Bone morphogenetic protein 2 functions via a conserved signaling pathway involving Wnt4 to regulate uterine decidualization in the mouse and the human. *Journal of Biological Chemistry*, *282*(43), 31725–31732. https://doi.org/10.1074/jbc.M704723200

Li, X., Kodithuwakku, S. P., Chan, R. W. S., Yeung, W. S. B., Yao, Y., Ng, E. H. Y., Chiu, P. C. N., & Lee, C. L. (2022). Three-dimensional culture models of human endometrium for studying trophoblast-endometrium interaction during implantation. *Reproductive Biology and Endocrinology : RB&E*, *20*(1). https://doi.org/10.1186/S12958-022-00973-8

Li, X., Sun, H., Lin, N., Hou, X., Wang, J., Zhou, B., Xu, P., Xiao, Z., Chen, B., Dai, J., & Hu, Y. (2011). Regeneration of uterine horns in rats by collagen scaffolds loaded with collagen-binding human basic fibroblast growth factor. *Biomaterials*, *32*(32), 8172–8181. https://doi.org/10.1016/J.BIOMATERIALS.2011.07.050

Li, X., & Wang, C. Y. (2021). From bulk, single-cell to spatial RNA sequencing. *International Journal of Oral Science 2021 13:1*, *13*(1), 1–6. https://doi.org/10.1038/s41368-021-00146-0

Li, Y., de Haar, C., Peppelenbosch, M. P., & van der Woude, C. J. (2012). SOCS3 in immune regulation of inflammatory bowel disease and inflammatory bowel disease-related cancer. *Cytokine & Growth Factor Reviews*, *23*(3), 127–138. https://doi.org/10.1016/J.CYTOGFR.2012.04.005

Lien, H. E., Berg, H. F., Halle, M. K., Trovik, J., Haldorsen, I. S., Akslen, L. A., & Krakstad, C. (2023). Single-cell profiling of low-stage endometrial cancers identifies low epithelial vimentin expression as a marker of recurrent disease. *EBioMedicine*, *92*. https://doi.org/10.1016/J.EBIOM.2023.104595

Lin, Y., Li, Y., Chen, P., Zhang, Y., Sun, J., Sun, X., Li, J., Jin, J., Xue, J., Zheng, J., Jiang, X. C., Chen, C., Li, X., Wu, Y., Zhao, W., Liu, J., Ye, X., Zhang, R., Gao, J., & Zhang, D. (2023). Exosome-Based Regimen Rescues Endometrial Fibrosis in Intrauterine Adhesions Via Targeting Clinical Fibrosis Biomarkers. *Stem Cells Translational Medicine*, *12*(3), 154–168. https://doi.org/10.1093/STCLTM/SZAD007

Ling, L., Nurcombe, V., & Cool, S. M. (2009). Wnt signaling controls the fate of mesenchymal stem cells. *Gene*, *433*(1–2), 1–7. https://doi.org/10.1016/J.GENE.2008.12.008

Liu, Z., Sun, Z., Liu, H., Niu, W., Wang, X., Liang, N., Wang, X., Wang, Y., Shi, Y., Xu, L., & Shi, W. (2021). Single-cell transcriptomic analysis of eutopic endometrium and ectopic lesions of adenomyosis. *Cell & Bioscience*, *11*(1). https://doi.org/10.1186/S13578-021-00562-Z

Llen, A., Ilcox, J. W., Onna, D., Ay, D., Aird, B., Larice, C., & Einberg, R. W. (1999). Time of Implantation of the Conceptus and Loss of Pregnancy. *Https://Doi.Org/10.1056/NEJM199906103402304*, *340*(23), 1796–1799. https://doi.org/10.1056/NEJM199906103402304

Loke, Y. W., Gardner, L., Burland, K., & King, A. (1989). Laminin in human trophoblast—decidua interaction. *Human Reproduction*, *4*(4), 457–463. https://doi.org/10.1093/OXFORDJOURNALS.HUMREP.A136926

Lou, Y., Han, M., Liu, H., Niu, Y., Liang, Y., Guo, J., Zhang, W., & Wang, H. (2019). Essential roles of S100A10 in Toll-like receptor signaling and immunity to infection. *Cellular & Molecular Immunology 2019 17:10*, *17*(10), 1053–1062. https://doi.org/10.1038/s41423-019-0278-1

Luan, H. H., Wang, A., Hilliard, B. K., Carvalho, F., Rosen, C. E., Ahasic, A. M., Herzog, E. L., Kang, I., Pisani, M. A., Yu, S., Zhang, C., Ring, A. M., Young, L. H., & Medzhitov, R. (2019). GDF15 Is an Inflammation-Induced Central Mediator of Tissue Tolerance. *Cell*, *178*(5), 1231-1244.e11. https://doi.org/10.1016/J.CELL.2019.07.033

Lucas, E. S., Vrljicak, P., Muter, J., Diniz-da-Costa, M. M., Brighton, P. J., Kong, C. S., Lipecki, J., Fishwick, K. J., Odendaal, J., Ewington, L. J., Quenby, S., Ott, S., & Brosens, J. J. (2020). Recurrent pregnancy loss is associated with a pro-senescent decidual response during the peri-implantation window. *Communications Biology*, *3*(1). https://doi.org/10.1038/S42003-020-0763-1

Luo, F., Liu, F., Guo, Y., Xu, W., Li, Y., Yi, J., Fournier, T., Degrelle, S., Zitouni, H., Hernandez, I., Liu, X., Huang, Y., & Yue, J. (2023). Single-cell profiling reveals immune disturbances landscape and HLA-F-mediated immune tolerance at the maternal-fetal interface in preeclampsia. *Frontiers in Immunology*, *14*. https://doi.org/10.3389/FIMMU.2023.1234577

Lv, H., Sun, H., Wang, L., Yao, S., Liu, D., Zhang, X., Pei, Z., Zhou, J., Wang, H., Dai, J., Yan, G., Ding, L., Wang, Z., Cao, C., Zhao, G., & Hu, Y. (2023). Targeting CD301 + macrophages inhibits endometrial fibrosis and improves pregnancy outcome. *EMBO Molecular Medicine*, *15*(9). https://doi.org/10.15252/EMMM.202317601

Lv, H., Zhao, G., Jiang, P., Wang, H., Wang, Z., Yao, S., Zhou, Z., Wang, L., Liu, D., Deng, W., Dai, J., & Hu, Y. (2022). Deciphering the endometrial niche of human thin endometrium at single-cell resolution. *Proceedings of the National Academy of Sciences of the United States of America*, *119*(8). https://doi.org/10.1073/PNAS.2115912119

Ma, J., Zhang, L., Zhan, H., Mo, Y., Ren, Z., Shao, A., & Lin, J. (2021). Single-cell transcriptomic analysis of endometriosis provides insights into fibroblast fates and immune cell heterogeneity. *Cell & Bioscience*, *11*(1). https://doi.org/10.1186/S13578-021-00637-X

Macdonald, L. J., Sales, K. J., Grant, V., Brown, P., Jabbour, H. N., & Catalano, R. D. (2011). Prokineticin 1 induces Dickkopf 1 expression and regulates cell proliferation and decidualization in the human endometrium. *Molecular Human Reproduction*, *17*(10), 626–636. https://doi.org/10.1093/MOLEHR/GAR031

Maenhoudt, N., De Moor, A., & Vankelecom, H. (2022). Modeling Endometrium Biology and Disease. *Journal of Personalized Medicine 2022, Vol. 12, Page 1048*, *12*(7), 1048. https://doi.org/10.3390/JPM12071048

Makieva, S., Giacomini, E., Ottolina, J., Sanchez, A. M., Papaleo, E., & Viganò, P. (2018). Inside the Endometrial Cell Signaling Subway: Mind the Gap(s). *International Journal of Molecular Sciences*, *19*(9). https://doi.org/10.3390/IJMS19092477

Malone, J. H., & Oliver, B. (2011). Microarrays, deep sequencing and the true measure of the transcriptome. *BMC Biology*, *9*. https://doi.org/10.1186/1741-7007-9-34

Manchanda, R., Rathore, A., Carugno, J., Della Corte, L., Tesarik, J., Török, P., Vilos, G. A., & Vitale, S. G. (2021). Classification systems of Asherman's syndrome. An old problem with new directions. *Minimally Invasive Therapy & Allied Technologies : MITAT : Official Journal of the Society for Minimally Invasive Therapy*, *30*(5), 304–310. https://doi.org/10.1080/13645706.2021.1893190

Mára, M., Borčinová, M., Lisá, Z., Boudová, B., Richtárová, A., & Kuzel, D. (2023). The perinatal outcomes of women treated for Asherman syndrome: a propensity score-matched cohort study. *Human Reproduction (Oxford, England)*, *38*(7), 1297–1304. https://doi.org/10.1093/HUMREP/DEAD092

March, C. M. (2011). Management of Asherman's syndrome. *Reproductive Biomedicine Online*, *23*(1), 63–76. https://doi.org/10.1016/J.RBMO.2010.11.018

March, C. M., Israel, R., & March, A. D. (1978). Hysteroscopic management of intrauterine adhesions. *American Journal of Obstetrics and Gynecology*, *130*(6), 653–657. https://doi.org/10.1016/0002-9378(78)90322-8

Masuda, H., Anwar, S. S., Bühring, H. J., Rao, J. R., & Gargett, C. E. (2012). A novel marker of human endometrial mesenchymal stem-like cells. *Cell Transplantation*, *21*(10), 2201–2214. https://doi.org/10.3727/096368911X637362

Masuda, H., Kalka, C., Takahashi, T., Yoshida, M., Wada, M., Kobori, M., Itoh, R., Iwaguro, H., Eguchi, M., Iwami, Y., Tanaka, R., Nakagawa, Y., Sugimoto, A., Ninomiya, S., Hayashi, S., Kato, S., & Asahara, T. (2007). Estrogen-mediated endothelial progenitor cell biology and kinetics for physiological postnatal vasculogenesis. *Circulation Research*, *101*(6), 598–606. https://doi.org/10.1161/CIRCRESAHA.106.144006

Matsuzaki, S. (2011). DNA microarray analysis in endometriosis for development of more effective targeted therapies. *Frontiers in Bioscience (Elite Edition)*, *3*(3), 1139–1153. https://doi.org/10.2741/E317

McKay, D. B., Vazquez, M. A., Redline, R. W., Lu, C. Y., Schmalzried, S. R., & Shea, C. M. (1992). Macrophage functions are regulated by murine decidual and tumor extracellular matrices. *The Journal of Clinical Investigation*, *89*(1), 134–142. https://doi.org/10.1172/JCI115553

Messinis, I. E., Messini, C. I., & Dafopoulos, K. (2014). Novel aspects of the endocrinology of the menstrual cycle. *Reproductive BioMedicine Online*, *28*(6), 714–722. https://doi.org/10.1016/j.rbmo.2014.02.003

Mihm, M., Gangooly, S., & Muttukrishna, S. (2011). The normal menstrual cycle in women. *Animal Reproduction Science*, *124*(3–4), 229–236. https://doi.org/10.1016/J.ANIREPROSCI.2010.08.030

Milingos, D. S., Philippou, A., Armakolas, A., Papageorgiou, E., Sourla, A., Protopapas, A., Liapi, A., Antsaklis, A., Mastrominas, M., & Koutsilieris, M. (2011). Insulinlike growth factor-1Ec (MGF) expression in eutopic and ectopic endometrium: characterization of the MGF E-peptide actions in vitro. *Molecular Medicine (Cambridge, Mass.)*, *17*(1–2), 21–28. https://doi.org/10.2119/MOLMED.2010.00043

Milne, S. A., Critchley, H. O. D., Drudy, T. A., Kelly, R. W., & Baird, D. T. (1999). Perivascular interleukin-8 messenger ribonucleic acid expression in human endometrium varies across the menstrual cycle and in early pregnancy decidua. *The Journal of Clinical Endocrinology and Metabolism*, *84*(7), 2563–2567. https://doi.org/10.1210/JCEM.84.7.5833

Mints, M., Jansson, M., Sadeghi, B., Westgren, M., Uzunel, M., Hassan, M., & Palmblad, J. (2008). Endometrial endothelial cells are derived from donor stem cells in a bone marrow transplant recipient. *Human Reproduction (Oxford, England)*, *23*(1), 139–143. https://doi.org/10.1093/HUMREP/DEM342

Mirkin, S., Arslan, M., Churikov, D., Corica, A., Diaz, J. I., Williams, S., Bocca, S., & Oehninger, S. (2005). In search of candidate genes critically expressed in the human endometrium during the window of implantation. *Human Reproduction (Oxford, England)*, *20*(8), 2104–2117. https://doi.org/10.1093/HUMREP/DEI051

Mohsen, R. O. M., Halawa, A. M., & Hassan, R. (2019). Role of bone marrow-derived stem cells versus insulin on filiform and fungiform papillae of diabetic albino rats (light, fluorescent and scanning electron microscopic study). *Acta Histochemica*, *121*(7), 812–822. https://doi.org/10.1016/J.ACTHIS.2019.07.007

Mongkolpathumrat, P., Pikwong, F., Phutiyothin, C., Srisopar, O., Chouyratchakarn, W., Unnajak, S., Nernpermpisooth, N., & Kumphune, S. (2024). The secretory leukocyte protease inhibitor (SLPI) in pathophysiology of non-communicable diseases: Evidence from experimental studies to clinical applications. *Heliyon*, *10*(2). https://doi.org/10.1016/J.HELIYON.2024.E24550

Moreno, I., Capalbo, A., Mas, A., Garrido-Gomez, T., Roson, B., Poli, M., Dimitriadis, E., Santamaria, X., Vilella, F., & Simon, C. (2023). The human periconceptional maternal-embryonic space in health and disease. *Physiological Reviews*, *103*(3), 1965–2038. https://doi.org/10.1152/PHYSREV.00050.2021

Morrison, S. J., & Spradling, A. C. (2008). Stem cells and niches: mechanisms that promote stem cell maintenance throughout life. *Cell*, *132*(4), 598–611. https://doi.org/10.1016/J.CELL.2008.01.038

Murray, M. J., Meyer, W. R., Zaino, R. J., Lessey, B. A., Novotny, D. B., Ireland, K., Zeng, D., & Fritz, M. A. (2004). A critical analysis of the accuracy, reproducibility, and clinical utility of histologic endometrial dating in fertile women. *Fertility and Sterility*, *81*(5), 1333–1343. https://doi.org/10.1016/j.fertnstert.2003.11.030

Murray, P. J., & Wynn, T. A. (2011). Obstacles and opportunities for understanding macrophage polarization. *Journal of Leukocyte Biology*, *89*(4), 557–563. https://doi.org/10.1189/JLB.0710409

Nguyen, H. P. T., Sprung, C. N., & Gargett, C. E. (2012). Differential expression of Wnt signaling molecules between pre- and postmenopausal endometrial epithelial cells suggests a population of putative epithelial stem/progenitor cells reside in the basalis layer. *Endocrinology*, *153*(6), 2870–2883. https://doi.org/10.1210/EN.2011-1839

Nikas, G., & Psychoyos, A. (1997). Uterine pinopodes in peri-implantation human endometrium. Clinical relevance. *Annals of the New York Academy of Sciences*, *816*, 129–142. https://doi.org/10.1111/J.1749-6632.1997.TB52136.X

Noyes, R. W., Hertig, A. T., & Rock, J. (1950). Dating the Endometrial Biopsy. *Fertility and Sterility*, *1*(1), 3–25. https://doi.org/10.1016/S0015-0282(16)30062-0

Noyes, R. W., Hertig, A. T., & Rock, J. (1975). Dating the endometrial biopsy. *American Journal of Obstetrics and Gynecology*, *122*(2), 262–263. https://doi.org/10.1016/S0002-9378(16)33500-1

O'Dwyer, D. N., & Moore, B. B. (2017). The role of periostin in lung fibrosis and airway remodeling. *Cellular and Molecular Life Sciences : CMLS*, *74*(23), 4305–4314. https://doi.org/10.1007/S00018-017-2649-Z

IX. References

Owusu-Akyaw, A., Krishnamoorthy, K., Goldsmith, L. T., & Morelli, S. S. (2019). The role of mesenchymal-epithelial transition in endometrial function. *Human Reproduction Update*, *25*(1), 114–133. https://doi.org/10.1093/HUMUPD/DMY035

Palejwala, S., Tseng, L., Wojtczuk, A., Weiss, G., & Goldsmith, L. T. (2002). Relaxin gene and protein expression and its regulation of procollagenase and vascular endothelial growth factor in human endometrial cells. *Biology of Reproduction*, *66*(6), 1743–1748. https://doi.org/10.1095/BIOLREPROD66.6.1743

Patterson, A. L., Zhang, L., Arango, N. A., Teixeira, J., & Pru, J. K. (2013). Mesenchymal-to-epithelial transition contributes to endometrial regeneration following natural and artificial decidualization. *Stem Cells and Development*, *22*(6), 964–974. https://doi.org/10.1089/SCD.2012.0435

Pawar, S., Laws, M. J., Bagchi, I. C., & Bagchi, M. K. (2015). Uterine Epithelial Estrogen Receptor-α Controls Decidualization via a Paracrine Mechanism. *Molecular Endocrinology (Baltimore, Md.)*, *29*(9), 1362–1374. https://doi.org/10.1210/ME.2015-1142

Pickard, M. R., Mourtada-Maarabouni, M., & Williams, G. T. (2011). Candidate tumour suppressor Fau regulates apoptosis in human cells: an essential role for Bcl-G. *Biochimica et Biophysica Acta*, *1812*(9), 1146–1153. https://doi.org/10.1016/J.BBADIS.2011.04.009

Pistofidis, Dimitropoulos, & Mastrominas. (1996). Comparison of Operative and Fertility Outcome Between Groups of Women with Intrauterine Adhesions after Adhesiolysis. *The Journal of the American Association of Gynecologic Laparoscopists*, *3*(4, Supplement), S40. https://doi.org/10.1016/S1074-3804(96)80272-6

Poon, P. P., & Storms, R. K. (1991). The periodically expressed TMP1 gene of Saccharomyces cerevisiae is subject to START-dependent and START-independent regulation. *Journal of Biological Chemistry*, *266*(25), 16808–16812. https://doi.org/10.1016/S0021-9258(18)55373-4

Prasad, S. V., Fiedoruk, K., Daniluk, T., Piktel, E., & Bucki, R. (2019). Expression and Function of Host Defense Peptides at Inflammation Sites. *International Journal of Molecular Sciences*, *21*(1). https://doi.org/10.3390/IJMS21010104

Prašnikar, E., Kunej, T., Gorenjak, M., Potočnik, U., Kovačič, B., & Knez, J. (2022). Transcriptomics of receptive endometrium in women with sonographic features of adenomyosis. *Reproductive Biology and Endocrinology : RB&E*, *20*(1). https://doi.org/10.1186/S12958-021-00871-5

Prianishnikov, V. A. (1978). On the concept of stem cell and a model of functional-morphological structure of the endometrium. *Contraception*, *18*(3), 213–223. https://doi.org/10.1016/S0010-7824(78)80015-8

Qin, K., Yu, M., Fan, J., Wang, H., Zhao, P., Zhao, G., Zeng, W., Chen, C., Wang, Y., Wang, A., Schwartz, Z., Hong, J., Song, L., Wagstaff, W., Haydon, R. C., Luu, H. H., Ho, S. H., Strelzow, J., Reid, R. R., … Shi, L. L. (2024). Canonical and noncanonical Wnt signaling: Multilayered mediators, signaling mechanisms and major signaling crosstalk. *Genes & Diseases*, *11*(1), 103–134. https://doi.org/10.1016/J.GENDIS.2023.01.030

Qin, X., Zeng, B., Sooranna, S. R., & Li, M. (2024). LAMB3 Promotes Myofibrogenesis and Cytoskeletal Reorganization in Endometrial Stromal Cells via the RhoA/ROCK1/MYL9 Pathway. *Cell Biochemistry and Biophysics*, *82*(1), 127–137. https://doi.org/10.1007/S12013-023-01186-5

Queckbörner, S., von Grothusen, C., Boggavarapu, N. R., Francis, R. M., Davies, L. C., & Gemzell-Danielsson, K. (2021). Stromal Heterogeneity in the Human Proliferative Endometrium-A Single-Cell RNA Sequencing Study. *Journal of Personalized Medicine*, *11*(6). https://doi.org/10.3390/JPM11060448

Quenby, S., Nik, H., Innes, B., Lash, G., Turner, M., Drury, J., & Bulmer, J. (2009). Uterine natural killer cells and angiogenesis in recurrent reproductive failure. *Human Reproduction (Oxford, England)*, *24*(1), 45–54. https://doi.org/10.1093/HUMREP/DEN348

Radons, J. (2016). The human HSP70 family of chaperones: where do we stand? *Cell Stress & Chaperones*, *21*(3), 379–404. https://doi.org/10.1007/S12192-016-0676-6

Rajski, M., Zanetti-Dällenbach, R., Vogel, B., Herrmann, R., Rochlitz, C., & Buess, M. (2010). IGF-I induced genes in stromal fibroblasts predict the clinical outcome of breast and lung cancer patients. *BMC Medicine*, *8*(1), 1–18. https://doi.org/10.1186/1741-7015-8-1/FIGURES/5

Rawlings, T. M., Makwana, K., Taylor, D. M., Molè, M. A., Fishwick, K. J., Tryfonos, M., Odendaal, J., Hawkes, A., Zernicka-Goetz, M., Hartshorne, G. M., Brosens, J. J., & Lucas, E. S. (2021). Modelling the impact of decidual senescence on embryo implantation in human endometrial assembloids. *ELife*, *10*. https://doi.org/10.7554/ELIFE.69603

Reardon, S. N., King, M. L., II, J. A. M. L., Mann, J. L., DeMayo, F. J., Lydon, J. P., & Hayashi, K. (2012). Cdh1 is essential for endometrial differentiation, gland development, and adult function in the mouse uterus. *Biology of Reproduction*, *86*(5). https://doi.org/10.1095/BIOLREPROD.112.098871

Regenerative Medicine: The Pipeline Momentum Builds H1. (2022). www.alliancerm.org.

Ren, X., Liang, J., Zhang, Y., Jiang, N., Xu, Y., Qiu, M., Wang, Y., Zhao, B., & Chen, X. (2022). Single-cell transcriptomic analysis highlights origin and pathological process of human endometrioid endometrial carcinoma. *Nature Communications 2022 13:1*, *13*(1), 1–15. https://doi.org/10.1038/s41467-022-33982-7

Richards, J. A. S. (2018). The Ovarian Cycle. *Vitamins and Hormones*, *107*, 1–25. https://doi.org/10.1016/BS.VH.2018.01.009

Riesewijk, A., Martín, J., van Os, R., Horcajadas, J. A., Polman, J., Pellicer, A., Mosselman, S., & Simón, C. (2003). Gene expression profiling of human endometrial receptivity on days LH+2 versus LH+7 by microarray technology. *Molecular Human Reproduction*, *9*(5), 253–264. https://doi.org/10.1093/MOLEHR/GAG037

Robboy, S. J., Kurita, T., Baskin, L., & Cunha, G. R. (2017). New insights into human female reproductive tract development. *Differentiation; Research in Biological Diversity*, *97*, 9–22. https://doi.org/10.1016/J.DIFF.2017.08.002

Robertson, S. A., Seamark, R. F., Guilbert, L. J., & Wegmann, T. G. (1994). The Role of Cytokines in Gestation. *Critical Reviews™ in Immunology*, *14*(3–4), 239–292. https://doi.org/10.1615/CRITREVIMMUNOL.V14.I3-4.30

Ruiz-Alonso, M., Blesa, D., Díaz-Gimeno, P., Gómez, E., Fernández-Sánchez, M., Carranza, F., Carrera, J., Vilella, F., Pellicer, A., & Simón, C. (2013). The endometrial receptivity array for diagnosis and personalized embryo transfer as a treatment for patients with repeated implantation failure. *Fertility and Sterility*, *100*(3), 818–824. https://doi.org/10.1016/J.FERTNSTERT.2013.05.004

Ruiz-Alonso, M., Blesa, D., & Simón, C. (2012). The genomics of the human endometrium. *Biochimica et Biophysica Acta (BBA) - Molecular Basis of Disease*, *1822*(12), 1931–1942. https://doi.org/10.1016/J.BBADIS.2012.05.004

Saegusa, M., Hashimura, M., & Kuwata, T. (2012). Sox4 functions as a positive regulator of β-catenin signaling through upregulation of TCF4 during morular differentiation of endometrial carcinomas. *Laboratory Investigation 2012 92:4*, *92*(4), 511–521. https://doi.org/10.1038/labinvest.2011.196

Saichi, M., Ladjemi, M. Z., Korniotis, S., Rousseau, C., Ait Hamou, Z., Massenet-Regad, L., Amblard, E., Noel, F., Marie, Y., Bouteiller, D., Medvedovic, J., Pène, F., & Soumelis, V. (2021). Single-cell RNA sequencing of blood antigen-presenting cells in severe COVID-19 reveals multi-process defects in antiviral immunity. *Nature Cell Biology*, *23*(5), 538–551. https://doi.org/10.1038/S41556-021-00681-2

Salama, N. M., Zaghlol, S. S., Mohamed, H. H., & Kamar, S. S. (2020). Suppression of the inflammation and fibrosis in Asherman syndrome rat model by mesenchymal stem cells: histological and immunohistochemical studies. *Folia Histochemica et Cytobiologica*, *58*(3), 208–218. https://doi.org/10.5603/FHC.A2020.0024

Salamonsen, L. A., Dimitriadis, E., & Robb, L. (2000). Cytokines in implantation. *Seminars in Reproductive Medicine*, *18*(3), 299–310. https://doi.org/10.1055/S-2000-12567/ID/30/BIB

Santamaria, X., Cabanillas, S., Cervelló, I., Arbona, C., Raga, F., Ferro, J., Palmero, J., Remohí, J., Pellicer, A., & Simón, C. (2016). Autologous cell therapy with CD133+ bone marrow-derived stem cells for refractory Asherman's syndrome and endometrial atrophy: a pilot cohort study. *Human Reproduction (Oxford, England)*, *31*(5), 1087–1096. https://doi.org/10.1093/HUMREP/DEW042

Santamaria, X., Isaacson, K., & Simón, C. (2018). Asherman's Syndrome: it may not be all our fault. *Human Reproduction (Oxford, England)*, *33*(8), 1374–1380. https://doi.org/10.1093/HUMREP/DEY232

Santamaria, X., Mas, A., Cervelló, I., Taylor, H., & Simon, C. (2018). Uterine stem cells: from basic research to advanced cell therapies. *Human Reproduction Update*, *24*(6), 673–693. https://doi.org/10.1093/HUMUPD/DMY028

Saribas, G. S., Ozogul, C., Tiryaki, M., Alpaslan Pinarli, F., & Hamdemir Kilic, S. (2020). Effects of uterus derived mesenchymal stem cells and their exosomes on asherman's syndrome. *Acta Histochemica*, *122*(1). https://doi.org/10.1016/J.ACTHIS.2019.151465

Sato, T., Vries, R. G., Snippert, H. J., Van De Wetering, M., Barker, N., Stange, D. E., Van Es, J. H., Abo, A., Kujala, P., Peters, P. J., & Clevers, H. (2009). Single Lgr5 stem cells build crypt-villus structures in vitro without a mesenchymal niche. *Nature*, *459*(7244), 262–265. https://doi.org/10.1038/NATURE07935

Schatz, F., Aigner, S., Papp, C., Toth-Pal, E., Hausknecht, V., & Lockwood, C. J. (1995). Plasminogen activator activity during decidualization of human endometrial stromal cells is regulated by plasminogen activator inhibitor 1. *The Journal of Clinical Endocrinology and Metabolism*, *80*(8), 2504–2510. https://doi.org/10.1210/JCEM.80.8.7629251

Schenker, J., & Yaffe, H. (1978). Induction of intrauterine adhesions in experimental animals and in women. *Isr J Med Sci* , *14*(2), 261–266.

Schlingensiepen, K. H., Wollnik, F., Kunst, M., Schlingensiepen, R., Herdegen, T., & Brysch, W. (1994). The role of Jun transcription factor expression and phosphorylation in neuronal differentiation, neuronal cell death, and plastic

adaptations in vivo. *Cellular and Molecular Neurobiology*, *14*(5), 487–505. https://doi.org/10.1007/BF02088833

Schupp, J. C., Adams, T. S., Cosme, C., Raredon, M. S. B., Yuan, Y., Omote, N., Poli, S., Chioccioli, M., Rose, K. A., Manning, E. P., Sauler, M., Deiuliis, G., Ahangari, F., Neumark, N., Habermann, A. C., Gutierrez, A. J., Bui, L. T., Lafyatis, R., Pierce, R. W., … Kaminski, N. (2021). Integrated Single-Cell Atlas of Endothelial Cells of the Human Lung. *Circulation*, *144*(4), 286–302. https://doi.org/10.1161/CIRCULATIONAHA.120.052318

Schutgens, F., & Clevers, H. (2020). Human Organoids: Tools for Understanding Biology and Treating Diseases. *Annual Review of Pathology*, *15*, 211–234. https://doi.org/10.1146/ANNUREV-PATHMECHDIS-012419-032611

Schwab, K. E., & Gargett, C. E. (2007). Co-expression of two perivascular cell markers isolates mesenchymal stem-like cells from human endometrium. *Human Reproduction*, *22*(11), 2903–2911. https://doi.org/10.1093/humrep/dem265

Sharma, J. B., Roy, K. K., Pushparaj, M., Gupta, N., Jain, S. K., Malhotra, N., & Mittal, S. (2008). Genital tuberculosis: an important cause of Asherman's syndrome in India. *Archives of Gynecology and Obstetrics*, *277*(1), 37–41. https://doi.org/10.1007/S00404-007-0419-0

Shen, K., Ramirez, B., Mapes, B., Shen, G. R., Gokhale, V., Brown, M. E., Santarsiero, B., Ishii, Y., Dudek, S. M., Wang, T., & Garcia, J. G. N. (2015). Structure–Function Analysis of the Non-Muscle Myosin Light Chain Kinase (nmMLCK) Isoform by NMR Spectroscopy and Molecular Modeling: Influence of MYLK Variants. *PLOS ONE*, *10*(6), e0130515. https://doi.org/10.1371/JOURNAL.PONE.0130515

Simón, C. (2009). *El Endometrio Humano: Desde la investigación a la clínica*. 242. https://books.google.com/books?id=9UUQyEHPX7EC&pgis=1

Singh, N., Shekhar, B., Mohanty, S., Kumar, S., Seth, T., & Girish, B. (2020). Autologous Bone Marrow-Derived Stem Cell Therapy for Asherman's Syndrome and Endometrial Atrophy: A 5-Year Follow-up Study. *Journal of Human Reproductive Sciences*, *13*(1), 31. https://doi.org/10.4103/JHRS.JHRS_64_19

Slater, T., Haywood, N. J., Matthews, C., Cheema, H., & Wheatcroft, S. B. (2019). Insulin-like growth factor binding proteins and angiogenesis: from cancer to cardiovascular disease. *Cytokine & Growth Factor Reviews*, *46*, 28–35. https://doi.org/10.1016/J.CYTOGFR.2019.03.005

Smikle, C., Yarrarapu, S. N., & Khetarpal, S. (2023). *Asherman Syndrome*.

Smith, L. R., Cho, S., & Discher, D. E. (2018). Stem Cell Differentiation is Regulated by Extracellular Matrix Mechanics. *Physiology*, *33*(1), 16. https://doi.org/10.1152/PHYSIOL.00026.2017

Snijders, M. P., De Goeij, A. F., Koudstaal, J., Thunnissen, E. B., De Haan, J., & Bosman, F. T. (1992). Oestrogen and progesterone receptor immunocytochemistry in human hyperplastic and neoplastic endometrium. *The Journal of Pathology*, *166*(2), 171–177. https://doi.org/10.1002/PATH.1711660214

Song, M., Zhao, G., Sun, H., Yao, S., Zhou, Z., Jiang, P., Wu, Q., Zhu, H., Wang, H., Dai, C., Wang, J., Li, R., Cao, Y., Lv, H., Liu, D., Dai, J., Zhou, Y., & Hu, Y. (2021). circPTPN12/miR-21–5 p/ΔNp63α pathway contributes to human endometrial fibrosis. *ELife*, *10*. https://doi.org/10.7554/ELIFE.65735

Spessotto, P., Bulla, R., Danussi, C., Radillo, O., Cervi, M., Monami, G., Bossi, F., Tedesco, F., Doliana, R., & Colombatti, A. (2006). EMILIN1 represents a major stromal element determining human trophoblast invasion of the uterine wall. *Journal of Cell Science*, *119*(Pt 21), 4574–4584. https://doi.org/10.1242/JCS.03232

Spitzer, T. L. B., Rojas, A., Zelenko, Z., Aghajanova, L., Erikson, D. W., Meyer, F. B., Tamaresis, J. S., Hamilton, A. E., Irwin, J. C., & Giudice, L. C. (2012). Perivascular human endometrial mesenchymal stem cells express pathways relevant to self-renewal, lineage specification, and functional phenotype. *Biology of Reproduction*, *86*(2). https://doi.org/10.1095/BIOLREPROD.111.095885

Stamer, S. (1946). Partial and total Atresia of the Uterus after Excochleation. *Acta Obstetricia et Gynecologica Scandinavica*, *26*(2), 263–297. https://doi.org/10.3109/00016344609154456

Stewart, C. L., Kaspar, P., Brunet, L. J., Bhatt, H., Gadi, I., Köntgen, F., & Abbondanzo, S. J. (1992). Blastocyst implantation depends on maternal expression of leukaemia inhibitory factor. *Nature*, *359*(6390), 76–79. https://doi.org/10.1038/359076A0

Stillman, R., & Asarkof, N. (1985). Association between mullerian duct malformations and Asherman syndrome in infertile women. *Obstet Gynecol*, *65*(5), 673–677.

Strassmann, B. (1996). *Energy economy in the evolution of menstruation* (Vol. 5). https://onlinelibrary.wiley.com/doi/abs/10.1002/%28SICI%291520-6505%281996%295%3A5%3C157%3A%3AAID-EVAN4%3E3.0.CO%3B2-C

Su, V. Y. F., Lin, C. S., Hung, S. C., & Yang, K. Y. (2019). Mesenchymal Stem Cell-Conditioned Medium Induces Neutrophil Apoptosis Associated with Inhibition of the NF-κB Pathway in Endotoxin-Induced Acute Lung Injury. *International Journal of Molecular Sciences 2019, Vol. 20, Page 2208*, *20*(9), 2208. https://doi.org/10.3390/IJMS20092208

Sun, Y., Chen, X., Qian, Z., Cao, L., Zhan, S., & Huang, L. (2022). Estradiol and intrauterine device treatment for moderate and severe intrauterine adhesions after transcervical resection. *BMC Women's Health*, *22*(1). https://doi.org/10.1186/S12905-022-01940-6

Sutton, C., & Diamon, M. (1995). *Diagnostic Hysteroscopy: Technique and Documentation*. Lippincott Williams & Wilkins Publishers.

Tal, R., Shaikh, S., Pallavi, P., Tal, A., López-Giráldez, F., Lyu, F., Fang, Y. Y., Chinchanikar, S., Liu, Y., Kliman, H. J., Alderman, M., Pluchino, N., Kayani, J., Mamillapalli, R., Krause, D. S., & Taylor, H. S. (2019). Adult bone marrow progenitors become decidual cells and contribute to embryo implantation and pregnancy. *PLoS Biology*, *17*(9). https://doi.org/10.1371/JOURNAL.PBIO.3000421

Tamura, M., Sebastian, S., Yang, S., Gurates, B., Fang, Z., & Bulun, S. E. (2002). Interleukin-1β Elevates Cyclooxygenase-2 Protein Level and Enzyme Activity via Increasing Its mRNA Stability in Human Endometrial Stromal Cells: An Effect Mediated by Extracellularly Regulated Kinases 1 and 2. *The Journal of Clinical Endocrinology & Metabolism*, *87*(7), 3263–3273. https://doi.org/10.1210/JCEM.87.7.8594

Tan, J., Li, P., Wang, Q., Li, Y., Li, X., Zhao, D., Xu, X., & Kong, L. (2016). Autologous menstrual blood-derived stromal cells transplantation for severe Asherman's syndrome. *Human Reproduction (Oxford, England)*, *31*(12), 2723–2729. https://doi.org/10.1093/HUMREP/DEW235

Tan, Y., Flynn, W. F., Sivajothi, S., Luo, D., Bozal, S. B., Davé, M., Luciano, A. A., Robson, P., Luciano, D. E., & Courtois, E. T. (2022). Single-cell analysis of endometriosis reveals a coordinated transcriptional programme driving immunotolerance and angiogenesis across eutopic and ectopic tissues. *Nature Cell Biology*, *24*(8), 1306–1318. https://doi.org/10.1038/S41556-022-00961-5

Tan, Y., Qiao, Y., Chen, Z., Liu, J., Guo, Y., Tran, T., Tan, K. Sen, Wang, D. Y., & Yan, Y. (2020). FGF2, an Immunomodulatory Factor in Asthma and Chronic Obstructive Pulmonary Disease (COPD). *Frontiers in Cell and Developmental Biology*, *8*. https://doi.org/10.3389/FCELL.2020.00223

Tang, M., Naidu, D., Hearing, P., Handwerger, S., & Tabibzadeh, S. (2010). LEFTY, a Member of the Transforming Growth Factor-β Superfamily, Inhibits Uterine Stromal Cell Differentiation: A Novel Autocrine Role. *Endocrinology*, *151*(3), 1320–1330. https://doi.org/10.1210/EN.2009-1081

Tavcar, J., Movilla, P., Carusi, D. A., Loring, M., Reddy, H., Isaacson, K., & Morris, S. N. (2023). Incidence and Clinical Implications of Placenta Accreta Spectrum after Treatment for Asherman Syndrome. *Journal of Minimally Invasive Gynecology*, *30*(3), 192–198. https://doi.org/10.1016/J.JMIG.2022.11.013

Taylor, H. S. (2004). Endometrial cells derived from donor stem cells in bone marrow transplant recipients. *JAMA*, *292*(1), 81–85. https://doi.org/10.1001/JAMA.292.1.81

Teixeira, J., Rueda, B. R., & Pru, J. K. (2008). Uterine stem cells. *StemBook*. https://doi.org/10.3824/STEMBOOK.1.16.1

Theocharis, A. D., Manou, D., & Karamanos, N. K. (2019). The extracellular matrix as a multitasking player in disease. *The FEBS Journal*, *286*(15), 2830–2869. https://doi.org/10.1111/FEBS.14818

Toth, B., Würfel, W., Germeyer, A., Hirv, K., Makrigiannakis, A., & Strowitzki, T. (2011). Disorders of implantation--are there diagnostic and therapeutic options? *Journal of Reproductive Immunology*, *90*(1), 117–123. https://doi.org/10.1016/J.JRI.2011.05.002

Turco, M. Y., Gardner, L., Hughes, J., Cindrova-Davies, T., Gomez, M. J., Farrell, L., Hollinshead, M., Marsh, S. G. E., Brosens, J. J., Critchley, H. O., Simons, B. D., Hemberger, M., Koo, B. K., Moffett, A., & Burton, G. J. (2017). Long-term, hormone-responsive organoid cultures of human endometrium in a chemically defined medium. *Nature Cell Biology*, *19*(5), 568–577. https://doi.org/10.1038/NCB3516

Ulbrich, S. E., Groebner, A. E., & Bauersachs, S. (2013). Transcriptional profiling to address molecular determinants of endometrial receptivity--lessons from studies in livestock species. *Methods (San Diego, Calif.)*, *59*(1), 108–115. https://doi.org/10.1016/J.YMETH.2012.10.013

Urbich, C., & Dimmeler, S. (2004). Endothelial progenitor cells: characterization and role in vascular biology. *Circulation Research*, *95*(4), 343–353. https://doi.org/10.1161/01.RES.0000137877.89448.78

Vaamonde, D., du Plessis, S. S., & Agarwal, A. (2016). Exercise and human reproduction: Induced fertility disorders and possible therapies. In *Exercise and Human Reproduction: Induced Fertility Disorders and Possible Therapies*. Springer New York. https://doi.org/10.1007/978-1-4939-3402-7

Van Den Heuvel, M. J., Chantakru, S., Xie, X., Evans, S. S., Tekpetey, F., Mote, P. A., Clarke, C. L., & Croy, B. A. (2005). Trafficking of circulating pro-NK cells to the decidualizing uterus: regulatory mechanisms in the mouse and human. *Immunological Investigations*, *34*(3), 273–293. https://doi.org/10.1081/IMM-200064488

Vasilevska, D., Rudaitis, V., Adamiak-Godlewska, A., Semczuk-Sikora, A., Lewkowicz, D., Vasilevska, D., & Semczuk, A. (2022). Cytokeratin Expression Pattern in Human Endometrial Carcinomas and Lymph Nodes Micrometastasis: a Mini-review. *Journal of Cancer*, *13*(6), 1713. https://doi.org/10.7150/JCA.70550

Vento-Tormo, R., Efremova, M., Botting, R. A., Turco, M. Y., Vento-Tormo, M., Meyer, K. B., Park, J. E., Stephenson, E., Polański, K., Goncalves, A., Gardner, L., Holmqvist, S., Henriksson, J., Zou, A., Sharkey, A. M., Millar, B., Innes, B., Wood, L., Wilbrey-Clark, A., … Teichmann, S. A. (2018). Single-cell reconstruction of the early maternal-fetal interface in humans. *Nature*, *563*(7731), 347–353. https://doi.org/10.1038/S41586-018-0698-6

Vilella, F., Wang, W., Moreno, I., Quake, S. R., & Simon, C. (2021). Understanding the human endometrium in the 21st century. *American Journal of Obstetrics and Gynecology*, *225*(1), 1–2. https://doi.org/10.1016/j.ajog.2021.04.224

Waites, G. T., James, R. F. L., & Bell, S. C. (1988). Immunohistological localization of the human endometrial secretory protein pregnancy-associated endometrial alpha 1-globulin, an insulin-like growth factor-binding protein, during the menstrual cycle. *The Journal of Clinical Endocrinology and Metabolism*, *67*(5), 1100–1104. https://doi.org/10.1210/JCEM-67-5-1100

Wang, J., Movilla, P., Morales, B., Wang, J., Williams, A., Reddy, H., Chen, T., Tavcar, J., Morris, S., Loring, M., & Isaacson, K. (2021). Effects of Asherman Syndrome on Maternal and Neonatal Morbidity with Evaluation by Conception Method. *Journal of Minimally Invasive Gynecology*, *28*(7), 1357-1366.e2. https://doi.org/10.1016/J.JMIG.2020.10.004

Wang, L., Chikama, T. –I., Hayashi, Y., Kao, C. W., & Kao, W. W. (2005). Role of FGF7 in Maintenance of Corneal Homeostasis. *Investigative Ophthalmology & Visual Science*, *46*(13), 2176–2176.

Wang, Q., Xu, X., He, B., Li, Y., Chen, X., & Wang, J. (2013). A critical period of progesterone withdrawal precedes endometrial breakdown and shedding in mouse menstrual-like model. *Human Reproduction (Oxford, England)*, *28*(6), 1670–1678. https://doi.org/10.1093/HUMREP/DET052

Wang, Vilella, F., Alama, P., Moreno, I., Mignardi, M., Isakova, A., Pan, W., Simon, C., & Quake, S. R. (2020). Single-cell transcriptomic atlas of the human endometrium during the menstrual cycle. *Nature Medicine*, *26*(10), 1644–1653. https://doi.org/10.1038/S41591-020-1040-Z

Wang, W., Wu, S., Guo, M., & He, J. (2016). LMO4 is a prognostic marker involved in cell migration and invasion in non-small-cell lung cancer. *Journal of Thoracic Disease*, *8*(12), 3682–3690. https://doi.org/10.21037/JTD.2016.12.22

Wang, X. B., Qi, Q. R., Wu, K. L., & Xie, Q. Z. (2018). Role of osteopontin in decidualization and pregnancy success. *Reproduction (Cambridge, England)*, *155*(5), 423–432. https://doi.org/10.1530/REP-17-0782

Wang, X., Mamillapalli, R., Mutlu, L., Du, H., & Taylor, H. S. (2015). Chemoattraction of bone marrow-derived stem cells towards human endometrial stromal cells is mediated by estradiol regulated CXCL12 and CXCR4 expression. *Stem Cell Research*, *15*(1), 14–22. https://doi.org/10.1016/J.SCR.2015.04.004

Wang, X., Wu, S. P., & DeMayo, F. J. (2017). Hormone dependent uterine epithelial-stromal communication for pregnancy support. *Placenta*, *60 Suppl 1*(Suppl 1), S20–S26. https://doi.org/10.1016/J.PLACENTA.2017.07.003

Wang, Y., Kang, X., Kang, X., & Yang, F. (2023). S100A6: molecular function and biomarker role. *Biomarker Research*, *11*(1), 1–14. https://doi.org/10.1186/S40364-023-00515-3/TABLES/3

Wang, & Yu. (2018). An update on the progress of transcriptomic profiles of human endometrial receptivity. *Biology of Reproduction*, *98*(4), 440–448. https://doi.org/10.1093/BIOLRE/IOY018

Wray, S., & Prendergast, C. (2019). The Myometrium: From Excitation to Contractions and Labour. *Advances in Experimental Medicine and Biology*, *1124*, 233–263. https://doi.org/10.1007/978-981-13-5895-1_10/FIGURES/5

Wynn, R. M. (1989). The Human Endometrium. *Biology of the Uterus*, 289–331. https://doi.org/10.1007/978-1-4684-5589-2_11

Xin, X., Liu, H., Zhang, S., Li, P., Zhao, X., Zhang, X., Li, S., Wu, S., Zhao, F., & Tan, J. (2024). S100A8/A9 promotes endometrial fibrosis via regulating RAGE/JAK2/STAT3 signaling pathway. *Communications Biology*, *7*(1). https://doi.org/10.1038/S42003-024-05814-5

Xu, F., Shen, X., Sun, C., Xu, X., Wang, W., & Zheng, J. (2020). The Effect of Mitomycin C on Reducing Endometrial Fibrosis for Intrauterine Adhesion. *Medical Science Monitor : International Medical Journal of Experimental and Clinical Research*, *26*. https://doi.org/10.12659/MSM.920670

Xue, X., Li, X., Yao, J., Zhang, X., Ren, X., & Xu, S. (2022). Transient and Prolonged Activation of Wnt Signaling Contribute Oppositely to the Pathogenesis of Asherman's Syndrome. *International Journal of Molecular Sciences*, *23*(15). https://doi.org/10.3390/IJMS23158808

Yamaguchi, M., Yoshihara, K., Suda, K., Nakaoka, H., Yachida, N., Ueda, H., Sugino, K., Mori, Y., Yamawaki, K., Tamura, R., Ishiguro, T., Motoyama, T., Watanabe, Y., Okuda, S., Tainaka, K., & Enomoto, T. (2021). Three-dimensional understanding of the morphological complexity of the human uterine endometrium. *IScience*, *24*(4). https://doi.org/10.1016/J.ISCI.2021.102258

Yanaihara, A., Otsuka, Y., Iwasaki, S., Aida, T., Tachikawa, T., Irie, T., & Okai, T. (2005). Differences in gene expression in the proliferative human endometrium. *Fertility and Sterility*, *83 Suppl 1*(4 SUPPL.), 1206–1215. https://doi.org/10.1016/J.FERTNSTERT.2004.11.032

Yang, L., Zhu, Y., Tian, D., Wang, S., Guo, J., Sun, G., Jin, H., Zhang, C., Shi, W., Gershwin, M. E., Zhang, Z., Zhao, Y., & Zhang, D. (2021). Transcriptome landscape of double negative T cells by single-cell RNA sequencing. *Journal of Autoimmunity*, *121*. https://doi.org/10.1016/J.JAUT.2021.102653

Yao, S., Zhou, Z., Wang, L., Lv, H., Liu, D., Zhu, Q., Zhang, X., Zhao, G., & Hu, Y. (2023). Targeting endometrial inflammation in intrauterine adhesion ameliorates endometrial fibrosis by priming MSCs to secrete C1INH. *IScience*, *26*(7). https://doi.org/10.1016/J.ISCI.2023.107201

Ye, X. (2020). Uterine Luminal Epithelium as the Transient Gateway for Embryo Implantation. *Trends in Endocrinology and Metabolism: TEM*, *31*(2), 165. https://doi.org/10.1016/J.TEM.2019.11.008

Yi, K. W., Mamillapalli, R., Sahin, C., Song, J., Tal, R., & Taylor, H. S. (2019). Bone marrow-derived cells or C-X-C motif chemokine 12 (CXCL12) treatment improve thin endometrium in a mouse model. *Biology of Reproduction*, *100*(1), 61–70. https://doi.org/10.1093/BIOLRE/IOY175

Yoo, I., Han, J., Kim, M., Jang, H., Sa, S., Choi, S. H., & Ka, H. (2017). Expression and regulation of interleukin 6 and its receptor at the maternal-conceptus interface during pregnancy in pigs. *Theriogenology*, *96*, 85–91. https://doi.org/10.1016/J.THERIOGENOLOGY.2017.04.007

IX. References

Yoshida, S., Asanoma, K., Yagi, H., Onoyama, I., Hori, E., Matsumura, Y., Okugawa, K., Yahata, H., & Kato, K. (2021). Fibronectin mediates activation of stromal fibroblasts by SPARC in endometrial cancer cells. *BMC Cancer*, *21*(1). https://doi.org/10.1186/S12885-021-07875-9

Yu, D., Wong, Y. M., Cheong, Y., Xia, E., & Li, T. C. (2008). Asherman syndrome--one century later. *Fertility and Sterility*, *89*(4), 759–779. https://doi.org/10.1016/J.FERTNSTERT.2008.02.096

Yu, L., Hu, R., Sullivan, C., Swanson, R. J., Oehninger, S., Sun, Y. P., & Bocca, S. (2016). MFGE8 regulates TGF-β-induced epithelial mesenchymal transition in endometrial epithelial cells in vitro. *Reproduction (Cambridge, England)*, *152*(3), 225–233. https://doi.org/10.1530/REP-15-0585

Yuan, L., Cao, J., Hu, M., Xu, D., Li, Y., Zhao, S., Yuan, J., Zhang, H., Huang, Y., Jin, H., Chen, M., & Liu, D. (2022). Bone marrow mesenchymal stem cells combined with estrogen synergistically promote endometrial regeneration and reverse EMT via Wnt/β-catenin signaling pathway. *Reproductive Biology and Endocrinology : RB&E*, *20*(1). https://doi.org/10.1186/S12958-022-00988-1

Zakrzewski, W., Dobrzyński, M., Szymonowicz, M., & Rybak, Z. (2019). Stem cells: past, present, and future. *Stem Cell Research & Therapy*, *10*(1). https://doi.org/10.1186/S13287-019-1165-5

Zeng, Y., Qiu, Y., Jiang, W., Shen, J., Yao, X., He, X., Li, L., Fu, B., & Liu, X. (2022). Biological Features of Extracellular Vesicles and Challenges. *Frontiers in Cell and Developmental Biology*, *10*. https://doi.org/10.3389/FCELL.2022.816698

Zhang, L., Li, Y., Guan, C. Y., Tian, S., Lv, X. D., Li, J. H., Ma, X., & Xia, H. F. (2018). Therapeutic effect of human umbilical cord-derived mesenchymal stem cells on injured rat endometrium during its chronic phase. *Stem Cell Research and Therapy*, *9*(1), 1–15. https://doi.org/10.1186/S13287-018-0777-5/FIGURES/8

Zhang, L. ping, Wang, M., Shang, X., Zhang, Q., Yang, B. jun, Xu, Y., Li, J. hua, & Feng, L. min. (2020). The incidence of placenta related disease after the hysteroscopic adhesiolysis in patients with intrauterine adhesions. *Taiwanese Journal of Obstetrics & Gynecology*, *59*(4), 575–579. https://doi.org/10.1016/J.TJOG.2020.05.018

Zhang, X. H., Liang, X., Liang, X. H., Wang, T. S., Qi, Q. R., Deng, W. B., Sha, A. G., & Yang, Z. M. (2013). The Mesenchymal–Epithelial Transition During In Vitro Decidualization. *Reproductive Sciences*, *20*(4), 354. https://doi.org/10.1177/1933719112472738

Zhang, X., Ren, D., Guo, L., Wang, L., Wu, S., Lin, C., Ye, L., Zhu, J., Li, J., Song, L., Lin, H., & He, Z. (2017). Thymosin beta 10 is a key regulator of tumorigenesis and metastasis and a novel serum marker in breast cancer. *Breast Cancer Research*, *19*(1), 1–15. https://doi.org/10.1186/S13058-016-0785-2/FIGURES/6

Zhang, X., Zhang, S., Qi, J., Zhao, F., Lu, Y., Li, S., Wu, S., Li, P., & Tan, J. (2023). PDGFBB improved the biological function of menstrual blood-derived stromal cells and the anti-fibrotic properties of exosomes. *Stem Cell Research & Therapy*, *14*(1). https://doi.org/10.1186/S13287-023-03339-Y

Zhang, Y., Shi, L., Lin, X., Zhou, F., Xin, L., Xu, W., Yu, H., Li, J., Pan, M., Pan, Y., Dai, Y., Zhang, Y., Shen, J., Zhao, L., Lu, M., & Zhang, S. (2021). Unresponsive thin endometrium caused by Asherman syndrome treated with umbilical cord mesenchymal stem cells on collagen scaffolds: a pilot study. *Stem Cell Research & Therapy*, *12*(1). https://doi.org/10.1186/S13287-021-02499-Z

Zhao, G., Cao, Y., Zhu, X., Tang, X., Ding, L., Sun, H., Li, J., Li, X., Dai, C., Ru, T., Zhu, H., Lu, J., Lin, C., Wang, J., Yan, G., Wang, H., Wang, L., Dai, Y., Wang, B., … Hu, Y. (2017). Transplantation of collagen scaffold with autologous bone marrow mononuclear cells promotes functional endometrium reconstruction via downregulating ΔNp63 expression in Asherman's syndrome. *Science China. Life Sciences*, *60*(4), 404–416. https://doi.org/10.1007/S11427-016-0328-Y

Zhao, G., Li, R., Cao, Y., Song, M., Jiang, P., Wu, Q., Zhou, Z., Zhu, H., Wang, H., Dai, C., Liu, D., Yao, S., Lv, H., Wang, L., Dai, J., Zhou, Y., & Hu, Y. (2020). ΔNp63α-induced DUSP4/GSK3β/SNAI1 pathway in epithelial cells drives endometrial fibrosis. *Cell Death & Disease*, *11*(6). https://doi.org/10.1038/S41419-020-2666-Y

Zhou, Q., Wu, X., Hu, J., & Yuan, R. (2018). Abnormal expression of fibrosis markers, estrogen receptor α and stromal derived factor-1/chemokine (C-X-C motif) receptor-4 axis in intrauterine adhesions. *International Journal of Molecular Medicine*, *42*(1), 81–90. https://doi.org/10.3892/IJMM.2018.3586

Zhou, Q., Yan, G., Ding, L., Liu, J., Yu, X., Kong, S., Zhang, M., Wang, Z., Liu, Y., Jiang, Y., Kong, N., Sun, J., & Sun, H. (2019). EHD1 impairs decidualization by regulating the Wnt4/β-catenin signaling pathway in recurrent implantation failure. *EBioMedicine*, *50*, 343–354. https://doi.org/10.1016/j.ebiom.2019.10.018

Zhou, Z., Wang, H., Zhang, X., Song, M., Yao, S., Jiang, P., Liu, D., Wang, Z., Lv, H., Li, R., Hong, Y., Dai, J., Hu, Y., & Zhao, G. (2022). Defective autophagy contributes to endometrial epithelial-mesenchymal transition in intrauterine adhesions. *Autophagy*, *18*(10), 2427–2442. https://doi.org/10.1080/15548627.2022.2038994

Zhu, H., Li, T., Xu, P., Ding, L., Zhu, X., Wang, B., Tang, X., Li, J., Zhu, P., Wang, H., Dai, C., Sun, H., Dai, J., & Hu, Y. (2024). Effect of autologous bone marrow stem cells-scaffold transplantation on the ongoing pregnancy rate in intrauterine adhesion women: a randomized, controlled trial. *Science China. Life Sciences*, *67*(1), 113–121. https://doi.org/10.1007/S11427-023-2403-7

Zhu, Q., Yao, S., Ye, Z., Jiang, P., Wang, H., Zhang, X., Liu, D., Lv, H., Cao, C., Zhou, Z., Zhou, Z., Pan, W., Zhao, G., & Hu, Y. (2023). Ferroptosis contributes to endometrial fibrosis in intrauterine adhesions. *Free Radical Biology & Medicine*, *205*, 151–162. https://doi.org/10.1016/J.FREERADBIOMED.2023.06.001

Zieba, A., Sjöstedt, E., Olovsson, M., Fagerberg, L., Hallström, B. M., Oskarsson, L., Edlund, K., Tolf, A., Uhlen, M., & Ponten, F. (2015). The Human Endometrium-Specific Proteome Defined by Transcriptomics and Antibody-Based Profiling. *Omics : A Journal of Integrative Biology*, *19*(11), 659–668. https://doi.org/10.1089/OMI.2015.0115